

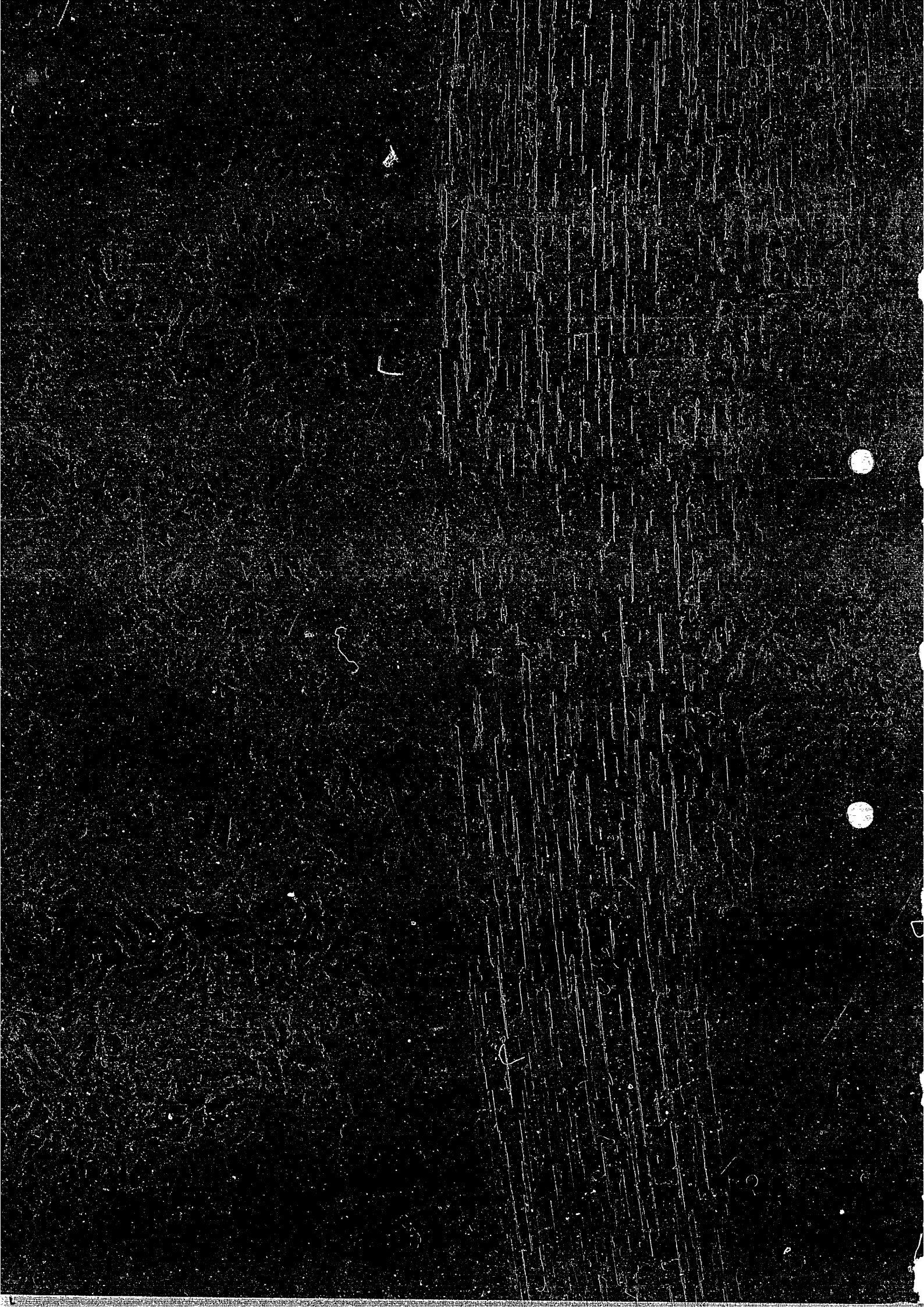
IPPJ-AM-43

THE COLLECTED PAPERS
OF
NICE PROJECT / IPP, NAGOYA

EDITED BY H. TAWARA

INSTITUTE OF PLASMA PHYSICS
NAGOYA UNIVERSITY

NAGOYA, JAPAN



THE COLLECTED PAPERS OF NICE PROJECT/IPP, NAGOYA

Edited by
Hiroyuki TAWARA

Institute of Plasma Physics, Nagoya University
Chikusa-ku, Nagoya 464, Japan

September 1985

This document is prepared as a preprint of compilation of atomic data for fusion research sponsored fully or partly by the IPP/Nagoya University. This is intended for future publication in a journal or will be included in a data book after some evaluations or rearrangements of its contents. This document should not be referred without the agreement of the authors. Enquiries about copyright and reproduction should be addressed to Research Information Center, IPP/Nagoya University, Nagoya, Japan.

Preface

This volume is a collection of the recent papers which the NICE-1 (Naked Ion Collision Experiment) group, an atomic collision study group organized at the Institute of Plasma Physics, Nagoya University, has published in International Journals and Books.

The Editor of the present volume would like to thank the Editors of the following Journals and Books for their permission of reproducing our papers which have been published in their Journals:

Journal of Physics B (papers 2,5,6,7,12,18)

Journal of Physical Society of Japan (papers 10,14,16)

Nuclear Instruments and Methods in Physical Research
(papers 1,9,17)

Physics of Electronic and Atomic Collisions
(papers 3,15)

Physica Scripta (paper 11)

Physical Review (papers 4,8,13)

日本物理学会誌

H. Tawara
Editor

Contents

I. FOREWORD	1
II. List of Publications and Talks	5
III. Reprints of Papers Published	19

I. FOREWORD

This is a collection of papers on the work of the NICE project at the Institute of Plasma Physics (IPP), Nagoya University from 1977 through 1984.

In 1977, Y. Kaneko and T. Iwai were invited to be Guest Professors of the IPP and to make experiments on atomic processes involving highly-charged ions, which were supposed to be extremely important in studies of high temperature plasmas. A research group was organized and several researchers were invited from various institutions in the country to take part in the project. The primary purpose of the project was not only to produce A-M data useful for the nuclear fusion research, but also to deepen our understanding of the basic physics of the atomic processes involving highly-charged ions at relatively low energies. In order to obtain clear conclusions, it was most desirable to make collision experiments using beams of fully-stripped or nearly fully-stripped ions with a narrow energy spread. The project, accordingly, was named NICE (Naked Ion Collision Experiments).

In the first stage of the project, an ion source of EBIS type with a conventional magnet was built and some preliminary experiments were made. In the second stage, an EBIS type ion source using a super conducting magnet was built. A beam of fully-stripped oxygen ions O^{8+} was successfully extracted from the source in 1980, and the source was named NICE-1. Since then, systematic and exhaustive studies on the electron

capture processes by various highly-charged ions from He atoms have been made through cross section measurements and by means of translational energy spectroscopy. The charge state of ions studied has reached up to as high as 41 by the end of the project.

Last spring, the NICE project closed its first phase as the Guest Research Program of the IPP. The whole apparatus including the ion source NICE-1 is still running in a good shape, but the project has been reduced in its scale and taken over to the Collaboration Program of the IPP. In commemoration of the collaboration of the NICE group and for the convenience of reviewing the work of NICE, this collection of papers was edited by H. Tawara as a part of IPPJ-AM series. The names of the people who have taken part in this project are listed below in an alphabetical order:

Toshihiko Hino (IPP→Hamamatsu Photonics Co.)

Hironobu Imamura (Kyushu University→Kyushu Electric Power Co.)

Tsuruji Iwai (Osaka University → Kansai Medical University)

Yozaburo Kaneko (Tokyo Metropolitan University)

Masahiro Kimura (Osaka University)

Nobuo Kobayashi (Tokyo Metropolitan University)

Atsushi Matsumoto (IPP)

Shunsuke Ohtani (IPP)

Kazuhiko Okuno (Tokyo Metropolitan University)

Hiroyuki Tawara (Kyushu University → IPP)

Seiji Tsurubuchi (Osaka University → Tokyo University of
Agriculture and Technology)

Tsutomu Watanabe (The University of Tokyo → The Institute of
Physical and Chemical Research, RIKEN).

It was really an enjoyable collaboration. We appreciate very much the wonderful team work brought into existence by all members of the group, and believe so do they. S. Ohtani has filled the role of secretary of the group throughout the project.

On behalf of the members of the NICE group, we appreciate the whole staff of the Institute of Plasma Physics for their kind support extended to the project. Especially, we would like to express our sincere appreciation to Professor Emeritus Kazuo Takayama who invited us to start this project when he was the Director of the Institute, and to the Former Director Professor Emeritus Hidetake Kakihana who encouraged our group throughout the work. We thank Mr. Genji Takamatsu and his company for their skillful machining of the ion source. Finally, we thank all wives of the NICE members for their tolerance of frequent neglect of home by their husbands who stayed out of homes often for the three consecutive nights, supposedly due to the experiments, over a long period of the project.

January 11, 1985

Yozaburo Kaneko

Tsuruji Iwai

II. List of Publications and Talks

II-1. Original Papers

1. Some Characteristics of an Electron Beam Ion Source:
H. Imamura, Y. Kaneko, T. Iwai, S. Ohtani,
K. Okuno, N. Kobayashi, S. Tsurubuchi, M. Kimura
and H. Tawara
Nucl. Instr. Meth. 188, 233 (1981)
2. Symmetric Resonance Multiple Charge Transfer of Ne^{q+}
and Ar^{q+} ($q \leq 4$):
Y. Kaneko, T. Iwai, s. Ohtani, K. Okuno,
N. Kobayashi, S. Tsurubuchi, M. Kimura
and H. Tawara
J. Phys. B 14, 881 (1981)
3. Cross Sections for One-Electron Capture from He by
Highly Stripped Ions of C, N, O, F, Ne and S below
1 keV/amu:
Y. Kaneko, T. Iwai, S. Ohtani, K. Okuno,
N. Kobayashi, S. Tsurubuchi, M. Kimura, H. Tawara
and S. Takagi
Physics of Electronic and Atomic Collision.
(ed. by S. Datz, North Holland, 1982), p.697.
4. Cross Section for One-Electron Capture by Highly
Stripped Ions of B, C, N, O, F, Ne and S from He
below 1 keV/amu:
T. Iwai, Y. Kaneko, M. Kimura, N. Kobayashi,
S. Ohtani, K. Okuno, S. Takagi, H. Tawara
and S. Tsurubuchi
Phys. Rev. A 27, 105 (1982)

5. Observation of Electron Capture into Selective State by Fully Stripped Ions from He Atom:
S. Ohtani, Y. Kaneko, M. Kimura, N. Kobayashi,
T. Iwai, A. Matsumoto, K. Okuno, S. Takagi,
H. Tawara and S. Tsurubuchi
J. Phys. B 15, L533 (1983)

6. Two-Electron Capture into Autoionizing States of N^{5+} ($3\ell 3\ell'$) and O^{5+} ($1s3\ell 3\ell'$) in Collisions of N^{7+} and O^{7+} with He:
S. Tsurubuchi, T. Iwai, Y. Kaneko, M. Kimura,
N. Kobayashi, S. Ohtani, K. Okuno, A. Matsumoto,
S. Takagi and H. Tawara
J. Phys. B 15, L733 (1983)

7. The (n, ℓ) Distributions in Electron Capture Reactions for C^{3+} , N^{4+} and O^{5+} Ions Colliding with He:
M. Kimura, T. Iwai, Y. Kaneko, N. Kobayashi,
A. Matsumoto, S. Ohtani, K. Okuno, S. Takagi,
H. Tawara and S. Tsurubuchi
J. Phys. B 15, L851 (1983)

8. Energy-Spectroscopic Studies of Electron-Capture Processes by Low-Energy, Highly Stripped C, N, and O ions from He:
K. Okuno, H. Tawara, T. Iwai, Y. Kaneko,
M. Kimura, N. Kobayashi, A. Matsumoto, S. Ohtani,
S. Takagi and S. Tsurubuchi
Phys. Rev. A 28, 127 (1983)

9. Gain Characteristics of Micro-Channel Plate and Channel-Electron Multiplier for Multiply Charged Ions:
S. Takagi, T. Iwai, Y. Kaneko, M. Kimura,
N. Kobayashi, A. Matsumoto, S. Ohtani, K. Okuno,
H. Tawara and S. Tsurubuchi
Nucl. Instr. Meth. 215, 207 (1983)

10. Measurement of Relative Population between B^{2+} (2s) and B^{2+} (2p) in Electron Capture Collision of B^{3+} with He:
A. Matsumoto, T. Iwai, Y. Kaneko, M. Kimura,
N. Kobayashi, S. Ohtani, K. Okuno, S. Takagi,
H. Tawara and S. Tsurubuchi
J. Phys. Soc. Japan 52, 3291 (1983)
11. Recent Activities at NICE Nagoya:
S. Ohtani
Phys. Scripta T 3, 110 (1983)
12. The Dependence on R_c of Cross Sections for One-Electron Capture by S^{11+} , S^{13+} and Kr^{q+} ($q=7-25$) Ions from He Atoms:
T. Iwai, Y. Kaneko, M. Kimura, N. Kobayashi,
A. Matsumoto, S. Ohtani, K. Okuno, S. Takagi,
H. Tawara and S. Tsurubuchi
J. Phys. B 17, L 95 (1984)
13. Energy-Spectroscopic Studies of Electron Capture Processes by Low-Energy, Highly Stripped F and Ne Ions in Collisions with He atoms:
H. Tawara, T. Iwai, Y. Kaneko, M. Kimura,
N. Kobayashi, A. Matsumoto, S. Ohtani, K. Okuno,
S. Takagi and S. Tsurubuchi
Phys. Rev. A 29, 1529 (1984)
14. Landau-Zener Model Calculations of One-Electron Capture from He Atoms by Highly Stripped Ions at Low Energies:
M. Kimura, T. Iwai, Y. Kaneko, N. Kobayashi,
A. Matsumoto, S. Ohtani, K. Okuno, S. Takagi,
H. Tawara and S. Tsurubuchi
J. Phys. Soc. Japan 53, 2224 (1984)

15. One-Electron Capture by Highly Stripped Ions from He Atoms-Final State Analysis-:

S. Ohtani

Eelctronic and Atomic Collisions (Ed. by J. Eichler, I. V. Hertel and N. Stolterfoht, North-Holland, 1984) p.353

16. Translational-Energy Spectroscopy of One-Electron Capture Processes in He^{2+} - H_2 and - N_2 Collisions:

N. Kobayashi, T. Iwai, Y. Kaneko, M. Kimura, A. Matsumoto, S. Ohtani, K. Okuno, S. Takagi, H. Tawara and S. Tsurubuchi

J. Phys. Soc. Japan 53, 3736 (1984)

17. Electron Capture in I^{q+} ($q=10-41$) + He Collisions at Low Energies:

H. Tawara, T. Iwai, Y. Kaneko, M. Kimura, N. Kobayashi, A. Matsumoto, S. Ohtani, K. Okuno, S. Takagi and S. Tsurubuchi

Nucl. Instr. Meth. B9,432 (1985)

18. Electron Capture Processes of I^{q+} Ions with Very High Charge State ($41 \geq q \geq 10$) in Collisions with He Atoms:

H. Tawara, T. Iwai, Y. Kaneko, M. Kimura, N. Kobayashi, A. Matsumoto, S. Ohtani, K. Okuno, S. Takagi and S. Tsurubuchi

J. Phys. B 18, 337 (1985)

II-2. Talks in International Conferences

1. NICE Project at IPP:

Y. Kaneko

Invited Talk at the Nagoya Seminar on Atomic Processes in Fusion Plasmas, Nagoya, 1979

2. Cross Sections for One-Electron Capture from He by Highly Stripped Ions of C, N, O, F and Ne below 1 keV/amu:

Y. Kaneko, T. Iwai, S. Ohtani, K. Okuno, N. Kobayashi, S. Tsurubuchi, M. Kimura, H. Tawara and S. Takagi

Invited Talk at XII International Conference on Physics of Electronic and Atomic Collisions (ICPEAC), Gatlinburg, 1981

3. Recent Activities at NICE Nagoya:

S. Ohtani

Invited Talk at the Symposium on Production and Physics of Highly Charged Ions, Stockholm, 1982

4. Electron Transfer Processes of Highly Ionized Heavy Ions Investigated Through Energy Loss Spectroscopy:

H. Tawara, T. Iwai, Y. Kaneko, M. Kimura, N. Kobayashi, A. Matsumoto, K. Okuno, S. Takagi and S. Tsurubuchi

Symposium on Production and Physics of Highly Charged Ions, Stockholm, 1982

5. Some Trends in Highly Ionized Ion-Atom Collision Experiments: Summary Talk

H. Tawara

Symposium on Production and Physics of Highly Charged Ions, Stockholm, 1982

6. Experimental Studies of Electron Capture Processes by Low Energy, Highly Stripped Heavy Ions:
H. Tawara, T. Iwai, Y. Kaneko, M. Kimura,
N. Kobayashi, A. Matsumoto, S. Ohtani, K. Okuno,
S. Takagi and S. Tsurubuchi
Invited Talk at U.S.-Japan Cooperative
Seminar of Physics of Highly Ionized Ions
Produced in Heavy Ion Collisions, Hawaii,
1983
7. Final-State Analysis of Electron Capture Processes in Collision of Highly Stripped C, N, and O Ions with He atoms:
M. Kimura, T. Iwai, Y. Kaneko, N. Kobayashi,
A. Matsumoto, S. Ohtani, K. Okuno, S. Takagi,
H. Tawara and S. Tsurubuchi
XIII ICPEAC, Berlin, 1983
8. Final-State Analysis of Electron Capture Processes in Collision of Highly Stripped F and Ne Ions with He atoms:
H. Tawara, T. Iwai, Y. Kaneko, M. Kimura,
N. Kobayashi, A. Matsumoto, S. Ohtani, K. Okuno,
S. Takagi and S. Tsurubuchi
XIII ICPEAC, Berlin, 1983
9. One-Electron Capture by Highly Stripped Ions from He Atoms (Final-State Analysis):
S. Ohtani
Invited Talk at XIII ICPEAC, Berlin, 1983
10. Electron Capture by Slow Multi-Charged Ions Colliding with Neutral Atoms:
Y. Kaneko
Invited Talk at the Asia Pacific Physics
Conference, Singapore, 1983

11. Report on the Present Status of the Naked Ion Collision Experiment (NICE):
Y. Kaneko
2nd IAEA Coordinated Research Program Meeting on Atomic Collision Data for Diagnostics of Magnetic Fusion Plasmas, Nagoya, 1983.

12. One-Electron Capture Processes of Very Highly Ionized I^{q+} ($q \leq 41$) Ions in Collisions with He Atoms at Low Energies:
H. Tawara, T. Iwai, Y. Kaneko, M. Kimura, N. Kobayashi, A. Matsumoto, S. Ohtani, K. Okuno, S. Takagi and S. Tsurubuchi
International Conference on the Physics of Highly Ionized Atoms, Oxford, 1984.

13. One-Electron Capture Processes by Highly Charged Ions from He:
Y. Kaneko
US-Japan Workshop on Tokamak Diagnostics by X-Ray, VUV and Optical Radiations, Nagoya, 1984.

14. Electron Capture by Slow and Highly Stripped Iodine form He:
M. Kimura
International Conference on the Physics of Electronic and Atomic Collisions, Stanford, 1985.

15. Energy-Spectroscopic Studies of Electron Capture Processes of Very High Charge at Low Energies:
H. Tawara, T. Iwai, Y. Kaneko, M. Kimura, N. Kobayashi, A. Matsumoto, S. Ohtani, K. Okuno, S. Takagi and S. Tsurubuchi
Invited Talk at Satellite Meeting on Atomic Physics of Highly Charged Ions, Stanford, 1985.

II-3. Progress Reports

1. On the NICE Project:
Y. Kaneko, T. Iwai, S. Ohtani, K. Okuno,
N. Kobayashi, S. Tsurubuchi, M. Kimura, H. Tawara
and H. Imamura
Atomic Collision Research in Japan-Progress
Report 4, 117 (1978)
2. Experimental Study on Multiply-Charged Ion
Collisions:
A. Matsumoto, S. Ohtani, S. Tsurubuchi, K. Okuno,
T. Iwai and Y. Kaneko
Atomic Collision Research in Japan-Progress
Report 4, 78 (1978)
3. Study of Charge Transfer Processes Involving Multiply
Charged Ions:
A. Matsumoto, M. Kimura, S. Tsurubuchi, T. Iwai,
S. Ohtani, H. Tawara, Y. Itoh, M. Namiki,
T. Koizumi, N. Kobayashi and K. Okuno
Annual Review (1979/1980, Inst. Plasma Phys.,
Nagoya Univ.) p.118
4. Cross Sections for One-Electron Capture from He by
Highly Stripped Ions of Be, B, C, N, O, F, Ne and S
below 1 keV/amu:
Y. Kaneko, T. Iwai, S. Ohtani, K. Okuno,
N. Kobayashi, S. Tsurubuchi, M. Kimura, H. Tawara
and S. Takagi
Atomic Collision Research in Japan-Progress
Report 7, 71 (1981)
5. The Nagoya EBIS (NICE-1):
T. Iwai, Y. Kaneko, K. Okuno, N. Kobayashi,
S. Tsurubuchi, M. Kimura, H. Tawara, S. Takagi and
S. Ohtani
Annual Review (1980/1981, Inst. Plasma Phys.,
Nagoya Univ.) p.116

6. Cross Sections for One-Electron Capture from He by Highly Stripped Ions of C, N, O, F and Ne below 1 keV/amu:
Y. Kaneko, T. Iwai, K. Ohkuno, N. Kobayashi, S. Tsurubuchi, M. Kimura, H. Tawara, S. Takagi and S. Ohtani
Annual Review (1980/1981, Inst. Plasma Phys., Nagoya Univ.) p.118
7. Observation of Electron Capture into Selective State by Multicharged C, N and O Ions:
S. Ohtani, Y. Kaneko, M. Kimura, N. Kobayashi, T. Iwai, A. Matsumoto, K. Okuno, S. Takagi, H. Tawara and S. Tsurubuchi
Atomic Collision Research in Japan-Progress Report 8, 309 (1982)
8. Recent Activities in NICE:
S. Ohtani, T. Hino, A. Matsumoto, S. Takagi, T. Iwai, Y. Kaneko, M. Kimura, N. Kobayashi, K. Okuno, H. Tawara and S. Tsurubuchi
Annual Review (1981/1982, Inst. Plasma Phys., Nagoya Univ.) p.155
9. Energy-Spectroscopic Studies of Electron Capture Processes in Collisions of Highly Stripped Ions:
S. Ohtani, T. Iwai, Y. Kaneko, M. Kimura, N. Kobayashi, A. Matsumoto, K. Okuno, S. Takagi, H. Tawara and S. Tsurubuchi
Atomic Collision Research in Japan-Progress Report 9, 51 (1983)
10. NICE Experiments:
T. Iwai, Y. Kaneko, N. Kobayashi, K. Okuno, M. Kimura, S. Tsurubuchi, T. Hino, A. Matsumoto, S. Ohtani, S. Takagi and H. Tawara
Annual Review (1982/1983, Inst. Plasma Phys., Nagoya Univ.) p.134

11. Electron Capture Processes of Kr^{q+} ($7 \leq q \leq 25$) and I^{q+} ($10 \leq q \leq 41$) Ions in Collisions with He Atoms:
 S. Ohtani, T. Iwai, Y. Kaneko, M. Kimura,
 N. Kobayashi, A. Matsumoto, K. Okuno, S. Takagi,
 H. Tawara and S. Tsurubuchi
 Atomic Collisions Research in Japan-Progress
 Report 10, 57 (1984)

12. Electron Capture Processes of Kr^{q+} ($7 \leq q \leq 25$) and I^{q+} ($10 \leq q \leq 41$) Ions in Collisions with He Atoms:
 T. Iwai, Y. Kaneko, N. Kobayashi, K. Okuno,
 M. Kimura, S. Takagi, S. Tsurubuchi, A. Matsumoto,
 H. Tawara and S. Ohtani
 Annual Review (1983/1984, Inst. Plasma Phys.,
 Nagoya Univ.) p.160

13. Dependence of the Gain of Micro-Channel Plate on
 Incident Charge State:
 M. Kimura, S. Takagi, T. Iwai, Y. Kaneko,
 N. Kobayashi, K. Okuno, S. Tsurubuchi,
 A. Matsumoto, S. Ohtani and H. Tawara
 Annual Review (1983/1984, Inst. Plasma Phys.,
 Nagoya Univ.) p.161

14. One-Electron Capture Processes by Highly Charged
 Ions from Helium:
 Y. Kaneko
 Proc. US-Japan Workshop on Tokamak
 Diagnostics by X-Ray, VUV and Optical
 Radiations (IPPJ-703, Inst. Plasma Phys.,
 Nagoya Univ., 1984) P.68.

15. electron Capture by Low Multi-Charged Ions Colliding
 with Neutral Atoms:
 Y. Kaneko
 Proc. First Asia-Pacific Physics Conference
 (Ed. A. Arima, C.K. Chew, T. Ninomiya, P.P.
 Ong, K.K. Phua and K.L. Tan, World
 Scientific Publ. Co., Singapore, 1984)
 Val.1. P.44.

II-4. 邦文誌報告

1. NICE計画の経過報告

金子洋三郎、NICEグループ

核融合研究 別冊 42-3、47 (1979)

2. NICE計画とそれによる多価イオンの共鳴電荷移行反応の研究

金子洋三郎、岩井鶴二、大谷俊介

核融合研究 43-3、23 (1980)

3. NICE実験について

大谷俊介

核融合研究 45-1、61 (1981)

4. 低エネルギー領域における多価イオンの電荷移行

奥野和彦

核融合研究 46-13、85 (1981)

5. 電子ビームイオン源用水平設置超電導コイルおよびクライオスタットの製作

小林信夫、大谷俊介、金子洋三郎、岩井鶴二、奥野和彦、鶴淵誠二、
木村正広、俵博之、日野利彦

名古屋大学プラズマ研究所資料技術報告 IPPJ-DT-84
(1981)

6. 多価イオンの一電子捕獲断面積の荷数依存に見られる振動

木村正広

日本物理学会誌 37、763 (1982)

7. 多価イオン ($q \leq 41$) による一電子捕獲

岩井鶴二

日本物理学会誌 40、213 (1985)

II - 5 . 国内学会発表

1 . E B I S 形高電離重イオン源 - N I C E 計画 :

金子洋三郎、奥野和彦、小林信夫、大谷俊介、岩井鶴二、鶴瀬誠二、
木村正広、今村博信、俵博之

第3回イオン源とその応用技術シンポジウム (東海大)

1979年2月19日

2 . Ne^{q+} , Ar^{q+} ($q \leq 4$) の対称共鳴多重電荷移行 :

金子洋三郎、岩井鶴二、大谷俊介、奥野和彦、小林信夫、鶴瀬誠二、
木村正広、俵博之

物理学会 (福井大学) 1980年10月2日

3 . 多価イオン衝突実験と N I C E 計画 :

金子洋三郎

物理学会 原子分子シンポジウム (北海道大学) 1982年10月2日

4 . 低エネルギー用 E B I S 型多価イオン源の原理と特性 :

大谷俊介

物理学会 原子分子シンポジウム (北海道大学) 1982年10月2日

5 . 高電離イオンと He 衝突による電子捕獲全断面積 :

小林信夫

物理学会 原子分子シンポジウム (北海道大学) 1982年10月2日

6 . 低エネルギー電子捕獲全断面積の荷数依存に見られる振動構造 :

俵博之

物理学会 原子分子シンポジウム (北海道大学) 1982年10月2日

7 . 電子捕獲過程のイオン分光法による研究 :

木村正広

物理学会 原子分子シンポジウム (北海道大学) 1982年10月2日

- 8 . 特定準位への選択的電子捕獲：
奥野和彦
物理学会 原子分子シンポジウム（北海道大学）1982年10月2日
- 9 . 自動電離状態への二電子捕獲：
鶴淵誠二
物理学会 原子分子シンポジウム（北海道大学）1982年10月2日
- 10 . N I C E 計画の今後：
岩井鶴二
物理学会 原子分子シンポジウム（北海道大学）1982年10月2日
- 11 . $K r^{q+} + H e$ ($q = 10 \sim 25$) における電子移行反応：
岩井鶴二、金子洋三郎、木村正広、小林信夫、松本淳、大谷俊介、
奥野和彦、高木祥示、俵博之、鶴淵誠二
物理学会（岡山大学）1983年10月11日
- 12 . L a n d a u - Z e n e r モデルによる多価イオンの電荷移行反応
木村正広、岩井鶴二、金子洋三郎、小林信夫、松本淳、大谷俊介、
奥野和彦、高木祥示、俵博之、鶴淵誠二
物理学会（岡山大学）1983年10月11日
- 13 . ヨウ素多価イオンの電荷移行反応：
木村正広、岩井鶴二、金子洋三郎、小林信夫、松本淳、大谷俊介、
奥野和彦、高木祥示、俵博之、鶴淵誠二
物理学会（九州大学）1984年4月3日
- 14 . M C P ゲインの特性の荷数 ($26 > q > 3$) 依存性：
高木祥示、岩井鶴二、金子洋三郎、木村正広、小林信夫、松本淳、
大谷俊介、奥野和彦、俵博之、鶴淵誠二
物理学会（九州大学）1984年4月3日

III. Reprints of Papers Published

SOME CHARACTERISTICS OF AN ELECTRON BEAM ION SOURCE

H. IMAMURA ¹⁾*, Y. KANEKO ²⁾, T. IWAI ³⁾, S. OHTANI, K. OKUNO ²⁾, N. KOBAYASHI ²⁾
S. TSURUBUCHI ⁴⁾, M. KIMURA ⁵⁾ and H. TAWARA ⁶⁾

Institute of Plasma Physics, Nagoya University, Nagoya 464, Japan

Received 18 August 1980 and in revised form 17 March 1981

Some characteristics of a medium-sized EBIS have been investigated in the continuous and pulsed operation modes. It is found that a 1 keV and 100 mA electron beams, H-like ions such as C⁵⁺, N⁶⁺ and O⁷⁺ as well as He-like ions are produced with intensities comparable to those of doubly ionized ions. A weak trace of naked carbon ions (¹³C⁶⁺) is also seen in the spectra.

1. Introduction

In atomic collision physics, astrophysics and other fields of applications, the importance of collision processes between highly ionized heavy ions and atoms has recently been recognized. In particular, the impurity ions of heavy elements in a thermonuclear fusion plasma are expected to play a key role in cooling and disturbing a high temperature plasma and energy loss from the plasma. Therefore, cross sections for collision processes involving highly ionized ions are urgently required. Production mechanisms of such highly ionized ions in the ion sources are also closely related with atomic collision physics itself.

It seems that a Penning type ion source, which is commonly used as a heavy ion source, can not produce completely ionized heavy ions. On the other hand, an electron beam ion source (EBIS) [1,2] seems to be a good candidate for production of highly ionized and possibly naked heavy ions. In

EBIS, highly ionized ions are produced mainly through successive impact ionization by energetic electrons which are confined with a strong axial magnetic field. A space charge potential well generated by these high density electron beams traps the ion radially. On the other hand, these ions are axially (along the electron beam flow direction) confined with the blocking electric potential applied to some electrodes until the ionization of ions in a desired charge state distribution is achieved.

In the present paper we describe the EBIS operation briefly and report some measurements of characteristics of prototype EBIS constructed to investigate the collision processes involving highly ionized heavy ions.

2. EBIS operation

By assuming that (1) the successive ionization processes by electron impact play a main role in ion production, (2) multiple electron ionization processes contribute negligibly to total ion production and (3) ion losses due to the diffusion and other processes are negligibly small, the ion production in EBIS is governed by the following equation:

$$dn_q/dI = n_{q-1}\sigma_{q-1,q} - n_q\sigma_{q,q+1},$$

where n_q is the ion density with charge ($q+$), $\sigma_{q,q+1}$ is the ionization cross section from charge q to ($q+1$) by electron impact and I is the ionization factor which is equal to product of electron current density and confinement time. The above equation can be

* Present addresses:

¹⁾ Kyushu Electric Power Co., Inc.

²⁾ Department of Physics, Tokyo Metropolitan University, Tokyo 158, Japan.

³⁾ Department of the Liberal Arts, Kansai Medical College, Hirakata, Osaka 573, Japan.

⁴⁾ Department of Applied Physics, Tokyo University of Agriculture and Technology, Koganei, Tokyo 184, Japan.

⁵⁾ Department of Physics, Osaka University, Osaka 560, Japan.

⁶⁾ Nuclear Engineering Department, Kyushu University, Fukuoka 812, Japan.

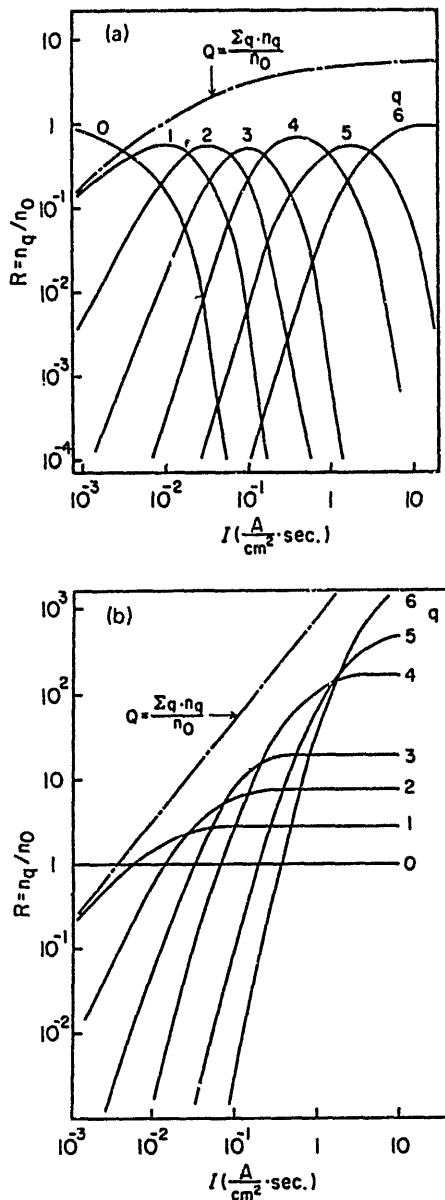


Fig. 1. The calculated charge distributions of C^{q+} ions as a function of the ionization factor under the pulsed neutral gas injection mode (a) and the continuous neutral gas injection mode (b).

solved under such conditions that (a) the neutral gas atoms are continuously supplied and (b) the gas is injected under a pulsed mode. The calculated results for carbon ions are shown in fig. 1 using Lotz's empirical formula [3] to estimate the ionization cross sections. From these figures, it is found that the charge distributions are quite different in both operation modes. For the pulsed gas injection mode, the charge distribution of ions changes with the ionization factor and ions with each charge state have a maximum

intensity at a particular value of the ionization factor and finally all ions become completely ionized (naked). On the other hand, for the continuous gas injection, the production of ions becomes equilibrated ($dn_q/dI = 0$) at large values of the ionization factor and their intensity ratios are given by $n_q/n_{q-1} = \sigma_{q-1,q}/\sigma_{q,q+1}$ at equilibrium. The normalized total ion density ($Q = \sum n_q/n_0$; n_0 is the density of neutral atoms injected) becomes saturated for the pulsed gas injection, meanwhile this increases with I for the continuous gas injection.

3. Experimental setup

Fig. 2 shows a schematic drawing of our prototype EBIS (called PROTO-NICE) with a medium-sized ionization region of 40 cm. The electron gun is of Frost type [4] with about $3 \mu\text{m}$ perveance and operated under the condition of the Brillouin flow [5]. The cathode is concave with a 20 mm diameter. The diameter of electron beams at the waist was measured to be about 1 mm in diameter at 1 keV–100 mA and 2 kG at the center. The typical current density of the electron beam was estimated to be 10 A/cm^2 . There are two differently functioning solenoids, both being water-cooled: One is the main coil for generating the magnetic field which confines the electron beam, the other is the compensation coil for forming a sharply rising magnetic field near the electron gun and the electron collector. Mu-metal sheets of 2 mm in thickness were used to shield the magnetic field at both ends. The magnetic field distribution near the gun is shown in fig. 3. The magnetic field strength at the waist of the electron beams was more than half of its maximum field strength, and less than a few Gauss at the anode–cathode region. With this system, more than 99% of the electron beams emitted from the cathode (100–200 mA) could reach the electron collector electrode. Fourteen drift tubes made of 6 mm ϕ stainless steel cylinder, whose potentials can be independently varied, are used to control the operation modes of PROTO-NICE. The ions produced are extracted and accelerated to desired energies. The charge states of the ions are analyzed using the sector magnet and these ions are detected by continuous-type electron multiplier. The system was evacuated with one 450 l/s and two 100 l/s turbo-molecular pumps and its final vacuum reached 8×10^{-9} Torr measured at the end of the drift tubes.

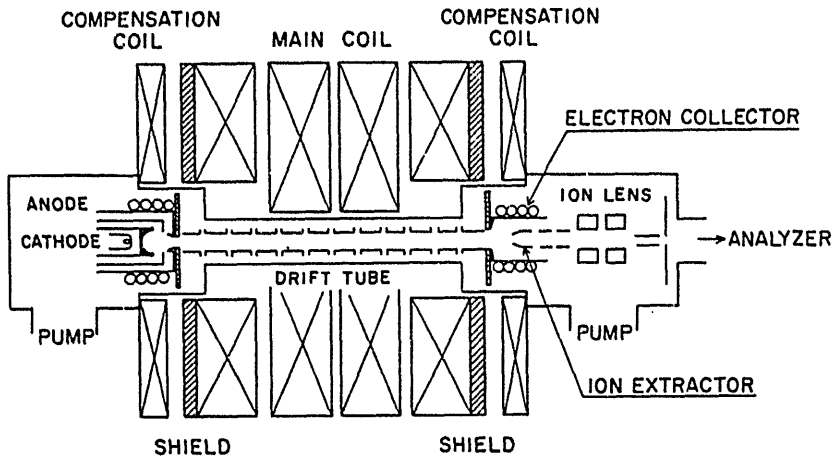


Fig. 2. A schematic drawing of PROTONICE.

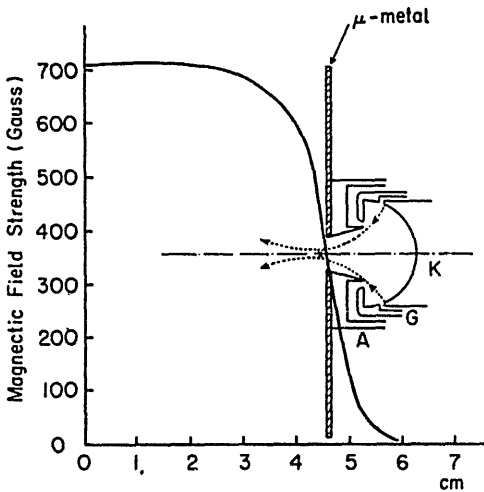


Fig. 3. Measured distribution of magnetic field near the electron with 2 mm thick μ -metal shield. The cross mark (x) shows the calculated position of the waist of the electron beam. (K: cathode, G: grid, A: anode.)

4. Results

The EBIS can be operated both in continuous or time-of-flight mode (continuous gas injection and continuous electron beam) and in confining or pulsed mode (pulsed gas injection and/or pulsed electron beam, or confinement by the blocking electrodes).

4.1. Continuous mode

In this operation mode, electron beams and also gas atoms (in the present case residual gases) were supplied continuously. No time-varying potentials

were applied but all the potentials applied to the drift tubes were constant, and there was no gradient in their distribution along the drift tubes. A typical example of the charge distribution of residual gas ions produced in PROTONICE is shown in fig. 4 which was obtained under the condition of 1.3 keV/89 mA electron beams and 3×10^{-8} Torr vacuum. H-like

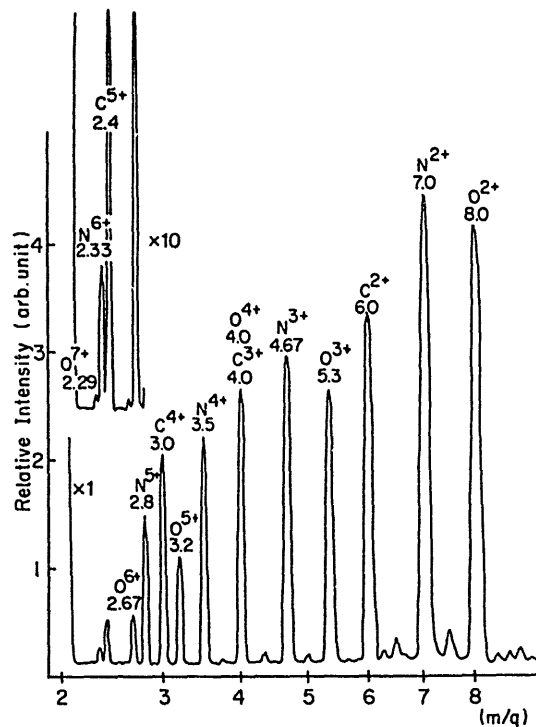


Fig. 4. Typical spectrum of the charge distribution of residual gas ions from PROTONICE under the conditions that the electron beam intensity is 89 mA at 1.3 keV and the background pressure is 3×10^{-8} Torr.

ions such as C^{5+} , N^{6+} and O^{7+} ions can be seen in the same scale as those in doubly ionized ions (C^{2+} , N^{2+} and O^{2+} ions). It is also noteworthy to find in the expanded spectrum that naked carbon ions $^{13}C^{6+}$ ions ($m/e = 2.17$) are produced with an intensity of about $1/20$ of $^{13}C^{5+}$ ions ($m/e = 2.60$). Therefore, it can be expected that some of $^{12}C^{6+}$, N^{7+} and O^{8+} ions are also produced in this PROTO-NICE, though it is impossible to distinguish these naked ions ($m/e = 2.0$ for these ions) from H_2^+ ions in the present analyzing system.

In fig. 5 are shown ratios of ions which charge q^+ to doubly ionized ions. As clearly seen in fig. 5, He-like ions (C^{4+} , N^{5+} and O^{6+} ions) with two 1s-shell electrons are quite intense (70 to 15%) relative to the doubly ionized ions.

In fig. 5 are also shown the calculated charge distributions for the carbon ions which are based upon the ionization factor of $0.1 \text{ A/cm}^2 \cdot \text{s}$. The calculation is in rough agreement with the observed charge distributions. This ionization factor corresponds to the ion confinement time of 10 ms in the present ion source. This is much longer than the thermal drift time of ions along the drift tubes and indicates that some confining potential wells are produced along the beam axis and that ions are trapped in these wells and ionized by successive collisions, resulting in enhancement of higher charge state components.

It is also interesting to compare ion yields in the Penning ion source and in PROTO-NICE. In typical PIGs, the ratios of N^{3+}/N^{2+} and of N^{4+}/N^{2+} are 0.3 and 0.02, respectively, while the ratios of N^{3+}/N^{2+} ,

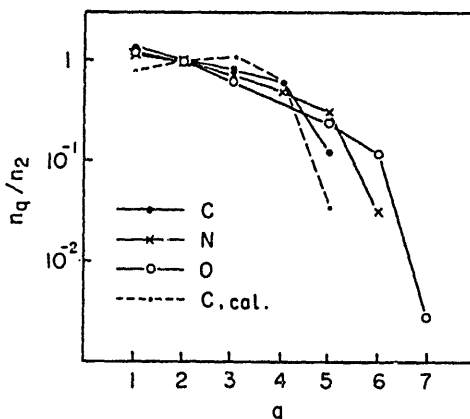


Fig. 5. Relative measured charge distributions of C, N and O ions under the same conditions as in fig. 4. The dotted line shows the calculated results for carbon ions with an ionization factor of $0.1 \text{ A/cm}^2 \cdot \text{s}$.

N^{4+}/N^{2+} and N^{5+}/N^{2+} ions in PROTO-NICE are 0.65, 0.49 and 0.21, respectively. This can be understood from the fact that in PIGs highly ionized ions are produced mainly through multiple electron ionization processes in single collisions, whereas in PROTO-NICE the successive collision of single electron ionization processes is dominant under better confinement.

4.1.1. Pressure dependence

In fig. 6 is shown the dependence of ion production on the gas pressure in the source. The residual gas pressure was controlled by adjusting the opening of the vacuum valves. Production of N^{3+} and N^{4+} ions depends weakly on the gas pressure, while those of He-like and H-like ions (N^{5+} and N^{6+} ions) are strongly dependent on the gas pressure. For example, the intensities of N^{6+} ions increased almost one order of magnitude when the gas pressure decreases only by a factor 2 (from 6×10^{-8} to 3×10^{-8} Torr). This clearly indicates the importance of high vacuum in the source in order to produce highly ionized ions, particularly, He-like, H-like and naked ions in the EBIS.

4.1.2. Electron energy dependence

The production of N^{6+} ions also shows a strong dependence on the ionizing electron energy, increasing one order of magnitude when the electron energy increases from 1 keV to 1.5 keV. This is quite understandable by considering the ionization potential of

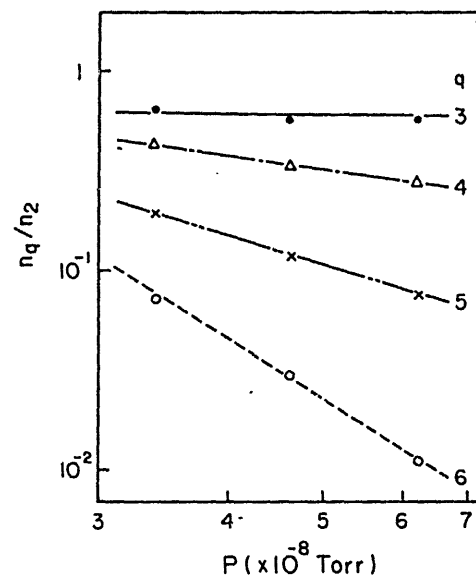


Fig. 6. Pressure dependence of the relative charge distribution of the nitrogen ions.

electrons in N^{5+} ions ($E_b = 524$ eV) and the fact that the maximum ionization cross sections occur at about 3–4 times E_b .

4.1.3. Effect of the ion drift motion

To investigate the effect of the mobility of ions in the drift tubes which changes the retaining time of the ions, the variation of ion intensity was measured as a function of the potential gradient along the drift tubes. The results are shown in fig. 7. It is interesting to note the sharp drop of the intensity of highly ionized ions above 8 V. Particularly, the decrease is prominent for N^{5+} and N^{6+} ions. On the other hand, the intensity of N^{2+} ions increases at this potential. This result can be understood by assuming that the space charge potential of about 8 V is generated along the electron beam axis. If the applied potential becomes larger than 8 V, ions can not be confined along the drift tubes and, as a result, the intensity of highly ionized ions decreases significantly.

4.2. Pulsed mode

There are a lot of different operation modes in the pulsed beam production. In our system, the electron beams and also (residual) gases are continuously supplied. Therefore, the ion yields were measured as a function of some important parameters such as the ion confining time and the pulse width of ion extraction in order to understand the characteristics of PROTO-NICE in the pulsed operation mode.

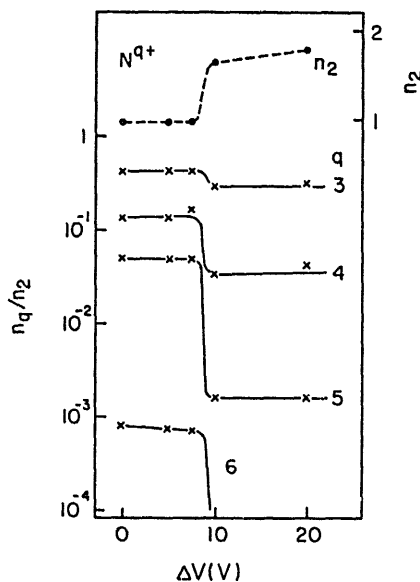


Fig. 7. Effect of potential gradient (ΔV) along the drift tubes on the charge distribution of nitrogen ions.

4.2.1. Pulse width of extraction

Ions were extracted by applying a square-pulsed voltage with various widths to the last drift tube. The confinement time was fixed to 2 ms. The ion beam pulse shape was observed as a function of the pulse width of ion extraction. The ion beam intensities increase with lengthening pulse width and at least 70 μs of the pulse width is necessary to extract ions from the ion source and longer pulses add only weak tails of ion beams which are probably produced in ionization collisions after all ions confined are extracted.

4.2.2. Confinement time

In fig. 8 is shown the dependence of carbon ion yields on the confinement time. In the present case, the ion confinement time is controlled by applying a potential barrier with various widths at the last drift tube. For all the charge state ions, the peak currents increase with increasing the confinement time and reach saturation values. This increase is due to the confinement of ions in the electron space charge potential and the effective successive ionization. Because the residual gas atoms are continuously supplied, the calculated yield of C^{2+} ions can reach equilibrium a few ms after the ion confinement starts; such a behavior is in rough agreement with the observed data. For C^{5+} ions, according to the calculation, some hundreds of ms are necessary before the equilibrium of C^{5+} ion production is established. However, the observed data show that the production of C^{5+} ions reaches equilibrium after 15 ms confinement. This

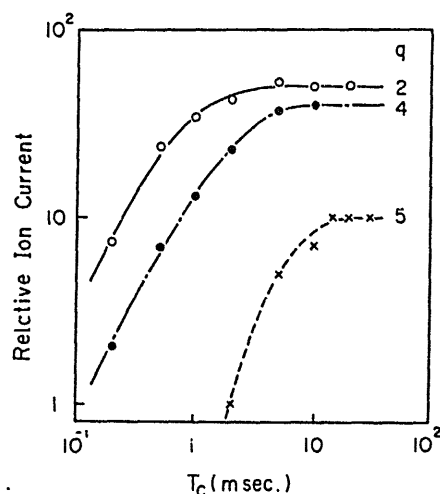


Fig. 8. Charge distribution of carbon ions measured as a function of the confinement time.

discrepancy may be due to the beam loss after the natural neutralization of the electron space charge potential occurs. The calculated natural neutralization time, which is caused by the ionization of the residual ions, is estimated to be about 10 ms at a vacuum of 10^{-7} Torr which is a reasonable estimate of the vacuum inside the drift tubes. It is clear from fig. 8 that it is essential to attain a background pressure (of residual gases) that should be as low as possible in order to obtain the highest charge state ions from PROTO-NICE.

5. Concluding remarks

We have described some characteristics of our PROTO-NICE, which is an EBIS with a medium-sized ionization length of 40 cm. At 1 keV–100 mA electron beams, which corresponds to about 10 A/cm² beam density, H-like ions as well as He-like ions of residual gases (C⁵⁺, N⁶⁺ and O⁷⁺ ions) are found to be produced in a continuous operation. There is also a weak but certain trace of the naked carbon ions (¹³C⁶⁺ ions). In the confinement mode by controlling the potential of the last drift tube, pulsed ion beams were extracted. It is found that there exists a best

pulse width of the potential in order to extract effectively all ions generated and confined in the source. It is also found by observing the beam intensity as a function of the confinement time that the natural neutralization time in the present PROTO-NICE is much shorter than the calculated confinement time necessary to produce C⁶⁺ ions with the best intensity. It becomes clear that the lowest background pressure is prerequisite in order to obtain the highest charge state heavy ions.

Based upon these results, a CRYO-NICE, an EBIS with a superconducting solenoid which can generate a magnetic field up to 20 kG, is now under development in our laboratory.

References

- [1] E.D. Donets, V.I. Ilyushchenko and V.A. Alpert, JINR-p7-4124 (1968).
- [2] J. Arianer and Ch. Goldstein, IEEE Trans. Nucl. Sci. NS-23 (1976) 979.
- [3] W. Lotz, Z. Physik 232 (1968) 101.
- [4] R. Frost, Proc. IRE 56 (1962) 1800.
- [5] G.R. Brewer, Focusing of charged particles, vol. 2 (Academic Press, 1967) p. 73.

Symmetric resonance multiple charge transfer of Ne^{q+} and Ar^{q+} ($q \leq 4$)

Y Kaneko†, T Iwai‡, S Ohtani, K Okuno†, N Kobayashi†, S Tsurubuchi§,
M Kimura|| and H Tawara¶

Institute of Plasma Physics, Nagoya University, Nagoya 464, Japan

Received 15 September 1980

Abstract. Cross sections for resonance charge transfer processes, $\text{A}^{q+} + \text{A} \rightarrow \text{A} + \text{A}^{q+}$, have been measured for Ne^{1-4+} and Ar^{1-4+} at ion acceleration voltages of 2, 3 and 4 kV. The cross sections obtained at 2 kV are 6.9×10^{-16} , 1.74×10^{-16} , 4.9×10^{-17} and $3.4 \times 10^{-18} \text{ cm}^2$ for Ne^+ , Ne^{2+} , Ne^{3+} and Ne^{4+} , respectively, and 2.4×10^{-15} , 5.5×10^{-16} , 9.0×10^{-17} and $3 \times 10^{-18} \text{ cm}^2$ for Ar^+ , Ar^{2+} , Ar^{3+} and Ar^{4+} , respectively. This is the first measurement of resonance charge transfer cross sections for quadruply charged ions. The results obtained are discussed in terms of the total ionisation energies $\sum_j^q I_j$ of the ions, where I_j is the j th ionisation potential. A concept of the 'survival factor' is introduced.

1. Introduction

So far, relatively little attention has been paid to symmetric resonance multiple charge transfer processes,



compared with asymmetric charge transfer processes. Especially for $q \geq 3$, only a few measurements have been reported. Flaks and Filippenko (1959) determined cross sections ${}_{30}\sigma_{03}$ for process (1) for Ne^{3+} and Kr^{3+} with ion energies of 9–90 keV. Latyrov *et al* (1968) measured ${}_{30}\sigma_{03}$ for Ne, Ar and Xe with ion energies of 0.75–9 keV. Beuhler *et al* (1979) measured ${}_{30}\sigma_{03}$ for Xe at 150 keV, and Okuno *et al* (1980) reported ${}_{30}\sigma_{03}$ for Kr with ion energies of 0.6–7.5 keV. There are no reports of cross section measurements of resonance charge transfer for $q \geq 4$, except for that by Beuhler *et al* (1979) who estimated only the order of magnitude of ${}_{40}\sigma_{04}$ for Xe at 200 keV.

A few theoretical papers have been published on resonance double charge transfer processes (Gurnee and Magee 1957, Ferguson and Moiseiwitsch 1959, Fetisov and Firsov 1959, Lichten 1963, Komarov and Yanev 1966). The concept that a resonance charge transfer cross section is determined in terms of the internuclear distance R_c where the u-g oscillation of the colliding system becomes appreciable is well established. All the theories cited above are based on this concept except for those

† Permanent address: Department of Physics, Tokyo Metropolitan University, Tokyo 158, Japan.

‡ Permanent address: Department of Liberal Arts, Kansai Medical University, Hirakata, Osaka 573, Japan.

§ Permanent address: Department of Applied Physics, Faculty of Technology, Tokyo University of Agriculture and Technology, Koganei, Tokyo 184, Japan.

|| Permanent address: Department of Physics, Osaka University, Osaka 560, Japan.

¶ Permanent address: Nuclear Engineering Department, Kyushu University, Fukuoka 812, Japan.

(Fetisov and Firsov 1959) taking account of escaping processes via pseudocrossings of the potential curves to the $A^+ + A^+$ states. No theories for resonance charge transfer for $q \geq 3$ are known to us.

Recently Okuno *et al* (1978) made cross section measurements of ${}_{20}\sigma_{02}$ for Kr and Xe in the energy range from 0.04 to 10 eV (centre-of-mass system). They used the injected-ion drift tube technique with isotope-selected primary ions, which is considered to be one of the most reliable ways of determining absolute integral cross sections in that energy range (Kaneko 1980). They found that the cross sections ${}_{20}\sigma_{02}$ increase as $E^{-1/2}$ with the decrease of the collision energy E below 1 eV, and become almost equal to the classical orbiting cross sections multiplied by a factor of $\frac{1}{2}$. Their results are summarised as follows: (i) the resonance double charge transfer occurs with a probability about $\frac{1}{2}$ once the ion gets within a certain distance R_c from the atom, (ii) the cross sections ${}_{20}\sigma_{02}$ exceed ${}_{10}\sigma_{01}$ at room temperature and (iii) the cross section curves of ${}_{20}\sigma_{02}$ are almost parallel to those of ${}_{10}\sigma_{01}$ above 1 eV, and the ratios ${}_{20}\sigma_{02}/{}_{10}\sigma_{01}$ are close to $I_1/(I_1 + I_2)$, where I_1 and I_2 are the first and second ionisation potentials, respectively.

Although these results were not unexpected from the existing theories, they are so striking and definitive that we were stimulated to discover what would happen to more highly charged ions. Of course, however, the experimental technique which Okuno *et al* used cannot be applied to the ions with $q > 2$ because highly charged ions may change their charge states in collisions with the He buffer gas (Kr²⁺ and Xe²⁺ are exceptions whose recombination energies are smaller than the ionisation potential of He). Therefore, a beam experiment at relatively high energies was performed, and some results on Ne^{q+} and Ar^{q+} ($q \leq 4$) are presented here.

2. Experimental

The experimental set-up for this study is shown schematically in figure 1. The ion source nicknamed cryo-NICE is of the EBIS type developed by Donets (1967, 1976). The cryo-NICE was designed as a source of highly stripped ions with low kinetic energies for studies of elementary processes in hot plasmas, and it was built at the Institute of Plasma Physics (IPP), Nagoya University. The ions are produced by a high-density electron beam confined by a strong magnetic field applied along the axis of the electron beam. The ions produced are trapped in the radial direction by the space charge potential of the electron beam. In the direction of the electron beam axis, the ions are confined by applying suitable potential barriers. Further stripping of the trapped ions proceeds through successive ionisation by electron bombardment. The ions can be extracted either in the pulse mode or in the continuous mode. The cryo-NICE has a superconducting magnet (SCM) for generating a strong and stable magnetic field. A surface of the liquid helium reservoir for the SCM is expected to have a cryogenic pumping function and to ensure an ultra-high vacuum in the source region. Because it has recently been constructed and no fine adjustment has been made, the full performance expected has not yet been achieved. Details of the source will be reported elsewhere after satisfactory adjustments are finished. Nevertheless, it provides enough intensity of ion beams for the present purpose.

The ions accelerated to the desired energy are mass analysed with a sector magnet B of 10 cm radius, and pass through a collision cell C. Then the beam is detected with a secondary electron multiplier M placed behind the cell. A pair of deflectors D₁ and D₂

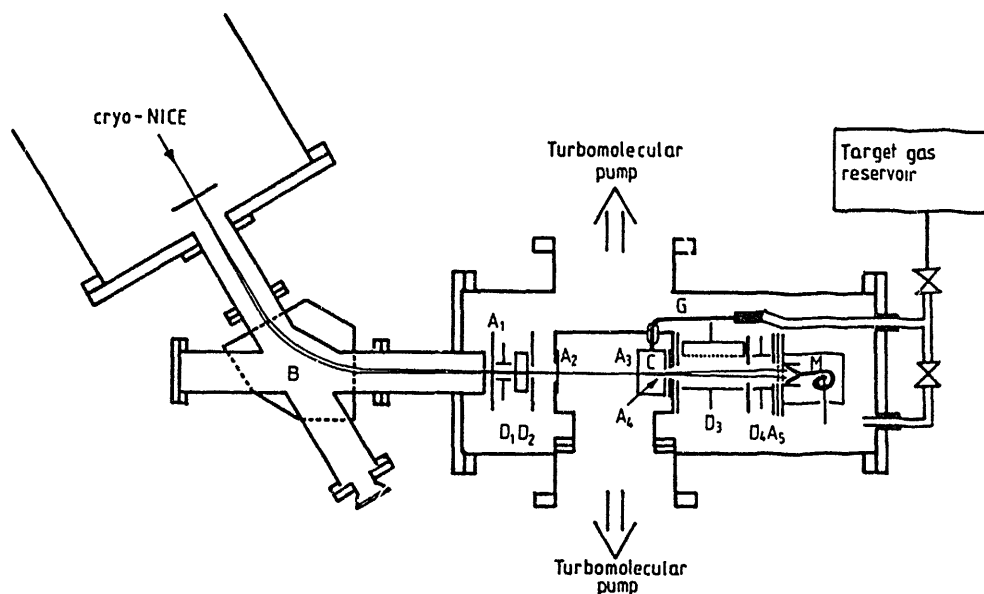


Figure 1. A schematic diagram of the apparatus used. B is a sector magnet of 10 cm radius, C is a collision cell, D_1 and D_2 are defectors for manipulating ion beams, D_3 and D_4 are defectors for complete separation of charged particles from the beam path, M is a Mullard-B419 multiplier and G is a capillary tube for target gas introduction. The diameter of the apertures are as follows: A_1 (1.0 mm), A_2 (0.8 mm), A_3 (0.5 mm), A_5 (2 mm) and A_4 (10 mm). Collision length L which is the distance between A_3 and A_4 is 2.0 cm.

is used to manipulate the primary ion beams. Another pair of defectors D_3 and D_4 is for complete separation of charged particles from the beam path. The beam intensities are measured by the single-counting mode. A channel-type continuous multiplier Mullard-B419 was used for the detector. It has a cone shaped opening 10 mm in diameter. The guard ring A_5 and the input end of the multiplier are kept at the ground potential, and a positive high voltage is applied on the output end of the multiplier. The distance between the exit of the collision cell and the detector is 8.0 cm. The diameters of the apertures around the collision cell are as follows: A_1 (1.0 mm), A_2 (0.8 mm), A_3 (0.5 mm), A_4 (2.0 mm) and A_5 (10 mm). The collision path length L which is the distance between A_3 and A_4 is 2.0 cm. Target gas is introduced into the collision cell through a capillary tube G from the reservoir, the pressure of which is measured with a Pirani gauge calibrated carefully with an MKS Baratron capacitance manometer. By the use of the conductance of the capillary tube and cell apertures, the target gas pressure inside the cell is determined.

The cross sections are determined by

$${}_{q0}\sigma_{0q} = \frac{\alpha_q S_0}{\alpha_0 S_q N L} \quad (2)$$

where S_0 and S_q are the counting rates with and without the double deflector field, N is the target gas density, L is the collision path length, α_0 and α_q are the detection efficiencies of the fast neutrals and the primary ions of charge state q .

Since, in the single-particle-counting technique, a single particle impinging on the multiplier is detected as a single output pulse of the multiplier, the detection efficiency should not depend on the charge state of the incoming particle as long as the missing counts due to the failure of ejection of secondary electrons are negligible. Therefore, we always assume $\alpha_0 = \alpha_q = 1$ in this experiment. This assumption may not be correct at

least for low-energy beams, and we shall discuss this problem later. Throughout the measurements, the primary ion beam intensities were reduced to be of the order of 1×10^4 counts/s in order to prevent the counting loss due to piling up.

The target gas density is given by $N = 3.54 \times 10^{16} P(273/T_g)$, where P is the target gas pressure in Torr and T_g is the gas temperature which is around 300 K. The target gas pressure is determined by $P = P_0(F_0/F)$, where P_0 is the pressure of the gas reservoir, F_0 is the conductance of the capillary tube and F is that of the cell apertures. The vacuum theory provides $F_0/F = 2.67 d^3 / l(K_3 a_3^2 + K_4 a_4^2)$, where d and l are the radius and length of the capillary tube, a_3 and a_4 are the radii of the apertures A_3 and A_4 , respectively, and K_3 and K_4 are the correction factors for the aperture thickness (Clausing factor). Given the values $d = 0.4$ mm, $l = 200$ mm, $a_3 = 0.25$ mm, $a_4 = 1$ mm, $K_3 = 0.95$ (for 0.03 mm thickness) and $K_4 = 0.91$ (for 0.2 mm thickness), the target pressure is given by $P = 0.88 \times 10^{-3} P_0$. When a measurement was made in a high-pressure range, the capillary tube was replaced by a shorter one of 100 mm length.

The ultimate vacuum measured with an ionisation gauge mounted on the vacuum chamber of cryo-NICE is 8×10^{-10} Torr. The pressure in the ion source region cannot be measured because it is surrounded by the walls of the liquid helium reservoir, and because the source pressure is supposed to depend on the vapour pressure of the gas at unknown temperatures inside the source. When a gas is introduced into the source region, the indicator of the ionisation gauge rises up to around 1×10^{-9} Torr. The target pressure inside the collision cell is usually kept below 5×10^{-5} Torr, and below 3×10^{-5} Torr in case of Ar^{4+} , in order to ensure single-collision conditions (see next section), while the pressure outside the cell is kept below 8×10^{-9} Torr by double differential pumping with two turbomolecular pumps.

Because multi-collision processes are more likely than single-collision processes to produce neutral atoms from highly charged ions, the target gas pressure must be kept as low as possible (see next section). Therefore, it is most important to minimise background S_0 signals, which are observed without target gas introduced but with the deflection fields at D_3 and D_4 . In order to minimise the background signals, the following efforts were made: (i) the collision cell housing was baked for some days to reduce background gas pressure, (ii) each aperture edge was made as thin as possible, and especially A_3 was pierced in a copper foil 0.03 mm thick to reduce the possibility of neutralisation of the primary ion beams on the aperture walls and (iii) a double deflector system was used and one of the deflector plates D_3 was covered with a tungsten mesh and coated with carbon soot in order to minimise reflection of ions. The ultimate background signals were a few counts per minute while the noise level of the detector itself was less than one count per minute. Even this low-level background hindered the cross section measurement for ions with $q \geq 6$ as mentioned in the next section. Time-of-flight measurements showed that signals by photons produced along the beam path were negligibly small.

3. Results

3.1. Pressure dependence of S_0/S_q

In order to ensure that the fast neutral particles detected are produced through single-collision processes, the dependence of S_0/S_q on the target thickness $\pi = NL$ was examined. In figure 2, the results obtained for Ar^{q+} with acceleration voltage 2 kV are

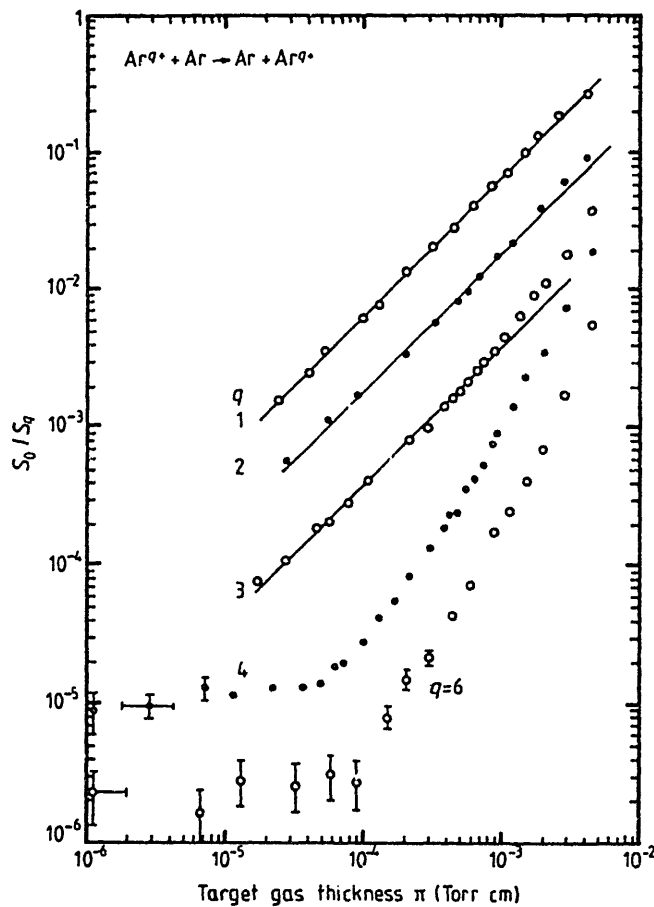


Figure 2. Dependence of S_0/S_q on the target thickness for processes $\text{Ar}^{q+} + \text{Ar} \rightarrow \text{Ar} + \text{Ar}^{q+}$ at the ion acceleration voltage 2 kV. The full lines are 45° lines.

illustrated for a wide range of target thicknesses. As is seen in figure 2, S_0/S_q for Ar^+ is proportional to the target thickness in the wide range studied. For Ar^{2+} and Ar^{3+} , some upward deviation from 45° lines is seen at high values of π indicating contributions from two-step processes. For Ar^{4+} , the slope of the S_0/S_q curve tends to be 2 at high values of π , and tends to be independent of π at low values of π . The former trend indicates that two-step processes are dominant for high values of π , and the latter trend is attributed to the background S_0 signals which are observed even without the introduction of the target gas. In figures 3(a) and 3(b), linear plots of S_0/S_q in the low π region are shown for Ne^{4+} and Ar^{4+} . The broken curves indicate quadratic equations $S_0/S_q = a_0 + a_1\pi + a_2\pi^2$, which are best fitted to the experimental points by the method of least squares. The full lines indicate the linear parts of the equations, and the true cross sections can be deduced from the slopes. Because it takes quite a long time to measure each dependence of S_0/S_q on π , the cross sections for other acceleration voltages were determined by setting the target thickness at appropriate values and measuring the differences of neutral signals with and without target gases. This procedure is evidently safe for Ne^{q+} ($q \leq 4$) and Ar^{q+} ($q \leq 3$) when the target thickness is below 1×10^{-4} Torr cm (5×10^{-5} Torr). In the case of Ar^{4+} , this procedure will result in an overestimation of S_0 even though the target thickness is set below 6×10^{-5} Torr cm (3×10^{-5} Torr). Then, the S_0 are corrected for the quadratic term indicated above by neglecting the energy dependence of the quadratic term. This correction is 30% at most.

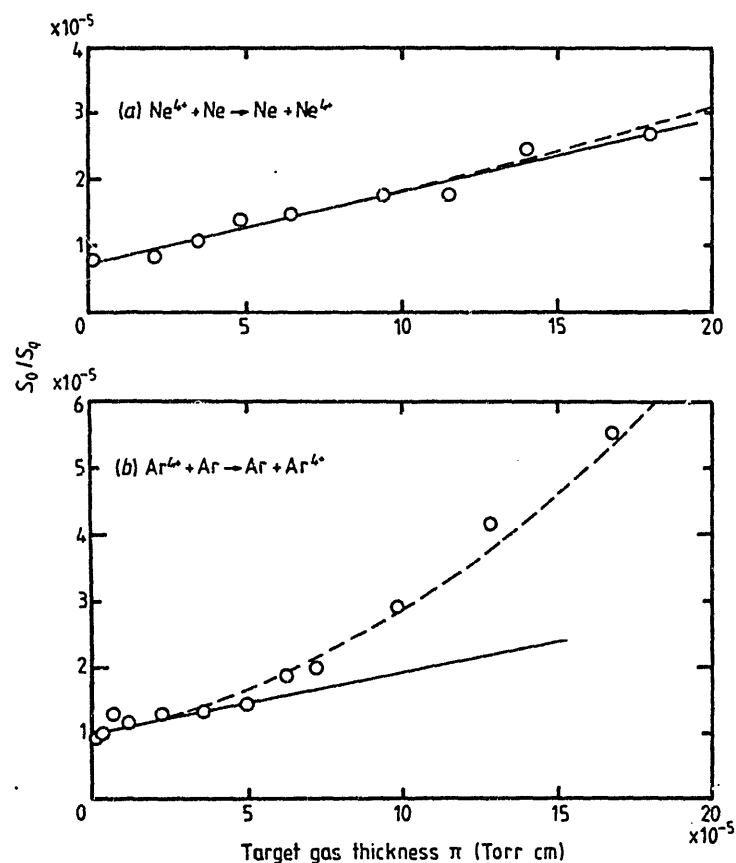


Figure 3. Linear plot of S_0/S_q at 2 kV against target gas thickness π in the low π region. The broken curves are quadratic equations $S_0/S_q = a_0 + a_1\pi + a_2\pi^2$ which are best fitted to the experimental points by the method of least squares. The full lines are linear parts of them.

For ions with $q = 5$, cross section measurements could not be made, because Ne^{5+} ($M/q = 4$) and Ar^{5+} ($M/q = 8$) could not be separated from some impurity ions such as C^{3+} and O^{2+} in the primary beams. The S_0/S_q curve for Ar^{6+} in figure 2 indicates that even three-step processes contribute to some extent in this case. Efforts were made to minimise background signals as mentioned in the previous section, but the ultimate background signals hindered the separation of the linear portion from the measured S_0/S_q curve. In a preliminary experiment (Kaneko 1979) we overestimated these cross sections because of underestimation of multi-collision processes.

3.2. Cross sections

The cross sections obtained are shown in figures 4(a) and (b) and table 1. The acceleration voltages of primary ions are set at 2, 3 and 4 kV. In the case of Ar^+ , no measurement was made at 4 kV because the field of the sector magnet was not strong enough to select the ions. Each point indicates the average of cross sections determined on different occasions. On each occasion several runs of measurements of S_0/S_q were made. The errors indicated in the figures and table are only for reference of the extent of data scattering.

The most ambiguous factors are the detection efficiencies α_0 and α_q in equation (2). As mentioned already, we have always assumed $\alpha_0 = \alpha_q$ in this experiment. This

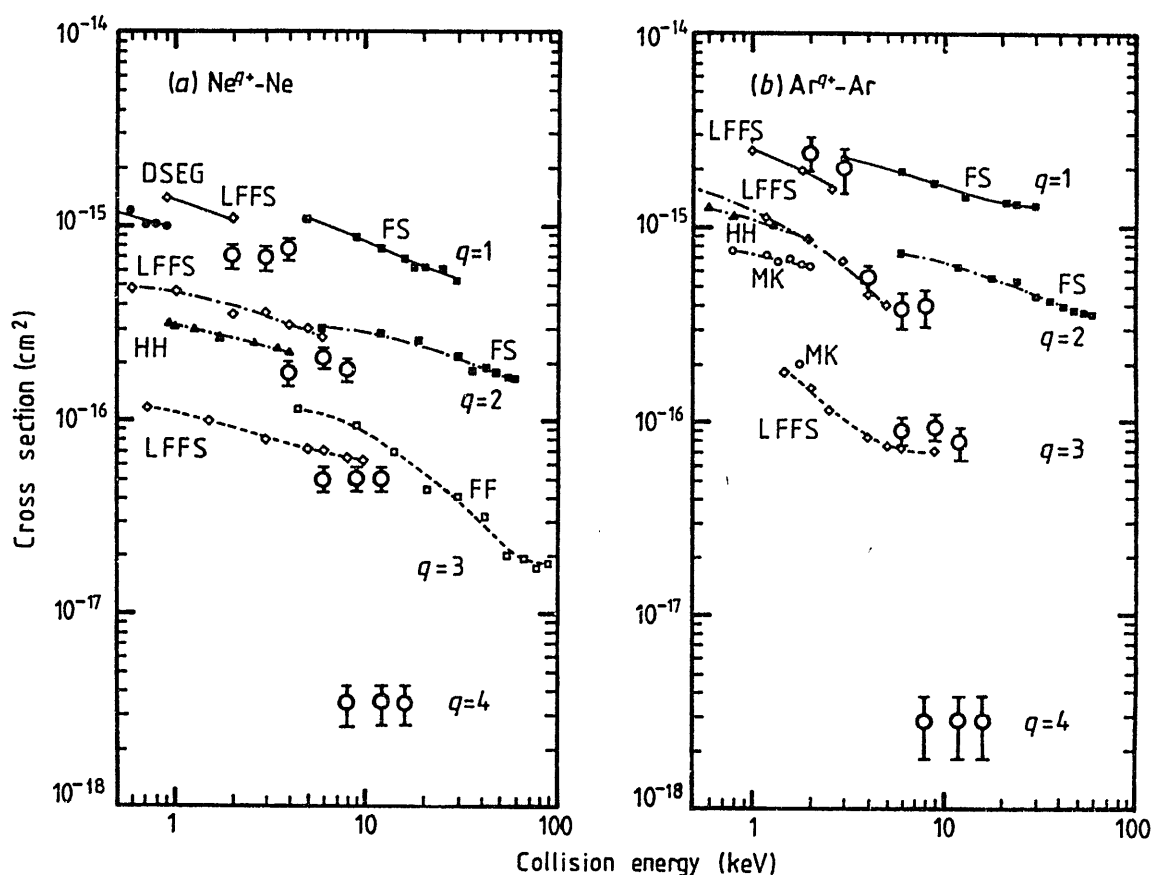


Figure 4. Cross sections ${}_{q_0}\sigma_{0q}$ for Ne^{q+} and Ar^{q+} ($q \leq 4$). \bar{O} , present results; DSEG, Dillon *et al* (1955); LFFS, Latyrov *et al* (1968); FS, Flaks and Solv'ev (1958); HH, Hasted and Hussain (1964); FF, Flaks and Filippenko (1959); MK, McGowan and Kervin (1967).

Table 1. The cross sections ${}_{q_0}\sigma_{0q}$ obtained for Ne^{q+} and Ar^{q+} .

Acceleration voltages (kV)		$10\sigma_{01}$ (10^{-16} cm 2)	$20\sigma_{02}$ (10^{-16} cm 2)	$30\sigma_{03}$ (10^{-17} cm 2)	$40\sigma_{04}$ (10^{-18} cm 2)
Ne^{q+}	2	6.9 ± 1.0	1.74 ± 0.25	4.9 ± 0.7	3.4 ± 0.8
	3	6.8 ± 1.0	2.08 ± 0.25	5.0 ± 0.7	3.4 ± 0.8
	4	7.6 ± 1.0	1.82 ± 0.25	5.0 ± 0.7	3.4 ± 0.8
Ar^{q+}	2	24 ± 5	5.5 ± 0.8	9.0 ± 1.5	3 ± 1
	3	20 ± 5	3.8 ± 0.8	9.5 ± 1.5	3 ± 1
	4	—	3.9 ± 0.8	7.8 ± 1.5	3 ± 1

assumption may not be correct at least for low-energy collisions. The present results for ions with $q = 1$, however, do not indicate any certain deviation from the results previously reported by other investigators. When the acceleration voltage was decreased below 2 kV, the reproducibility of the apparent cross sections becomes very poor. It may be explained partly by the inadequacy of the assumption of $\alpha_0 = \alpha_q$. However, the reproducibility became even worse for more highly charged ions for which the assumption $\alpha_0 = \alpha_q$ was expected to be safer than for lower charge state ions

because higher velocities were gained by higher charge state ions at the same acceleration voltage. In the preliminary experiment we used a detector system consisting of a secondary electron converter plate and a multiplier. An aluminium plate and an Ag-Mg plate were tested for the converter, but always we observed poor reproducibility of S_0/S_q below 2 kV. Since we had to change the potentials of the lens system drastically to focus the ion beams with acceleration voltages below 2 kV, a slight change of impinging positions of ions and neutrals on the detector might cause appreciable changes in the detection efficiencies α_0 and α_q . The causes of these phenomena are not yet clear. With acceleration voltages higher than 2 kV, the reproducibility was almost satisfactory and within the errors indicated. The uncertainty caused from α_0/α_q is estimated as 20%. The uncertainty associated with the determination of the target gas thickness is estimated to be 10%. The total uncertainty for the absolute values of the cross sections is therefore estimated to be 30%. In the case of Ar^{4+} , an additional 20% uncertainty arises from the determination of the slope of S_0/S_q on target thickness, and it makes the total uncertainty 50%.

There are some results of other groups previously reported for ions with $q \leq 3$ and they are also shown in figures 4(a) and (b). These previous results scatter to some extent, and the present results are within the scattering of these data. No cross sections have been reported for ions with $q = 4$. Beuhler *et al* (1979) estimated ${}_{40}\sigma_{04}$ for Xe to be $0.1 \times 10^{-16} \text{ cm}^2$ at 200 keV which seems to be a little too large. Since the energy range studied is narrow, we cannot say much about the energy dependence of the cross sections obtained; nor can we say whether the primary ions are extracted in their ground state although it is said that the ions extracted from an EBIS type source include few ions in metastable states (Klinger *et al* 1975).

4. Discussion

No theories for symmetric resonance multiple charge transfer processes for ions with $q \geq 3$ are known. As mentioned in the introduction, it is well established that a resonance double charge transfer cross section is given by $\frac{1}{2}\pi R_c^2$. Here R_c is the internuclear distance where the u-g oscillation starts (Gurnee and Magee 1957). There are several ways of estimating R_c . In a study of symmetric resonance double charge transfer of Kr^{2+} and Xe^{2+} Okuno *et al* (1978) found that the ratios ${}_{20}\sigma_{02}/{}_{10}\sigma_{01}$ are close to $I_1/(I_1 + I_2)$ above 1 eV. Here, I_1 and I_2 are the first and second ionisation potentials, respectively. This suggests that one of the simplest ways of estimation of R_c for resonance multiple charge transfer is to assume

$$R_c^2 \propto \frac{1}{\sum_j^q I_j} \quad (3)$$

where I_j is the j th ionisation potential. In table 2, a comparison of ${}_{q0}\sigma_{0q}/{}_{10}\sigma_{01}$ and $I_1/\sum_j^q I_j$ is made. Although ${}_{q0}\sigma_{0q}$ and ${}_{10}\sigma_{01}$ should be taken at the same energy for this purpose, we reluctantly take them at the same acceleration voltage 2 kV, because the energy ranges studied do not overlap. The agreement between ${}_{q0}\sigma_{0q}/{}_{10}\sigma_{01}$ and $I_1/\sum_j^q I_j$ may be said to be fairly good for $q = 2$ if one takes into account that they are not at the same energy. For $q = 3$ and 4, the agreement is poor. This is quite natural from the following point of view.

In figures 5(a) and 5(b), some potential curves are schematically shown for $(\text{Ar}-\text{Ar})^{2+}$ and $(\text{Ar}-\text{Ar})^{3+}$ systems. These curves are drawn taking only the levels at

Table 2. Comparison of cross sections with ionisation potentials.

	q	$q_0\sigma_{0q}/10\sigma_{01}^\dagger$	$I_1/\sum I_i^\ddagger$	$\frac{q_0\sigma_{0q}/10\sigma_{01}}{I_1/\sum I_i}$
Ne^{q+}	1	1	1	1
	2	0.25	0.34	0.74
	3	0.071	0.17	0.42
	4	0.0049	0.096	0.051
Ar^{q+}	1	1	1	1
	2	0.22	0.36	0.61
	3	0.038	0.19	0.21
	4	0.0012	0.11	0.012

† At the ion acceleration voltage 2 kV.

‡ Moore (1971).

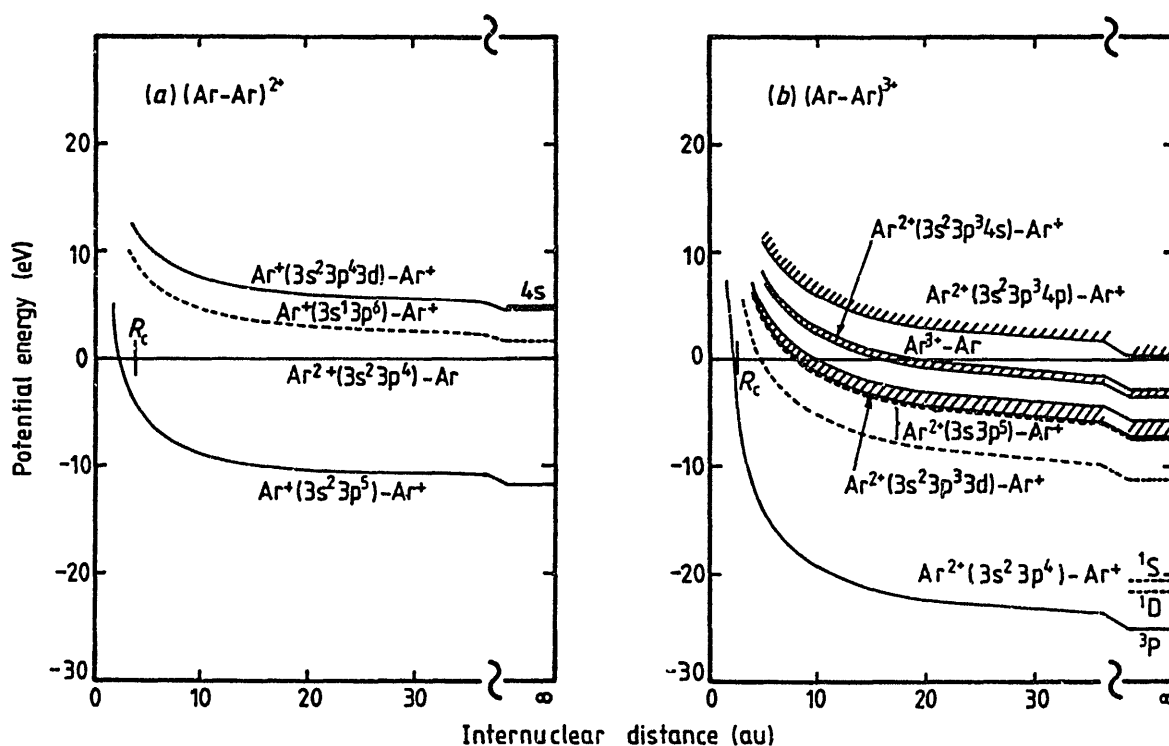


Figure 5. A schematic diagram of potential curves for $(\text{Ar}-\text{Ar})^{2+}$ and $(\text{Ar}-\text{Ar})^{3+}$ systems. The positions of R_c determined from the ratios of total ionisation energies and the single charge transfer cross sections (see text) are shown approximately.

infinity and the Coulomb repulsions into account. In the case of $(\text{Ar}-\text{Ar})^{2+}$, no potential curves for the final state $(\text{Ar}^+-\text{Ar}^+)$ cross the curve for the initial state $(\text{Ar}^{2+}-\text{Ar})$ at a distance larger than R_c . In contrast, in the case of $(\text{Ar}-\text{Ar})^{3+}$, a number of potential curves for $(\text{Ar}^{2+*}-\text{Ar}^+)$ cross the potential curve for the initial state $(\text{Ar}^{3+}-\text{Ar})$ outside R_c . Generally speaking, there are four collision paths at each potential crossing as indicated in figure 6. The initial collision pair $\underline{\text{Ar}^{3+}}-\text{Ar}$ results in elastic scattering by path (1), or results in $\underline{\text{Ar}^{2+*}}-\text{Ar}$ state by path (2) (the underlines indicate fast particles). Some of the initial collision pairs penetrate the crossing and may reach R_c . On the way back, however, some of the pairs in the state $\underline{\text{Ar}}-\text{Ar}^{3+}$ which have experienced

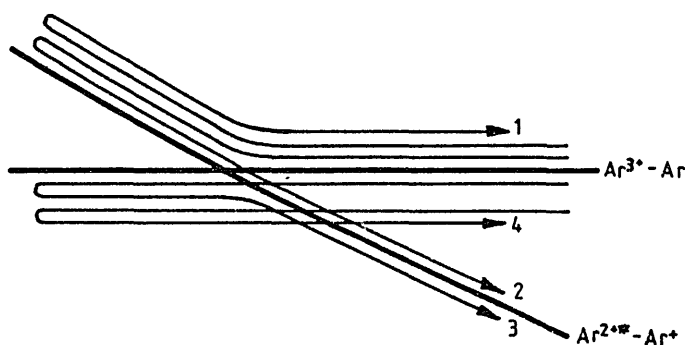


Figure 6. Collision paths at a potential curve crossing.

resonance charge transfer escape to $\underline{\text{Ar}}^+ - \text{Ar}^{2+*}$ state by path (3). Thus, only the initial collision pairs going in and coming out by path (4) are eligible to be observed as the resonance charge transferred state $\underline{\text{Ar}} - \text{Ar}^{3+}$ except for the charge transfer probability. From this point of view, the ratios of experimental cross sections to hypothetical ones, which are given in table 2, are providing some idea on the 'survival factor'. That is, the survival factor is the possibility of getting to R_c and coming back without suffering from adiabatic processes at potential crossings. If the probabilities of penetration at the k th potential crossing is taken to be $(1 - P_k)$, the survival factor corresponds to $\prod_k^n (1 - P_k)^2$, where n is the number of the crossings outside R_c . Of course, this is a very crude argument especially as the effects of potential crossings inside R_c are neglected. However, the fact that the ratio of ${}_{q0}\sigma_{0q}/{}_{10}\sigma_{01}$ to $I_1/\sum_j^q I_j$ is much smaller for Ar^{4+} than for Ne^{4+} is quite understandable because there are much more potential crossings in the $(\text{Ar}-\text{Ar})^{4+}$ system than in $(\text{Ne}-\text{Ne})^{4+}$. It would be most interesting to see what will happen to resonance multiple charge transfer processes in very low-energy regions where the classical orbiting cross sections become large.

Acknowledgments

This work was carried out as a part of the Guest Research Program at the Institute of Plasma Physics, Nagoya University. The authors are grateful to Professor Kazuo Takayama, who retired from the office of Director of the Institute in April, for his encouragement through this work.

References

- Beuhler R J, Friedman L and Porter R F 1979 *Phys. Rev. A* **19** 486-94
 Donets E D 1967 *Sov. Bul. Disc. Invent* No 24
 — 1976 *IEEE Trans. Nucl. Sci.* **NS-23** 897-903
 Dillon J A Jr, Sheridan W F, Edwards H D and Ghosh S N Jr 1955 *J. Chem. Phys.* **23** 776-9
 Ferguson A F and Moiseiwitsch B L 1959 *Proc. Phys. Soc.* **74** 457-62
 Fetisov I K and Firsov O B 1959 *Zh. Eksp. Teor. Fiz.* **37** 95-7 (1960 *Sov. Phys.-JETP* **10** 67-8)
 Flaks I P and Filippenko L G 1959 *Zh. Tekh. Fiz.* **29** 1100-9 (1960 *Sov. Phys.-Tech. Phys.* **4** 1005-13)
 Flaks I P and Solv'ev E S 1958 *Zh. Tekh. Fiz.* **28** 599 (1958 *Sov. Phys.-Tech. Phys.* **3** 564-76)
 Gurnee E F and Magee J L 1957 *J. Chem. Phys.* **26** 1237-48
 Hasted J B and Hussain M 1964 *Proc. Phys. Soc.* **83** 911-24

- Kaneko Y 1979 Institute of Plasma Physics, Nagoya University preprint IPPJ-AM-13 pp 28-37
— 1980 *Proc. 11th Int. Conf. on Physics of Electronic and Atomic Collisions* (Amsterdam: North-Holland)
Invited papers and progress reports pp 109-24
- Klinger H, Müller A and Salzborn E 1975 *J. Phys. B: At. Mol. Phys.* **8** 230-8
- Komarov I V and Yanev R K 1966 *Zh. Eksp. Teor. Fiz.* **51** 1712-21 (1967 *Sov. Phys.-JETP* **24** 1159-64)
- Latyrov Z Z, Fedrenko N V, Flaks I P and Shaporenko A A 1968 *Zh. Eksp. Teor. Fiz.* **55** 847-53 (1969 *Sov. Phys.-JETP* **28** 439-42)
- Lichten W 1963 *Phys. Rev.* **131** 229-38
- McGowan J W and Kerwin L 1967 *Can. J. Phys.* **45** 1451-67
- Moore C E 1971 *Atomic Energy Levels* NSRDS-NBS35 vol 1 (Washington, DC: US Govt Printing Office)
- Okuno K, Koizumi T and Kaneko Y 1978 *Phys. Rev. Lett.* **40** 1708-10
— 1980 *Proc. 11th Int. Conf. on Physics of Electronic and Atomic Collisions* (Amsterdam: North-Holland)
Abstracts pp 594-5

CROSS SECTIONS FOR ONE-ELECTRON CAPTURE FROM He
BY HIGHLY STRIPPED IONS OF C, N, O, F, Ne AND S BELOW 1 keV/amu

Y. Kaneko*, T. Iwai*, S. Ohtani, K. Okuno*, N. Kobayashi*,
S. Tsurubuchi⁺, M. Kimura[‡], H. Tawara[#] and S. Takagi^{##}

Institute of Plasma Physics, Nagoya University,
Nagoya 464, Japan

The cross sections for one-electron transfer from He atom into the fully stripped, hydrogen-like, helium-like and lithium-like C^{q+} , N^{q+} , O^{q+} , F^{q+} , Ne^{q+} ions and also highly stripped S^{q+} ions have been measured at the energy range of 0.5q - 4.0q keV. It is found that the measured cross sections are nearly independent of the collision energy with a few exceptions. When plotted as a function of the ionic charge q of ion, strong oscillations in the cross sections are observed which are very similar in phase but different in absolute values for ions with different isoelectronic sequence. On the other hand, the measured cross sections come together on a single curve when plotted as a function of the effective core charge Z_1^* of ion by taking into account the screening by electrons. This oscillatory behavior can be explained reasonably well through the modified classical one electron model of Ryufuku-Sasaki-Watanabe.

1. INTRODUCTION

The electron transfer process between highly stripped heavy ion with charge q and atomic hydrogen at low energies



is important not only in basic collision physics but also in many applications such as astrophysics and high temperature plasma physics. In particular, the process(1) involving impurity ions plays a key role in the energy and particle loss from the Tokamak plasma¹⁾. Because only a single electron is involved in the collision process of the fully stripped ion, theoretical treatment is considerably simple and a number of theoretical calculations have been reported. Most of the theories are based upon the concept of formation of the quasi-molecule $(A-H)^{q+}$ during collision. Progress in theories is summarized by Olson²⁾. On the other hand, it is difficult

* Department of Physics, Tokyo Metropolitan University, Setagaya-ku, Tokyo 158

‡ Department of Liberal Arts, Kansai Medical University, Hirakata, Osaka 573

+ Department of Applied Physics, Tokyo University of Agriculture and Technology, Koganei, Tokyo 184

‡ Department of Physics, Osaka University, Osaka 560

Nuclear Engineering Department, Kyushu University, Fukuoka 812

Department of Electric Engineering, Doshisha University, Kyoto 602

to obtain the highly ionized heavy ions at low energies and, therefore, experimental results are particularly scarce for the fully stripped ions. Data up to early 1980 have been compiled³⁾. Presently both theoretical²⁾ and experimental works⁴⁻⁵⁾ are concentrated on investigations of the dependence of the cross sections on the ionic charge of ion q and its nuclear charge Z_1 and on the collision energy. Most of theories predict that the cross sections change monotonically with the ionic charge q and its dependence is given as q^α , α being roughly equal to 2 but slightly depending on the model used, and the cross sections are nearly independent of the collision energy below energies corresponding to the velocity of 1 a.u. with a few exceptions.

Experimental aspects including targets other than atomic hydrogen are reviewed by Salzborn and Müller⁶⁾. Most of the data have been obtained at energies higher than a few keV/amu for partially ionized heavy ions. Again, almost all the experimental data show the monotonic dependence of the cross sections on q . However, there is also experimental evidence that the cross sections do not change monotonically but some bumps or dips exist in some collision systems. For example, Müller⁷⁾ and Crandall et al.⁸⁾ reported the cross sections for Xe^{q+} ions show a significant bump at $q=5$ in collisions with H and Xe targets. Very recently, Bliman et al.⁹⁾ also reported the non-monotonic variation of the cross sections for C^{q+} , N^{q+} , O^{q+} and Ar^{q+} ions incident on D_2 and Ar gas targets at the energies of $1q - 10q$ keV. They concluded that such an oscillatory variation of the cross sections is not due to the presence of the metastable ions but due to the electronic structure of the projectile ions. Similar variations have also been observed by Cocke et al.¹⁰⁾

Meanwhile, Ryufuku, Sasaki and Watanabe (RSW)¹¹⁾, based on their unitarized distorted-wave approximation (UDWA)¹²⁾, predict that such an oscillation of the cross sections at low energies occurs due to the crossings of the diabatic potential curves and that the amplitude of the oscillation is large at lower energies and the oscillation disappears at intermediate energies (≈ 25 keV/amu). They also showed that at low energies the UDWA treatment is equivalent to the classical treatment (see 3.3).

The present paper describes our effort in measuring the cross sections for one-electron capture processes in highly stripped C, N, O, F, Ne and S ions including the fully stripped ions in collisions with He gas target :



at the energy range of $0.5q - 4.0q$ keV. This is, to our knowledge, the first systematic measurements of the cross sections for highly stripped heavy ions with the isoelectronic sequence.

2. Experimental

2.1 Ion source and charge state distribution of ions

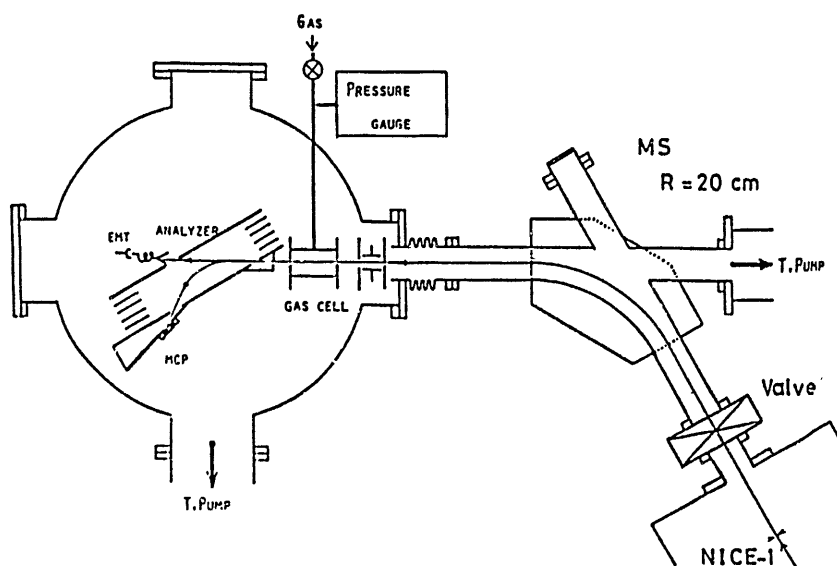


Fig. 1

In the present work, ions are produced in NICE-1¹³⁾, an electron beam type ion source (EBIS), which has a superconducting magnet to confine the high density electron beam. The surface of the superconducting magnet container at liquid He temperature works as a cryogenic pump to reduce background gas pressure in the ionization region. The background pressure measured at the outer vacuum vessel is usually 2×10^{-10} Torr. The present experimental set-up is schematically shown in Fig. 1. Ions, accelerated to a desired energy, are mass-analyzed and injected into a collision chamber. To make separation and identification of the charge and mass of ions easy and sure, the stable isotope gases, ^{13}CO , $^{15}\text{N}_2$ and $^{18}\text{O}_2$, are used for C, N and O ions. Ne and SF_6 gases are used for Ne, F and S ions.

A typical charge state distribution of ^{15}N ions is shown in Fig. 2 which is observed with a continuous electron multiplier (EMT). In contrast to the ordinary EBIS¹⁴⁾, the present NICE-1 is operated in a mode where gas and electron beam are continuous-

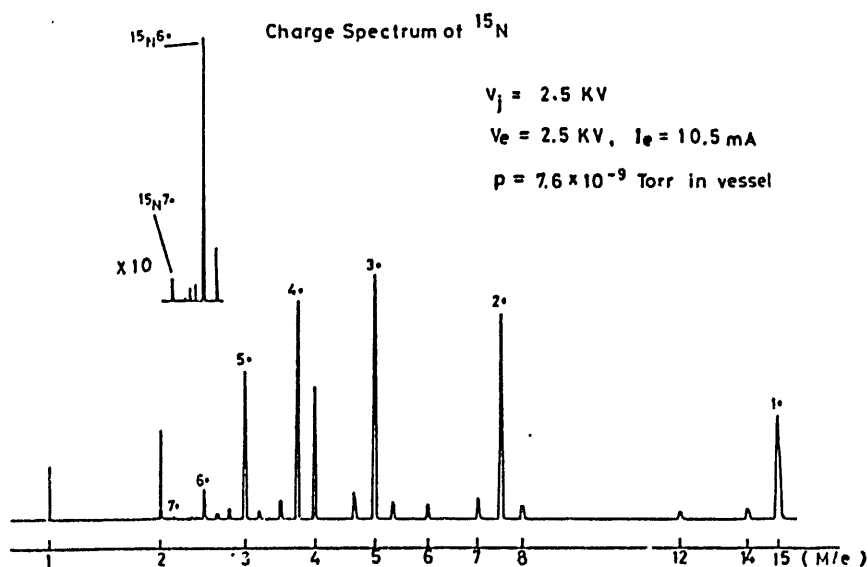


Fig. 2

q \ Z _i	C	N	O	F	Ne	///	S
	6	7	8	9	10	///	16
3	□					///	
4	△	□				///	
5	○	△	□			///	
6	◆	○	△	□		///	
7	-	◆	○	△	□	///	
8	-	-	◆	○	△	///	
9	-	-	-		○	///	
10	-	-	-	-		///	
11	-	-	-	-	-	///	×
///	///	///	///	///	///	///	///
13	-	-	-	-	-	///	□

- ◆ fully stripped ion
- hydrogen-like ion
- △ helium-like ion
- lithium-like ion
- × boron-like ion

Fig. 3

ly supplied¹⁵⁾. Therefore, the charge of ions produced is fairly widely distributed over from $q=1$ to $q=7$ for N ions; their distribution is strongly dependent on the gas pressure in the ion source and the electron energy. The intensity of the fully stripped N^{7+} ions shown in Fig. 2 is typically 2×10^3 counts per second (cps).

Because of such a wide charge distribution, ions with different charge state are obtained without changing the ion source parameters.

2.2 Cross section measurements

To reduce background signals, the present collision chamber is evacuated down to 10^{-8} Torr with a 500 l/s turbo-molecular pump. The target density of the collision cell containing He gas atoms is estimated through the pressure in a gas reservoir measured with a capacitance manometer BAROCELL and the calculated conductance of the capillary-aperture system used. Ions which pass through the collision cell are charge separated with a parallel plate electrostatic analyzer and detected with a multichannel plate detector (MCP) which works in a single particle counting mode. In this detection system, it is assumed that the sensitivity of the MCP is identical for all ions with different charge state because the ion impact energy on the MCP is always higher than a few keV where the coefficient of the secondary electron emission is usually larger than unity. It is found that the pulse height distribution from MCP used is dependent on the count rate. Therefore, in the course of measurements, care is taken to minimize the counting loss due to reduction of the pulse height by monitoring the pulse height distribution from MCP through a multichannel pulse height analyzer and an oscilloscope. The intensity of the primary ion beams is always kept less than 1.5×10^4 cps.

The cross sections for electron capture processes are determined through the initial growth of the charge-changed ions. The errors of the measured cross sections are estimated to be about $\pm 30\%$ where most uncertainties come from the determination of the growth rate, the target thickness and reproducibility.

In Fig.3 is shown a matrix of the ion and charge state which has been investigated in the present work. As seen in Fig.3, we are concentrating ourselves on measurements of the cross sections of the fully stripped, hydrogen-like, helium-like and lithium-like ions.

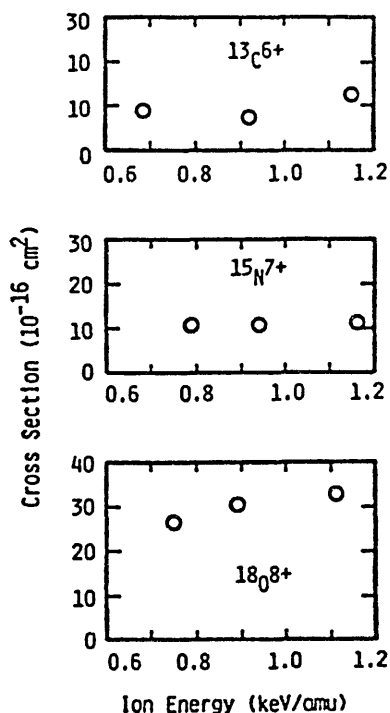


Fig.4

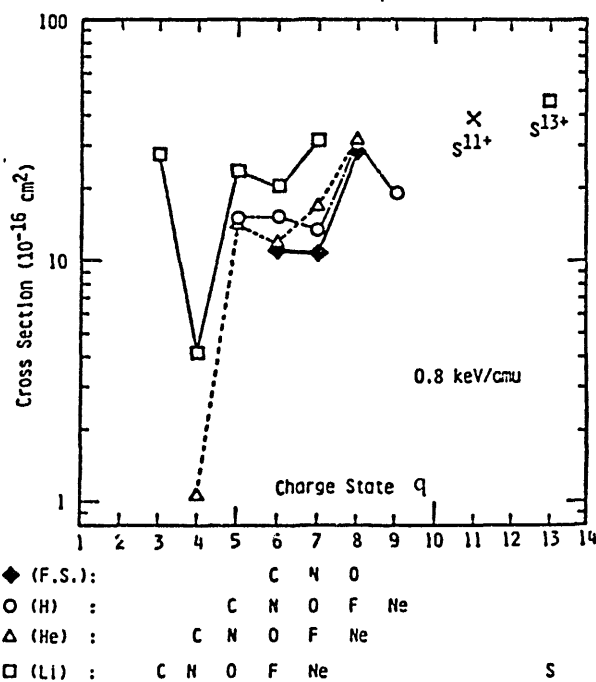


Fig.5

3. Results and discussions

3.1 Energy dependence of the cross sections

As those in previous works, the measured cross sections for one-electron capture of multiply-charged heavy ions are nearly independent of the collision energy over $0.5q - 4.0q$ keV investigated in the present work, except for a few collision systems such as C^{3+} , F^{8+} , Ne^{8+} and S^{13+} ions where the cross sections increase slightly with collision energy. As a typical example, the cross sections for the fully stripped C^{6+} , N^{7+} and O^{8+} ions are shown in Fig.4. Full details of these results will be published elsewhere.

It is found from these data that the cross sections are varied with the charge state q and also with the nuclear charge Z_1 of the projectile ions at the present energy range. The

variation of the cross sections is particularly large for highly stripped low Z_1 ions and seems to be not so simple and monotonic as predicted by theories but depends on both q and Z_1 .

3.2 Ionic charge dependence

In Fig.5 are shown the cross sections at 0.8 keV/amu as a function of the initial charge state for all ions investigated. The lines are drawn to connect the initial charge of the isoelectronic sequence. As seen in Fig.5, the cross sections oscillate strongly with q for all ions. These oscillations are particularly significant at low q . For example, the cross sections for $q=3$ and 5 are almost

one order of the magnitude larger than those for $q=4$. Also the oscillation of the cross sections as a function of q is very similar for ions with different isoelectronic sequence. Further, for the same q , the cross sections depend on the atomic number Z_1 of the projectile ions. These oscillation and variation with q and Z_1 tend to disappear with increasing q and Z_1 . In fact, the measured cross sections in the present work, averaged over the oscillation, are very similar to those obtained from an empirical formula of Müller and Salzborn¹⁶⁾.

3.3 The classical one-electron model with effective charge

As mentioned already, similar oscillations of the cross sections as a function of Z_1 are predicted by RSW¹¹⁾ for the electron capture process between the naked ion and atomic hydrogen where only a single electron is involved. However, in the present case, the target of He has two electrons and the ion, partially ionized, also has a few electrons. Therefore, both nuclei of the target and projectile ion are screened by electrons and, then, the electron involved in the capture process feels a potential by such screened nuclei. The effective core charge, Z_1^* , of the ion, as seen by the electron to be transfer, is not the same as the ionic charge of the ion q .

In order to understand the oscillation phenomena observed in the present work, we follow the classical one-electron model in the electron capture process by RSW with the following modifications :

1. It is assumed that the partially stripped projectile ion consisting of the core with the nuclear charge Z_1 and the screening electrons is equivalent to a naked ion with the effective core charge Z_1^* and the target He atom consists of the hydrogen-like nucleus with the effective charge Z_2^* and an electron which is transferred into the projectile ion.
2. Such a core + electron system behaves hydrogenically, that is, the energy of the level of ion with the effective charge Z^* is given by $-(Z^*)^2/2n^2$ where n is the principal quantum number of the level concerned.
3. The effective charge Z^* of such a partially stripped ion and helium atom is determined through the ionization potential I_g in the ground state (n_g) of the core + electron system :

$$Z^* = n_g (I_g/I_H)^{1/2} \quad (3)$$

where I_H represents the ionization potential of hydrogen atom in the ground state. For He target atom, $Z_2^* = 1.34$.

Then, the level energy for the excited state is calculated as follows :

$$-(Z^*)^2/2n^2 = -I_g n_g^2 / (2n^2 I_H). \quad (4)$$

As the ionization potential I_g of the ground state ion with the nuclear charge Z , empirical values of Lotz¹⁷⁾ are used.

According to the classical one-electron model of RSW, the electron transfer to multiply charge ion at low collision energies occurs when the energy levels of the

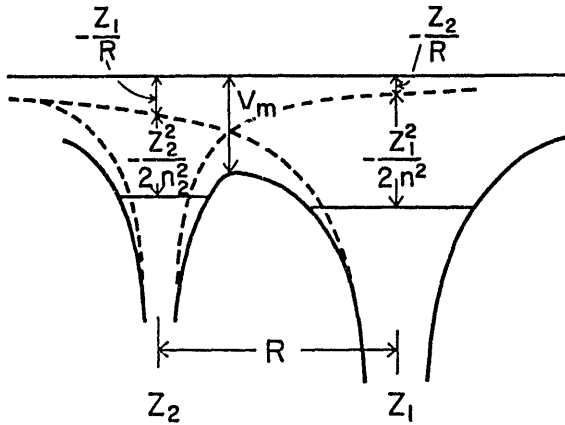


Fig.6

with the effective charge Z_1^* before collision and the right-hand side of eq.(5) does to that in the n_1 state of the projectile ion with the effective charge Z_1^* perturbed by the Coulomb potential of the He^+ ion with the effective charge Z_2^* after collision (see Fig.6).

The electron transfer becomes possible when the diabatic potential energy before collision (the left-hand side of eq.(5)) exceeds the maximum value of the potential barrier formed between the projectile ion and target atom V_m :

$$-Z_1^*/R - (Z_2^*)^2/2n_2^2 \geq -V_m, \tag{6}$$

$$V_m = \{(Z_1^*)^{1/2} + (Z_2^*)^{1/2}\}^2/R. \tag{7}$$

From two equations (5) and (6), the integer n corresponding to the level where the electron is transferred can be determined as follows :

$$n \leq n_1, \tag{8}$$

$$n_1 = (Z_1^*/Z_2^*) \{(Z_2^* + 2(Z_1^*Z_2^*)^{1/2})/(Z_1^* + 2(Z_1^*Z_2^*)^{1/2})\}^{1/2}.$$

Then, the distance R_n , corresponding to the crossing point of the diabatic potential curves, is given by the following equation :

$$R_n = (Z_1^* - Z_2^*) / \{(Z_1^*)^2/2n^2 - (Z_2^*)^2/2n_2^2\}. \tag{9}$$

Therefore, the classical one-electron transfer cross section $\sigma_{q,q-1}$ is given as follows :

$$\sigma_{q,q-1} = (1/2)\pi R_n^2. \tag{10}$$

3.4 Comparison between the measured cross sections and the classical model

In Fig. 7 are shown the measured cross sections plotted as a function of the effective charge Z_1^* calculated from eq.(3), instead of the charge state q, together with those calculated from eq.(10) based on the classical model (dotted line).

The number of n in Fig.7 represents the principal quantum number of the level of the projectile ion into which the electron is captured. It is remarkable that almost all the measured cross sections come close together on a single curve. The oscillation is large for low Z_1^* and tends to vanish for higher Z_1^* . This oscillatory

collision system before and after collision cross diabatically, that is,

$$-Z_1^*/R - (Z_2^*)^2/2n_2^2 = -(Z_1^*)^2/2n_1^2 - Z_2^*/R \tag{5}$$

where R is the nuclear distance between the projectile ion and target atom. In the present case, $n_2=1$ as the electron is in the ground state of He atom.

The left-hand side of eq.(5) corresponds to the diabatic potential energy of electron in the He target with the effective charge Z_2^* perturbed by the Coulomb potential of the projectile ion

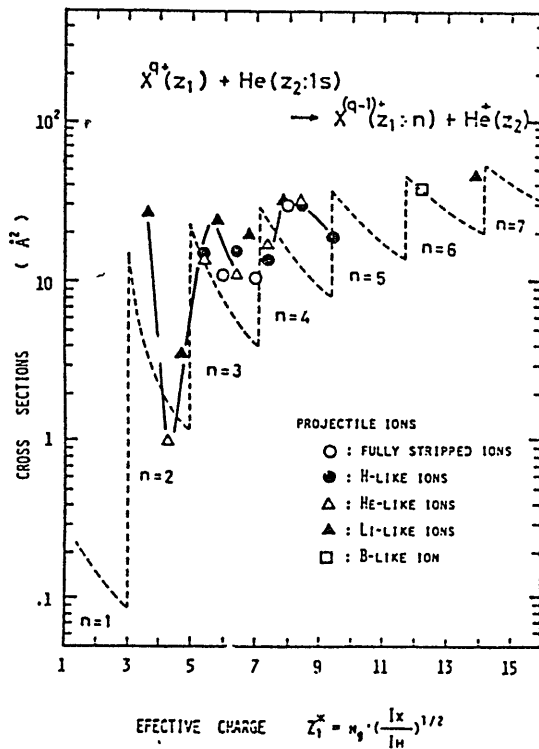


Fig.7

of the effective charges Z_1^* and Z_2^* . In either case, this effect may be large for higher Z_1^* ions.

3. Because the energy level of the excited states is not purely hydrogenic in character, some corrections are necessary to obtain the accurate level energy. These corrections cause the change of the effective charge Z_1^* which, in turn, may give rise to some systematic deviations between different isoelectronic sequences.

In essence, however, the oscillatory behavior of the measured cross sections observed in the present work is a good indication that, in highly stripped heavy ion collision at low energies, the electron is captured dominantly into a particular single level of the projectile ion through the crossing of the diabatic energy levels in the collision system. The oscillation is particularly significant for low Z ions. For low Z ions, the energy level responsible for the electron capture has a small value of n and then the adjacent levels are largely separated. This causes a great increase in the cross section even if the n -value is promoted by one. On the other hand, for high Z ions, the electron is captured into a level having a large n , where the energy levels are densely located, and then more than a single levels have a chance to capture electron from the target atom. This may be a reason why the amplitude of the oscillation in the cross sections tends to diminish toward higher Z ions.

behavior is quite similar to the calculated one, though the agreement in the phase of the oscillation is not so good.

Such a poor agreement in the phase of the oscillation seems to be understandable from the following reasons :

1. In the present classical model, the tunnel effect is neglected and the possibility of the electron being captured into more than a single levels is neglected. If these effects are taken into account, the oscillation should damp.
2. The charge cloud of the target atom and of the partially stripped ion will be deformed during collision because of their finite size of the charge distribution. This polarization effect may result in the change of the electron transfer probability or in the change

4. Conclusions

We have measured the cross sections for one-electron transfer from He atom into highly stripped C^{q+} , N^{q+} , O^{q+} , F^{q+} , Ne^{q+} and S^{q+} ions produced in an electron beam ion source at energies less than 1 keV/amu. The measured cross sections plotted as a function of the ionic charge of ion q show significant oscillations with q which tend to disappear at large q . These oscillations are very similar for ions with different isoelectronic sequence but the observed cross sections are considerably different from each other. On the other hand, when plotted as a function of the effective charge Z_1^* of ion, the cross sections measured come close together on a single curve with an oscillation which is reasonably well reproduced with the classical one-electron model, though their phase of the oscillation is not in good agreement with each other.

In order to understand the oscillatory phenomena in the cross sections for electron transfer processes, measurements of the cross sections for lower Z_1 ions such as B^{q+} , Be^{q+} and Li^{q+} ions seem to be important at the low energy range and also more sophisticated calculations of the cross sections would be of great help.

5. References

- 1) M. P. C. McDowell (ed.), Atomic and Molecular Processes in Controlled Thermonuclear Fusions (Plenum Press, 1979).
- 2) R. E. Olson, Electronic and Atomic Collisions (ed. O. Oda and K. Takayanagi, North-Holland, 1980) p.391.
- 3) Y. Kaneko, T. Arikawa, Y. Itikawa, T. Iwai, T. Kato, M. Matsuzawa, Y. Nakai, K. Okuno, H. Ryufuku, H. Tawara and T. Watanabe, IPPJ-AM-15 (Inst. Plasma Physics, Nagoya Univ., 1980).
- 4) H. J. Kim, R. A. Phaneuf, F. W. Feyer and P. H. Stelson, Phys. Rev. A17,854 (1978).
- 5) L. D. Gardner, J. E. Bayfield, P. M. Koch, I. A. Sellin, D. J. Pegg, R. S. Peterson and D. H. Crandall, Phys. Rev. A21, 1397 (1980).
- 6) E. Salzbom and A. Müller, p.407 in ref.2).
- 7) A. Müller, PhD thesis (Univ. Giessen, 1977).
- 8) D. H. Crandall, R. A. Phaneuf and F. W. Meyer, Phys. Rev. A22,379 (1980).
- 9) S. Bliman, J. Aubert, R. Geller, B. Jacquot and D. van Houffte, Phys. Rev. A23, 1703 (1981).
- 10) C. L. Cocke, R. D. DuBoir, T. J. Gray and E. Justiniano, IEEE NS=28,1032 (1981)
- 11) H. Ryufuku, K. Sasaki and T. Watanabe, Phys. Rev. A21,745 (1980).
- 12) H. Ryufuku and T. Watanabe, Phys. Rev. A19,1538 (1979).
- 13) T. Iwai, Y. Kaneko, S. Ohtani, K. Okuno, N. Kobayashi, S. Tsurubuchi, M. Kimura, H. Tawara and S. Takagi, Proc. Sym. Ion Sources and its Application Technology (ISIAT-81,1981) p.167. Further details will be published soon.
- 14) E. D. Donets, IEEE NS-23,827 (1976).
- 15) H. Imamura, Y. Kaneko, T. Iwai, S. Ohtani, N. Kobayashi, K. Okuno, S. Tsurubuchi, M. Kimura and H. Tawara, Nucl. Instr. Meth. (in press).
- 16) A. Müller and E. Salzbom, Phys. Letters 62A,391 (1977).
- 17) W. Lotz, J. Opt. Soc. Am. 57, 873 (1967).

Cross sections for one-electron capture by highly stripped ions of B, C, N, O, F, Ne, and S from He below 1 keV/amu

T. Iwai,* Y. Kaneko,[†] M. Kimura,[‡] N. Kobayashi,[†] S. Ohtani, K. Okuno,[†]
S. Takagi,[§] H. Tawara,^{||} and S. Tsurubuchi,**

Institute of Plasma Physics, Nagoya University, Nagoya 464, Japan

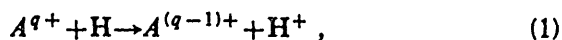
(Received 31 August 1981)

Cross sections for one-electron transfer from a He atom into the fully stripped, hydrogenlike, heliumlike, and lithiumlike B^{q+} , C^{q+} , N^{q+} , O^{q+} , F^{q+} , Ne^{q+} ions, and also highly stripped S^{q+} ions have been measured at the energy range of $1.5q - 3.0q$ keV. The measured cross sections are nearly independent of the collision energy with a few exceptions, and most of the cross sections measured are about $(1 \sim 4) \times 10^{-15}$ cm², but the cross sections for B^{4+} , C^{4+} , and N^{4+} ions are very small in the energy range studied. When the cross sections measured are plotted as a function of the ionic charge q of isoelectronic projectile ions, strong oscillations in the cross sections are observed. As a first approximation, this oscillatory behavior can be explained in terms of the classical one-electron model.

I. INTRODUCTION

The electron capture process by highly stripped ions is currently of great importance not only in basic atomic collision physics but also in such diverse fields as controlled-thermonuclear-fusion research, developments of x-ray laser devices and astrophysics.

In particular, the electron-capture process by highly stripped ions A^{q+} from atomic hydrogen at low energies,



plays a key role in the energy and particle losses from high-temperature plasmas.¹ Because of a simple situation in the collision process of the fully stripped ion, a number of theoretical calculations have been reported.² On the other hand, it is difficult to obtain highly stripped ions at low energies and, therefore, experimental results are scarce for the fully stripped ions.³ Until now, theoretical and experimental works including partially stripped ions have been concentrated on investigations of the dependence of the cross sections on the ionic charge q of the projectile ion and its nuclear charge Z_1 and on the collision energy.

Most of the theories are based on the concept of the quasimolecule $(A-H)^{q+}$ during collisions. Then, the cross sections are mainly determined by interactions at the crossings between the diabatic potential curves of the initial $(A^{q+}-H)$ and the final

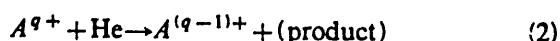
$(A^{(q-1)+}-H^+)$ states. For the high-charge states of projectile ions, there are many curve crossings and it is possible to model the collision processes. These theories predicted that the cross sections change monotonically with the ionic charge q and are proportional to q^α , where α is equal to $1 \sim 2$ dependent on the model used, and that the cross sections are nearly independent of the collision velocity at low and intermediate velocities ($10^6 \sim 10^8$ cm/s). Meanwhile, for the low- q states, several theories showed that the cross sections do not scale according to such a simple rule as q changes. Aside from detailed calculations for the specified collision processes, Ryufuku, Sasaki, and Watanabe (RSW)⁴ predicted a strongly oscillatory dependence of the cross sections on certain effective charges of projectile ions at low and intermediate energies (< 10 keV/amu) using a model in which the projectiles are replaced by bare nuclei having the effective charges. They also showed the oscillation disappears at higher energies.

Experimental aspects including target atoms other than atomic hydrogen have been reviewed by Salzborn and Müller.⁵ Most of the data have been obtained for partially stripped ions at energies higher than a few keV/amu. Almost all the experimental data show the monotonic dependence of the cross sections on q . However, there are experimental evidences that in some collisions cross sections do not change monotonically, but some bumps or dips exist. As for the H target atom, for example,

Crandall *et al.*^{6,7} and Gardner *et al.*⁸ reported that the cross sections for C, N, O, F, and Xe ions show significant bumps at $q=3$ and 5 in the keV/amu energy region; Phaneuf reported very recently that the cross sections for C ions show neither monotonic change with q nor uniform velocity dependence below 500 eV/amu.⁹ Recently, Bliman *et al.*¹⁰ reported the nonmonotonic variation of the cross sections for C, N, O, and Ar ions incident on D₂ and Ar gas targets in the energy range of $1q \sim 10q$ keV. They concluded that such an oscillatory behavior of the cross sections is not due to the presence of metastable projectile ions but due to the electronic structure of the ions. Similar oscillations were observed by Cocke *et al.*¹¹ Mann *et al.*¹² also reported that the cross sections for the one-electron capture by highly stripped heavy ions change drastically in the magnitude with the ionization potential of the target atoms.

The helium atom, among others, is an interesting target atom, because its electronic structure is simple enough to treat theoretically, and because it is easily prepared as a target atom in collision experiments. The electron-capture process by highly stripped ions from He atom has been studied experimentally by several authors¹³⁻¹⁹. Zwally *et al.*^{15,16} measured the cross sections of one-electron capture for C⁴⁺ and B³⁺ ions in the wide energy range of 0.3~40 keV. Crandall¹⁸ and Gardner *et al.*¹⁹ measured the cross sections of one-electron capture for the He-like and the Li-like ions such as B^{q+}, C^{q+}, N^{q+}, and O^{q+} ions in the energy range of $6q \sim 23q$ keV, and observed the nonmonotonic variation with the charge state q . They also measured the cross section of two-electron capture and found that this cross section becomes greater than that of one-electron capture for the C⁴⁺ ion as the collision energy is reduced. No measurement of the cross sections, however, was reported for fully stripped ions or the H-like ions except for B⁴⁺ at low energies.²⁰

The present paper describes our effort in measuring the cross sections of one-electron capture for highly stripped B, C, N, O, F, Ne, and S ions including the fully stripped ions in collision with helium target,



at the collision energies below $3.0q$ keV. This is, to our knowledge, the first systematic measurement of the one-electron-capture cross section for highly stripped ions with the isoelectronic sequence.

II. EXPERIMENTAL TECHNIQUE

A. Ion source and experimental setup

The ion source in the present work, called NICE-1, is an electron-beam-ion source (EBIS) originally developed by Donets.²¹ The ions are produced by a high-density electron beam confined by a strong magnetic field applied along the electron-beam axis.

The NICE-1 has a superconducting magnet (SCM) for generating a strong and stable magnetic field; the solenoid made of Nb-Ti is 100 cm in length and 10 cm in inside diameter (i.d.); the magnetic field can be varied up to 2 T; a persistent current-mode operation is chosen. A surface of the liquid-helium reservoir for the SCM works as a cryogenic pump to reduce the background gas pressure in the ionization region. An electron beam is extracted from a thoriated tungsten hair-pin-type gun and passes through an anode hole of 2 mm in radius and the subsequent 14 pieces of drift tubes of 3 cm in i.d. surrounded by the liquid-helium reservoir. A very small amount of gases is injected through a gap between the first and second drift tubes. Ions produced by electron impacts are trapped radially by the space-charge potential of the electron beam and axially by the potential barriers applied to the drift tubes. The step-by-step ionization of the trapped ions proceeds by successive electron bombardments. The diameter of the electron beam was not measured directly, but is estimated to be less than 0.5 mm. After passing through the drift tubes, the electron beam is received by an electron collector shielded from the magnetic field by a soft-iron plate and a μ -metal cylinder. A typical electron current is 15 mA at 2 kV and 1.2 T. The background gas pressure measured at the vacuum vessel of the NICE-1 is usually 2×10^{-10} Torr. Then the residual gas pressure in the ionization region is expected to be much less than 1×10^{-10} Torr. Such an ultrahigh vacuum is essentially important for producing the fully stripped ions. For the fully stripped C⁶⁺, N⁷⁺, and O⁸⁺ ions, stable isotope gases ¹³CO, ¹⁵N₂, and ¹⁸O₂ are used to separate from impurity ions having $M/q=2$. BF₃, Ne, and SF₆ gases are used for B, Ne, F, and S ions.

The present experimental setup is schematically shown in Fig. 1. Ions extracted from the source are accelerated to a desired energy. An ion beam, formed after passing through an einzel lens and a pair of quadrupole lenses, is mass analyzed with a

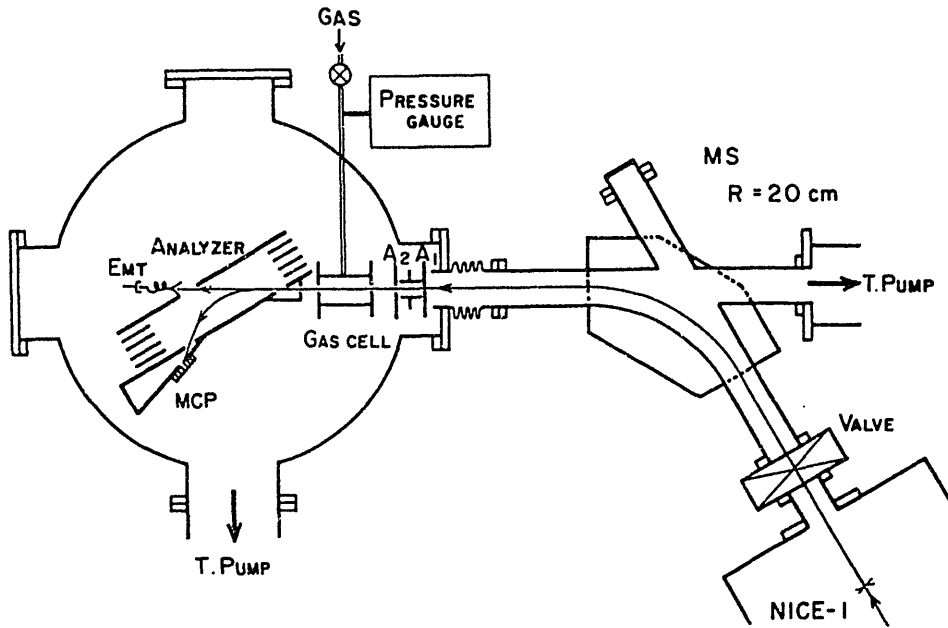


FIG. 1. Schematic view of the apparatus.

60° sector of 20-cm radius and injected into a collision cell. The ion beam is well collimated by a pair of beam-defining apertures of 1 mm diam A_1 and A_2 ; the distance between A_1 and A_2 is 5 cm and A_2 is placed 4 cm in front of the gas cell. The gas cell is 2 cm in length and its entrance and exit apertures are 0.8 and 1 mm in diameter, respectively. Ions which pass through the cell are charge separated with a parallel plate electrostatic analyzer located 1 cm behind the cell; the entrance and exit apertures of the analyzer plate are 5 mm in width and 8 mm in height. By changing the voltage applied to the analyzer, both the primary A^{q+} ions and the charge-changed $A^{(q-1)+}$ ions are detected with the same microchannel plate detector (MCP, HTV F1158) in a single-counting mode. Another detector, a continuous electron multiplier (EMT), aligned to the ion-beam axis, is used to identify the charge and mass of the primary ion. In order to reduce background signals, the pressure outside the collision cell is kept below 2×10^{-8} Torr with a 500-l/s turbomolecular pump. Figure 2 shows a typical charge-state spectrum of ^{15}N at the acceleration voltage of 2.5 kV. In contrast to the ordinary EBIS operation,²¹ the NICE-1 is operated in a mode where gas atoms to be ionized and the electron beam are continuously supplied.²² Therefore the charge of ions produced is widely distributed over from $q=1$ to 7 for N ions; their distribution is strongly dependent on the gas pressure in the ion

source and the electron energy. The intensity of the fully stripped N^{7+} ions shown in Fig. 2 is typically 2×10^3 counts per s (cps). Because of such a wide charge distribution, ions with different charge state are obtained without changing the ion source parameters.

The He target gas is introduced through a stainless-steel tubing from a cylinder containing He of high purity (99.999%). In order to avoid any contamination with impurities, the tubing is carefully connected and preheated.

B. Measurement of cross sections

1. Determination of cross sections

Cross section for the one-electron-capture process $\sigma_{q,q-1}$ is determined by

$$\sigma_{q,q-1} = \frac{\alpha_q S_{q-1}}{\alpha_{q-1} S_q N L}, \quad (3)$$

where S_q is the count rate for the primary A^{q+} ions, S_{q-1} for the charge-changed $A^{(q-1)+}$ ions, N the number density of the target He atom, L the collision-path length, and α_q and α_{q-1} are the detection efficiencies for the A^{q+} and $A^{(q-1)+}$ ions. In the present detection system, we assumed that the detection efficiency of the MCP is identical for all the ions with different charge states, that is,

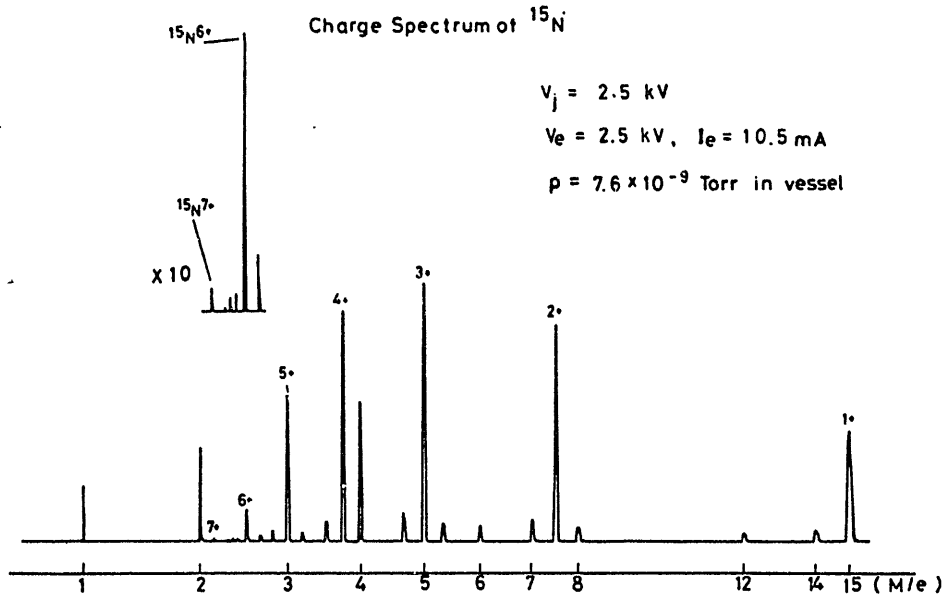


FIG. 2. Typical spectrum of the charge-state distribution of $^{15}\text{N}^{q+}$ ions extracted at 2.5 kV from the NICE-1 under the condition that the electron beam intensity is 10.5 mA at 2.5 kV. Ion detection is made by the EMT shown in Fig. 1.

$\alpha_q = \alpha_{q-1}$, because the ion impact energy on the MCP is always higher than a few keV where the coefficient of the secondary electron emission is usually larger than unity.

It is found that the pulse-height distribution from the MCP used is nearly independent of the ion impact energy for all the charge states, but dependent on the charge state and the count rate. The maximum of the pulse-height distribution shifts towards higher values as the charge state increases, and the pulse-height distribution becomes broader and its maximum shifts towards lower values as the count rate increases. Therefore, for each experimental run, care is taken to minimize the counting loss due to reduction of the pulse height by monitoring the pulse-height distribution from the MCP with a multichannel pulse-height analyzer and an oscilloscope. The count rate of the primary ion beam is always kept less than 5×10^3 cps. Spatial detection efficiency of the MCP used is checked by varying the analyzer voltage, and is confirmed to be fairly uniform over the detection area within the limits of stabilities of incident ion beams.

The target density N in the gas cell is determined by the use of the calculated conductance of the capillary tube and cell apertures and by measurements of the pressure in the He gas reservoir with a capacitance manometer (BAROCELL). Details of the determination have been described in Ref. 23. The collision-path length L is assumed to be the

distance between the apertures of the cell which is 2 cm.

Actually, cross sections for the one-electron-capture process are determined through the initial growth of the charge-changed $A^{(q-1)+}$ ions. This procedure is illustrated in Fig. 3 as an example, which shows the count rate for the primary N^{7+} ions and charge-changed N^{6+} ions as a function of the target thickness NL . At first, the analyzer voltage is set for the primary ions to impact on the MCP while the collision cell is evacuated, and then

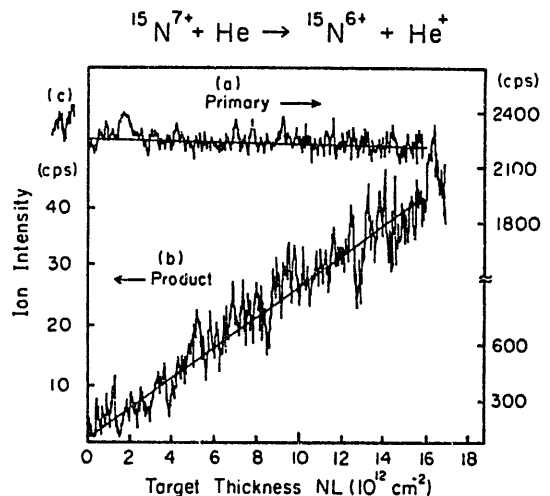


FIG. 3. Growth-rate curve of the charge-changed N^{6+} ion for the primary N^{7+} ion. See text for detail.

the target He gas is introduced into the cell until a few % reduction of the count rate of the primary ions is observed [part (a) in Fig. 3]. Secondly, the analyzer voltage is set for the charge-changed ions and the target gas pressure is reduced continuously [part (b) in Fig. 3]. Finally, the analyzer voltage is returned for the primary ions in order to check the reproducibility of the count rate of the primary ions [part (c) in Fig. 3]. Then the cross section can be determined from the slope of the growth-rate curve. This procedure has four advantages at least. First, it is easy and sure to check for single-collision conditions, which are necessary to apply Eq. (3), by directly observing the linearity of the growth-rate curve. Second, background noise signals are readily subtracted from the count rate of the charge-changed ions S_{q-1} which is usually several tens cps when S_q is of the order of 10^3 cps. Third, it is very useful to reduce statistical errors, because the continuous variation of the target thickness corresponds to average out a lot of point-to-point measurements. Fourth, the identification of the primary ions, which is usually not so easy because of the presence of impurity ions in the primary beam, can be reconfirmed by the analyzer potentials to be applied for the A^{q+} and $A^{(q-1)+}$ ions.

2. Uncertainties

Most of uncertainties come from the stability of the primary ion beam, determination of the slope of the growth-rate curve and of the target thickness. The uncertainty in the stability of the primary ion beam is estimated to be less than $\pm 8\%$. The uncertainty associated with determination of the slope of the growth-rate curve is less than $\pm 20\%$. Determination of the target thickness involves about $\pm 10\%$ uncertainty as estimated in the previous work.²³ Further uncertainty arises from the dependence of counting efficiency of the detector on the ionic charge state and count rate. This uncertainty, however, is elaborately reduced as mentioned in Sec. II B, and estimated at $\pm 5\%$. The total uncertainty for the absolute value of the cross section therefore is estimated to be about $\pm 30\%$ in quadrature sum except for the uncertainty in the primary ion-beam purity. All ions studied are completely separated and well identified by the use of stable isotopes. However, we cannot say whether the primary ions are extracted in their ground state although it is said that an EBIS-type ion source produces few ions in the metastable states.²⁴

III. RESULTS AND DISCUSSION

A. General results and comparison with others

Table I presents the measured cross sections for the one-electron capture by highly stripped B, C, N, O, F, Ne, and S ions together with total uncertainties. In general, most of the cross sections measured are about $1\sim 4 \times 10^{-15}$ cm² in the collision energy range of 1.5q ~ 3.0q keV investigated in the present work. However, it is quite remarkable that the cross sections obtained for B^{4+} , C^{4+} , and N^{4+} ions are anomalously small. The measured cross sections are nearly independent of the collision energy, though the present energy range is rather narrow. Some cross sections, however, increase with the collision energy in such collisions as B^{4+} , C^{3+} , F^{8+} , Ne^{8+} , and S^{13+} -He systems.

There are several groups which have studied experimentally the A^{q+} -He system. All of the present data are illustrated in Figs. 4(a)–4(g) for comparison with others. Owing to the different energy range studied, the present data cannot be compared directly to others except for the data of Zwally *et al.* Nikolaev *et al.*¹⁴ reported the cross sections $\sigma_{q,q-1}$ for the fully stripped B^{5+} ion, the H-like B^{4+} and N^{6+} ions, the He-like B^{3+} , C^{4+} , N^{5+} , and O^{6+} ions, and the Li-like B^{2+} , C^{3+} , N^{4+} , and O^{5+} ions. Their data, however, were obtained in the energy range about 100 times as high as the present ones; in their energy range $\sigma_{q,q-1}$ sharply decreases with the collision energy; their data are not shown in Fig. 4. Crandall¹⁸ and Gardner *et al.*¹⁹ obtained their data at energies a few times as high as the present ones. In their energy range, most of the cross sections are nearly independent of energy. As seen in Figs. 4(a)–4(d), rough extrapolation of their data indicates that the present data seem to be in fairly good agreement with theirs for the $B^{3,4+}$, $C^{3,4+}$, $N^{4,5+}$, and $O^{5,6+}$ ions which are the only ionic species available for comparison. Data of Zwally and Koopman¹⁵ for the C^{4+} ion and of Zwally and Cable¹⁶ for the B^{3+} ion, which can be directly compared with ours, are in good agreement with the present data as seen in Figs. 4(a) and 4(b). As for the fully stripped C^{6+} , N^{7+} , and O^{8+} ions, the present data are compared with the results of Afrosimov *et al.*²⁰ Though the collision energy range tested is different, both data seem to be smoothly connected with each other.

It is found from the present data that the cross sections $\sigma_{q,q-1}$ vary with the ionic charge q drastically and also with nuclear charge Z_1 of projectile

TABLE I. One-electron-capture cross sections $\sigma_{q,q-1}$ for the highly stripped ion from He at collision energy E .

Ion	E (keV/amu)	$\sigma_{q,q-1}$ (10^{-16} cm 2)	Ion	E (keV/amu)	$\sigma_{q,q-1}$ (10^{-16} cm 2)
B^{3+}	0.44	12.2 \pm 2.4	O^{5+}	0.47	22.7 \pm 4.5
	0.55	17.3 \pm 3.5		0.63	25.1 \pm 5.0
	0.68	13.2 \pm 2.6		0.78	23.9 \pm 4.8
	0.82	14.6 \pm 2.9	O^{6+}	0.56	9.0 \pm 1.8
B^{4+}	0.58	0.92 \pm 0.28		0.75	11.6 \pm 2.3
	0.73	1.36 \pm 0.41		0.94	12.1 \pm 2.4
	0.91	1.53 \pm 0.47	$^{18}O^{7+}$	0.58	12.3 \pm 2.5
	1.09	2.87 \pm 0.86		$^{16}O^{7+}$	0.66
B^{5+}	0.73	8.4 \pm 1.7		0.88	12.8 \pm 2.6
	0.91	8.3 \pm 1.7	1.09	14.6 \pm 2.9	
	1.14	11.6 \pm 2.3	$^{18}O^{8+}$	0.76	27.3 \pm 5.5
	1.36	9.2 \pm 1.8		0.89	30.6 \pm 6.1
C^{3+}	0.38	14.7 \pm 2.9		1.11	34.4 \pm 6.9
	0.50	18.8 \pm 2.9	F^{6+}	0.54	18.5 \pm 3.7
	0.63	22.5 \pm 4.5		0.63	18.8 \pm 3.8
C^{4+}	0.50	0.85 \pm 0.26		0.79	19.4 \pm 3.9
	0.67	1.72 \pm 0.52	F^{7+}	0.63	16.2 \pm 3.2
	0.83	1.16 \pm 0.35		0.74	17.6 \pm 3.5
C^{5+}	0.63	15.2 \pm 3.0		0.92	21.7 \pm 4.3
	0.83	14.8 \pm 3.0	F^{8+}	0.72	26.7 \pm 5.3
	1.04	14.2 \pm 2.8		0.84	30.4 \pm 6.1
$^{13}C^{6+}$	0.69	9.0 \pm 1.8		1.05	34.5 \pm 6.9
	0.92	7.9 \pm 1.6	$^{20}Ne^{7+}$	0.53	30.4 \pm 6.1
	1.15	13.2 \pm 2.6		$^{22}Ne^{7+}$	0.64
N^{4+}	0.43	3.0 \pm 0.9		0.80	32.2 \pm 6.4
	0.57	3.7 \pm 1.1	$^{20}Ne^{8+}$	0.60	28.0 \pm 5.6
	0.71	3.5 \pm 1.1		$^{22}Ne^{8+}$	0.73
N^{5+}	0.54	13.4 \pm 2.7		0.91	33.9 \pm 6.8
	0.71	16.8 \pm 3.4	$^{20}Ne^{9+}$	0.77	18.1 \pm 3.6
	0.89	14.4 \pm 2.9		0.90	20.1 \pm 4.0
$^{15}N^{6+}$	0.68	14.2 \pm 2.8		1.13	19.3 \pm 3.9
	0.80	15.5 \pm 3.1	S^{11+}	0.58	40.2 \pm 8.0
	1.00	15.0 \pm 3.0		0.69	37.7 \pm 7.5
$^{15}N^{7+}$	0.78	10.5 \pm 2.1		0.86	37.5 \pm 7.5
	0.93	10.9 \pm 2.2	S^{13+}	0.69	44.8 \pm 9.0
	1.17	11.9 \pm 2.4		0.81	45.3 \pm 9.1
		1.02		50.5 \pm 10.1	

ions at the present energy range. The variation of the cross sections is enhanced for highly stripped

low- Z_1 ions and is not simple and monotonic as q changes, but really depends on both q and Z_1 .

B. Ionic charge dependence

In Fig. 5 are shown the cross sections reasonably interpolated at 0.8 keV/amu as a function of the initial charge state q for all ions investigated. The lines are drawn to connect data for ions having the same isoelectronic sequences such as fully stripped, H-like, He-like, and Li-like ions. As seen in Fig. 5, the cross sections oscillate strongly with q for all ions. These oscillations are particularly significant at low q . For example, the cross sections for $q=3$ and 5 are almost one order of magnitude larger than those for $q=4$. Furthermore, for the same q , the cross sections depend on the atomic number Z_1 of

the projectile ions. These oscillations with q and variations with Z_1 tend to disappear with increasing q and Z_1 . In fact, when the oscillation of the measured cross sections in the present work is smoothed out, the q dependence is quite similar to that obtained from an empirical formula of Müller and Salzborn,²⁵ which is shown as a dotted line in Fig. 5.

C. Classical one-electron model with effective charge

Few theoretical studies have been made on the electron-capture process for A^{q+} -He collisions.

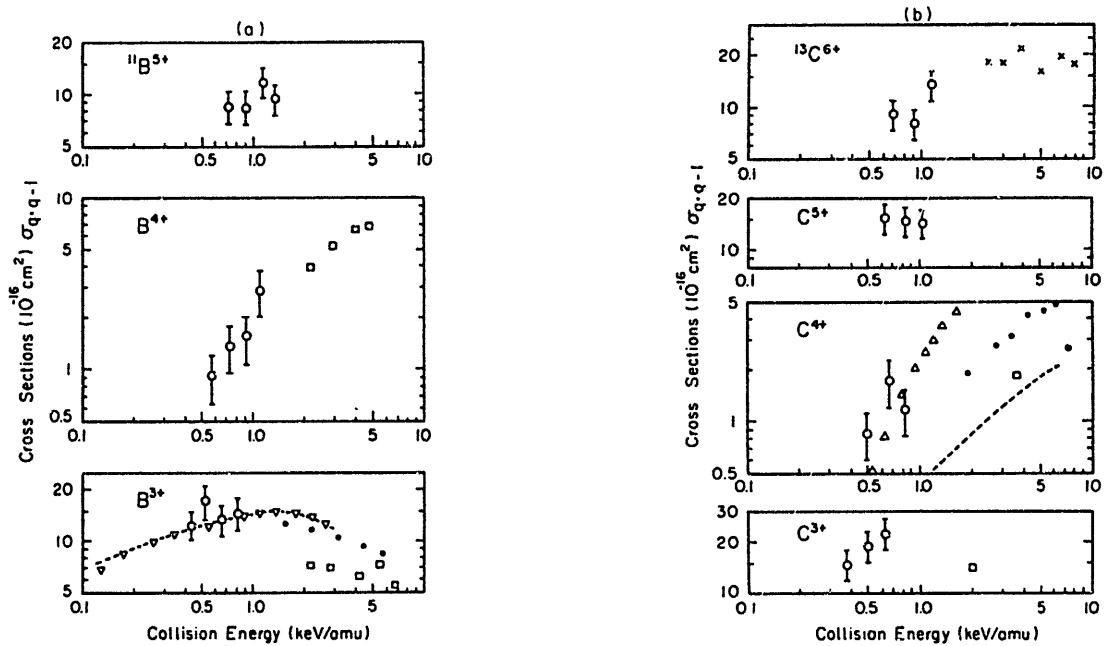


FIG. 4. (a) Cross section of one-electron capture by B^{3+} , B^{4+} , and B^{5+} ions incident on He. Open circles are the present data, triangles the data of Zwally and Cable (Ref. 16), solid circles the data of Crandall (Ref. 18), squares the data of Gardner *et al.* (Ref. 19). Dashed line is the theoretical result of Shipsey *et al.* (Ref. 26). (b) Cross sections of one-electron capture by C^{3+} , C^{4+} , C^{5+} , and C^{6+} ions incident on He. Open circles are the present data, triangles the data of Zwally and Koopman (Ref. 15), solid circles the data of Crandall (Ref. 18), squares the data of Gardner *et al.* (Ref. 19), crosses the data of Afrosimov *et al.* (Ref. 20). Dashed line is the theoretical result of Shipsey *et al.* (Ref. 26). (c) Cross sections of one-electron capture by N^{4+} , N^{5+} , N^{6+} , and N^{7+} ions incident on He. Open circles are the present data, solid circles the data of Crandall (Ref. 18), squares the data of Gardner *et al.* (Ref. 19), crosses the data of Afrosimov *et al.* (Ref. 20). (d) Cross sections of one-electron capture by O^{5+} , O^{6+} , O^{7+} , and O^{8+} ions incident on He. Open circles are the present data, solid circles the data of Crandall (Ref. 18), squares the data of Gardner *et al.* (Ref. 19), crosses the data of Afrosimov *et al.* (Ref. 20). (e) Cross sections of one-electron capture by F^{6+} , F^{7+} , and F^{8+} ions incident on He. (f) Cross sections of one-electron capture by Ne^{7+} , Ne^{8+} , and Ne^{9+} ions incident on He. (g) Cross sections of one-electron capture by S^{11+} and S^{13+} ions incident on He.

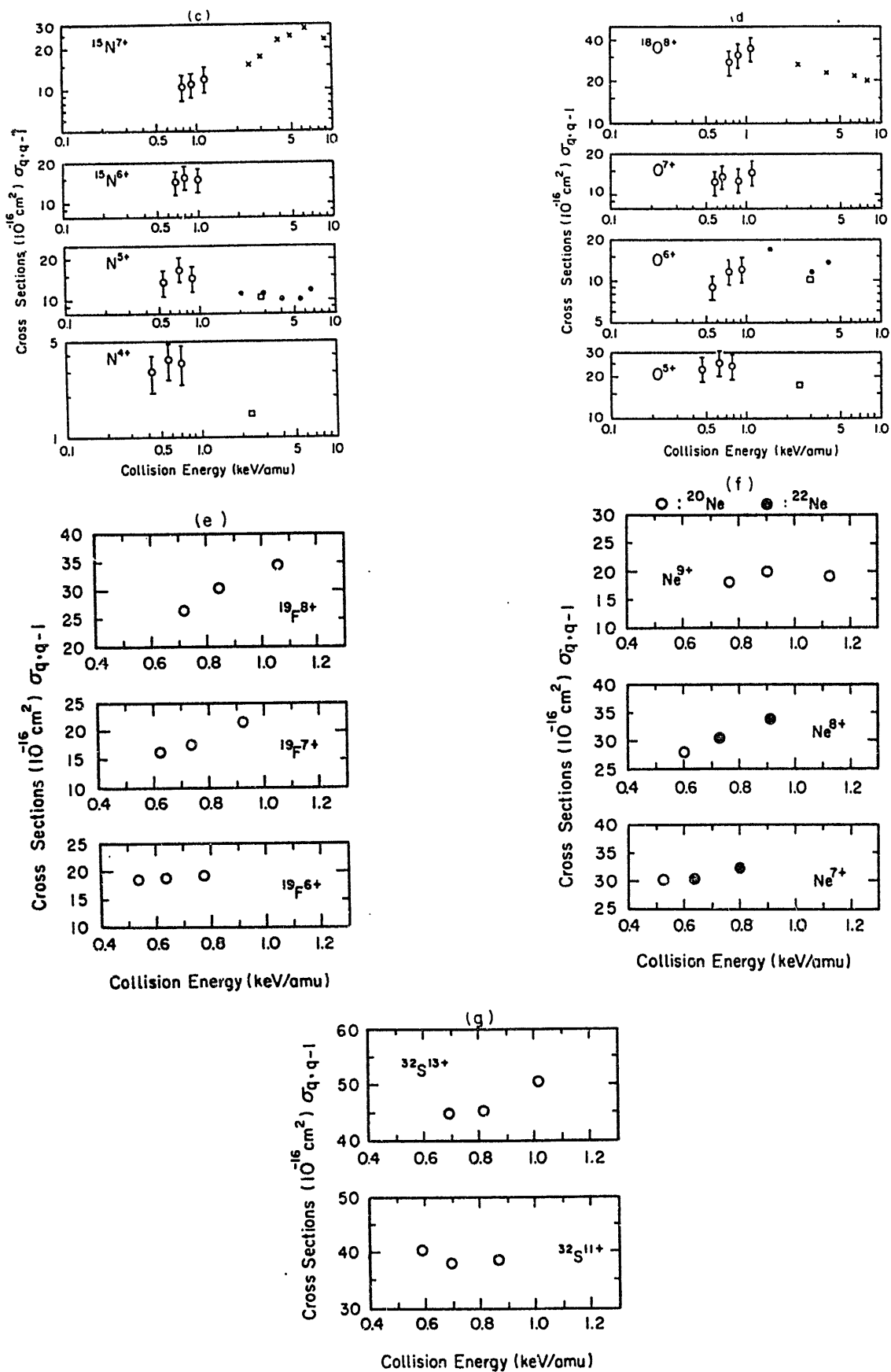


FIG. 4. (Continued.)

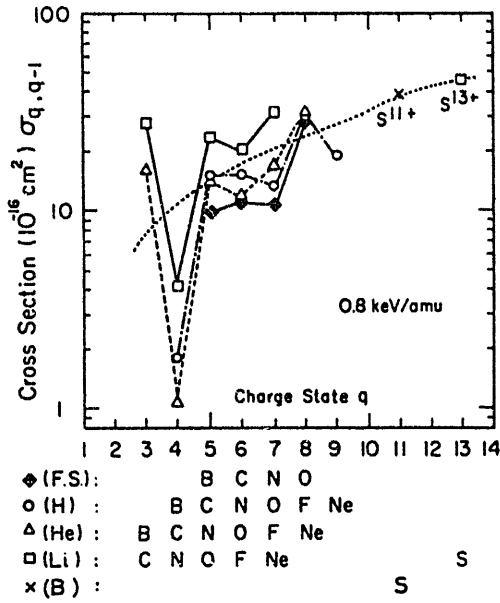


FIG. 5. Measured cross sections $\sigma_{q,q-1}$ at 0.8 keV/amu as a function of the ionic charge q of projectile ions. The dotted line is obtained from the empirical formula of Müller and Salzborn (Ref. 25).

Shipsey *et al.*²⁶ calculated the cross sections for B^{3+} - and C^{4+} -He collisions by the use of the molecular-orbital method, and their results for the one-electron-capture process are shown as dashed lines in Figs. 4(a) and 4(b). Their results agree with the present data and those of Zwally and Cable¹⁶ for B^{3+} ions, but their cross sections are somewhat smaller than the experimental results for C^{4+} ions. Except for their calculations, there has been neither detailed calculation of individual collision processes nor overall treatment for better understanding of the A^{q+} -He collision systems systematically.

As mentioned in Sec. I, similar oscillations of the cross sections were predicted by RSW⁴ as a function of the effective charge of projectiles for the A^{q+} -H collisions. Their calculation is based upon the unitarized-distorted-wave approximation²⁷ (UDWA), but they also showed that the UDWA treatment becomes equivalent to the classical treatment at low energies. Hence, as a first approximation, we adopt a classical one-electron model in the sense of RSW in order to understand the oscillation phenomena observed in the present work.

In the classical one-electron model, the projectile ions are replaced by bare nuclei having the effective charge Z_1^* and the He atom is replaced by the system of a bare nucleus having the effective charge Z_2^* plus one electron which is to be transferred into the projectile ion. Such a bare nucleus plus one-

electron system behaves hydrogenically, that is, its energy level is given by $-(Z^*)^2/2n^2$, where n is the principal quantum number of the level concerned. The effective charge Z^* is determined from the ionization potential I_g of the ground state (n_g) of the system

$$Z^* = n_g (I_g / I_H)^{1/2}, \quad (4)$$

where I_H is the ionization potential of the H atom. As the ionization potential I_g , empirical values of Lotz²⁸ are used. Then, the energy level of the excited state (n) is calculated by

$$\frac{-(Z^*)^2}{2n^2} = \frac{-I_g n_g^2}{(2n^2 I_H)}. \quad (5)$$

According to the classical one-electron model, the electron transfer from He atom to projectile ions occurs when the energy levels of the collision system before and after collision coincide diabatically with each other, that is, the quaresonance condition is fulfilled:

$$\frac{-Z_1^*}{R} - \frac{(Z_2^*)^2}{2n_2^2} = \frac{-(Z_1^*)^2}{2n_1^2} - \frac{Z_2^*}{R}, \quad (6)$$

where R is the internuclear distance between projectile ion and the target He atom. The left-hand side of Eq. (6) corresponds to the diabatic potential energy of the n_2 state of the target He atom perturbed by the Coulomb potential of the projectile ion before collision, and the right-hand side of Eq. (6) does to that of the n_1 state of the projectile ion plus one electron perturbed by the Coulomb potential of the He⁺ ion after collision. In the present case, $n_2 = 1$ since the electron is in the ground state of the He atom.

The solution R in Eq. (6) gives the crossing point of the two diabatic potential curves. There are many possible crossing points corresponding to many different n_1 states into which the electron is to be transferred. According to the classical model, however, the electron transfer becomes possible when the diabatic potential energy before collision exceeds the maximum value of the potential barrier $-V_m$ formed between the projectile ion and the target atom:

$$\frac{-Z_1^*}{R} - \frac{(Z_2^*)^2}{2n_2^2} \geq -V_m. \quad (7)$$

and

$$V_m = [(Z_1^*)^{1/2} + (Z_2^*)^{1/2}]^2 / R. \quad (8)$$

From Eqs. (6) and (7), the integer n corresponding to the state where the electron can be transferred is

determined as follows:

$$n \leq n_1, \quad (9)$$

where

$$n_1 = \left[\frac{Z_1^*}{Z_2^*} \right] \left[\frac{[Z_2^* + 2(Z_1^* Z_2^*)^{1/2}]}{[Z_1^* + 2(Z_1^* Z_2^*)^{1/2}]} \right]^{1/2}. \quad (10)$$

Then the distance R_n where one-electron transfer takes place is given by

$$R_n = \frac{(Z_1^* - Z_2^*)}{[(Z_1^*)^2/2n^2 - (Z_2^*)^2/2n^2]}. \quad (11)$$

Assuming the probability of one-electron transfer to be $\frac{1}{2}$, the classical cross section $\sigma_{q,q-1}$ is given as

$$\sigma_{q,q-1} = \left(\frac{1}{2}\right) \pi R_n^2. \quad (12)$$

D. Comparison between the measured cross sections and the classical model

Figure 6 shows the measured cross sections at 0.8 keV/amu plotted as a function of the effective charge Z_1^* derived from Eq. (4) together with those calculated from Eq. (12) based on the classical one-electron model (dotted curve). The number of n in

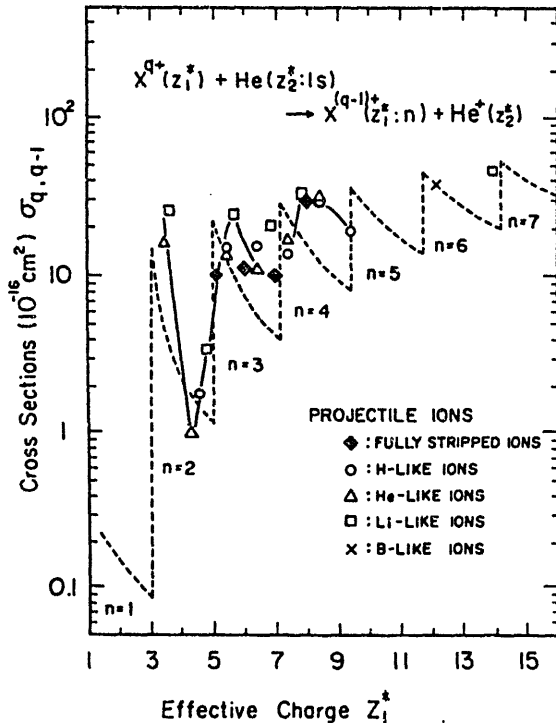


FIG. 6. Comparison of the measured cross sections at 0.8 keV/amu with the cross sections calculated in terms of the classical one-electron model shown as the dotted curve. Cross sections are plotted as a function of the effective charge Z_1^* of projectile ions.

Fig. 6 represents the principal quantum number of the level of the ion (projectile plus one electron) into which the electron is captured. It is noted that almost all the measured cross sections come together on a single curve. The oscillation is enhanced for low- Z_1^* ions and tends to vanish for high- Z_1^* ions. This oscillatory behavior is similar to the calculated one, though the agreement in the phase of the oscillation is not so good. Since the present calculation based on the classical model is very crude, the poor agreement between the calculation and the experimental results is not surprising. The discrepancy is partly due to neglect of the tunnel effect, neglect of the polarization effect, and so on.

In essence, however, the oscillatory behavior of the cross sections observed in the present work is a good indication that in highly stripped ion collisions at low energies, the electron is captured selectively into the level with a particular quantum number n in the collision system. The observed oscillation is significant for low- Z_1^* ions. For low- Z_1^* ions, the energy level into which the electron is transferred has a small value of n , and then its adjacent levels are largely separated. This causes a significant change in the cross section if the n value changes from n to $n+1$. On the other hand, for high- Z_1^* ions, the electron is captured into a level having a large n around which a number of energy levels are densely located. This gives rise to a minor change in the cross section if n is changed by one, and more than a single level may have a chance to capture one electron from the target atom. These should be reasons why the amplitude of the oscillation in the cross section tends to diminish towards higher- Z_1^* ions.

Such an oscillatory behavior should be dependent on the collision energy. The data of Gardner *et al.*,¹⁹ which were obtained at energies a few times as high as the present energy range, show oscillations around $q=4$ for B^{q+} , C^{q+} , and N^{q+} ions, but the amplitude of their oscillation is smaller than the present one. The present classical model is essentially independent of energy. More sophisticated calculations would be desired.

ACKNOWLEDGMENTS

This work was carried out as a part of the Guest Research Program at the Institute of Plasma Physics, Nagoya University. The authors are grateful to Professor H. Kakihana, Director of the Institute, and to Emeritus Professor K. Takayama, the former Director of the Institute, for their encouragement throughout this work.

- *Permanent address: Department of Liberal Arts, Kansai Medical University, Hirakata, Osaka 573, Japan.
- †Permanent address: Department of Physics, Tokyo Metropolitan University, Setagaya-ku, Tokyo 158, Japan.
- ‡Permanent address: Department of Physics, Osaka University, Toyonaka, Osaka 560, Japan.
- §Permanent address: Department of Electric Engineering, Doshisha University, Kyoto 602, Japan.
- ||Permanent address: Nuclear Engineering Department, Kyushu University, Fukuoka 812, Japan.
- **Permanent address: Department of Applied Physics, Tokyo University of Agriculture and Technology, Koganei, Tokyo 184 Japan.
- ¹*Atomic and Molecular Processes in Controlled Thermonuclear Fusion*, edited by M. P. C. McDowell (Plenum, New York, 1979).
- ²Progress in theories is summarized by R. E. Olson, in *Electronic and Atomic Collisions*, edited by N. Oda and K. Takayanagi (North-Holland, Amsterdam, 1980), p. 391.
- ³Experimental data up to the early 1980's including partially stripped ions are compiled by Y. Kaneko, T. Arikawa, Y. Itikawa, T. Iwai, T. Kato, M. Matsuzawa, Y. Nakai, K. Okuno, H. Ryufuku, H. Tawara, and T. Watanabe in Institute of Plasma Physics Report No. IPPJ-AM-15, Nagoya University, 1980 (unpublished).
- ⁴H. Ryufuku, K. Sasaki, and T. Watanabe, *Phys. Rev. A* **21**, 745 (1980).
- ⁵E. Salzbom and A. Müller, Ref. 2, p. 407.
- ⁶D. H. Crandall, R. A. Phaneuf, and F. W. Meyer, *Phys. Rev. A* **19**, 504 (1979).
- ⁷D. H. Crandall, R. A. Phaneuf, and F. W. Meyer, *Phys. Rev. A* **22**, 379 (1980).
- ⁸L. D. Gardner, J. E. Bayfield, P. M. Koch, I. A. Sellin, D. J. Pegg, R. S. Peterson, and D. H. Crandall, *Phys. Rev. A* **21**, 1397 (1980).
- ⁹R. A. Phaneuf, *Phys. Rev. A* **24**, 1138 (1981).
- ¹⁰S. Bliman, J. Aubert, R. Geller, B. Jacquot, and D. van Houtte, *Phys. Rev. A* **23**, 1703 (1981).
- ¹¹C. L. Cocke, R. D. DuBoir, T. J. Gray, and E. Justiano, *IEEE Trans. Nucl. Sci.* **NS-28**, 1032 (1981).
- ¹²R. Mann, F. Folkmann, and H. F. Beyer, *J. Phys. B* **14**, 1161 (1981).
- ¹³C. W. Sherwin, *Phys. Rev.* **57**, 814 (1940).
- ¹⁴V. S. Nikolaev, L. N. Fateeva, I. S. Dmitriev and Ya. A. Teplova, *Zh. Eksp. Teor. Fiz.* **40**, 989 (1961) [*Sov. Phys.—JETP* **13**, 659 (1961)].
- ¹⁵H. J. Zwally and D. W. Koopman, *Phys. Rev. A* **2**, 1851 (1970).
- ¹⁶H. J. Zwally and P. G. Cable, *Phys. Rev. A* **4**, 2301 (1971).
- ¹⁷J. Goldhar, R. Mariella, Jr., and A. Javan, *Appl. Phys. Lett.* **29**, 96 (1976).
- ¹⁸D. H. Crandall, *Phys. Rev. A* **16**, 958 (1977).
- ¹⁹L. D. Gardner, J. E. Bayfield, P. M. Koch, I. A. Sellin, D. J. Pegg, R. S. Peterson, M. S. Mallory, and D. H. Crandall, *Phys. Rev. A* **20**, 766 (1979).
- ²⁰Very recently, preliminary reports appeared in the XII-ICPEAC, Gatlinburg, Tennessee, 1981: Data for fully stripped C, N, O, and Ne ions by Afrosimov *et al.*, in *Abstracts of the XII ICPEAC, Gatlinburg, Tennessee, 1981*, edited by S. Datz (North-Holland, Amsterdam, 1981), p. 690; data for C⁵⁺, N⁶⁺, O^{7,8+}, F⁸⁺, and Ne⁹⁺ by our group in the papers, p. 696. A brief report of the present work except for B⁹⁺ ions is described by Kaneko *et al.* in *Physics of Electronic and Atomic Collisions*, edited by S. Datz (North-Holland, Amsterdam, 1982), p. 697.
- ²¹E. D. Donets, *IEEE Trans. Nucl. Sci.* **NS-23**, 897 (1976).
- ²²H. Imamura, Y. Kaneko, T. Iwai, S. Ohtani, N. Kobayashi, K. Okuno, S. Tsurubuchi, M. Kimura, and H. Tawara, *Nucl. Instrum. Methods.* **188**, 233 (1981).
- ²³Y. Kaneko, T. Iwai, S. Ohtani, K. Okuno, N. Kobayashi, S. Tsurubuchi, M. Kimura, and H. Tawara, *J. Phys. B* **14**, 881 (1981).
- ²⁴H. Klinger, A. Müller, and E. Salzbom, *J. Phys. B* **8**, 230 (1975).
- ²⁵A. Müller and E. Salzbom, *Phys. Lett.* **62A**, 391 (1977).
- ²⁶E. J. Shipsey, J. C. Browne, and R. E. Olson, *Phys. Rev. A* **15**, 2166 (1977).
- ²⁷H. Ryufuku and T. Watanabe, *Phys. Rev. A* **19**, 1538 (1979).
- ²⁸W. Lotz, *J. Opt. Soc. Am.* **57**, 873 (1967).

LETTER TO THE EDITOR

Observation of electron capture into selective state by fully stripped ions from He atom

S Ohtani, Y Kaneko†, M Kimura‡, N Kobayashi†, T Iwai§,
A Matsumoto, K Okuno†, S Takagi, H Tawara|| and S Tsurubuchi¶
Institute of Plasma Physics, Nagoya University, Nagoya 464, Japan

Received 2 June 1982

Abstract. Energy spectra of charge-changing projectile ions are measured for one-electron capture by fully stripped C and O ions from He atoms. The electron is selectively captured into a single level of principal quantum number $n = 3$ of C^{6+} and $n = 4$ of O^{7+} , respectively, at a collision energy of $0.45 \text{ keV amu}^{-1}$.

Recently, total cross sections for one-electron transfer from He atoms into multi-charged B, C, N, O, F, Ne and S ions, including fully stripped ions, have been measured at low collision energies below 1.5 keV amu^{-1} (Iwai *et al* 1982, Kaneko *et al* 1982). The measured cross sections are nearly independent of the collision energy investigated with only a few exceptions. When the cross sections are plotted as a function of the ionic charge q of isoelectronic projectile ions, strong oscillations in the cross sections are observed for all ions. This oscillatory behaviour is interpreted as follows. At low energies an electron is captured selectively into a level with a particular quantum number n . Such a level drastically changes from n to $n + 1$ with an increase of q . This level change results in an increase of the crossing distance of the potential curves: it causes a significant increase in the q dependence of the cross sections. Similar oscillations in cross sections have been reported in other collision systems (Bliman *et al* 1981, Mann *et al* 1981, Cocke *et al* 1981).

In order to see whether the oscillation is caused by the change of the level into which the electron is transferred in the collision system, we have measured energy spectra of charge-changing projectile ions scattered in the forward direction for the collision systems mentioned above. These measurements give us information on the level into which the electron is captured.

The experimental set-up is shown in figure 1. The ion beam extracted from an ion source of EBIS type, called NICE-1, is focused, mass analysed by a sector magnet and well collimated by a pair of apertures of 1 mm in front of the target gas cell. The gas cell is 2 cm in length and its entrance and exit apertures are 0.8 mm and 1 mm in

† Permanent address: Department of Physics, Tokyo Metropolitan University, Setagaya-ku Tokyo 158, Japan.

‡ Permanent address: Department of Physics, Osaka University, Toyonaka, Osaka 560, Japan.

§ Permanent address: Department of Liberal Arts, Kansai Medical University, Hirakata, Osaka 573, Japan.

|| Permanent address: Nuclear Engineering Department, Kyushu University, Fukuoka 812, Japan.

¶ Permanent address: Department of Applied Physics, Tokyo University of Agriculture and Technology, Koganei, Tokyo 184, Japan.

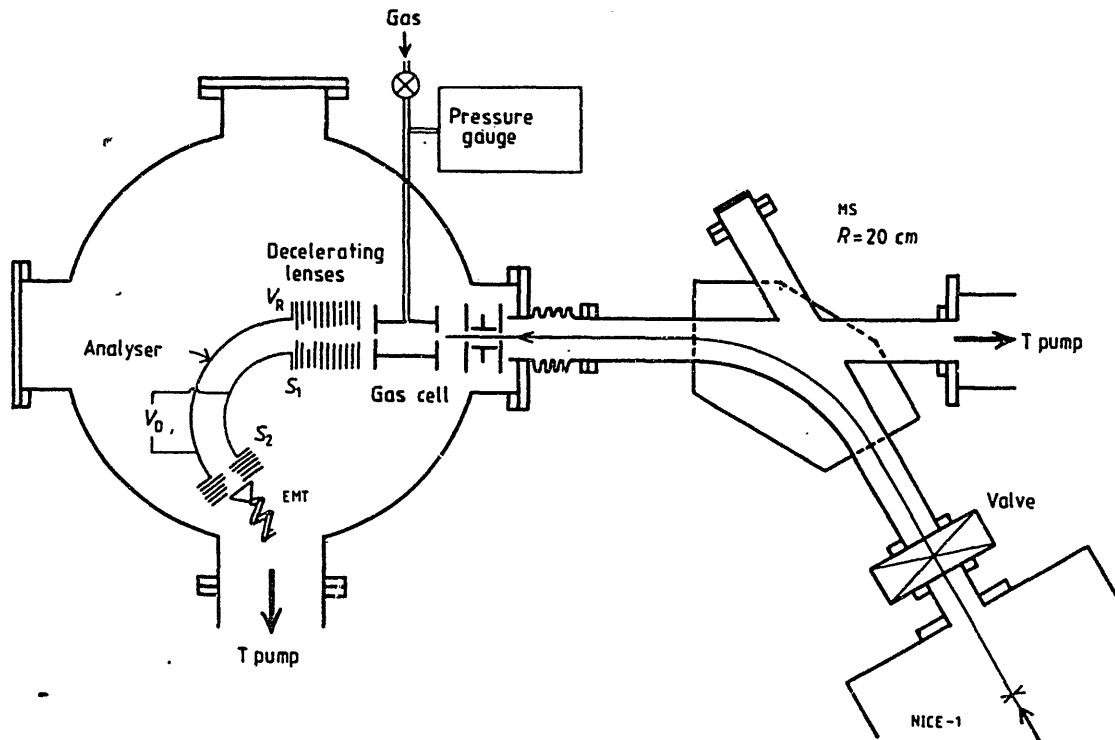


Figure 1. Schematic view of the spectrometer used for ion energy analysis.

diameter, respectively. Ions which pass through the cell are decelerated by electrostatic lenses before entering a 127° cylindrical analyser. An entrance aperture of the decelerating lens system having 14 electrodes is located 22 mm behind the cell. The mean radius of the analyser is $r = 125$ mm and the slit widths are $S_1 = 1.0$ mm and $S_2 = 1.5$ mm. The deceleration voltage V_R is so adjusted that the energy of the ions passing the analyser is between 30–60($\times q$) eV. Then the energy resolution is just limited by the energy spread of incident ions extracted from NICE-1. It is usually

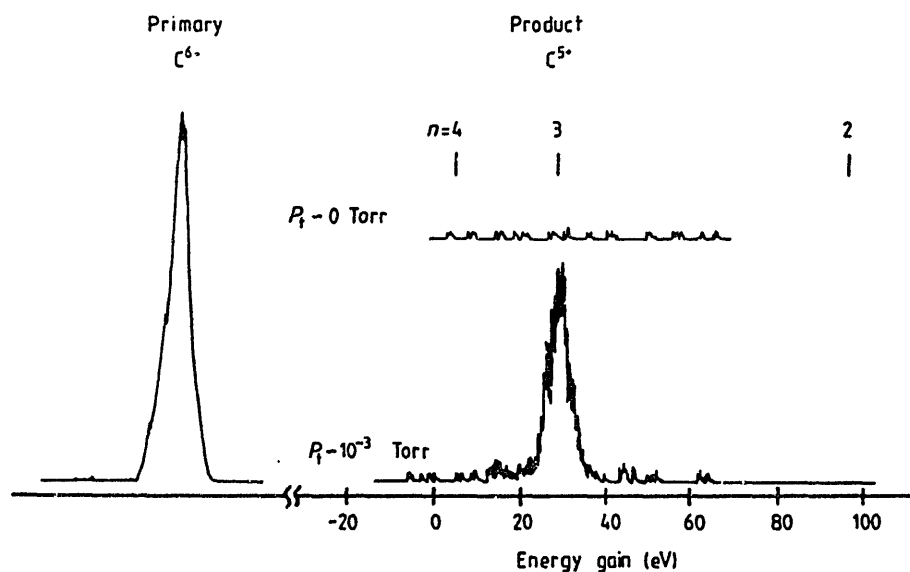


Figure 2. Energy gain and loss spectrum of scattered C^{5+} ions from $C^{6+} + He$ collisions at a collision energy of 6 keV. No peak was observed without target He gas ($P_1 \sim 0$).

$0.8 \times q$ eV, depending a little on the current density of the electron beam and on the potential distribution applied to the drift tubes in the ion source. The energy spectra of charge-changing projectiles are obtained by scanning an additional variable voltage superimposed on the deceleration voltage while the deflection voltage V_D of the analyser is fixed. The energy-analysed ions are detected by an electron multiplier (EMT).

In figure 2 is shown the energy gain spectrum of scattered C^{5+} ion from $C^{6+} + He$ collisions. Only a single peak is observed, which corresponds to the following electron transfer process: $C^{6+} + He(1s^2) \rightarrow C^{5+}(n=3) + He^+(1s)$.

For the case of $O^{8+} + He$ collisions, as seen in figure 3, the electron is selectively captured into the $n=4$ level of O^{7+} . This change of the level from $n=3$ to $n=4$ gives rise to a significant difference in the cross sections for one-electron capture by C^{6+} and O^{8+} ions. Actually, as reported previously (Iwai *et al* 1982), the cross section for O^{8+} is about three times larger than that for C^{6+} . Similar measurements are in progress for various projectiles including fully stripped, H-, He- and Li-like ions.

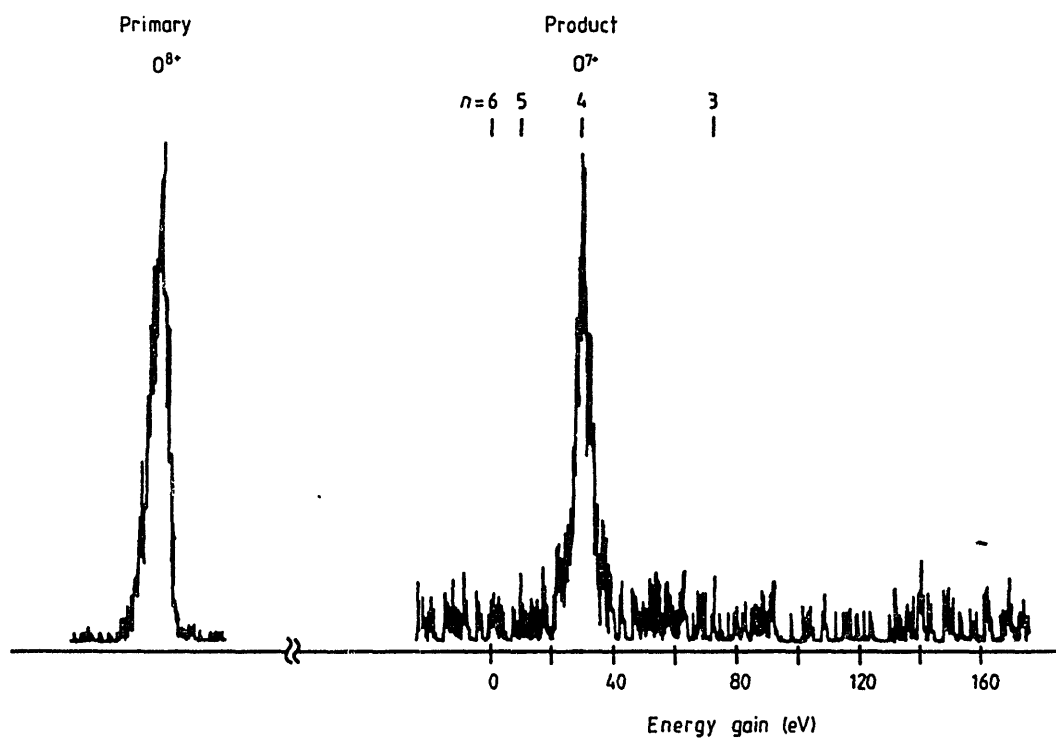


Figure 3. Energy spectrum of scattered O^{7+} ions from $O^{8+} + He$ collisions at a collision energy of 8 keV.

References

- Bliman S, Aubert J, Geller R, Jacquot B and van Houtte D 1981 *Phys. Rev. A* **23** 1703-7
 Cocke C L, DuBois R, Gray T J and Justiniano E 1981 *IEEE Trans. Nucl. Sci.* **NS-28** 1032-5
 Kaneko Y, Iwai T, Ohtani S, Okuno K, Kobayashi N, Tsurubuchi S, Kimura M, Tawara H and Takagi S 1981 *Proc. 12th Int. Conf. on Electronic and Atomic Collisions, Gatlinburg* ed S Datz (Amsterdam: North-Holland) Invited papers and progress reports pp 697-705
 Iwai T, Kaneko Y, Kimura M, Kobayashi N, Ohtani S, Okuno K, Takagi S, Tawara H and Tsurubuchi S 1982 *Phys. Rev. A* **27** No 1 in press
 Mann R, Folkmann F and Beyer H F 1981 *J. Phys. B: At. Mol. Phys.* **14** 1161-81

LETTER TO THE EDITOR

Two-electron capture into autoionising states of $N^{5+}(3l3l')$ and $O^{5+}(1s3l3l')$ in collisions of N^{7+} and O^{7+} with He

S Tsurubuchi†, T Iwai‡, Y Kaneko§, M Kimura||, N Kobayashi§,
A Matsumoto, S Ohtani, K Okuno§, S Takagi and H Tawara¶
Institute of Plasma Physics, Nagoya University, Nagoya 464, Japan

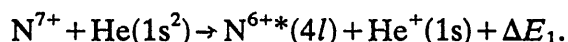
Received 10 August 1982

Abstract. Transfer ionisation processes are studied for the $N^{7+} + He$ and $O^{7+} + He$ systems by means of ion beam spectroscopy at 7 keV. The autoionising states ($3l3l'$) of N^{5+} and ($1s3l3l'$) of O^{5+} are identified.

The identification of satellite lines of highly charged ions plays an important role in the spectroscopic diagnostics of high-temperature sources such as laser-produced plasmas and vacuum spark sources, and also in the observation of the solar corona. To the authors' knowledge, however, no experimental data is available for those satellite lines with the configuration of $N\text{ VI}(3ln'l')$ and $O\text{ VI}(1s3ln'l')$.

In our previous paper, we showed that ion beam spectroscopy is one of the very powerful tools in determining the final electronic state of the projectile ions after charge transfer collision with He (Ohtani *et al* 1982). The ion source used is the NICE-1 built at IPPJ. A detailed description of the present experimental apparatus will be published soon. Briefly, a 127° cylindrical energy analyser with a retardation lens system is set behind a target cell to measure the energy gain ΔE of the charge-changed projectile in the forward direction.

In figure 1 is shown the energy gain spectrum of N^{6+} ions obtained in $N^{7+} + He$ collision. The dominant peak around $\Delta E \approx 17$ eV is assigned as being due to the selective one-electron capture,



The energy balance consideration in figure 2(a) shows that the N^{6+} ions should be in the $n = 4$ state. Furthermore, a small peak around $\Delta E \approx 60$ eV is recognised. The intensity of the peak increases with an increase of target pressure as shown in the figure. The purity of the target He gas was increased up to 99.999% to ensure no impurity effect involved in the spectrum. The typical resolution of the analyser is less than 4.8 eV in the present case. Thus, we are certain that the peak is due to N^{6+} ions

† Permanent address: Department of Applied Physics, Tokyo University of Agriculture and Technology, Koganei-shi, Tokyo 184, Japan.

‡ Permanent address: Department of Liberal Arts, Kansai Medical University, Hirakata, Osaka 573, Japan.

§ Permanent address: Department of Physics, Tokyo Metropolitan University, Setagaya-ku, Tokyo 158, Japan.

|| Permanent address: Department of Physics, Osaka University, Toyonaka, Osaka 560, Japan.

¶ Permanent address: Nuclear Engineering Department, Kyushu University, Fukuoka 812, Japan.

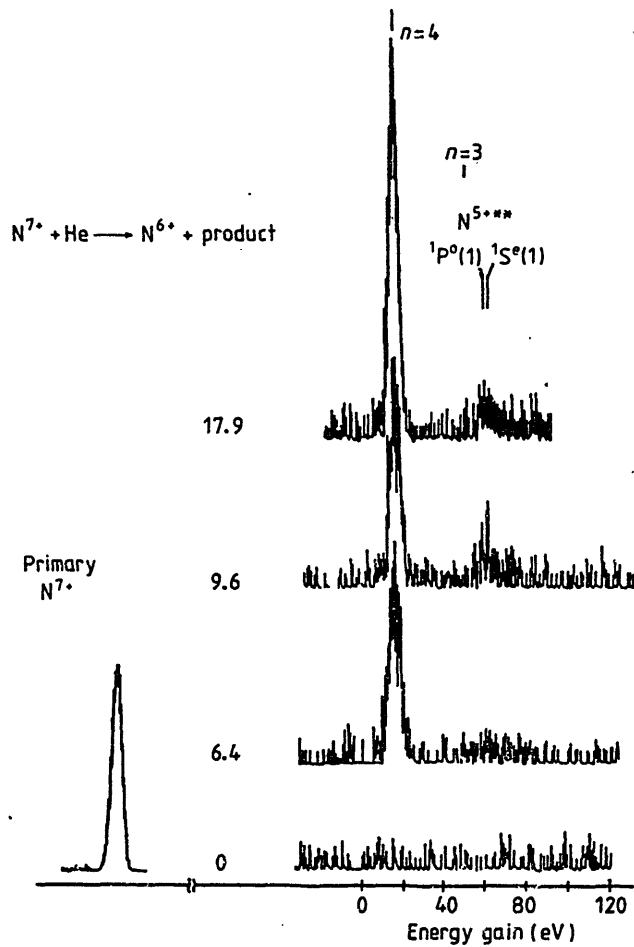


Figure 1. Energy gain spectra of N^{6+} obtained in $N^{7+} + He$ collisions at $0.47 \text{ keV amu}^{-1}$. The numbers with the various spectra are the values of NL in units of 10^{13} cm^{-2}

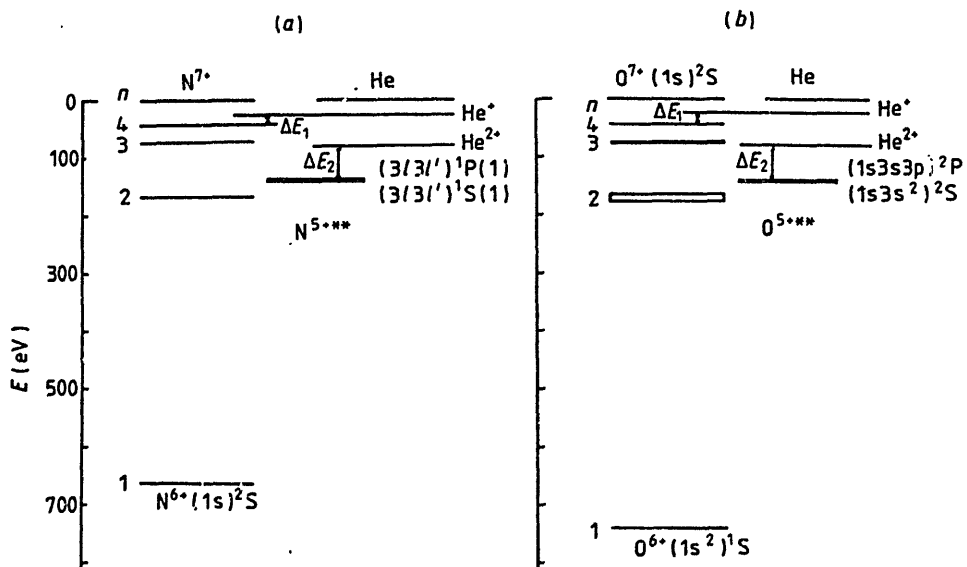


Figure 2. Schematic energy level diagrams for (a) $N^{7+} + He$ system, and (b) $O^{7+} + He$ system. The values of the energy levels are taken from Bashkin and Stoner (1975), Pradhan *et al* (1981), and Ho (1979).

formed through a different reaction channel from the one-electron transfer process in which an electron is captured into the $n = 3$ state of N^{6+} .

According to the calculation of Ho (1979), the doubly excited autoionising states 1S , 1P , and 3P in which two electrons occupy the $n = 3$ shell are located 7.7760 to 10.2160 Ryd below the N^{7+} state. In figure 2(a), the $^1S(1)$ and $^1P(1)$ states are presented. The energy gain ΔE_2 (see figure 2(a)) estimated from those levels is in good harmony with the result obtained from the position of the second weak peak in the present experiment. Thus, we assign the small peak observed in the spectrum as being due to the following transfer ionisation via two-electron capture into the autoionising states of N^{5+} ,

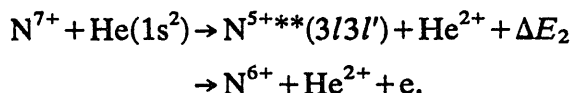


Figure 3 shows the schematic potential curves relevant to the proposed mechanism. Another transfer ionisation, in which one-electron capture into N^{6+} and target ionisation of He^+ take place simultaneously, would contribute to continuum background spectra and will not form a peak. Such a continuum was not observed in the present spectrum.

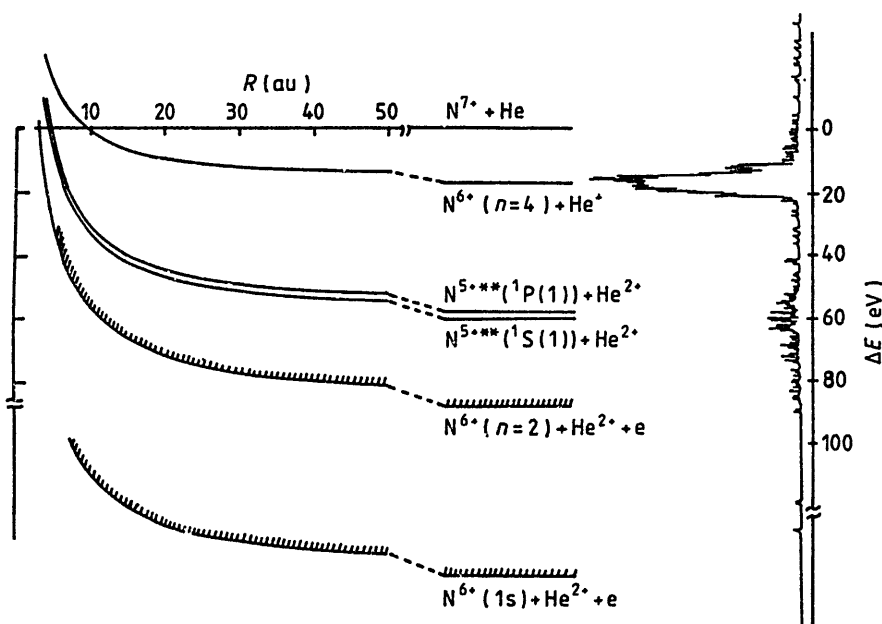
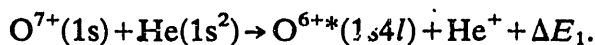


Figure 3. Schematic potential curves relevant to the energy gain spectrum of N^{6+} in $N^{7+} + He$ collisions at $0.47 \text{ keV amu}^{-1}$.

The O^{6+} spectrum obtained in the $O^{7+} + He$ collision is given in figure 4. A similar pattern of spectrum is obtained but the second peak is more clearly recognised. The first dominant peak is assigned as being due to one-electron capture into the $1s4l$ state of O^{6+} from figure 2(b),



From the resolution of the analyser, the second peak corresponds neither to the one-electron capture into $O^{6+}(1s2l)$ nor to $O^{6+}(1s3l)$. Because the energy positions

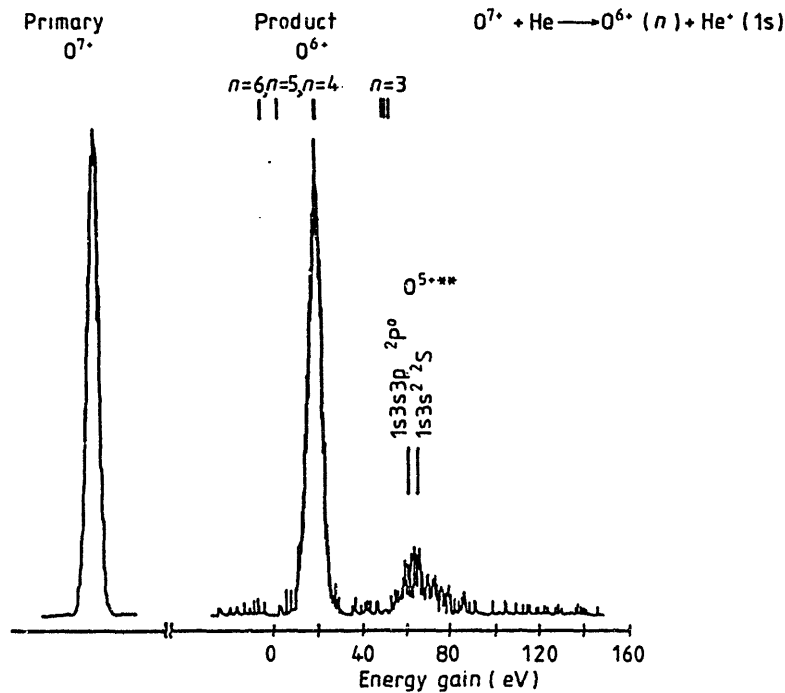
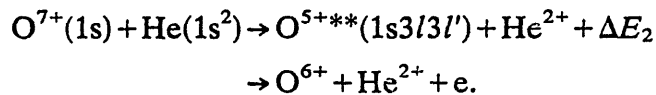


Figure 4. Energy gain spectrum of O^{6+} obtained in $O^{7+} + He$ collision at $0.39 \text{ keV amu}^{-1}$

of the $(1s3s3p)^2P$ and $(1s3s^2)^2S$ states of O^{5+**} (Pradhan *et al* 1981) agree quite well with the maximum position of the weak peak, we provisionally assign this peak as due to the following transfer ionisation process by means of two-electron capture into the autoionising states of O^{5+**} ,



The importance of the transfer ionisation has been pointed out by Kishinevskii and Parillis (1969), and recently by Groh *et al* (1982) in the measurement of recoil target ions in coincidence with the projectile ions. The transfer ionisation process in multiply charged ion collisions has been studied by measuring the energy spectrum of the ejected electrons (Winter *et al* 1977, 1978, Woerlee *et al* 1979).

Several types of transfer ionisation are possible according to the scheme of potential curve interactions. These are well compiled in the literature of Niehaus (1980). The two-electron capture into the autoionising state of the projectile ion with subsequent Auger effect is typical of transfer ionisation (Kishinevskii and Parillis 1969).

The lifetime of the $^1P(1)$ and $^1S(1)$ states of N^{5+**} can be estimated as $1.6 \times 10^{-15} \text{ s}$ and $4.9 \times 10^{-15} \text{ s}$ respectively from the resonant parameter Γ of Ho (1979). In the present experiment, the kinetic energy of N^{7+} projectile is $0.47 \text{ keV amu}^{-1}$ which corresponds to the velocity of $3.0 \times 10^7 \text{ cm s}^{-1}$. Assuming the effective interacting distance is about 10 au, then the collision time is comparable with the lifetimes of the doubly excited states $^1P(1)$ and $^1S(1)$ of N^{5+} . A molecular autoionisation would be possible to some extent as well as atomic autoionisation of N^{5+} . The energy profile of ejected electrons will be asymmetric and have a tail to the lower energy side. It is noticed that the observed transfer ionisation peak has a tail extending to the side of higher energy gain, which may be considered as a reflection of the molecular

autoionisation process. A similar situation seems to be the case for the spectrum observed in the $O^{7+} + He$ collision. The measurement of the energy spectrum of ejected electrons will give a definite answer to this question.

The total cross sections for $N^{7+} + He \rightarrow N^{6+}(n=4) + He^+$ and $O^{7+} + He \rightarrow O^{6+}(n=4) + He^+$ are 1.1×10^{-15} and $1.3 \times 10^{-15} \text{ cm}^2$ respectively at 0.8 keV amu^{-1} (Iwai *et al* 1982). The cross sections for the two-electron capture into the autoionising states of N^{5+**} and O^{5+**} in $N^{7+} + He$ and $O^{7+} + He$ collisions are one order of magnitude smaller than that of the one-electron capture process. In conclusion, we have found, for the first time, the two-electron capture processes into the doubly excited autoionising states of N^{5+} and O^{5+} converging to the $n=3$ state of N^{6+} and O^{6+} in collisions of N^{7+} and O^{7+} with He.

References

- Bashkin S and Stoner J R Jr 1975 *Atomic Energy Levels and Grotrian Diagrams* (Amsterdam: North-Holland)
- Groh W, Schlachter A S, Müller A and Salzborn E 1982 *J. Phys. B: At. Mol. Phys.* **15** L207-12
- Ho Y K 1979 *J. Phys. B: At. Mol. Phys.* **12** 387-99
- Iwai T, Kaneko Y, Kimura M, Kobayashi N, Ohtani S, Okuno K, Takagi S, Tawara H and Tsurubuchi S 1982 *Phys. Rev. A* **26** 105-15
- Kishinevskii L M and Parilis E S 1969 *Sov. Phys.-JETP* **28** 1020-5
- Niehaus A 1980 *Comment. At. Mol. Phys.* **9** 153-63
- Ohtani S, Kaneko Y, Kimura M, Kobayashi N, Iwai T, Matsumoto A, Okuno K, Takagi S, Tawara H and Tsurubuchi S 1982 *J. Phys. B: At. Mol. Phys.* **15** L533-5
- Pradhan A K, Norcross D W and Hummer D G 1981 *Phys. Rev. A* **23** 619-31
- Winter H, Bloemen E and de Heer F J 1977 *J. Phys. B: At. Mol. Phys.* **10** L599-604
- Winter H, El-Sherbini T M, Bloemen E, de Heer F J and Salop A 1978 *Phys. Lett.* **68A** 211-4
- Woerlee P H, El-Sherbini T M, de Heer F J and Saris F W 1979 *J. Phys. B: At. Mol. Phys.* **12** L235-41

LETTER TO THE EDITOR

The (n, l) distributions in electron capture reactions for C^{3+} , N^{4+} and O^{5+} ions colliding with He

M Kimura[†], T Iwai[‡], Y Kaneko[§], N Kobayashi[§], A Matsumoto,
S Ohtani, K Okuno[§], S Takagi, H Tawara^{||} and S Tsurubuchi[¶]

Institute of Plasma Physics, Nagoya University, Nagoya 464, Japan

Received 4 October 1982

Abstract. Distributions of captured electrons in the reaction $A^{q+} + He \rightarrow A^{(q-1)+}(n, l) + He^+$ over the final-state quantum numbers n and l are measured using a beam spectroscopy method at the energy of $1.0q$ keV. Projectile ions A^{q+} are Li-like species of carbon ($q = 3$), nitrogen ($q = 4$) and oxygen ($q = 5$).

Electron capture by highly-charged ions from neutral atoms has been intensively studied in recent years. Most work has been directed toward the determination of total electron capture cross sections in such collisions. In a previous paper (Iwai *et al* 1982) we reported measurements of the cross sections for one-electron capture from He by highly stripped ions A^{q+} ($A =$ boron, carbon, nitrogen, oxygen, fluorine, neon and sulphur) below 1.5 keV amu^{-1} , and found strong oscillatory behaviour of cross sections as a function of charge q . This observation was qualitatively explained using the classical one-electron model (Ryufuku *et al* 1980). One of the important assumptions of this model is that an electron is transferred to a particular single energy level of charge-changed ions. As q increases, the principal quantum number n of the capturing level increases in a stepwise fashion. As a result the cross sections show oscillatory structure.

With this prediction in mind, we have recently measured the energy gain spectra of the charge-changed ions in collisions of fully stripped, H-like and He-like ions of C, N and O with He at the energies of $1q$ and $2q$ keV (Ohtani *et al* 1982, Tsurubuchi *et al* 1982, Tawara *et al* 1982, Okuno *et al* 1982). It was confirmed that an electron really transfers to a single level n of the ions in the process of one-electron capture and that the number n agrees with that of the classical model except in one case (Tawara *et al* 1982).

Though the energy resolution of our apparatus is good enough to resolve the n distributions for the above-mentioned systems, distributions of orbital angular quantum number l within the same principal quantum number n could not be resolved.

[†] Present address: Department of Physics, Osaka University, Toyonaka, Osaka 560, Japan.

[‡] Present address: Department of Liberal Arts, Kansai Medical University, Hirakata, Osaka 573, Japan.

[§] Present address: Department of Physics, Tokyo Metropolitan University, Setagaya-ku, Tokyo 158, Japan.

^{||} Present address: Department of Energy Conversion, Kyushu University, Kasuga, Fukuoka 816, Japan.

[¶] Present address: Department of Applied Physics, Tokyo University of Agriculture and Technology, Koganei, Tokyo 184, Japan.

Both theoretical and experimental studies are quite scarce on the l distributions. Theoretical studies have been exclusively directed toward the collisions of fully-stripped ions with H atoms (Ryufuku *et al* 1979, Salop 1979). Since the product ions in such collision systems have almost degenerate sublevels within one principal quantum number, their predictions cannot be applied to our observations. Winter *et al* (1977) and Matsumoto *et al* (1980a, b) have measured cross sections for one-electron capture into several excited (n, l) states by observing radiations from charge-changed ions in collisions of 100 keV Ne^{q+} ($q = 1-4$) with He, H_2 and Ar, and Ar^{2+} of keV energy with Na, respectively. Afrosimov *et al* (1977) and Huber (1980) have also determined one-electron capture cross sections into several states by energy-loss spectroscopy for the systems Ar^{q+} ($q = 3-7$)-He, and for the systems Ar^{2+} -He, Ne and Ar, respectively.

The present paper is concerned with electron-capturing collisions of Li-like ions of C, N and O on He. Since product ions from one-electron capture are Be-like and they have wide energy separations among sublevels, the l distributions may be observed as well as the n distributions. These distributions are compared with cross sections calculated by means of the Landau-Zener model.

The present measurements were performed using a beam spectroscopy method and procedures described previously (Ohtani *et al* 1982). In all cases studied here the n distributions are consistent with the prediction of the classical one-electron model; $\text{C}^{2+}(n = 2)$, $\text{N}^{3+}(n = 2)$ and $\text{O}^{4+}(n = 3)$.

(i) $\text{C}^{3+} + \text{He}$. In figure 1 is shown the energy spectrum at a collision velocity of $2.1 \times 10^7 \text{ cm s}^{-1}$. Isotope gas ^{13}CO was used to separate impurity ions having $m/q = 4$. In this figure the calculated energy levels are also indicated which correspond to the

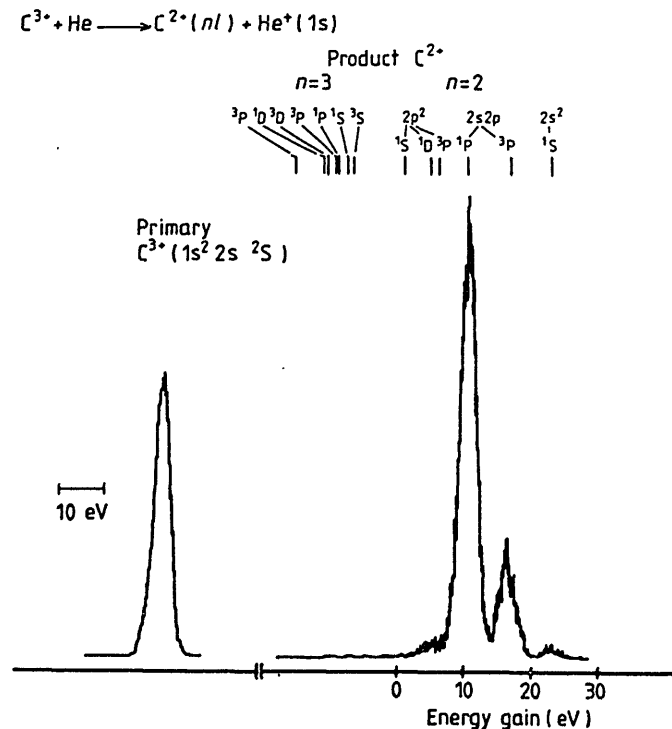


Figure 1. Energy gain spectrum of forward scattered C^{2+} ions from $\text{C}^{3+} + \text{He}$ collisions at a collision velocity of $2.1 \times 10^7 \text{ cm s}^{-1}$.

levels of the charge-changed C^{2+} ions for the process, $C^{3+} + He \rightarrow C^{2+}(nl) + He^+(1s)$, together with the energy profile of the primary C^{3+} ions. All the peaks observed correspond to the electron configurations, $1s^2 2l 2l'$, which have six terms. Relative intensity for each term was determined from the best fit to the observed spectrum by deconvolution with the energy profile of the primary ions. Normalisation of the relative intensities to the total one-electron capture cross section, which was measured previously at a slightly higher velocity $2.6 \times 10^7 \text{ cm s}^{-1}$, gives the cross sections for the final channels. They are listed in table 1 (i) along with the energy gain values ΔE , calculated from tabulated values (Bashkin and Stoner 1975). One can estimate the

Table 1. Energy gains ΔE and crossing distances R_c for capture into various states in the collision systems C^{3+} , N^{4+} and $O^{5+} + He$. Crossing distances were estimated using equation (1). Measured cross sections are normalised to total one-electron capture cross sections obtained by Iwai *et al* (1982) at slightly higher velocities and compared with the Landau-Zener cross sections.

Final ionic state	ΔE (eV)	R_c (Å)	Measured σ^a (10^{-16} cm^2)	LZ σ (10^{-16} cm^2)
<i>(i) C³⁺(1s²2s²S) incident</i>				
$C^{2+} 2p^2 \ ^1S$	0.67	43.0	0	0
$\ ^1D$	5.21	5.5	0.03	0.01
$\ ^3P$	6.26	4.6	0.3	0.17
$2s2p \ ^1P$	10.61	2.7	11.4	10.1
$\ ^3P$	16.80	1.7	2.8	0.01
$2s^2 \ ^1S$	23.30	1.2	0.2	0
		Total	14.7 ± 2.9^b	10.3
<i>(ii) N⁴⁺(1s²2s²S) incident</i>				
$N^{3+} 2p^2 \ ^1S$	23.70	1.8	3	0.04
$\ ^1D$	29.47	1.5	~0	$\ll 0.001$
$\ ^3P$	31.11	1.4	~0	0
$2s2p \ ^1P$	36.68	1.2	0	0
$\ ^3P$	44.54	1.0	0	0
$2s^2 \ ^1S$	53.15	0.8	0	0
		Total	3.0 ± 0.9^c	0.04
<i>(iii) O⁵⁺(1s²2s²S) incident</i>				
$O^{4+} 2p3s \ ^1P$	6.93	8.3	0	0
$\ ^3P$	8.34	6.9	0	0
$2s3d \ ^1D$	13.36	4.3	small	2.8
$\ ^3D$	14.83	3.9	small	5.3
$2s3p \ ^3P$	17.04	3.4	^e	8.0
$\ ^1P$	17.30	3.3	^e	7.0
$2s3s \ ^1S$	19.72	2.9	^e	5.9
$\ ^3S$	21.49	2.7	small	2.8
		Total	22.7 ± 4.5^d	31.8

^a Total one-electron capture cross sections measured at slightly higher velocities are decomposed into the constituents according to their relative peak heights.

^{b,c,d} Total one-electron capture cross sections at collision velocities, 2.6, 2.9 and $3.0 \times 10^7 \text{ cm s}^{-1}$ respectively (Iwai *et al* 1982), while the present measurements were performed at 2.1, 2.3 and $2.5 \times 10^7 \text{ cm s}^{-1}$.

^e Relative cross sections could not be determined.

crossing distance R_c for the two diabatic potential curves from the following relation, by considering pure Coulomb repulsion in the final channel $A^{(q-1)+}(n, l) + \text{He}^+$ and disregarding polarisation attractions in the initial channel $A^{q+} + \text{He}$,

$$R_c = 14.4(q-1)/\Delta E \text{ (\AA)} \quad (1)$$

where ΔE is expressed in eV. The R_c value obtained from equation (1) is also listed in table 1.

According to the Landau-Zener model, the probability of a transition between the two states at a crossing distance R_c is given by

$$p = \exp(-2H_{12}^2/v|\Delta F|) \quad (2)$$

where

$$\Delta F = \frac{d}{dR}(H_{11} - H_{22})_{R=R_c}. \quad (3)$$

Here v is the radial velocity and H_{12} is the coupling matrix element between the initial and final states at the crossing point. For the case of a single crossing, the probability of a transition from the initial state to the final state is given by the relation:

$$P = 2p(1-p). \quad (4)$$

This expression can be generalised to the case of N crossings as described by Salop and Olson (1976) if interference between adjacent channels are neglected. The interaction potential H_{12} at each crossing point is estimated using the semi-empirical formula given by Olson and Salop (1976). By integrating the probabilities over the impact parameter, the cross section for each channel can be obtained. The calculations of the Landau-Zener cross sections are carried out for the collision velocity of $2.1 \times 10^7 \text{ cm s}^{-1}$ and the results are also listed in table 1 (i). Compared with the observation the Landau-Zener cross section gives a similar total one-electron capture cross section, though indicating stronger selectiveness to the $2s2p \ ^1P$ state.

(ii) $\text{N}^{4+} + \text{He}$. The energy spectrum for the $\text{N}^{4+} + \text{He}$ collision is shown in figure 2. One strong peak and a few weak peaks are observed. The strong one is assigned to the $1s^2 2p^2 \ ^1S$ state. A small peak at around 10 eV remains almost unchanged even when the target He is evacuated. Therefore it is thought to come from the background gas (1×10^{-7} Torr). Since the cross section of one-electron capture for this collision system is relatively small, the background signal becomes observable. A small tail located at the higher energy wing of the main peak is due to $2p^2 \ ^1D$ and possibly 3P . It is noted that the two-electron process, in which the one-electron capture together with the projectile excitation ($2s \rightarrow 2p$) occurs simultaneously, is predominant compared with simple one-electron capture. Energy gain values, crossing distances of potential curves calculated from equation (1) and relative cross sections determined similarly as for the $\text{C}^{3+} + \text{He}$ case are listed in table 1 (ii). In this case the crossing distances R_c are so small that our simple approximations to estimate R_c and H_{12} would make serious errors. This could be the reason for a significant discrepancy between the calculated cross sections and the measured ones.

(iii) $\text{O}^{5+} + \text{He}$. The observed energy spectrum is shown in figure 3. A broad peak corresponding to $\text{O}^{4+}(n=3)$ is observed. Since the $n=3$ state consists of substates densely located, each substate could not be resolved. Deconvoluting the observed

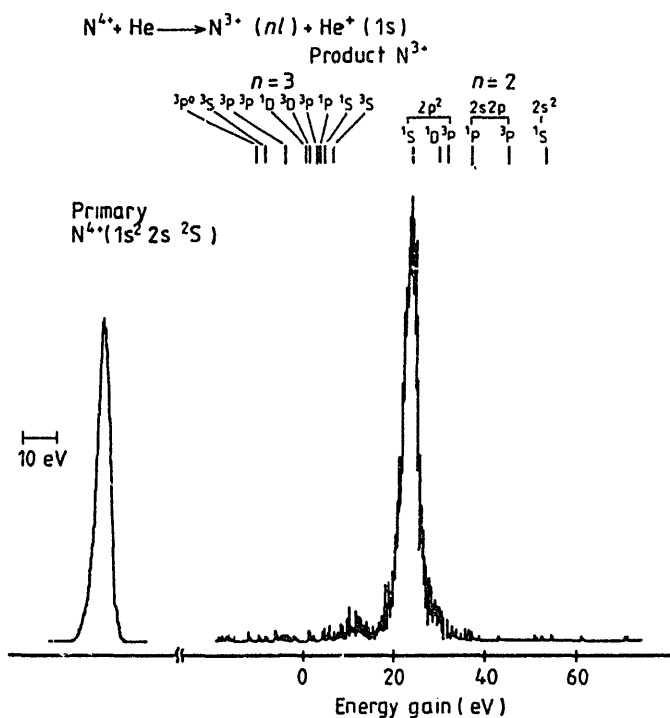


Figure 2. Energy gain spectrum of forward scattered N^{3+} ions from $N^{4+} + He$ collisions at a collision velocity of $2.3 \times 10^7 \text{ cm s}^{-1}$.

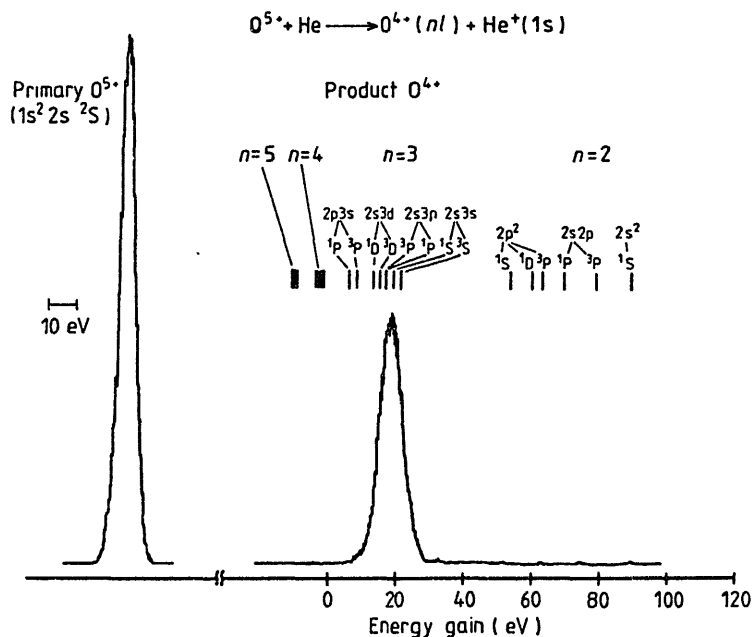


Figure 3. Energy gain spectrum of forward scattered O^{4+} ions from $O^{5+} + He$ collisions at a collision velocity of $2.5 \times 10^7 \text{ cm s}^{-1}$.

spectrum with the primary energy profile does not give a unique solution in this case because of the too narrow separations of the sublevels. One can say at least that the $2s3l$ states are selectively populated, and among them the cross sections for the $2s3d$ levels are much smaller than those for the $2s3s$ and the $2s3p$ levels. Energy gain

values and crossing distances of the potential curves are listed in table 1 (iii) along with the Landau-Zener cross sections.

In all the cases studied here any signals due to endothermic processes are not observed. As seen in table 1, the process of one-electron capture seems to be most favoured when the potential curve of the final state crosses with that of the initial state at a distance of about 1.5–4 Å. These results are consistent with those observed in other multicharged-ion-He systems (Tawara *et al* 1982, Okuno *et al* 1982). Regardless of one- or two-electron processes, the crossing distance appears to be most important in determining the l distributions.

References

- Afrosimov V V, Basalaev A A, Panov M N and Leiko G A 1977 *Zh. Eksp. Teor. Fiz. Pis. Red.* **26** 699 (1977 *JETP Lett.* **26** 537)
- Bashkin S and Stoner J R Jr 1975 *Atomic Energy Levels and Grotrian Diagrams I* (Amsterdam: North-Holland)
- Huber B A 1980 *J. Phys. B: At. Mol. Phys.* **13** 809
- Iwai T, Kaneko Y, Kimura M, Kobayashi N, Ohtani S, Okuno K, Takagi S, Tawara H and Tsurubuchi S 1982 *Phys. Rev. A* **26** 105
- Matsumoto A, Tsurubuchi S, Iwai T, Ohtani S, Okuno K and Kaneko Y 1980a *J. Phys. Soc. Japan* **48** 567
— 1980b *J. Phys. Soc. Japan* **48** 575
- Ohtani S, Kaneko Y, Kimura M, Kobayashi N, Iwai T, Matsumoto A, Okuno K, Takagi S, Tawara H and Tsurubuchi S 1982 *J. Phys. B: At. Mol. Phys.* **15** L533
- Okuno K, Iwai T, Kaneko Y, Kimura M, Kobayashi N, Matsumoto A, Ohtani S, Takagi S, Tawara H and Tsurubuchi S 1982 *Phys. Rev. A* submitted
- Olson R E and Salop A 1976 *Phys. Rev. A* **14** 579
- Ryufuku H, Sasaki K and Watanabe T 1980 *Phys. Rev. A* **21** 745
- Ryufuku H and Watanabe T 1979 *Phys. Rev. A* **20** 1828
- Salop A 1979 *J. Phys. B: At. Mol. Phys.* **12** 919
- Salop A and Olson R E 1976 *Phys. Rev. A* **13** 1312
- Tawara H, Iwai T, Kaneko Y, Kimura M, Kobayashi N, Matsumoto A, Ohtani S, Okuno K, Takagi S and Tsurubuchi S 1982 *Phys. Rev. A* submitted
- Tsurubuchi S, Iwai T, Kaneko Y, Kimura M, Kobayashi N, Matsumoto A, Ohtani S, Okuno K, Takagi S and Tawara H 1982 *J. Phys. B: At. Mol. Phys.* **15** L733
- Winter H, Bloemen E and de Heer F J 1977 *J. Phys. B: At. Mol. Phys.* **10** L453

Energy-spectroscopic studies of electron-capture processes by low-energy, highly stripped C, N, and O ions from He

K. Okuno,* H. Tawara, T. Iwai,[†] Y. Kaneko,* M. Kimura,[‡] N. Kobayashi
A. Matsumoto, S. Ohtani, S. Takagi, and S. Tsurubuchi[§]

Institute of Plasma Physics, Nagoya University, Nagoya 464, Japan

(Received 9 August 1982; revised manuscript received 22 February 1983)

Translation-energy spectra of charge-state-changed projectile ions scattered in the forward direction in collisions of C^{q+} ($q=5,4$), N^{q+} ($q=6,5$), and O^{q+} ($q=6$) ions with He atoms have been measured at collision energies of q and $2q$ keV. All the product peaks observed in the spectra come from exothermic electron-capture processes. From the measured energy gains of the product $(q-1)$ -charge-state ions, it has been found that an electron is captured selectively into a single shell with a particular principal quantum number $n=2$ for the incident C^{4+} ion and $n=3$ for the incident C^{5+} , N^{5+} , N^{6+} , and O^{6+} ions. This fact is in accord with the prediction of the one-electron classical theory. It has also been revealed that there is good similarity among the energy-spectral patterns obtained for the ions having the same charge $+q$, irrespective of ionic species; such a similarity results from the similarity among diabatic potential curves for the collision systems of the q -charge-state ions and He. In the case of $C^{4+} + \text{He}$ collision, the two-electron-capture process into the ground state of C^{2+} occurs more efficiently than the one-electron-capture process at the low energies studied.

I. INTRODUCTION

Recently one-electron-capture cross sections from neutral He atoms by multiply charged B, C, N, O, F, Ne, and S ions including fully stripped ions have been measured at collision energies below 1.5 keV/amu.¹ A remarkable oscillation of cross sections with incident-ionic charge q was found. Similar oscillation was predicted by Ryufuku, Sasaki, and Watanabe for the case of the H atom target using a classical model of charge transfer.² The oscillation has been interpreted as follows. The transferred electron is captured selectively into a shell having a principal quantum number n . This quantum number changes from n to $n+1$ at some value of q as q is increased, with an accompanying drastic increase in cross section. Before the quantum number n changes, the larger q gives the smaller interaction distance, leading instead to a gradual decrease in cross section. After all, the cross sections show a sawtooth type oscillation with the change of ionic charge q . Though the classical model may be crude, the model has been found to be adequate also for the case of the He target.¹ The essential assumption of this model is that the electron is captured only into a single shell. We have made a series of experiments intending to find some evidence for it and to determine into which shell the transferred electron goes. The results obtained should be most important for basic understanding of charge transfer involving multiply charged ions and useful for development of x-ray laser and controlled-thermonuclear-fusion research.

In our preceding papers,^{3,4} energy gains of the charge-state changed projectile ions scattered into the forward direction for the collisions of fully stripped C^{6+} , N^{7+} , and O^{8+} with neutral He atoms have been reported, and it has been verified that an electron is captured selectively into a shell of principal quantum number $n=3$, 4, and 4 of the

product C^{5+} , N^{6+} , and O^{7+} ions, respectively. In the continuation of the previous experiments for fully stripped ions, energy-spectroscopic studies of collisions of hydrogenlike and heliumlike ions of carbon, nitrogen, and oxygen with neutral He atoms have been made systematically. The two-electron-capture process and the transfer ionization process have also been studied in addition to the one-electron-capture process; among these, the transfer ionization process has been reported⁴ for the collision systems of $N^{7+} + \text{He}$ and $O^{7+} + \text{He}$.

In the present paper, we report mainly on the one-electron-capture process at keV collision energies. The experimental details are described in Sec. II. The measured translation-energy spectra are displayed and similarity among the spectral patterns for ions having the same charge q is discussed in relation to diabatic potential curves concerned in Sec. III. Concluding remarks follow in Sec. IV, where the results obtained from the series of energy-spectroscopic measurements including fully stripped ions are compared with the classical one-electron theory.²

II. EXPERIMENTS

The apparatus used and the experimental procedure have been reported in Ref. 3. Therefore, we describe here the principle of translation-energy spectroscopy and the related problems such as determination of the parameter depending on the apparatus geometry and the energy resolution in detail. A brief description of the experimental setup is given.

A. Principle of translation-energy spectroscopy

We consider the following electron-capture process at low energies:



where Q is the total inelastic energy gain. In this inelastic electron-capture process, the incident projectile ion A^{q+} with the mass M_1 and the energy E_q is scattered into an angle of θ with the energy $E_{q'}$; meanwhile the neutral target B atom with the mass M_2 is recoiled with the energy

$$\Delta E(E_q, Q, \theta) = \frac{2M_1M_2}{(M_1+M_2)^2} E_q \left\{ 1 + \frac{M_1}{M_2} \sin^2\theta + \frac{M_1+M_2}{M_1} \frac{Q}{2E_q} - \cos\theta \left[1 - \left(\frac{M_1}{M_2} \right)^2 \sin^2\theta - \frac{M_1+M_2}{M_2} \frac{Q}{E_q} \right]^{1/2} \right\} \quad (3)$$

If it is assumed that the energy gain is much smaller than the incident kinetic energy of the projectile ion, that is, $Q \ll E_q$, the energy gain of the projectile ion scattered into the zero-degree direction ($\theta \simeq 0^\circ$) becomes independent of E_q as follows:

$$\Delta E(\theta \simeq 0^\circ) \simeq Q. \quad (4)$$

That is, by measuring the energy gain ΔE of the projectile ion (energy gain spectroscopy) scattered into the forward direction, we can determine straightforwardly the reaction energy Q which provides important information on mechanisms in the inelastic collision processes.

In order to get good energy resolution, the energy of the projectile ions should be reduced before they enter an electrostatic energy analyzer as shown schematically in Fig. 1. If the decelerating potential to the projectile ion is V_R , the energy of the incident projectile ion is reduced to $E_q - qV_R$ at the entrance of the energy analyzer. When the ion is to pass through the analyzer of which the deflection voltage is V_D and to reach a detector, the following relation should be fulfilled:

$$E_q - qV_R = qKV_D, \quad (5)$$

where K is a constant depending mainly on the geometry of the analyzer and probably on the deflection voltage of the analyzer V_D . On the other hand, the energy of the charge-state-changed projectile ion ($A^{q'+}$) with the charge $+q'$ has to be decelerated through V_R , which is different from V_R for the incident projectile in order to pass through the analyzer with the same deflection voltage V_D as that for the incident projection ion and to reach the detector. Then, the following condition is necessary:

$$E_{q'} - q'V_R = q'KV_D. \quad (6)$$

From the energy conservation, we obtain the following relation:

$$V_R = (q/q')V_R + [(q-q')/q']KV_D + (1/q')\Delta E. \quad (7)$$

That is, we can determine the energy change ΔE in the absolute scale by scanning the decelerating potential V_R for the charge-state-changed projectile ions while keeping the deflection voltage V_D constant, provided that K is known.

B. Experimental setup and determination of the parameter K

Actually, projectile ions are produced in an EBIS-type ion source called NICE-1 and are injected into a collision

cell. Then, the total gain Q is defined as

$$Q = (E_{q'} + E_r) - E_q. \quad (2)$$

In this energy spectroscopy, the gain of the kinetic energy of the scattered ion, $\Delta E = E_{q'} - E_q$, may be measured at the scattering angle θ . The kinematical consideration leads to the following relation:

cell after acceleration and mass-charge analysis. Ions passing through the cell are decelerated through electrostatic lenses, are energy analyzed by an electrostatic 127° cylindrical analyzer, and finally reach a Channeltron-type detector as shown in Fig. 1. The decelerating lens system having 14 electrodes consists of a part of linear field distribution, an einzel lens, and a pair of deflection electrodes to control the position of projectile ions and to optimize the transmission through the energy analyzer as well as to obtain good energy resolution. Dimensions of the present apparatus are as follows: The collision cell is 2 cm in length and its entrance and exit apertures are 0.8 and 1.0 mm in diameter, respectively; the first decelerating electrode is located 22 mm behind the cell; the entrance and exit slit widths of the analyzer with the mean radius of 125 mm are 1.0 and 1.5 mm, respectively. This geometry enables one to detect the ions scattered only into an extremely forward direction.

By the use of 10-keV C^{5+} ions, the energy resolution of the present analyzer was tested as a function of the deflection voltage V_D . When the voltage V_D is reduced, the resolution becomes high and then tends to be nearly constant; a typical operating resolution was about $0.8 \times 5 = 4.0$ eV with the deflection voltage V_D of 25–35 V after the ion energy was decelerated by about 90% of the original acceleration energy. Therefore, the deflection voltage V_D was usually set at 30 V throughout the present experiment. From these experiments it was found that the energy resolution is mainly limited by the energy spread of extracted ions from the NICE-1 and it was estimated to be smaller than $0.8 \times q$ eV under the continuous operation mode,⁵ which is much smaller than that prevailed in the litera-

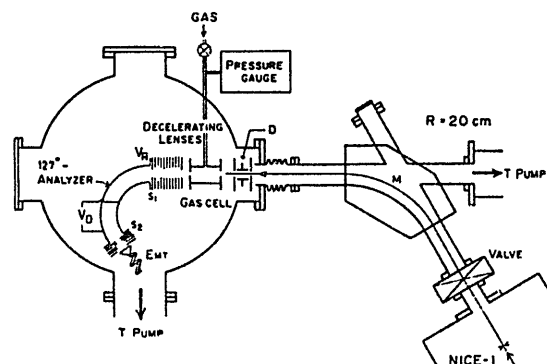


FIG. 1. Schematic view of the apparatus used for translation-energy spectroscopy.

tures.⁶

The translation-energy spectra of the charge-state-changed projectile ions are obtained by scanning the decelerating voltage V_R' while the deflection voltage V_D of the analyzer is kept at the same voltage, 30 V, as that for the incident projectile ions. In order to obtain the absolute scale of the energy in the energy spectra, the parameter K in Eq. (7) has to be determined. First, we determined K using a Li^+ -ion beam which is generated from a thermal-emission-type ion source. In this case the ion energy is entirely determined by the acceleration voltage, and then K is found to be equal to 1.21. This number is very close to that estimated from the geometry of the analyzer ($K=1.24$). Secondly, we have checked this number by

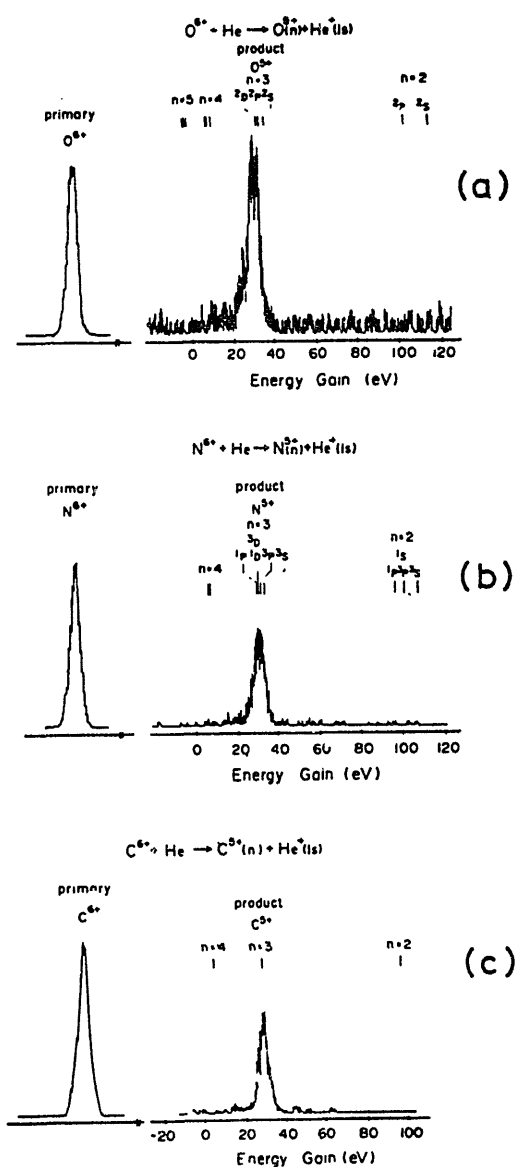


FIG. 2. (a) Typical energy spectrum of O^{5+} ions in the forward direction from the $\text{O}^{6+} + \text{He}$ collision at 0.33 keV/amu. (b) Typical energy spectrum of N^{5+} ions in the forward direction from the $\text{N}^{6+} + \text{He}$ collision at 0.30 keV/amu. (c) Typical energy spectrum of C^{5+} ions in the forward direction from the $\text{C}^{6+} + \text{He}$ collision at 0.46 keV/amu.

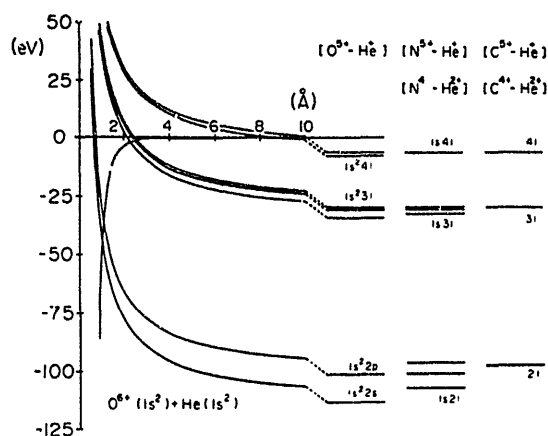


FIG. 3. Diabatic potential curves for the one-electron-capture process, $\text{O}^{6+}(1s^2) + \text{He} \rightarrow \text{O}^{5+}(1s^2n) + \text{He}^+(1s)$, and energy diagrams for channels of the one-electron capture into $\text{O}^{5+}(1s^2n)$, $\text{N}^{5+}(1sn)$, and $\text{C}^{5+}(nl)$ levels.

measuring the relationship between the deflection voltage V_D and the decelerating voltage V_R based upon Eq. (5). It was found that V_D changes very much linearly with V_R , resulting in $K=1.213 \pm 0.003$ for the deflection voltage ranging from 20 to 40 V, which is very close to the number obtained with Li^+ -ion beams. Therefore, $K=1.21$ is used in the present energy analysis.

The stable-isotope gases $^{18}\text{O}_2$, $^{15}\text{N}_2$, and ^{13}CO are used for source gases in order to separate the highly stripped ions from impurity ions. The helium gas used for the target is in a research grade with 99.999% purity. Background pressures were less than 10^{-10} Torr at the ion source and 10^{-7} Torr at the outside of the collision cell. Under the operation condition, the source pressure was around 10^{-9} Torr, the target pressure in the cell was kept at about 10^{-4} Torr, and the pressure outside the cell was about 10^{-6} Torr.

III. RESULTS AND DISCUSSION

The energy-spectroscopic measurements have been made for hydrogenlike and heliumlike ions of oxygen, nitrogen, and carbon such as O^{6+} , $\text{N}^{6,5+}$, and $\text{C}^{5,4+}$ at the energies of q and $2q$ keV, where $q+$ is the charge of the projectile ion incident upon the neutral-helium target. The present experiment has been made in extension of the previous one^{3,4} for fully stripped ions colliding with He. In this section, however, the experimental results are presented and classified according as the ionic charge state q rather than the isoelectronic sequence of the incident projectiles, because good similarity is found in the spectra obtained for the ions with the same incident-ionic charge state q . The measured energy gains ΔE of the charge-state-changed projectile ions are compared to the reaction energies Q calculated from the book of Bashkin and Stoner⁷ and then the electron-capturing levels of charge-state-changed projectiles are determined.

TABLE I. Observed energy gains and related levels of charge-state-changed projectiles. Energy gain ΔE is determined from the peak position in the energy spectrum measured. The reaction energy Q is calculated with energy levels given by Bashkin and Stoner (Ref. 7). R_c is the crossing distance of diabatic potential curves in consideration of the polarization for the initial channel and the Coulomb repulsion for the final channel; note that R_c is calculated by the use of the ionic charge state q . R_x is an internuclear distance limit at which an electron can get over the potential barrier between target and projectile in the classical model [see Eq. (14) in text].

Incident	ΔE (eV)	product	Q (eV)	R_c (Å)	R_x (Å)
O^{7+}	18.0 ^a	$O^{6+}(1s\ 4p\ ^1P)$	16.95	5.13	
		$(1s\ 4d\ ^{1,3}D)$	17.05	5.11	
		$(1s\ 4f\ ^{1,3}F)$	17.12	5.09	
		$(1s\ 4s\ ^3S)$	17.45	4.99	
		$(1s\ 4p\ ^3P)$	17.46	4.99	4.4
N^{7+}	16.8 ^a	$N^{6+}(4f\ ^2F)$	17.08	5.10	
		$(4d\ ^2D)$	17.09	5.10	
		$(4s\ ^2S)$	17.10	5.09	
		$(4p\ ^2P)$	17.10	5.09	4.4
O^{6+}	29.5	$O^{5+}(1s^2 3d\ ^2D)$	29.89	2.53	
		$(1s^2 3p\ ^2P)$	30.94	2.26	
		$(1s^2 3s\ ^2S)$	34.18	2.26	4.2
N^{6+}	30.0	$N^{5+}(1s\ 3p\ ^1P)$	29.51	2.56	
		$(1s\ 3d\ ^3D)$	29.89	2.53	
		$(1s\ 3d\ ^1D)$	29.93	2.53	
		$(1s\ 3p\ ^3P)$	30.78	2.47	
		$(1s\ 3s\ ^3S)$	32.66	2.34	4.2
C^{6+}	29.0 ^b	$C^{5+}(3d\ ^2D)$	29.84	2.53	
		$(3s\ ^2S)$	29.86	2.53	
		$(3p\ ^2P)$	29.86	2.53	4.1
N^{5+}	16.0	$N^{4+}(1s^2 3d\ ^2D)$	13.24	4.39	
		$(1s^2 3p\ ^2P)$	14.07	4.14	
		$(1s^2 3s\ ^2S)$	16.75	3.50	3.9
C^{5+}	13.6	$C^{4+}(1s\ 3p\ ^1P)$	12.98	4.48	
		$(1s\ 3d\ ^1D)$	13.21	4.40	
		$(1s\ 3d\ ^3D)$	13.24	4.39	
		$(1s\ 3p\ ^3P)$	13.97	4.17	
		$(1s\ 3s\ ^1S)$	14.00	4.16	
		$(1s\ 3s\ ^3S)$	15.44	3.78	3.9
C^{4+}	31	$C^{3+}(1s^2 2p\ ^2P)$	31.91	1.57	
		$(1s^2 2s\ ^2S)$	39.91	1.35	3.6

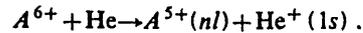
^aTaken from Ref. 4.

^bTaken from Ref. 1.

A. O^{6+} , N^{6+} + He collisions

The energy spectra of the product O^{5+} ion in the O^{6+} + He collision and of the product N^{5+} ion in the N^{6+} + He collision are shown in Figs. 2(a) and 2(b), together with the energy profile of the primary ions. Figure 2 clearly demonstrates that the energy-spectral patterns of the product O^{5+} and N^{5+} ions are quite similar not only to each other but also to that of the C^{5+} ion in the C^{6+} + He collision reported previously³ and is shown in Fig. 2(c) as a reference. In Fig. 2 are indicated the calcu-

lated energy levels which correspond to some principal quantum numbers n of the product A^{5+} ions for the one-electron-capture process,



As seen in Fig. 2, the electron is captured into neither the $n=2$ shell nor the $n=4$ shell. In each energy spectrum, only a single peak is observed at the energy gain of around 30 eV and it corresponds to the one-electron capture into the $n=3$ shell of the charge-state-changed projectiles of O^{5+} and N^{5+} as

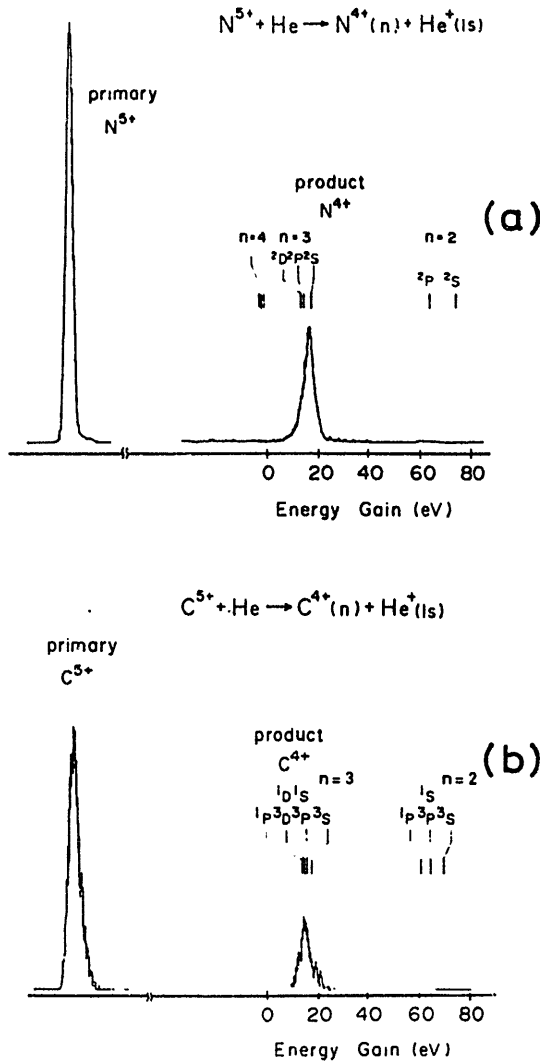


FIG. 4. (a) Typical energy spectrum of N^{4+} ions in the forward direction from the $N^{5+} + He$ collision at 0.33 keV/amu. (b) Typical energy spectrum of C^{4+} ions in the forward direction from the $C^{5+} + He$ collision at 0.38 keV/amu.

$$O^{6+}(1s^2) + He(1s^2) \rightarrow O^{5+}(1s^2 3l) + He^+(1s) + Q \quad (8)$$

and

$$N^{6+}(1s) + He(1s^2) \rightarrow N^{5+}(1s 3l) + He^+(1s) + Q, \quad (9)$$

where Q is distributed from 29.89 to 34.18 eV for the $O^{6+} + He$ collision and from 29.51 to 32.66 eV for the $N^{6+} + He$ collision. The energy resolution in the present experiment is not high enough to separate the sublevels of the $n=3$ shell.

In consideration of the polarization for the initial channel and the Coulomb repulsion for the final channel, the diabatic potential curves are presented in Fig. 3 for the collision systems of $O^{6+} + He$ and $N^{6+} + He$, along with the system of $O^{6+} + He$. This figure illustrates good similarity among the potential curves of these collision systems and such similarity is considered to give the simi-

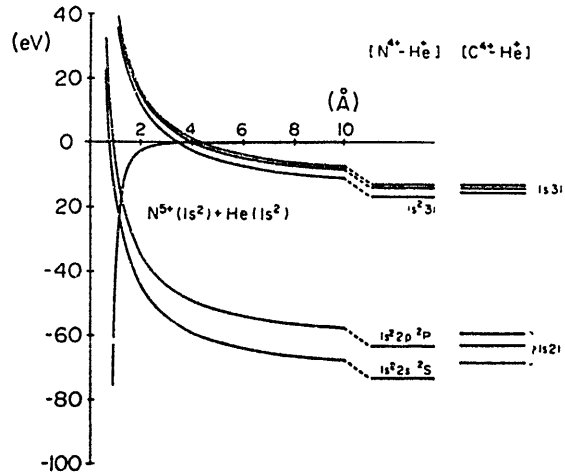


FIG. 5. Diabatic potential curves for the one-electron-capture process, $N^{5+}(1s^2) + He \rightarrow N^{4+}(1s^2nl) + He^+(1s)$, and energy diagrams for channels of one-electron capture into $N^{4+}(1s^2nl)$ and $C^{4+}(1s2nl)$ levels.

larity in the energy spectra obtained for the one-electron-capture process by the O, N, and C ions having the same charge $q=6$ from He. The calculated reaction energies Q and the crossing distances R_c in the related channels are listed in Table I.

It is noted here that the values of the R_c are slightly different from those of crossing distances R_n evaluated in Ref. 1; in the present paper, the R_c is calculated by the use of the ionic charge q , whereas the R_n is done by the use of the effective charge Z^* (see Ref. 1 for details).

B. $N^{5+}, C^{5+} + He$ collisions

Good similarity is also observed between the energy spectra obtained in the $N^{5+} + He$ and $C^{5+} + He$ collisions as shown in Figs. 4(a) and 4(b). This is expected from the similarity of the diabatic potential curves presented in Fig. 5.

For the $N^{5+} + He$ collision, as shown in Fig. 4(a), only a single peak is observed at the energy gain of 16 eV, and it corresponds to the one-electron capture into the $n=3$ shell of the product N^{4+} ion as

$$N^{5+}(1s^2) + He(1s^2) \rightarrow N^{4+}(1s^2 3l) + He^+(1s) + Q, \quad (10)$$

where Q is distributed from 13.24 to 16.75 eV as listed in Table I. In this case the energy resolution is too poor to allow separation of the sublevels.

Typical energy spectrum obtained in the $C^{5+} + He$ collision is shown in Fig. 4(b). Only a single peak is observed at the energy gain of 13.6 eV and it corresponds to the one-electron-capture process

$$C^{5+}(1s) + He(1s^2) \rightarrow C^{4+}(1s 3l) + He^+(1s) + Q. \quad (11)$$

The Q values are distributed from 12.98 to 15.44 eV for the $1s 3l$ states as listed in Table I. The observed peak re-

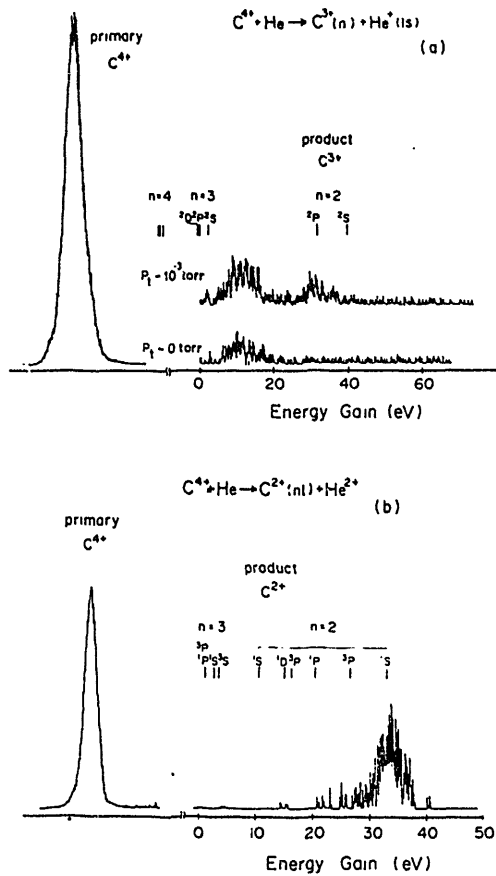


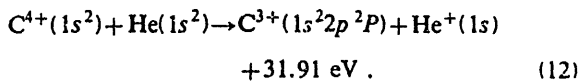
FIG. 6. (a) Typical energy spectrum of C^{3+} ions in the forward direction from the $C^{4+} + He$ collision at 0.31 keV/amu. (b) Typical energy spectrum of C^{2+} ions in the forward direction from the $C^{4+} + He$ collision at 0.31 keV/amu.

sults from these states, though the preferentially capturing sublevels cannot be definitely assigned.

C. $C^{4+} + He$ collision

In the energy gain spectra of the charge-state-changed C^{3+} ion in the $C^{4+} + He$ collision, two peaks are observed at around 12 and 31 eV as shown in Fig. 6(a). The former peak at 12 eV is considered to be due to collisions with background gases because it is still observed without the He target gas.

The latter peak at 31 eV increases with an increase of the target pressure of He gas and is originated from the charge-state-changed C^{3+} ion in the one-electron-capture process by C^{4+} from He. The energy spectrum of the product C^{3+} ion reveals clearly that an electron is not captured into the $C^{3+}(1s^2 2s^2 S)$ but into the $C^{3+}(1s^2 2p^2 P)$ level in the reaction such as



In Fig. 7 are shown the diabatic potential curves for one- and two-electron-capture processes. The small value of the observed cross section⁸ of reaction (12) may be re-

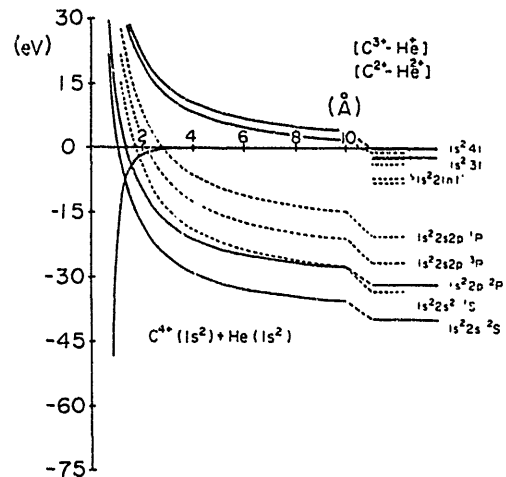
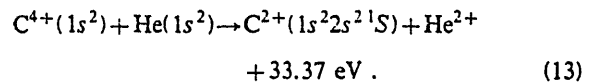


FIG. 7. Diabatic potential curves for the $C^{4+} + He$ collision and energy diagrams. Solid and dashed lines are for one- and two-electron-capture channels into $C^{3+}(1s^2 n)$ and $C^{2+}(1s^2 2l 2l')$ levels, respectively.

lated to the very short crossing distance (1.57 Å). There are some potential curve crossings at around 2 Å for the two-electron-capture process. The C^{2+} product peak is observed in the $C^{4+} + He$ collision as shown in Fig. 6(b) and it corresponds to the ground state of the C^{2+} ion in the two-electron-capture process



The two-electron-capture process takes place more efficiently than the one-electron capture at the low-energy region as reported by Crandall.⁹ From the comparison between the peak heights of the C^{3+} and C^{2+} product ions we estimated that the total cross section of two-electron capture by C^{4+} from He is about thirty times larger than that of one-electron capture at 0.31 keV/amu. This ratio agrees roughly with that calculated by Shipsey *et al.*¹⁰

Finally, we add mention of the $O^{7+} + He$ and $N^{7+} + He$ collisions which have been reported in connection with the transfer ionization process.⁴ Patterns of the energy spectra obtained in both the collisions are very similar to each other (see Figs. 3 and 4 in Ref. 4) as expected from the similarity in the diabatic potential curves concerned. Dominant peaks in the energy spectra are observed at the energy gains of about 17–18 eV and they correspond to the one-electron capture into the $n=4$ shell of the product O^{6+} and N^{6+} ions. The reaction energies Q and the crossing distances R_c in the related channels are listed in Table I.

IV. CONCLUDING REMARKS

In this paper, we classified the experimental results according to the ionic charge state q rather than the isoelectronic sequence of the incident projectiles. There is good similarity among the energy spectra for ions having the same charge state q . This is quite natural because the diabatic potential curves are not very dependent on the num-

ber of core electrons of incident ions and, as a result, are very similar for ions with the same charge state q .

It is clearly demonstrated that all the observed peaks in the energy spectra obtained in the forward direction are originated from the exothermic channels in the electron-capture processes without the excitation of the He^+ ion, and no signals due to the endothermic processes are found over noise levels in any energy spectra. In the one-electron-capture processes by fully stripped, hydrogenlike and heliumlike ions, O^{q+} , N^{q+} , and C^{q+} , from the neutral He atom, it is confirmed experimentally that an electron is captured selectively into only a single shell of charge-state-changed projectiles. As summarized in Table II, the principal quantum numbers n of the capturing levels of charge-state-changed ions are determined as $n=4$ for O^{8+} , O^{7+} , and $\text{N}^{7+} + \text{He}$ collisions, $n=3$ for O^{6+} , N^{6+} , C^{6+} , N^{5+} , and $\text{C}^{5+} + \text{He}$ collisions, and $n=2$ for the $\text{C}^{4+} + \text{He}$ collision.

It is interesting to compare these results with the prediction by the classical one-electron theory.² The theory characterizes an internuclear distance R_x at which the attractive force by the multiply charged ion becomes to exceed the binding force for the electron in the target atom. In other words, the R_x gives the outer limit of the internuclear distance where the one-electron-transfer reaction is possible. The R_x is given by

$$R_x = [Z_1^* + 2(Z_1^* Z_2^*)^{1/2}] / I_{\text{He}}, \quad (14)$$

where Z_1^* and Z_2^* are the effective charges of He^+ ion core and of q -charge-state ion core of the projectile, and I_{He} is the ionization energy of He atom in atomic units. The values of R_x given by Eq. (14) are listed in Table I. It is noted that most of the levels determined experimentally have the crossing distance R_c which is smaller than the R_x , but is the largest inside the R_x . In some cases including O^{7+} and N^{7+} , however, the R_c is slightly larger than the R_x .¹¹ This discrepancy may be due to the crudeness of the classical theory and the inaccuracy of the potential curves. For other cases the classical theory correctly predicts the principal quantum number n of the level into which the electron is captured. The theory could be a criterion for prediction of the electron-capturing levels. It should be

TABLE II. Principal quantum numbers n of selectively capturing levels of charge-state-changed projectiles $A^{(q-1)+}$ in the $A^{q+} + \text{He}$ collision.

A	$q=8$	$q=7$	$q=6$	$q=5$	$q=4$
O	4	4	3		
N		4*	3	3	
C			3	3	2

*The classical model (Ref. 1) predicts $n=3$.

most interesting to see what relation exists between the cross sections and the R_c of the reaction channels determined. Unfortunately, the present data are not enough for a discussion of this subject and an effect to accumulate sufficient data for discussion of this subject is now under way.

Transfer ionization process producing a $(q-1)$ -charge-state ion of the projectile via two-electron capture into autoionizing levels was observed in some cases; for example, the $\text{O}^{7+} + \text{He}$ and $\text{N}^{7+} + \text{He}$ collisions.⁴ The two-electron-capture process was found to be much more dominant than one-electron-capture process in the $\text{C}^{4+} + \text{He}$ collision. In the cases of one- and two-electron-capture processes by C^{4+} not only the principal quantum number n but also the orbital quantum number l could be determined because the energy separation of the sublevels becomes larger in low- n shells.

ACKNOWLEDGMENTS

This work was carried out as a part of the Guest Research Program at the Institute of Plasma Physics, Nagoya University. The authors are grateful to Professor H. Kakihana, the Director of the Institute, and to Professor Emeritus K. Takayama, the former Director of the Institute, for their encouragement throughout this work. Thanks are also due to Professor T. Watanabe of the University of Tokyo for his interest and helpful discussion and to Mr. T. Hino for his technical skill and help.

*Permanent address: Department of Physics, Tokyo Metropolitan University, Setagaya-ku, Tokyo 158, Japan.

†Permanent address: Department of Liberal Arts, Kansai Medical University, Hirakata, Osaka 573, Japan.

‡Permanent address: Department of Physics, Osaka University, Toyonaka, Osaka 560, Japan.

§Permanent address: Department of Applied Physics, Tokyo University of Agriculture and Technology, Koganei, Tokyo 184, Japan.

¹T. Iwai, Y. Kaneko, M. Kimura, N. Kobayashi, S. Ohtani, K. Okuno, S. Takagi, H. Tawara, and S. Tsurubuchi, *Phys. Rev. A* **26**, 105 (1982).

²H. Ryufuku, K. Sasaki, and T. Watanabe, *Phys. Rev. A* **21**, 745 (1980).

³S. Ohtani, Y. Kaneko, M. Kimura, N. Kobayashi, T. Iwai, A. Matsumoto, K. Okuno, S. Takagi, H. Tawara, and S. Tsurubuchi, *J. Phys. B* **15**, L533 (1982).

⁴S. Tsurubuchi, T. Iwai, Y. Kaneko, M. Kimura, N. Kobayashi, A. Matsumoto, S. Ohtani, K. Okuno, S. Takagi, and H. Tawara, *J. Phys. B* **15**, L733 (1982).

⁵H. Imamura, Y. Kaneko, T. Iwai, S. Ohtani, K. Okuno, N. Kobayashi, S. Tsurubuchi, M. Kimura, and H. Tawara, *Nucl. Instrum. Methods* **188**, 233 (1981).

⁶J. Arianer and Ch. Goldstein, *IEEE Trans. Nucl. Sci.* **NS-23**, 979 (1976); E. D. Donets, *ibid.* **NS-23**, 897 (1976).

⁷S. Bashkin and J. O. Stoner, Jr., *Atomic Energy Levels and Grottrian Diagram I* (North-Holland, Amsterdam, 1975).

⁸The total cross section of one-electron capture in the $\text{C}^{4+} + \text{He}$ collision was reported as $0.85 \times 10^{-16} \text{ cm}^2$ at 0.5 keV/amu in Ref. 1. However this value should be considered as an upper limit of the cross section because it could be affected by a small amount of the background gas.

⁹D. H. Crandall, *Phys. Rev. A* **16**, 958 (1977).

¹⁰E. J. Shipsey, J. C. Browne, and R. E. Olson, *Phys. Rev. A* **15**,

2166 (1977).

¹¹As mentioned in Sec. III A, the R_c value is slightly different from the R_n value which is evaluated in Ref. 1. If the R_n is used instead of the R_c , the classical theory correctly predicts

the experimentally determined principal quantum numbers n of the capturing levels with the sole exception in $N^{7+} + He$ collisions.

GAIN CHARACTERISTICS OF A MICROCHANNEL PLATE AND A CHANNEL-ELECTRON MULTIPLIER FOR LOW ENERGY MULTIPLY CHARGED IONS

S. TAKAGI, T. IWAI *, Y. KANEKO **, M. KIMURA ***, N. KOBAYASHI **, A. MATSUMOTO, S. OHTANI, K. OKUNO ⁶⁾, H. TAWARA + and S. TSURUBUCHI ++

Institute of Plasma Physics, Nagoya University, Nagoya 464, Japan

Received 15 November 1982 and in revised form 28 February 1983

Pulse height distributions are measured when multiply charged ions of S, Ne, F, O, N and C are incident on a microchannel plate of chevron type (MCP) and a channel electron multiplier (CEM) in the velocity range of $3-4.5 \times 10^5$ m/s. The pulse height distribution obtained with the CEM shows no significant dependence of the gain on the energy, mass and charge state of incident ions. On the other hand, for the case of the MCP, an increase of the gain is observed with an increase of the charge state of incident ions irrespectively of ionic species. Such behavior is discussed in connection with secondary electron emission yield at the input and electron multiplication mechanisms in the channels.

1. Introduction

A channel-electron multiplier (CEM) has been used widely as a detector for electrons, ions and energetic photons. Because of its simple structure, small size and ruggedness, the CEM was first applied to space research. The detector also has inherent advantages such as high gain, and low background noise. Therefore, the CEM is now a common instrument for the detection of charged particles in atomic collision experiments as well as space experiments. In parallel with the development of the CEM, microchannel plates (MCPs) are commercially available [1]. Since the MCP is array of 10^4-10^7 miniature channel-electron multipliers parallel to one another, it has good spacial resolution and rapid time response in addition to similar advantages as the CEM.

Both the detectors were operated in a pulse counting mode. In such a counting operation, the detection efficiency and the gain are the most important characteristics. The detection efficiency, which is defined as the number of output pulses per number of incident par-

ticles, has been investigated by many authors for charged particles and photons and a review of existing knowledge up to 1976 has been given by Macau et al. [2].

Recently, collision processes involving multiply charged ions have been of great importance in connection with thermonuclear fusion research. The characteristics of the CEM and MCP for multiply charged ions, however, has received little study to date. Fricke et al. reported the detection efficiency and gain characteristics of the CEM for multiply charged A^{q+} ($q \leq 6$) ions or rare gases in the incident energy range of 4-15 keV [3]. Meanwhile no investigation has been reported on the characteristics of the MCP.

In the present paper, we describe the gain characteristics of the MCP and CEM for multiply charged S, Ne, F, O, N and C ions at the incident energies from a few keV to a few tens of keV.

2. Experimental procedure

Fig. 1 shows a schematic of the experimental arrangement used in the present study. Multiply charged ions are produced by an electron beam ion source (EBIS), called NICE-1 [4]. Ions extracted from the source are accelerated to a desired energy and mass-analyzed by a 60° sector magnet. The ion beam is then collimated by a series of apertures, A_1 (1 mm in I.D.), A_2 (1 mm in I.D.), A_3 (0.8 mm in I.D.) and A_4 (1 mm in I.D.), and it then enters a parallel plate electrostatic analyzer. By applying an appropriate voltage to the analyzer, the ion beam was received with an MCP, while the ion beam was received directly with a CEM without

* Permanent address: Department of Liberal Arts, Kansai Medical University, Hirakata, Osaka 573, Japan.

** Permanent address: Department of Physics, Tokyo Metropolitan University, Setagaya-ku, Tokyo 158, Japan.

*** Permanent address: Department of Physics, Osaka University, Toyonaka, Osaka 560, Japan.

+ Permanent address: Nuclear Engineering Department, Kyushu University, Fukuoka 812, Japan.

++ Permanent address: Department of Applied physics, Tokyo University of Agriculture and Technology, Koganei, Tokyo 184, Japan.

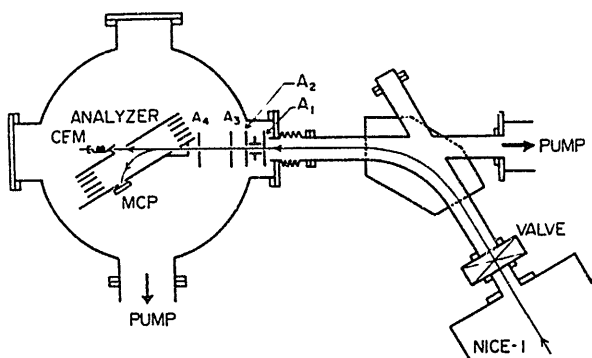


Fig. 1. Experimental apparatus.

the applied voltage. In order to avoid any acceleration and deceleration of the incident ions, the input of the CEM was grounded, and also the input of the MCP and the exit aperture plate of the analyzer were grounded.

The CEM used in the present experiment (MURATA EMS-1081B) has a cone-shaped input of 10 mm aperture and a spiraled amplification section with 1 mm in I.D. and 100 mm in total length; the operation voltage was 3 kV. The MCP used is of tandem type (HAMAMATSU TV F1158-11) having an effective aperture of 20 mm diameter. The diameter of each pore is $12 \mu\text{m}$ and the ratio of the length to the diameter is 45. The front and rear plates of MCPs have the same bias angle of 8° to the input surface normal and the plate separation is 0.03 mm. The operation voltage was 0.9 kV per plate. For the present experimental arrangement, the ion beam passing through the exit aperture ($5 \times 8 \text{ mm}^2$) of the analyzer was incident on the MCP at an angle of 60° to the plate normal.

The MCP and CEM were operated in a single pulse counting mode. The charge output of these multipliers for each input event was fed through a charge-sensitive preamplifier to a main amplifier-discriminator system. The discriminator threshold, however, was kept at zero throughout experiments. The output pulse was fed to a scaler and a multichannel analyzer. The gain characteristics of both the detectors were investigated by recording the output pulse height distribution (PHD) with the multichannel analyzer for a number of multiply charged S, Ne, F, O, N and C ions in the incident velocity range of $3\text{--}4.5 \times 10^5 \text{ m/s}$. The background pressure was maintained below 1×10^{-8} Torr throughout the present study.

3. Results

3.1. Pulse height distribution and the relative gain

In fig. 2 is shown a typical pulse height distribution (PHD) observed for the Ne^{9+} ion incident on the MCP;

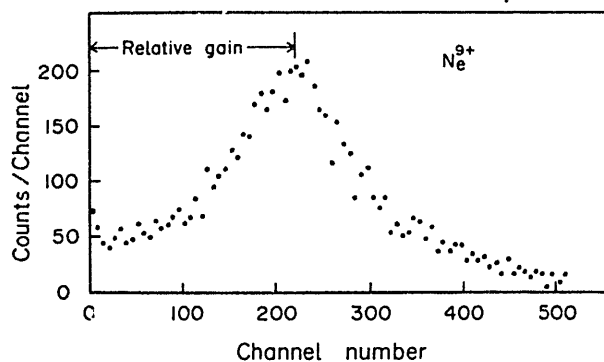


Fig. 2. Pulse height distribution for the Ne^{9+} ion incident on the MCP. The incident velocity is $3.4 \times 10^5 \text{ m/s}$ and the count rate is 1354 cps.

the incident velocity was $3.4 \times 10^5 \text{ m/s}$ and the count rate was 1354 cps; the channel number illustrated in the figure is proportional to the output pulse height. The PHD observed contains pulses from thermal, background noises as well as true signal pulses. Signals below a valley, which appears at around 20 of relative pulse height in fig. 2, are mainly due to pulses of the background noise. In fact, a negative exponential shape was observed at a low pulse height side in the PHD when no ion was incident on the MCP. This fact enables one to discriminate easily and surely between true pulses and background noise pulses.

Except for the background noise, the main feature of the observed PHD was a quasi-Gaussian shape for all the ions studied, as expected from the space-charge saturation effect [5]. Such a quasi-Gaussian shape in the PHD was also observed with the CEM.

The gain is usually defined as the ratio of the number of output electrons to the number of incident particles. Due to statistical fluctuations of the secondary electron emission, the gain also varies statistically. When the PHD is a quasi-Gaussian shape as observed in the present case, it is convenient to define the average gain of the MCP to be the modal (most probable) number of output electrons per pulse. Therefore, we define the relative gain to be the pulse height value at the peak in the observed PHD (see fig. 2).

3.2. Gain characteristics of MCP

The measured relative gain of the MCP is illustrated in fig. 3 as a function of the count rate. In order to get a general feeling, the data for almost all the ions studied are shown in this figure. It is quite remarkable that the gain decreases when the count rate exceeds about 1000 cps. Such gain reduction may be due to the dense injection of the incident beam [6,7] (beam diameter $\sim 1 \text{ mm}^2/2500$ pores). If the incident particles are injected widely over the surface of the MCP, that is, the current

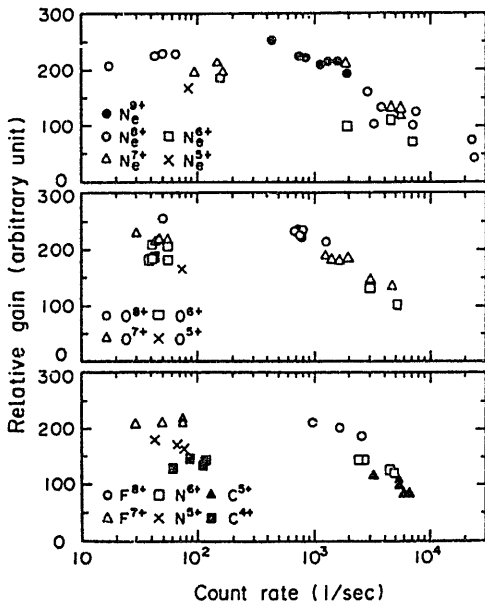


Fig. 3. The measured relative gain of the MCP as a function of the count rate.

density of the incident beam is decreased, a gain reduction does not occur when the count rate is in excess of 1000 cps. From this gain reduction, the recovery time is roughly estimated at about 250 ms, if a single burst of multiplied electrons from the front MCP is supposed to spread into about ten pores at the rear MCP. In the tandem MCP it is considered that the recovery time becomes longer than the estimation by Wiza [7] when many pores are used at the rear MCP for single ion input [8]. In the present work, detailed investigations were carried out under conditions of the count rate being less than 500 cps.

The relative gains measured for Ne⁹⁻⁵⁺, F⁷⁺, O⁸⁻⁵⁺, N⁵⁺ and C⁴⁺ ions are shown in fig. 4 as a function of the incident velocity; each data point is an average of several measurements and the statistical error is esti-

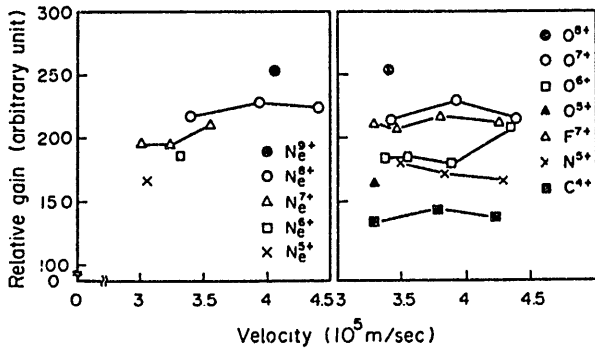


Fig. 4. The relative gain of the MCP as a function of the incident velocities.

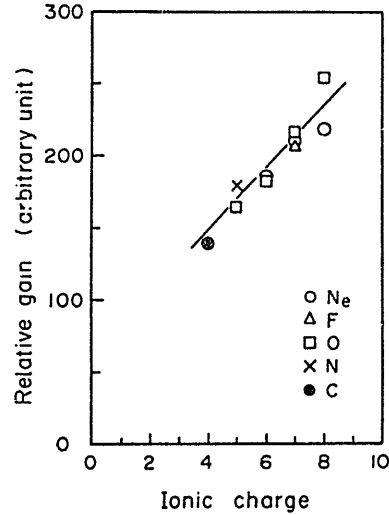


Fig. 5. The relative gain of the MCP as a function of the ionic charge. The incident velocity is about 3.5×10^5 m/s.

mated roughly to be $\pm 6\%$. The measured pulse height distributions show no significant dependence of the relative gain on the incident velocity, though the present velocity range is rather narrow ($3-4.5 \times 10^5$ m/s). Then, the relative gains reasonably interpolated at a velocity of 3.5×10^5 m/s are displayed in fig. 5 as a function of the ionic charge state q for all the A^{q+} ions observed. As seen in fig. 5, the relative gains increase with the charge state q and seem to line up on a straight line irrespectively of ionic species.

3.3. Gain characteristics of CEM

As mentioned in sect. 3.1. the pulse height distribution (PHD) obtained with the CEM was quite similar to that obtained with the MCP for all the ions investigated. In the space-charge saturation mode, the mea-

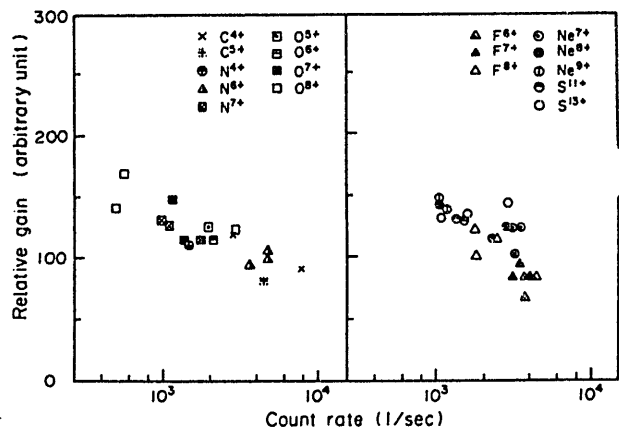


Fig. 6. The measured relative gain of the CEM as a function of the count rate.

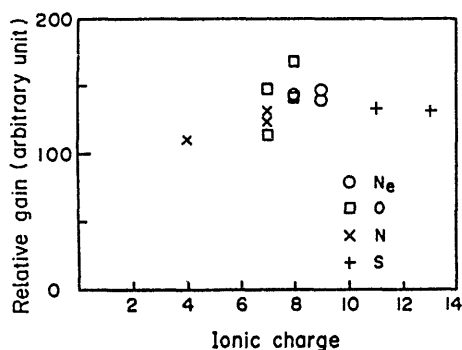


Fig. 7. The relative gain of the CEM as a function of the ionic charge. The gains are measured in the incident velocity range of $3\text{--}4.5 \times 10^5$ m/s.

sured PHD shows no significant dependence of the relative gain on the incident velocity. In fig. 6 is shown the relative gain as a function of the count rate for all the ions studied. Similarly to the case of the MCP, the relative gain decreases slowly with the count rate.

Then, by using the data obtained at a count rate less than 1500 cps, the relative gains are plotted as a function of the ionic charge state in fig. 7. Here the statistical error of each data point was approximately $\pm 11\%$. In contrast to the case of the MCP, the relative gain is nearly independent of the ionic charge state for the CEM.

4. Discussion

The present result of the gain characteristics obtained with the CEM is in agreement with that reported by Fricke et al. [3]; the gain depression with the count rate and no significant dependence of the gain on ionic species, velocities or charge states.

According to the study of the electron multiplication mechanism of the CEM, the output pulse height distribution changes from a negative exponential to a quasi-Gaussian shape with increasing gain levels and such a peaked distribution is the result of space-charge saturation near the channel output [5]. Therefore, the modal gain is expected to be independent of the charge state, velocity and mass of incident ions, as far as the CEM is operated in the space-charge saturation mode. This is verified by the present and Fricke et al. experiments.

The next problem, then, is why the gain of the MCP does depend on the charge state, although its pulse height distribution is quasi-Gaussian. In order to remove ion feedback and to get stable operations at high gain levels, the MCP used was a chevron type which consists of front and rear plates. Secondary electrons emitted from each channel of the front plate fires several channels of the rear plate owing to the space charge

effect. Wiza observed that the PHD from a MCP (not a chevron) is nearly a negative exponential [7]. His result suggests that the space charges do not saturate at the output of the front section, but the saturation is attained in the rear section. Therefore, even in a saturation mode as a whole, an increase of the space charge density is still possible at the output of the front section. This increase results in an increase in the number of the fired channels in the rear section and finally in an increase of the gain.

In a non-saturation mode as expected in the front section of the MCP, the space charge density should be closely related to the secondary electron emission yield by impact of ions. As is well known, the secondary electron ejection is explained by two mechanisms, potential ejection and kinetic ejection [9]. We observed no significant dependence of the gain on the impact velocity. This fact suggests that the contribution of potential ejection dominates that of kinetic ejection in the velocity range studied.

Now consider the dependence of the electron emission yield at the front surface on the charge state of the incident ion, based upon the potential ejection mechanism. The secondary electron is ejected by Auger neutralization or Auger deexcitation. As the multiply charged ion comes close to the surface, the Auger process is expected to occur several times at one impact. As a result, the secondary electron emission yield at the input surface of the front section may increase with the charge state of the incident ion, which in turn causes an increase of the gain with the charge state.

On the other hand, such an increase of the gain could not be expected for the CEM, because it consists of a single channel and its gain is limited by the space-charge saturation in one continuous channel.

5. Conclusion

Relative gain characteristics of a CEM and a MCP have been measured for various kinds of incident ions in the velocity range of $3\text{--}4.5 \times 10^5$ m/s. The relative gains for both detectors are independent of the impact velocities of the incident ions investigated here. As for the dependence on the charge state q of the incident ions, the relative gains of the CEM are almost similar for the various kinds of the incident ions, but those of the MCP increase with q . This q -dependence of the relative gain for the MCP is interpreted in connection with the q -dependence of secondary electron emission yield at the input and the electron multiplication mechanism in channels of the MCP.

The authors are grateful to Mr. Y. Kawasumi for helpful discussions and Mr. T. Hino for his technical support and assistance.

References

- [1] W.B. Colson, J. McPherson and F.T. King, *Rev. Sci. Instr.* 44 (1973) 1694.
- [2] J.P. Macau, J. Jamer and S. Gardier, *IEEE Trans. Nucl. Sci.* NS-23 (1976) 2049.
- [3] J. Fricke, A. Müller and E. Salzborn, *Nucl. Instr. and Meth.* 175 (1980) 379.
- [4] Y. Kaneko, T. Iwai, S. Ohtani, K. Okuno, N. Kobayashi, S. Tsurubuchi, M. Kimura and H. Tawara, *J. Phys. B: At. Mol. Phys.* 14 (1981) 881.
- [5] K. Schmidt and C.F. Hendee, *IEEE Trans. Nucl. Sci.* NS-13 (1966) 100.
- [6] W.G. Wolber, B.D. Klettke and H.K. Lintz, *Rev. Sci. Instr.* 40 (1969) 1364.
- [7] J.L. Wiza, *Nucl. Instr. and Meth.* 162 (1979) 587.
- [8] K. Oba, M. Sugiyama, Y. Suzuki and Y. Yoshimura, *IEEE Trans. Nucl. Sci.* NS-26 (1979) 346.
- [9] M. Kaminsky, *Atomic and Ionic Impact Phenomena on Metal Surface* (Springer-Verlag, Berlin, 1965) Ch. 12-14.

Measurement of Relative Population between $B^{2+}(2s)$ and $B^{2+}(2p)$ in Electron Capture Collision of B^{3+} with He

Atsushi MATSUMOTO, Tsuruji IWAI,* Yozaburo KANEKO,†
 Masahiro KIMURA,†† Nobuo KOBAYASHI,† Shunsuke OHTANI,
 Kazuhiko OKUNO,† Shoji TAKAGI, Hiroyuki TAWARA and
 Seiji TSURUBUCHI#

Institute of Plasma Physics, Nagoya University, Nagoya 464

(Received July 6, 1983)

One-electron capture processes into $B^{2+}(2s)$ and $B^{2+}(2p)$ have been investigated in B^{3+} -He collision at low velocities (1.3 - 2.3×10^7 cm/sec) using a translation energy spectroscopy. Energy dependence of the relative population between $B^{2+}(2s)$ and $B^{2+}(2p)$ is obtained and compared with the theoretical result of Shipsey *et al.*

Recently collision spectroscopy has become a useful means, as well as optical spectroscopy, to obtain a better understanding of electron capture processes by multiply charged ions from neutral atoms. We report here a measurement of relative population between $B^{2+}(2s)$ and $B^{2+}(2p)$ states in electron capture collision of B^{3+} with He at low collision energies using the technique of translation energy spectroscopy. Total cross sections for the one-electron capture by B^{3+} ion from He atom have been measured by several authors.¹⁻⁴⁾ Their data are roughly in agreement with each other, and the measured cross section has a broad maximum at the collision energy of around 20 keV (see Fig. 1). Shipsey *et al.*⁵⁾ calculated the electron capture cross sections for the present collision system by means of a molecular state close-coupling method; their result is in agreement with the experimental data as seen in Fig. 1. They also evaluated the contribution of electron

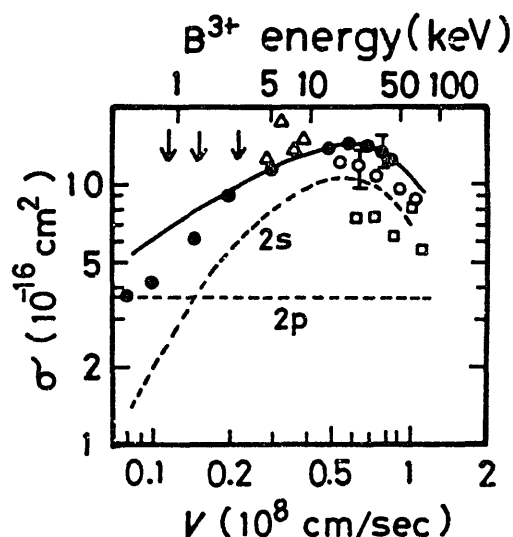


Fig. 1. Cross sections for one-electron capture by B^{3+} from He. Closed circles-Zwally and Cable (ref. 1), open circles-Crandall (ref. 2), squares-Gardner *et al.* (ref. 3), triangles-Iwai *et al.* (ref. 4). Solid curve is the result for total cross section of Shipsey *et al.* (ref. 5) and dashed curves are the partial cross sections for $B^{2+}(2s)$ and $B^{2+}(2p)$ states calculated by Shipsey *et al.* (ref. 5). Arrows indicate the energy points at which the present observation is made.

capture into the $B^{2+}(2s)$ and $B^{2+}(2p)$ states. Therefore, it is worthwhile to compare the present energy-spectroscopic data with the calculation of Shipsey *et al.*

The apparatus used and the experimental procedure have been described previously.^{6,7)} The energy spectra of the charge-changed

Permanent addresses:

* Department of Liberal Arts, Kansai Medical University, Hirakata, Osaka 573.

† Department of Physics, Tokyo Metropolitan University, Setagaya-ku, Tokyo 158.

†† Department of Physics, Osaka University, Toyonaka, Osaka 560.

Department of Applied Physics, Tokyo University of Agriculture and Technology, Koganei, Tokyo 184.

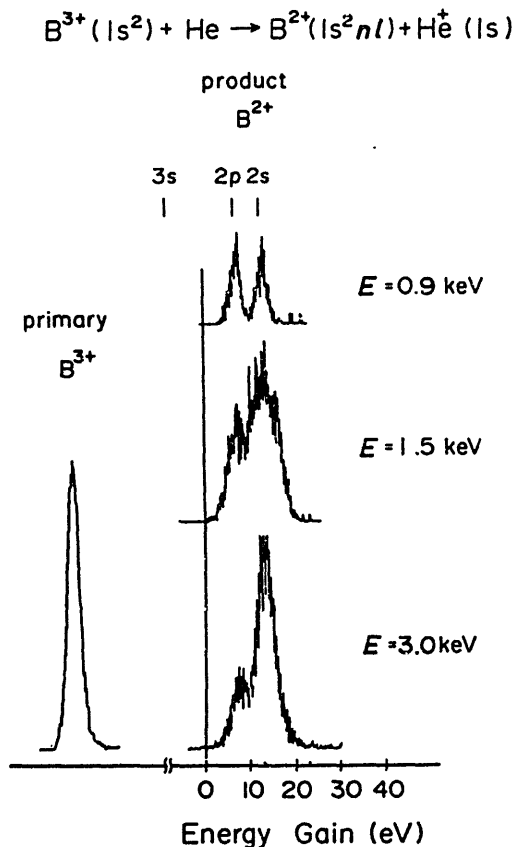
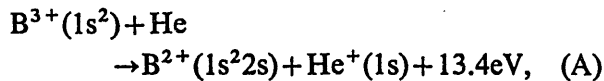
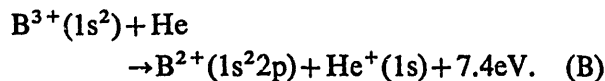


Fig. 2. Observed energy gain spectra of forwardly scattered B^{2+} ions in $B^{3+} + He$ collisions at collision energies of 0.9, 1.5 and 3 keV.

boron ions were observed at the collision energies of 0.9–3 keV, and the observed spectra are shown in Fig. 2, together with the energy profile of the primary B^{3+} ion. Two peaks are observed at the energy gain of 13.4 and 7.4 eV. By referring to the book of Bashkin and Stoner,⁸⁾ the two peaks are found to correspond to the following reactions:



and



No other peaks are observed in the collision energy range studied. This fact indicates that the metastable $B^{3+}(1s2s \ ^1,^3S)$ ion possibly contained in the primary ion beam does not contribute to these peaks. The present result reveals that an electron is captured selectively into the $n=2$ state, and this evidence is in accord with the prediction of the classical model discussed in the previous paper.⁴⁾

The relative peak intensity for the 2s and 2p states is quite sensitive to the collision energy as seen in Fig. 2. The relative intensity for the two states were determined from the best fit to the observed spectra by deconvolution with the energy profile of primary B^{3+} ions. The ratio $I(2s)/I(2p)$ obtained in this way is plotted as a function of the collision energy in Fig. 3, where the ratio of the respective cross section $\sigma(2s)/\sigma(2p)$ calculated by Shipsey *et al.* is also presented for comparison. The tendency that the ratio increases with an increase of the collision energy is seen in both the present experiment and the calculation. The measured ratio, however, increases more rapidly with the collision energy than the calculated result.

According to Shipsey *et al.*, the $B^{2+}(2s)$ state is populated via the radial coupling at the crossing distance $R_c \simeq 4.7a_0$ (a_0 : the Bohr radius), meanwhile the $B^{2+}(2p)$ state is populated through two rotational couplings between the Σ states and the Π state; the rotational coupling at the inner crossing $R_c \simeq 2a_0$ contributes at low energies and the coupling at the outer crossing $R_c \simeq 7a_0$ does at high energies. As a result, the population in the 2p state exhibits a weak energy dependence. Since the R_c values responsible for the reactions (A) and (B) are fairly small at low energies studied in the present experiment, the product ions may not be always scattered into the extremely forward direction. There-

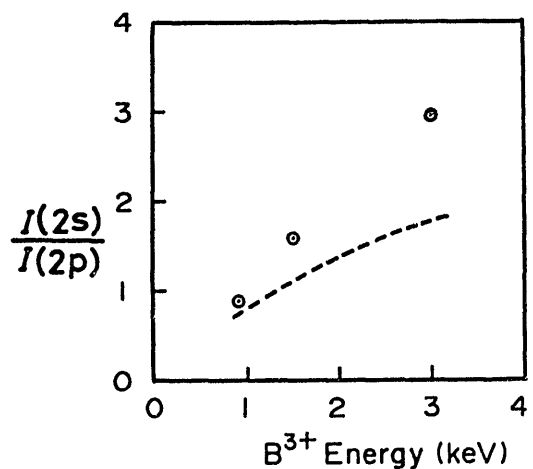


Fig. 3. Ratio $I(2s)/I(2p)$ as a function of the collision energy. Circles are the present data and the dashed curve is the theoretical result of Shipsey *et al.* (ref. 5).

fore, a part of the discrepancy between the observation and the theory mentioned above may arise from the incomplete collection of the product ions.* Optical measurements of the energy dependence of light emission from $B^{2+}(2p)$ would be complementary to the present work.

To our knowledge, this is the first observation which shows strong energy dependence of one-electron capture into the same n but different l states for multiply charged ions by the translation energy spectroscopy.

References

- 1) H. J. Zwally and P. G. Cable: *Phys. Rev. A* **4**

* If the product $B^{2+}(2s)$ and $B^{2+}(2p)$ ions are completely collected, $I(2s)/I(2p)$ is equal to $\sigma(2s)/\sigma(2p)$.

- (1971) 2301.
 2) D. H. Crandall: *Phys. Rev. A* **16** (1977) 958.
 3) L. D. Gardner, J. E. Bayfield, P. M. Koch, I. A. Sellin, D. J. Pegg, R. S. Peterson, M. L. Mallory and D. H. Crandall: *Phys. Rev. A* **20** (1979) 766.
 4) T. Iwai, Y. Kaneko, M. Kimura, N. Kobayashi, S. Ohtani, K. Okuno, S. Takagi, H. Tawara and S. Tsurubuchi: *Phys. Rev. A* **26** (1982) 105.
 5) E. J. Shipsey, J. C. Browne and R. E. Olson: *Phys. Rev. A* **15** (1977) 2166.
 6) S. Ohtani, Y. Kaneko, M. Kimura, N. Kobayashi, T. Iwai, A. Matsumoto, K. Okuno, S. Takagi, H. Tawara and S. Tsurubuchi: *J. Phys. B* **15** (1982) L533.
 7) K. Okuno, H. Tawara, T. Iwai, Y. Kaneko, M. Kimura, N. Kobayashi, A. Matsumoto, S. Ohtani, S. Takagi and S. Tsurubuchi: *Phys. Rev. A* **28** (1983) 127.
 8) S. Bashkin and J. O. Stoner, Jr: *Atomic Energy Levels and Grotrian Diagrams I* (Amsterdam, North-Holland, 1975).

7

Recent Activities at NICE Nagoya

S. Ohtani

Institute of Plasma Physics, Nagoya University, Nagoya 464, Japan

Received September 7, 1982; accepted September 24, 1982

Abstract

A report is given of recent activities at NICE Nagoya in atomic collision research. The measurements of the total and partial cross-sections for one-electron capture in collision of highly stripped light ions with helium are presented.

1. Introduction

Charge transfer recombination of highly stripped ionic species in collisions with atomic hydrogen and helium is an important atomic process in (D-T) burning plasmas where it may influence the particle and energy balances by lowering the ionization states and by leading to production of high energy photons. A detailed understanding of these processes is surely needed for the development of the fusion research.

On the other hand, the knowledge of state-selected, partial cross-sections for electron capture serves for plasma diagnostics. The intensity enhancement of a particular line emitted from impurity ions during the injection of neutral hydrogen or helium beam gives us information on the spatial distribution of such ions in a hot plasma.

In the course of experimental investigation on atomic processes at Institute of Plasma Physics (IPP), Nagoya University, a research program was started at the end of the summer 1977, for studies of collisional processes involving highly stripped ions, as a joint research program by guest staffs and collaborators in the IPP. The group consists of 16 physicists:

- T. Iwai (Kansai Medical Univ., Guest Prof. of IPP)
- Y. Kaneko (Tokyo Metropolitan Univ., Guest Prof. of IPP)
- M. Kimura (Osaka Univ.)
- N. Kobayashi (Tokyo Metropolitan Univ.)
- K. Okuno (Tokyo Metropolitan Univ.)
- H. Tawara (Kyushu Univ.)
- S. Tsurubuchi (Tokyo Univ. of Agriculture and Technology)
- A. Matsumoto (IPP)
- S. Takagi (IPP)
- S. Ohtani (IPP)

The research program done by this group is called the NICE project. NICE means Naked Ion Collision Experiments.

In the present paper, we will report on some recent activities of NICE; the measurements of total and partial cross-sections for one-electron capture processes of highly stripped, light ions in collisions with helium atoms.

2. Ion source

The ion source we have constructed is of EBIS type [1]. In the early stage of the NICE project, we built a prototype EBIS having conventional solenoids of about 50 cm in length, and, using this proto-NICE, we accumulated various experiences

on EBIS operation and got information on some characteristics of the ion source [2].

Based on these experiences, we have built a new ion source, called NICE-1, in 1979. A schematic view of NICE-1 is shown in Fig. 1. The NICE-1 has a superconducting magnet (SCM), which is 1 m in length and 10 cm in inside diameter. The magnetic field can be varied up to about 2 T. A surface of the liquid helium can of the magnet works as a cryogenic pump to reduce the background gas pressure in the ionization region. The background pressure measured at the outside of the vacuum vessel of the NICE-1 is usually around 1×10^{-10} torr and is expected to be less than this pressure in the ionization region inside the helium can. A very small amount of sample gas is continuously injected through the gap between the first and second drift tubes. A typical potential distribution applied to each element of the ion source for collision experiments is also shown in Fig. 1. All the potentials applied to the drift tubes (DT) are constant during the operation time. We call this operation a "continuous mode". Further details of the ion source are described in [3, 4].

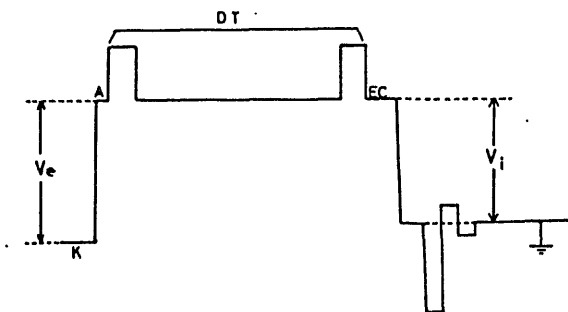
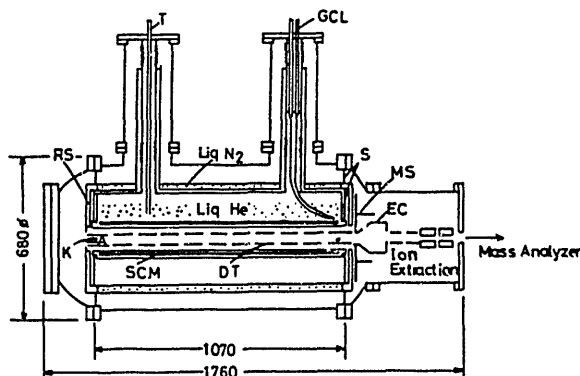


Fig. 1. Schematic view of NICE-1 and potential distribution applied to each element of the ion source.

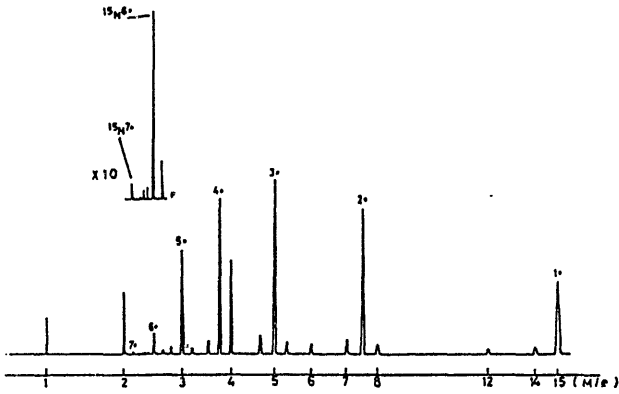


Fig. 2. Typical spectrum of $^{15}\text{N}^{q+}$ ions extracted at $V_i = 2.5$ kV from the NICE-1 under the condition that electron beam intensity is 10.5 mA at the $V_e = 2.5$ kV and beam diameter is less than 0.5 mm.

A typical charge state spectrum of ^{15}N extracted from the NICE-1 at the acceleration voltage of 2.5 kV is shown in Fig. 2. As mentioned above, the NICE-1 is operated in a continuous mode, where sample gas atoms and the electron beam are continuously supplied and, also, ions produced in the ion source are extracted continuously. Therefore, the charge state of ions extracted is widely distributed from 1+ to 7+. Their distribution is strongly dependent on the gas pressure in the ion source and on the energy and current of the electron beam. The intensity of the fully stripped N^{7+} ions is usually about 10 000 cps.

3. Collision experiments

3.1. Total cross-sections for one-electron capture

Using the ion source called NICE-1, we have recently measured cross-sections for one-electron capture by highly ionized atoms of B, C, N, O, F, Ne and S from He, at low energies [4, 5]. The

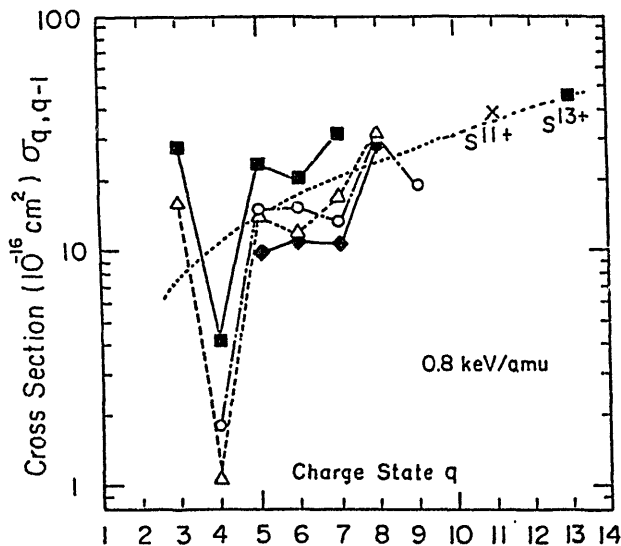


Fig. 3. Measured cross-sections $\sigma_{q, q-1}$ at 0.8 keV amu^{-1} as a function of the ionic charge q of projectile B, C, N, O, F, Ne and S ions. \bullet : fully stripped ions, \circ : H-like ions, Δ : He-like ions, \blacksquare : Li-like ions, \times : B-like ion. The dotted line is obtained from the empirical formula of Müller and Salzborn [15].

measured cross-sections are nearly independent of the collision energies investigated with only a few exceptions. When the cross-sections at 0.8 keV amu^{-1} are plotted as a function of the ionic charge q of isoelectronic projectile ions, strong oscillations in the cross-sections are observed for all ions (Fig. 3). This oscillatory behaviour is interpreted using the classical one-electron model [6] and the outline is as follows. In the one-electron capture processes at low energies, an electron is captured selectively into a level with a particular quantum number n . Such a level drastically changes from n to $n+1$ with an increase of q . This level-change results in an increase of the crossing distance of the potential curves: it causes a significant increase in the q -dependence of the cross-sections. Similar oscillations in cross-sections have been reported in other collision systems [7-9].

In order to see whether the electron is really captured into a single level and whether the oscillation is caused by the change of such a level, we have measured translational energy spectra of charge-changing projectile ions scattered in the forward direction for the collision systems mentioned above [10]. These measurements give us information on the level into which the electron is transferred in the collision system.

3.2. Translational energy spectroscopy

The experimental set-up for the translational energy spectroscopy is shown in Fig. 4. The ion beam extracted from NICE-1 is focused, mass-analysed by a sector magnet (MS), and well collimated by a pair of apertures of 1 mm in front of the target gas cell. After passing through the gas cell, ions are decelerated by electrostatic lenses before entering a 127° cylindrical analyser. The mean radius of the analyser is $r = 125$ mm and the slit widths are $S_1 = 1.0$ mm and $S_2 = 1.5$ mm. The deceleration voltage V_R is so adjusted that the energy of the ions passing the analyser is between $30-60 (\times q) \text{ eV}$. The energy spectra of ions are obtained by scanning an additional, variable voltage superimposed upon the deceleration voltage V_R , while the deflection voltage V_D of the analyser is kept constant.

In Fig. 5 is shown a typical energy profile of O^{6+} projectile ions extracted from NICE-1 at the continuous mode. The energy spread of the incident ions is usually $0.8 \times q \text{ eV}$, depending a little on the current density of the electron beam and other parameters of the ion source. Further details of the experimental procedure for the translational energy spectroscopy are described elsewhere [11].

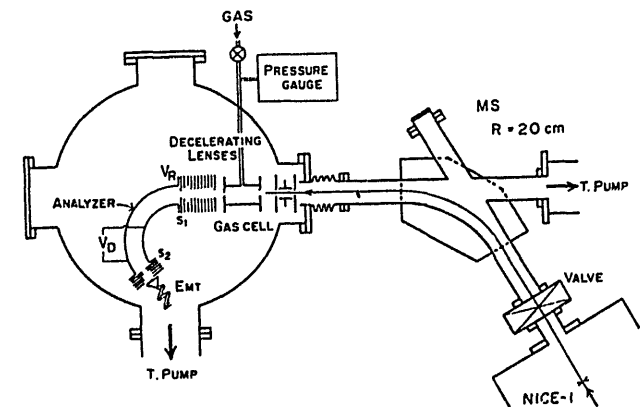


Fig. 4. Schematic view of the apparatus used for translational energy spectroscopy.

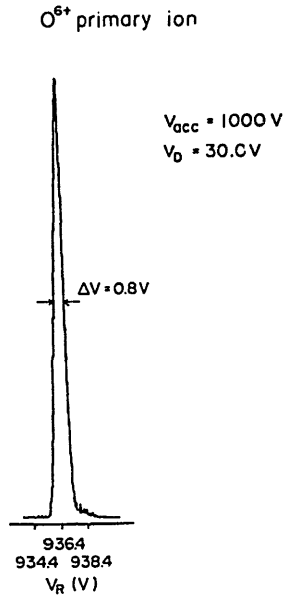


Fig. 5. Typical energy profile of O^{6+} projectile ions extracted from NICE-1.

In Fig. 6 is shown the energy spectrum of scattered C^{5+} ions from $C^{6+} + He$ collisions. Calculated energy levels are also indicated, corresponding to some principal quantum numbers n of the product C^{5+} ions for the process: $C^{6+} + He(1s^2) \rightarrow C^{5+}(n) + He^+(1s)$. In this figure, only a single peak is observed which corresponds to the energy of the $n = 3$ level in C^{5+} , and this is in good agreement with the prediction of the classical consideration in [4].

For the case of $O^{8+} + He$ collisions, as seen in Fig. 7, the electron is selectively captured into the $n = 4$ level of the product ion O^{7+} . This change of the level from $n = 3$ to 4 should give rise to a significant difference in the cross-sections for one-electron capture by C^{6+} and O^{8+} ions. Actually, as seen in Fig. 3, the cross-section for O^{8+} is about three times as large as that for C^{6+} .

An energy spectrum obtained in $C^{5+} + He$ collision is shown in Fig. 8. It is clear that the electron is captured into the $n = 3$ level of C^{4+} . In this case, some population distribution among the sublevels in the $n = 3$ level is observed. The population

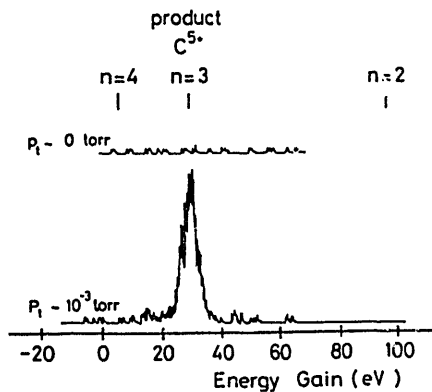


Fig. 6. Typical energy spectrum of scattered C^{5+} ions at forward direction from $C^{6+} + He$ collisions at a collision energy of 6 keV. No peak was observed without target He gas ($P_t \sim 0$ torr).

Physica Scripta T3

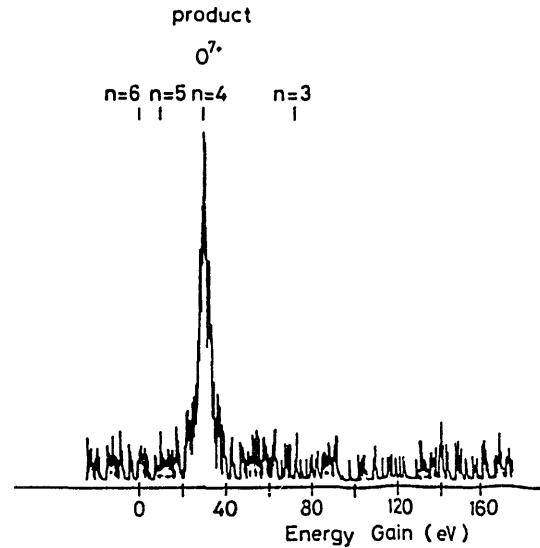


Fig. 7. Energy spectrum of product O^{7+} ions from $O^{8+} + He$ collisions at a collision energy of 8 keV.

distribution [12] is more clearly seen in $C^{3+} + He$ collisions, as is shown in Fig. 9. As for the principal quantum number, even in this case, the electron is captured only into the $n = 2$ level of C^{2+} .

Similar observations have been made for other fully stripped, H-like, He-like and Li-like ions of C, N and O incident on He, at collision energies of $1 \times q$ and $2 \times q$ keV. In all cases observed, it was clearly demonstrated that the electron is captured selectively into a single level with a particular quantum number n of the product ions [13], and that no signals due to endothermic processes and excitation of target He^+ ions are found. In Table I is listed the level n into which the electron is captured for all ions investigated and the energy gain ΔE measured in the energy spectra. As seen in Table I, it is found that, for the incident ions with the same charge state q , the electron is captured into the same n -level, and the measured energy gains ΔE are similar to each other. This similarity among the same q projectiles is due to the fact that the potential energy curves for $A^{q+} + He$

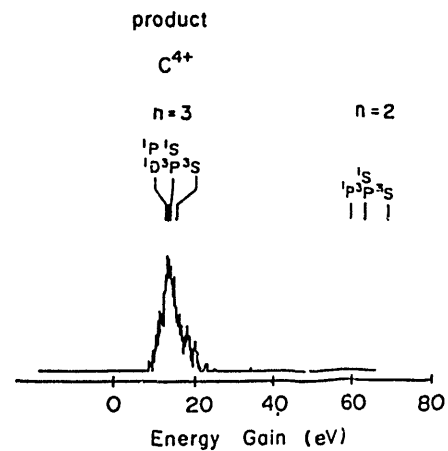
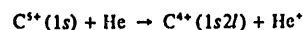


Fig. 8. Energy spectrum of product C^{4+} ions at a collision energy of 5 keV.



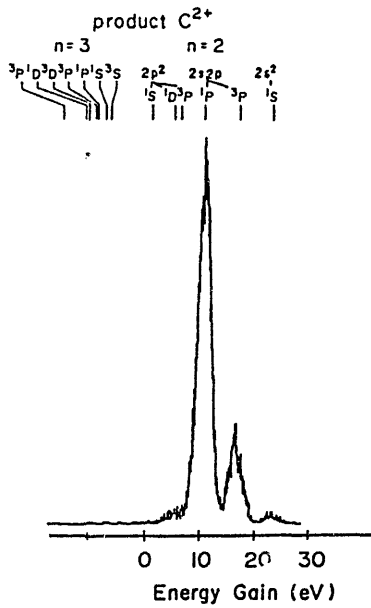
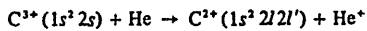


Fig. 9. Energy spectrum of product C²⁺ ions at a collision energy of 3 keV.



collision systems are very similar for larger values of principal quantum numbers in the final state [14].

The results summarized in Table I are in rather good agreement with the prediction of the classical consideration. However, there are some discrepancies between the prediction and the measured data. For example, according to the classical treatment, the change of the level from $n = 3$, for C⁶⁺, to $n = 4$ for N⁷⁺ should cause a significant increase in the q -dependence in the cross-sections. But, in point of fact, as seen in Fig. 3, the measured cross-section for N⁷⁺ is very similar to that for C⁶⁺. Accordingly, it is imaginable that there should be another rule in the determination of the q -dependence of cross-sections for one-electron capture, in addition to the selection and variation of the capturing level. In order to search for this additional rule, we arranged the measured total cross-sections $\sigma_{q,q-1}$ as a function of the crossing distances R_c at which an electron is transferred in the potential energy curves (Fig. 10). As seen in Fig. 10, where R_c of each collision system is derived from the observed energy gain, the R_c -dependence in the cross-sections seems to have a peak structure. This fact implies that the electron capture process prefers states of the product ions which correspond to crossing points at some suitable internuclear distances. It is very interesting to find out the relation

Table I. Principal quantum number n and measured energy gain ΔE (eV) for the collision systems:

		$A^{q+} + He \rightarrow A^{(q-1)+} + He^+ + \Delta E$ (eV)					
		$q = 3$	$q = 4$	$q = 5$	$q = 6$	$q = 7$	$q = 8$
C	n	2	2	3	3		
	ΔE	(11)	(31)	(14)	(29)		
N	n		2	3	3	4	
	ΔE		(24)	(16)	(30)	(17)	
O	n			3	3	4	4
	ΔE			(18)	(30)	(18)	(30)

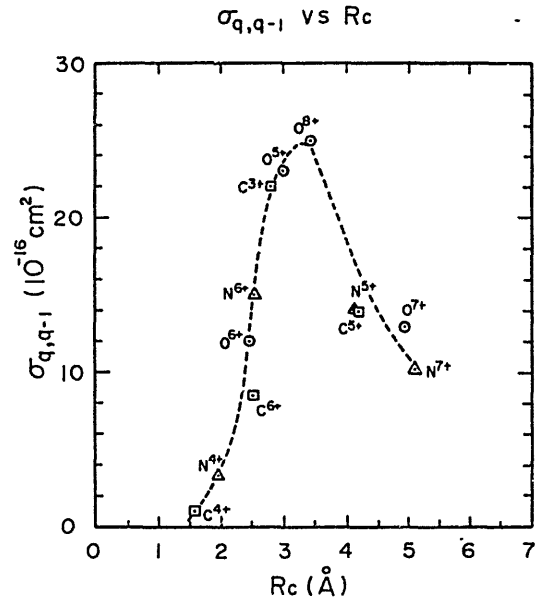


Fig. 10. Measured cross-section $\sigma_{q,q-1}$ as a function of crossing distances R_c in potential curves for various collision systems, $A^{q+} + He$.

between the total or partial cross-sections and the crossing distances, but, unfortunately, the present data studied here are not enough to derive the selection rule for one-electron capture processes at low energies, such as the preference of certain crossing distances, and to discuss this subject. It is urgently needed that a sufficient amount of data is accumulated for the various collision systems.

Acknowledgements

The author would like to thank Drs M. Barat, C. L. Cocke and D. H. Crandall for useful discussions at this Stockholm meeting.

The author is also grateful to Professor H. Kakihana, the Director of the Institute, and to Emeritus Professor K. Takayama, the former Director of the Institute and to Professors J. Fujita, M. Otsuka and H. Suzuki for their encouragement throughout this work. Thanks are also due to Professor T. Watanabe for his interest and helpful discussions and Mr T. Hino for his technical skill and help.

References

1. A review of EBIS is given by E. D. Donets at this Symposium.
2. Imamura, H., Kaneko, Y., Iwai, T., Ohtani, S., Kobayashi, N., Okuno, K., Tsurubuchi, S., Kimura M. and Tawara, H., Nucl. Instr. Meth. 188, 233 (1981).
3. Kobayashi, N., Ohtani, S., Kaneko, Y., Iwai, T., Okuno, K., Tsurubuchi, S., Kimura, M., Tawara, H. and Hino, T., Technical report of Institute of Plasma Physics, Nagoya University, IPPJ-DT-84. Design and Construction of a Horizontally Placed Superconducting Magnet and its Cryostat for an Electron Beam Ion Source (in Japanese).
4. Iwai, T., Kaneko, Y., Kimura, M., Kobayashi, N., Ohtani, S., Okuno, K., Takagi, S., Tawara, H. and Tsurubuchi, S., Phys. Rev. A26, 105 (1982).
5. Kaneko, Y., Iwai, T., Ohtani, S., Okuno, K., Kobayashi, N., Tsurubuchi, S., Kimura, M., Tawara, H. and Takagi, S., in Physics of Electronic and Atomic Collisions (Edited by S. Datz), p. 697. North Holland, Amsterdam (1982).
6. Ryufuku, H., Sasaki, K. and Watanabe, T., Phys. Rev. A21, 745 (1980).
7. Bliman, S., Aubert, J., Geller, R., Jacquot, B. and van Houtte, D., Phys. Rev. A23, 1703 (1981).
8. Cocke, S. L., DuBoir, R. D., Gray, T. J. and Justiniano, E., IEEE

- NS-28, 1032 (1981)
9. Mann, R., Folkmann, F. and Beter, H. F., *J. Phys. B: Atom. Mol. Phys.* **14**, 1161 (1981).
 10. Ohtani, S., Kaneko, Y., Kimura, M., Kobayashi, K., Iwai, T., Matsumoto, A., Okuno, K., Takagi, S., Tawara, H. and Tsurubuchi, S., *J. Phys. B: At. Mol. Phys.* **15**, L533 (1982).
 11. Tawara, H., Iwai, T., Kaneko, Y., Kimura, M., Kobayashi, N., Matsumoto, A., Ohtani, S., Okuno, K., Takagi, S. and Tsurubuchi, S., Submitted to *Phys. Rev. A*.
 12. Kimura, M., Iwai, T., Kaneko, Y., Kobayashi, N., Matsumoto, A., Ohtani, S., Okuno, K., Takagi, S., Tawara, H. and Tsurubuchi, S., *J. Phys. B: At. Mol. Phys.* **15**, No. 23 (1982).
 13. For $N^{7+} + He$, $O^{7+} + He$ collision systems, aside from the dominant peaks corresponding to $n = 4$ levels of the product N^{6+} and O^{6+} , weak peaks are observed. These peaks are assigned to be due to transfer ionization via two electron capture into the autoionizing states of N^{5+} and O^{5+} . (Tsurubuchi, S., Iwai, T., Kaneko, Y., Kimura, M., Kobayashi, N., Matsumoto, A., Ohtani, S., Okuno, K., Takagi, S. and Tawara, H., *J. Phys. B: At. Mol. Phys.* **15**, L733 (1982).
 14. Okuno, K., Iwai, T., Kaneko, Y., Kimura, M., Kobayashi, N., Matsumoto, A., Ohtani, S., Takagi, S., Tawara, H. and Tsurubuchi, S., Submitted to *Phys. Rev. A*.
 15. Müller, A. and Salzborn, E., *Phys. Lett.* **62A**, 391 (1977).

LETTER TO THE EDITOR

The dependence on R_c of cross sections for one-electron capture by S^{11+} , S^{13+} and Kr^{q+} ($q = 7-25$) ions from He atoms

T Iwai†, Y Kaneko‡, M Kimura§, N Kobayashi‡, A Matsumoto, S Ohtani, K Okuno‡, S Takagi, H Tawara and S Tsurubuchi||

Institute of Plasma Physics, Nagoya University, Nagoya 464, Japan

Received 1 December 1983

Abstract. Total cross section measurements and translational energy spectroscopy have been performed at collision energies of 1 q keV for one-electron capture processes by S^{11+} , S^{13+} and Kr^{q+} ($7 \leq q \leq 25$) ions from He atoms. When the measured cross sections are plotted as a function of the crossing radius R_c deduced from the observed energy gain, it is found that the cross sections in general increase with R_c and almost all of them lie between the $\frac{1}{2}\pi R_c^2$ and πR_c^2 curves. This dependence on R_c is very different from previous results for ions with relatively low q ($q < 10$).

We have systematically studied one-electron capture processes by highly stripped ions such as C^{q+} , N^{q+} , O^{q+} , F^{q+} and Ne^{q+} ions ($q \leq 9$) from He atoms at low collision energies. One of the important conclusions obtained from a series of our experiments (Kaneko *et al* 1982, Iwai *et al* 1982, Ohtani *et al* 1982, Tsurubuchi *et al* 1982, Kimura *et al* 1982, Okuno *et al* 1983, Tawara *et al* 1983) is that when the measured cross sections $\sigma_{q,q-1}$ are plotted as a function of the internuclear distance where electron transfer takes place predominantly, i.e., the crossing radius R_c of the diabatic potential curves deduced from the observed energy gain spectra, the cross sections do not follow the $\frac{1}{2}\pi R_c^2$ rule expected from the classical one-electron model, but seem to have a maximum around a particular crossing radius $R_c \approx 3.5 \text{ \AA}$ (Tawara *et al* 1983).

A similar dependence of the cross section on R_c has been reported by several investigators for various collision systems and various collision energies (Winter *et al* 1977, Smith *et al* 1980, Huber 1983, Winter 1983), and it has often been called the *reaction window*. However, as pointed out by Tawara *et al* (1983), it is questionable to assert that this window is *universal* for all the collision systems.

Concerning the dependence on R_c , all the measurements reported so far are restricted to projectile ions having the charge of $q < 10$; no experimental work has been done for projectile ions of $q > 10$ at low energies. When the charge state q of

† Permanent address: Department of Liberal Arts, Kansai Medical University, Hirakata, Osaka 573, Japan.

‡ Permanent address: Department of Physics, Tokyo Metropolitan University, Setagaya-ku Tokyo 158, Japan.

§ Permanent address: Department of Physics, Osaka University, Toyonaka, Osaka 560, Japan.

|| Permanent address: Department of Applied Physics, Tokyo University of Agriculture and Technology, Koganei, Tokyo 184, Japan.

the projectiles is increased, the corresponding R_c is expected to become large. Therefore, we extend a series of experiments to further high- q ions in order to see what happens in such cases of high- q ions. It will contribute to better understanding of the physics of the one-electron capture process by highly charged ions.

The present paper is a report on one-electron capture processes by S^{11+} , S^{13+} and Kr^{q+} ($q=7-25$) ions from He atoms. Measurements of total cross sections and translational energy spectra of the fast product ions were carried out using the same apparatus as the previous experiments (Ohtani *et al* 1982, Okuno *et al* 1983) with little change. A movable MCP detector with a retardation grids system was inserted between the collision cell and the energy analyser for the total cross section measurements. The movable detector is similar to that reported by Mann *et al* (1982) and its details will be reported elsewhere. The cross section of the $O^{7+} + He$ collision measured in this system agreed well with the previous result by Iwai *et al* (1982). All the present measurements were performed at collision energies of $1q$ keV.

The measured cross sections $\sigma_{q,q-1}$ for Kr^{q+} ions are shown in figure 1 as a function of the charge state q of the projectile ions; in this figure, other experimental results obtained by Cocke *et al* (1981) and Kusakabe *et al* (1983) are also shown for comparison. Though the energy ranges studied are different in these papers, and though the range of q concerned is quite different, all the results can be connected smoothly with each other. We note in figure 1 that strong oscillation of the cross section with q is observed for low- q ions as was seen in our previous measurements (Kaneko *et al* 1982, Iwai *et al* 1982), and that for high- q ions the oscillation tends to diminish and the q dependence of $\sigma_{q,q-1}$ becomes very similar to that derived from an empirical formula of Müller and Salzborn (1977) which is shown as a broken curve in the figure.

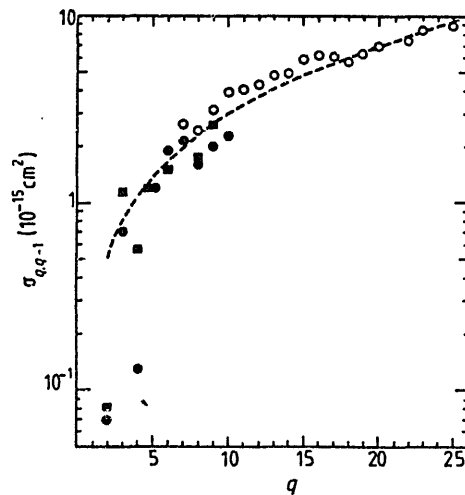


Figure 1. Total cross sections for one-electron capture $\sigma_{q,q-1}$ as a function of the charge state q of projectile Kr^{q+} ions. ●: Cocke *et al* (1981) at $0.78q$ keV, ■: Kusakabe *et al* (1983) at 0.286 keV amu^{-1} , ○: present results at $1q$ keV.

Figure 2 illustrates typical examples of translational energy gain spectra of the product $Kr^{(q-1)+}$ ions. In all the cases studied here the energy spectrum has a strong peak with rather a narrow width, and in some cases the spectrum seems to have a weak peak in addition to the main peak. Unfortunately, we can not assign the electron

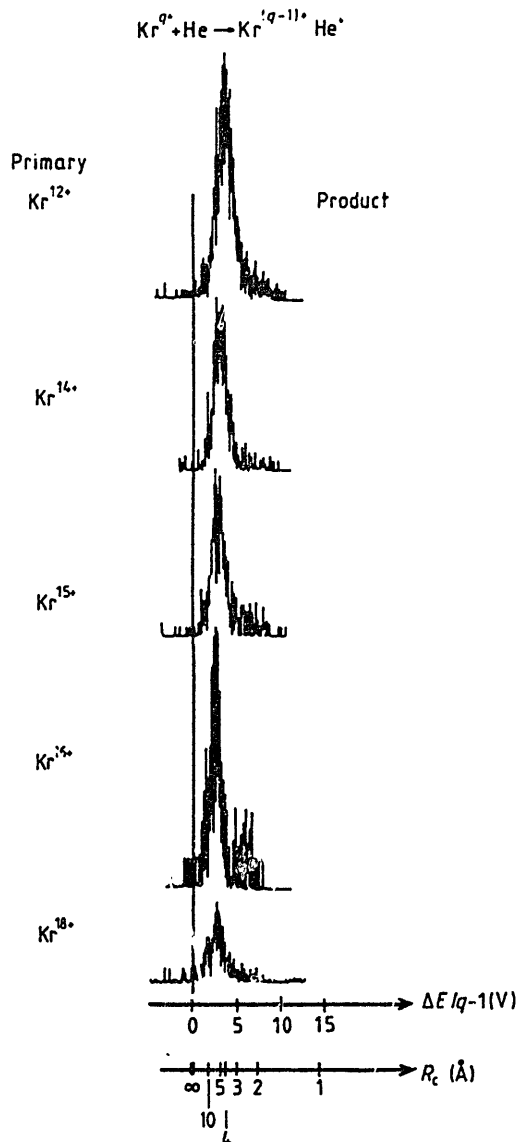


Figure 2. Energy gain spectra of product $\text{Kr}^{(q-1)+}$ ions at $1q$ keV for $q = 12, 14, 15, 16$ and 18 .

capturing level corresponding to the observed peak because of lack of information on the energy level of the $\text{Kr}^{(q-1)+}$ ion. However, as seen in figure 2, the quantity $\Delta E/(q-1)$, where ΔE is the observed energy gain at the main peak, becomes small with the increase of q in general. This means that the crossing radius R_c becomes large with the increase of q . The R_c is obtained from the observed energy gain ΔE through the equation: $R_c(\text{\AA}) = 14.4(q-1)/\Delta E(\text{eV})$, where only Coulomb repulsion is assumed for the diabatic potential.

In figure 3 we summarise all the measured cross sections $\sigma_{q,q-1}$ as a function of R_c for S^{11+} and S^{13+} ions as well as $\text{Kr}^{(q-1)+}$ ions, together with the result obtained previously (Tawara *et al* 1983). In contrast to the previous results for relatively low- q ions, the cross sections obtained here do not have any maximum around a particular crossing radius; almost all the present data points lie between the $\frac{1}{2}\pi R_c^2$ and πR_c^2 curves.

For high- q ions, an electron should be captured into the high Rydberg state of the product ion in which the l sublevels are nearly degenerate and around which the

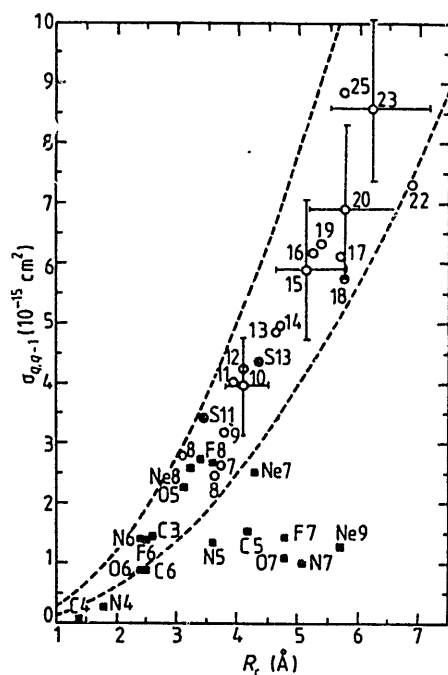


Figure 3. Dependence on R_c of total cross sections $\sigma_{q,q-1}$. \circ : present results for Kr^{q+} ions; q is indicated by the number in the figure. \bullet : present results for S^{11+} and S^{13+} ions. \blacksquare : previous results of Tawara *et al* (1983); in the figure, C4 means C^{4+} projectile ion, N5 means N^{5+} projectile ion, and so on. Lower broken curve is $\frac{1}{2}\pi R_c^2$, and upper broken curve is πR_c^2 . Uncertainties in the determination of $\sigma_{q,q-1}$ and R_c are denoted by bars for some cases for Kr^{q+} .

neighbouring n states are closely located. Therefore, the electron capture reaction must be shared among a large number of levels within a narrow energy separation. In the present experiment, however, the energy resolution is not good enough to separate such closely located levels, and the ΔE and the R_c deduced from the peak position of the observed energy spectrum should be considered as some sort of average values. Besides, the measured cross section is the sum of contributions from those many reaction channels. This being the case, it is expected that the cross sections tend to πR_c^2 with the increase in the number of crossings as pointed out by Kaneko (1983). Olson and Salop proposed the absorbing-sphere model for these cases (1976).

In conclusion, the multi-level crossing is responsible for the R_c dependence of cross sections observed in the present work. Detailed discussion will be given in a full paper.

References

- Cocke C L, DuBois R, Gray T J and Justiniano E 1981 *IEEE Trans. Nucl. Sci.* **NS-28** 1032
 Huber B A 1983 *Phys. Scr.* **T 3** 96
 Iwai T, Kaneko Y, Kimura M, Kobayashi N, Ohtani S, Okuno K, Takagi S, Tawara H and Tsurubuchi S 1982 *Phys. Rev. A* **26** 105
 Kaneko Y 1983 *Invited Talk at the Asia Pacific Physics Conference (Singapore)*
 Kaneko Y, Iwai T, Ohtani S, Okuno K, Kobayashi N, Tsurubuchi S, Kimura M, Tawara H and Takagi S 1982 *Physics of Electronic and Atomic Collisions* ed S Datz (Amsterdam: North-Holland) p 697
 Kimura M, Iwai T, Kaneko Y, Kobayashi N, Matsumoto A, Ohtani S, Okuno K, Takagi S, Tawara H and Tsurubuchi S 1982 *J. Phys. B: At. Mol. Phys.* **15** L851
 Kusakabe T, Hanaki H, Nagai N, Horinouchi T and Sakisaka M 1983 *Phys. Scr.* **T 3** 191

- Mann R, Cocke C L, Schlachter A S, Prior M and Marrus R 1982 *Phys. Rev. Lett.* **49** 1329
- Müller A and Salzborn E 1977 *Phys. Lett.* **62A** 391
- Ohtani S, Kaneko Y, Kimura M, Kobayashi N, Iwai T, Matsumoto A, Okuno K, Takagi S, Tawara H and Tsurubuchi S 1982 *J. Phys. B: At. Mol. Phys.* **15** L533
- Okuno K, Tawara H, Iwai T, Kaneko Y, Kimura M, Kobayashi N, Matsumoto A, Ohtani S, Takagi S and Tsurubuchi S 1983 *Phys. Rev. A* **28** 127
- Olson R E and Salop A 1976 *Phys. Rev. A* **14** 579
- Smith D, Adams N G, Alge E, Villinger H and Lindinger W 1980 *J. Phys. B: At. Mol. Phys.* **13** 2787
- Tawara H, Iwai T, Kaneko Y, Kimura M, Kobayashi N, Matsumoto A, Ohtani S, Okuno K, Takagi S and Tsurubuchi S 1983 *Phys. Rev. A* to be published
- Tsurubuchi S, Iwai T, Kaneko Y, Kimura M, Kobayashi N, Matsumoto A, Ohtani S, Okuno K, Takagi S and Tawara H 1982 *J. Phys. B: At. Mol. Phys.* **15** L733
- Winter H 1983 *Phys. Scr. T* **3** 159
- Winter H, Bloemen E and de Heer F J 1977 *J. Phys. B: At. Mol. Phys.* **10** L453

Energy-spectroscopic studies of electron-capture processes of low-energy, highly stripped F and Ne ions in collisions with He atoms

H. Tawara, T. Iwai,* Y. Kaneko,[†] M. Kimura,[‡] N. Kobayashi,[†]
 A. Matsumoto, S. Ohtani, K. Okuno,[†] S. Takagi, and S. Tsurubuchi[§]
Institute of Plasma Physics, Nagoya University, Furo-cho, Chikusa-ku, Nagoya 464, Japan
 (Received 5 July 1983)

The electron-capture processes of highly stripped ions of F^{q+} ($q=6,7,8$) and Ne^{q+} ($q=7,8,9$) in collisions with He atom were investigated using the energy-gain spectroscopy technique. A single dominant peak is observed in most of the energy-gain spectra except for the Ne^{7+} and Ne^{9+} spectra, in which two peaks are observed corresponding to the one-electron capture process into levels with different principal quantum number n .

I. INTRODUCTION

In our recent measurement of total cross sections for one-electron capture processes by highly stripped heavy ions from He atoms at low energies, it was found that the cross sections show significant oscillations when plotted as a function of the ionic charge of the projectile ions.^{1,2} This can be explained quantitatively by the classical one-electron model² where it is assumed that in such a collision the electron is selectively captured into a particular single level of the ion. To confirm this assumption, we already made a series of measurements of the energy gain of various projectile ions such as C^{q+} ($q=3-6$), N^{q+} ($q=4-7$), and O^{q+} ($q=5-8$) in collisions with He atoms using the translational energy-spectroscopy technique.³⁻⁶ In fact, most of the energy-gain spectra observed show only a single peak which is found to be due to exothermic processes, indicating that the classical one-electron model is valid for these collisions at low energies. However, in some cases such as in the $C^{3+} + He$ collision, four peaks are observed.⁵ It was found that they correspond to electron capture into levels with the same principal quantum number n but different orbital angular quantum number l . Similarly, the energy-gain spectra in N^{4+} and O^{5+} ions become broad indicating the contribution of a number of peaks corresponding to levels with different l .

It has also been found that there is good similarity among the energy-gain spectral patterns obtained for different projectile ions with the same ionic charge q , irrespective of the ion species: such similarity is considered to result from the similarity among the diabatic potential curves for $A^{q+} + He$ collision systems.⁶

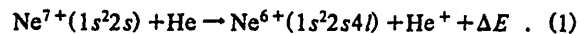
In the present paper, we present new results of our continuing investigation on the electron-capture processes of highly stripped F^{q+} ($q=6,7,8$) and Ne^{q+} ($q=7,8,9$) ions on He atoms. The present experimental principle and technique were already described in detail.⁶

In the following, first, some features in the collision systems investigated are described. All the following experiments have been done at the energy of $q \times 1$ keV, where q is the ionic charge of the ion. The energy levels of each ion are taken from the book of Bashkin and Stoner.⁷

II. EXPERIMENTAL RESULTS

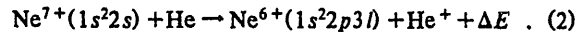
(i) $Ne^{7+} + He$ [see Fig. 1(a)]: Three peaks are clearly seen. The strongest peak at the energy gain $\Delta E \approx 20$ eV is

found to be due to the following one-electron-capture process into the $n=4$ level:



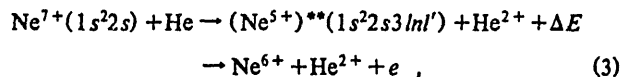
It is not possible to assign any particular single level because there are a number of closely spaced levels in Ne^{6+} ions.

The second peak at $\Delta E \approx 38$ eV is due to the following one-electron capture into the $n=3$ state:



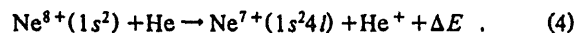
It should be noted that this process (2) involves two electrons; that is, one $2s$ electron in the projectile ion is excited into the $2p$ state and the other is captured into the excited $3l$ state of the projectile ion from the target atom. A similar two-electron process has also been observed in the $N^{4+} + He$ collision which results in $N^{3+}(1s^22p^21S)$.⁵ This observation is the first clear evidence that the electron is captured into levels with different n , in contrast to the classical one-electron model which assumes the involvement of only a single level in the one-electron-capture process at low energies.

The very weak peak at $\Delta E \approx 68$ eV is thought to be due to the transfer ionization, as discussed previously,⁴ as follows:

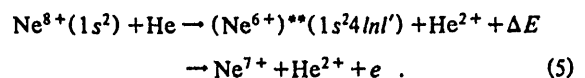


though it is not possible to assure this because no information on the energy levels of such doubly excited states of many-electron systems is available presently. By comparing the integrated areas under peaks with total cross sections previously measured, it is estimated that the cross sections for processes (1), (2), and (3) are 26.1, 4.9, and 1.0×10^{-16} cm², respectively.

(ii) $Ne^{8+} + He$ [Fig. 1(b)]: The dominant peak at $\Delta E \approx 31$ eV is found to correspond to the following one-electron capture into the $n=4$ state:



The weak peak at $\Delta E \approx 63$ eV may be due to the transfer ionization



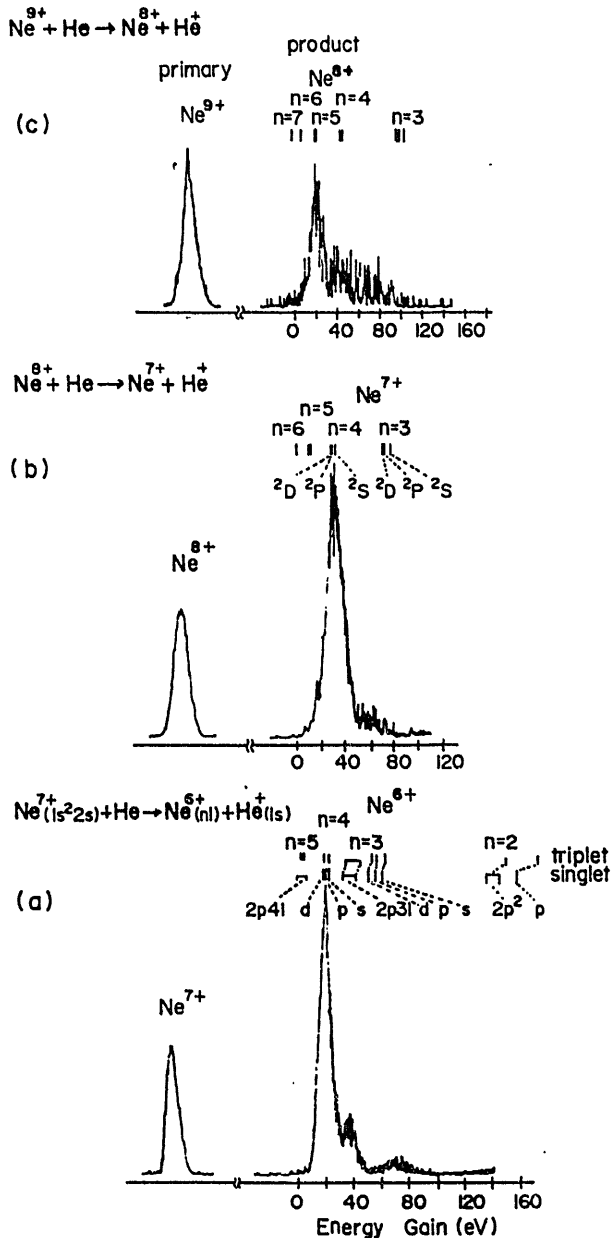


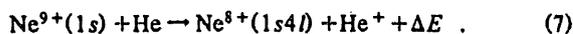
FIG. 1. Energy-gain spectra in (a) $\text{Ne}^{7+} + \text{He}$, (b) $\text{Ne}^{8+} + \text{He}$, and (c) $\text{Ne}^{9+} + \text{He}$ collisions.

The intensity for process (5) is roughly 10% of that for process (4).

(iii) $\text{Ne}^{9+} + \text{He}$ [Fig. 1(c)]: At least two peaks are seen. The stronger peak at $\Delta E \approx 20$ eV is due to the following one-electron capture into the $n=5$ state of Ne^{8+} ions:



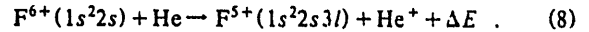
The second peak at $\Delta E \approx 44$ eV is due to the one-electron-capture process into the $n=4$ state:



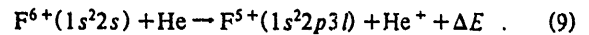
The partial cross sections for processes (6) and (7) are

roughly 14.5 and $5.5 \times 10^{-16} \text{ cm}^2$, respectively. The very weak peak at $\Delta E \approx 70$ eV may be due to the transfer ionization as discussed previously.⁴

(iv) $\text{F}^{6+} + \text{He}$ [Fig. 2(a)]: The observed peak at $\Delta E \approx 29$ eV is thought to correspond to the following simple one-electron capture:



It should be noted that this peak is broader because of the contribution of the levels with different l , with the highest intensity for the $1s^2 2s3d^1 D$ level. The weak shoulder at $\Delta E \approx 18$ eV is thought to be due to the following two-electron process, similar to process (2) in $\text{Ne}^{7+} + \text{He}$ collisions:



(v) $\text{F}^{7+} + \text{He}$ [Fig. 2(b)]: The stronger peak at $\Delta E \approx 18$

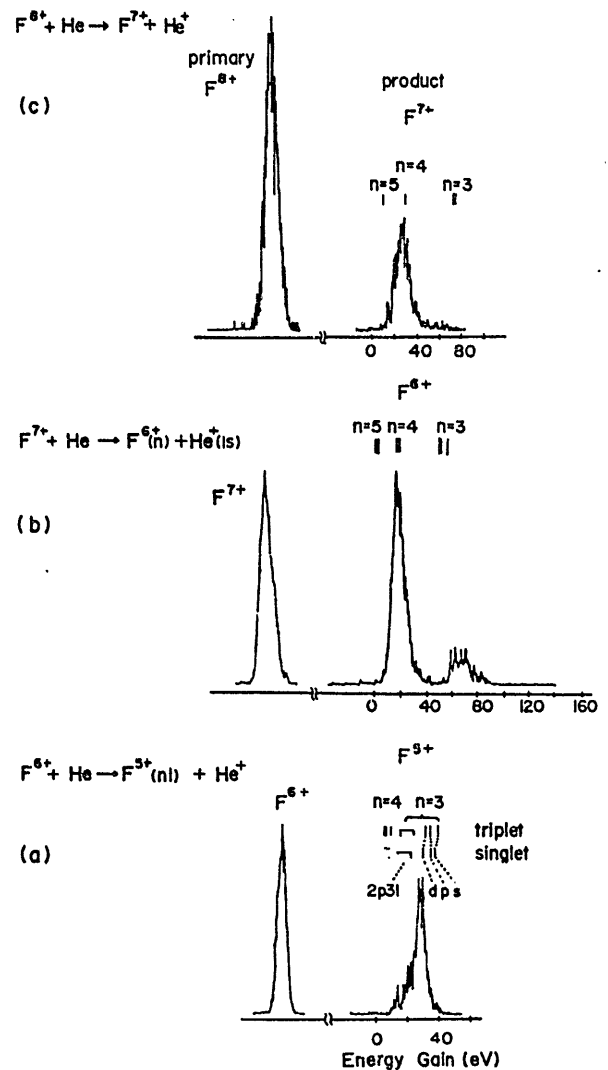
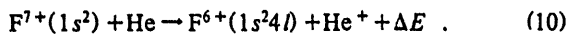
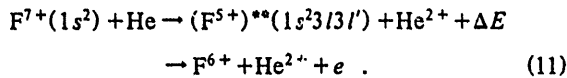


FIG. 2. Energy-gain spectra in (a) $\text{F}^{6+} + \text{He}$, (b) $\text{F}^{7+} + \text{He}$, and (c) $\text{F}^{8+} + \text{He}$ collisions.

eV is due to the following process:

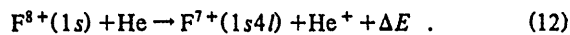


The weaker peak at $\Delta E \approx 66$ eV is probably due to the transfer ionization



By comparing spectra in Figs. 1(a) and 2(b) with previous spectra for N^{7+} and O^{7+} ions,⁶ the observed spectra are found to be very similar for all the ions with $q=7$ except for Ne^{7+} where two different n levels contribute. This similarity of the spectra among different ions with the same ionic charge has been already discussed in detail.⁶ However, it should be noted that the transfer-ionization process is much stronger for F^{7+} ions and its intensity amounts to about 20% of that for the main one-electron-capture process (10).

(vi) $F^{8+} + He$ [Fig. 2(c)]: Only a single peak at $\Delta E \approx 28$ eV is observed which corresponds to the following one-electron capture into the $n=4$ state of the F^{7+} ion:



As discussed above [see (v)], the very good similarity in the energy-gain spectra is observed in all ions with the ionic charge of $q=8$ and is understood to be due to the similar energy-level diagrams among them.

III. DISCUSSION

Comparing the observed energy-gain spectra with the energy levels tabulated by Bashkin and Stoner,⁷ the principal quantum number n of the electron-capturing levels can be deduced for collision processes and are summarized in Table I which includes our previous data. Data for $Ne^{10+} + He$ collisions are taken from the work of Mann *et al.*,⁸ where their collision energy was lower than ours. As can be seen in Table I, the electron-capturing levels are the same for projectile ions with the same ionic charge, irrespective of the ion species. From the observed energy gain ΔE , the curve crossing radius R_c for the one-electron-capture process in the quasimolecule can be determined as shown in Table II through $R_c = 14.4(q-1)/\Delta E$ (q : the ionic charge of projectile ion; ΔE : eV; R_c : Å).⁸

TABLE I. Principal quantum numbers n of the electron-capturing levels in $A^{q+} + He$ collisions.

q	10	9	8	7	6	5	4	3
Ne	5 ^a	5(4) ^b	4	4(3) ^b				
F			4	4	3			
O			4	4	3	3		
N				4	3	3	2	
C					3	3	2	2

^aData of Mann *et al.* (Ref. 8).

^bThe number in the parentheses is the principal quantum number n corresponding to the weak peak in the energy-gain spectrum.

TABLE II. Crossing radius R_c for the one-electron-capture process in $A^{q+} + He$ collisions (Å).

q	10	9	8	7	6	5	4	3
Ne	4.6 ^a	5.7	3.3	4.3				
F			3.6	4.8	2.5			
O			3.4	4.8	2.4	3.1		
N				5.1	2.4	3.6	1.8	
C					2.5	4.2	1.4	2.6

^aData of Mann *et al.* (Ref. 8)

In Fig. 3 are shown total one-electron-capture cross sections for various ions investigated in our previous experiment as a function of the crossing radius R_c . For the split distribution of the capturing levels the cross sections are divided according to the observed peak intensity in the energy-gain spectra. In the figure, only data for stronger peaks are shown. The solid line is drawn through data points just to guide the eye, whereas the dotted and dashed curves represent the classical cross sections, that is, πR_c^2 and $\frac{1}{2}\pi R_c^2$, respectively. Classically, it is assumed that the electron capture effectively takes place at the outermost crossing distance R_c inside a critical distance R_x where the attractive force of the projectile ion exceeds the binding force for the electron ion target atom.⁶

From Fig. 3, it is seen that the observed cross sections do not follow the classical cross section πR_c^2 rule. It should also be noted that they do not exceed πR_c^2 for all the range of R_c but are smaller than $\frac{1}{2}\pi R_c^2$ for $R_c < 2.5$ Å and decrease for $R_c > 4$ Å. The existence of a maximum in the cross sections at a particular crossing radius has been report-

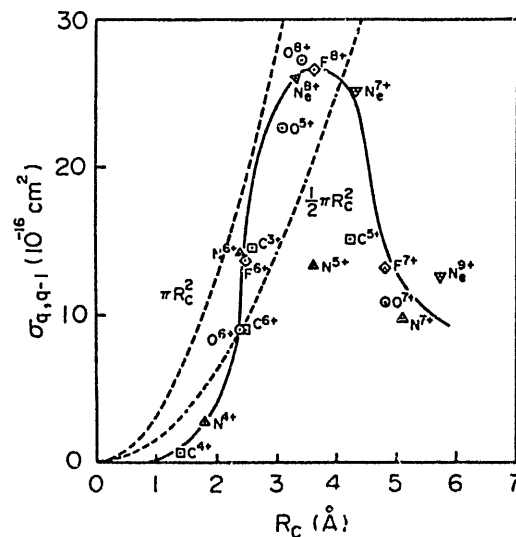


FIG. 3. Total one-electron-capture cross sections vs the crossing radius R_c in $A^{q+} + He$ collisions at around 0.5 keV/amu. Experimental data for C^{q+} , N^{q+} , and O^{q+} are taken from Refs. 5 and 6. The dotted and dashed lines correspond to the classical cross sections. The solid line is drawn through experimental data to guide the eye.

ed by some investigators for various collision systems at different energy ranges⁹ and is often called the "reaction window." This window shape seems to be similar for the various cases reported and it tends to be believed to be "universal" for all the collision systems. It is, however, necessary to look at and analyze more carefully the observed data before coming to such a conclusion.

Only in the single crossing system can we theoretically analyze the data relatively easily. In such a single crossing, a Landau-Zener model calculation predicts that the dependence of the cross sections for the charge transfer on the crossing radius R_c is indeed similar in shape to the observed curve (solid line) shown in Fig. 3.¹⁰ It is noted, however, that the R_c dependence of the cross section is strongly dependent on the shape of diabatic potential curves at R_c as well as the collision velocity and, then, could not be universal. Furthermore, even though the observed energy-gain spectrum consists of a single peak, this does not always guarantee a single crossing in the diabatic energy diagram. In fact, we have no accurate idea of how many crossings do contribute to the observed "apparent" single peak in the

energy-gain spectrum because of the limited energy resolution used in the experiments. For example, the sublevels having the same n but different l should result in many crossings closely located in the diabatic energy diagram.

On the other hand, if a number of crossings exist at larger crossing radii, many of them may contribute to the total charge-transfer process. Therefore the total cross section could increase with the number of crossings and finally reach the maximum cross section πR_c^2 . If there are only a limited number of crossings available in the collision system under investigation, the cross section may not reach the maximum value, as in the present case.

Systematic studies of the l distribution of the electron-capturing levels of higher charge state ions would make it possible to discuss the R_c dependence of the cross section for electron capture in more detail.

As we have shown in Figs. 1 and 2, we observed weak peaks in the energy-gain spectra which we attribute to transfer ionization involving highly stripped ions. Unfortunately, at present there is no accurate data on the energy levels of such doubly excited states of heavy ions.

*Permanent address: Department of Liberal Arts, Kansai Medical University, Hirakata, Osaka 573, Japan.

[†]Permanent address: Department of Physics, Tokyo Metropolitan University, Setagaya-ku, Tokyo 158, Japan.

[‡]Permanent address: Department of Physics, Osaka University, Toyonaka, Osaka 560, Japan.

[§]Permanent address: Department of Applied Physics, Tokyo University of Agriculture and Technology, Koganei, Tokyo 184, Japan.

¹Y. Kaneko, T. Iwai, M. Kimura, N. Kobayashi, S. Ohtani, K. Okuno, S. Takagi, H. Tawara, and S. Tsurubuchi, in *Physics of Electronic and Atomic Collisions*, edited by S. Datz (North-Holland, Amsterdam, 1982), p. 697.

²T. Iwai, Y. Kaneko, M. Kimura, N. Kobayashi, S. Ohtani, K. Okuno, S. Takagi, H. Tawara, and S. Tsurubuchi, *Phys. Rev. A* **26**, 105 (1982).

³S. Ohtani, Y. Kaneko, M. Kimura, N. Kobayashi, T. Iwai, A. Matsumoto, K. Okuno, S. Takagi, H. Tawara, and S. Tsurubuchi, *J. Phys. B* **15**, L533 (1982).

chi, *J. Phys. B* **15**, L533 (1982).

⁴S. Tsurubuchi, T. Iwai, Y. Kaneko, M. Kimura, N. Kobayashi, A. Matsumoto, S. Ohtani, K. Okuno, S. Takagi, and H. Tawara, *J. Phys. B* **15**, L733 (1982).

⁵M. Kimura, T. Iwai, Y. Kaneko, N. Kobayashi, A. Matsumoto, S. Ohtani, K. Okuno, S. Takagi, H. Tawara, and S. Tsurubuchi, *J. Phys. B* **15**, L851 (1982).

⁶K. Okuno, H. Tawara, T. Iwai, Y. Kaneko, M. Kimura, N. Kobayashi, A. Matsumoto, S. Ohtani, S. Takagi, and S. Tsurubuchi, *Phys. Rev. A* **28**, 127 (1983).

⁷S. Bashkin and J. R. Stoner, *Atomic Energy Levels and Grotian Diagrams I* (North-Holland, Amsterdam, 1975).

⁸R. Mann, C. L. Cocke, A. S. Schlachter, M. Prior, and R. Marrus, *Phys. Rev. Lett.* **99**, 1329 (1982).

⁹H. Winter, E. Bloemen, and F. J. de Heer, *J. Phys. B* **10**, L599 (1977); D. Smith, N. G. Adams, E. Alge, H. Villinger, and W. Lindinger, *ibid.* **13**, 2787 (1980).

¹⁰B. A. Huber, *Phys. Scr.* **T3**, 96 (1983).

Landau-Zener Model Calculations of One-Electron Capture from He Atoms by Highly Stripped Ions at Low Energies

Masahiro KIMURA,* Tsuruji IWAI,** Yozaburo KANEKO,***
Nobuo KOBAYASHI,*** Atsushi MATSUMOTO, Shunsuke OHTANI,
Kazuhiko OKUNO,*** Shoji TAKAGI, Hiroyuki TAWARA
and Seiji TSURUBUCHI****

Institute of Plasma Physics, Nagoya University, Nagoya 464
(Received March 13, 1984)

Cross sections for single electron capture from He atom by highly stripped, C^{q+} , N^{q+} , O^{q+} , F^{q+} , Ne^{q+} ($q=4-9$) and Kr^{q+} ($q=10-25$) ions have been calculated using the multichannel Landau-Zener model. The collision energy is 600 eV/amu except for Kr^{q+} , whose energy is $q \times 1$ keV. The selective electron capture into a single or at most two n -shells is predicted for the cases of $q \leq 9$. The n -distributions obtained by the present calculation are quite consistent with our earlier observation and the total cross sections agree reasonably well with the measured data in spite of the simple model. In the case of Kr^{q+} , where q is larger than 10, more and more shells can be populated and the total cross sections increase monotonically with the increase of q .

§1. Introduction

Recently we have measured total cross sections for one-electron capture processes by highly stripped ions A^{q+} ($q \leq 9$) from He atoms at low energies;



where A^{q+} is fully stripped ions of C, N and O, and H-like, He-like and Li-like ions of C, N, O, F and Ne.¹⁻²⁾ We have also measured the energy-gain ΔE spectra from which the distributions over the final state quantum number n and, in some cases, the distributions over l were also determined.³⁻⁷⁾ In almost all the cases except for Ne^{7+} and Ne^{9+} it was found that the electron is transferred into a particular single n -state and the capturing levels n are the same for projectiles with the same ionic

charge irrespective of the ion species.

If we assume that the interaction of the system is only the pure Coulomb repulsion between the product ions, the crossing radius R_c of the potential curves between the initial and final states can be estimated through¹⁾

$$R_c(\text{\AA}) = 14.4(q-1)/\Delta E \quad (\Delta E \text{ in eV}). \quad (1.2)$$

When one-electron capture cross sections are plotted as a function of R_c there seems to be a maximum at around 3.5 \AA.⁷⁾ Similar results have been reported for various collision systems and the region with maximum cross sections is sometimes called "reaction window".⁸⁾ When higher charged ions, such as Kr^{q+} ions with $7 \leq q \leq 25$, were employed as projectiles, the cross sections have shown no peak structure as a function of R_c , but both the cross sections and crossing distances which give dominant contributions increase almost monotonically with q .⁹⁾ In general, several product channels can contribute to the reaction and the number of possible channels increases with the increase of q . Accurate methods to calculate the cross sections, e.g., large basis molecular-orbital-close-coupling method, need enormous computation. When the number of channels is very large, a simple approximation called the

* Permanent address: Department of Physics, Osaka University, Toyonaka, Osaka 560.

** Permanent address: Department of Liberal Arts, Kansai Medical University, Hirakata, Osaka 573.

*** Permanent address: Department of Physics, Tokyo Metropolitan University, Setagaya-ku, Tokyo 158.

**** Permanent address: Department of Applied Physics, Tokyo University of Agriculture and Technology, Koganei, Tokyo 184.

absorbing-sphere model was proposed by Olson and Salop to predict total cross sections.¹⁰⁾ They assumed the unit probability for reaction inside some critical distance R_0 and that the charge-transfer cross section is simply given by $Q = \pi R_0^2$. Such an R_0 is determined through the condition that the probability p of electron remaining on the diabatic curve at the crossing R_0 becomes 0.86. This model is applicable only when the density of the curve crossings is high at internuclear distances in the vicinity of R_0 . The number 0.86 was empirically deduced irrespective of the final state distribution.

In the present work we calculate both total and partial cross sections of one-electron capture processes using the multichannel Landau-Zener model and compare the results with our previous measurements.

§2. Survey of the Landau-Zener Model

2.1 Method of calculations

According to the Landau-Zener model, the probability of the diabatic transition at a single potential crossing is given by the following formula:

$$p = \exp(-2\pi H_{12}^2 / v_b \Delta F), \quad (2.1)$$

where $v_b = v(1 - b^2/R_c^2)^{1/2}$ is the radial velocity of projectiles at the crossing, v being the relative velocity, b the impact parameter, H_{12} the one half of the diabatic splitting at the curve crossing and ΔF the difference in slopes of the diabatic potential energy curves at R_c .

Analytical expressions of the coupling matrix elements H_{12} for one-electron capture processes by multicharged ions were proposed by several

authors. Olson and Salop obtained an analytical fit to the coupling matrix elements for ionic charge $q=4-54$ by calculating the potential curves for a large number of stripped-ion-atomic-hydrogen systems and extending to systems of the targets other than atomic hydrogen.¹⁰⁾ The expression obtained by Butler and Dalgarno does not depend on q ,¹¹⁾ and is a factor of 4 smaller at $q=4$ than that of Olson and Salop. Another expression was also obtained for $q \leq 4$ by Olson, Smith and Bauer.¹²⁾ Their formula also gives values of H_{12} much smaller than those evaluated from Olson and Salop. After several trials, it is found that H_{12} , reduced by 40% from the matrix elements of Olson and Salop's H_{12} , shows a good agreement with a series of our measurements. Therefore, we adopt the following expression throughout our present calculations:

$$H_{12} = 5.48q^{-1/2} \exp(-1.324\alpha q^{-1/2} R_c), \quad (2.2)$$

where H_{12} and R_c are in a.u., $\alpha = (2I_t)^{1/2}$ and I_t is the ionization potential of the target atom in a.u. When there is only one crossing, the total probability of the electron transfer at a given impact parameter is given by

$$P = 2p(1-p). \quad (2.3)$$

This expression can be generalized to the case of multichannel crossings. The general expression of the probability P_i for a particular product ionic level i when there are N crossings is given by Salop and Olson assuming that there are no couplings between the adjacent exit channels as follows:¹³⁾

$$P_i = p_1 p_2 \cdots p_i (1-p_i) [1 + (p_{i+1} p_{i+2} \cdots p_N)^2 + (p_{i+1} p_{i+2} \cdots p_{N-1})^2 (1-p_N)^2 + (p_{i+1} p_{i+2} \cdots p_{N-2})^2 (1-p_{N-1})^2 + \cdots + p_{i+1}^2 (1-p_{i+2})^2 + (1-p_{i+1})^2]. \quad (2.4)$$

The partial cross section Q_i is obtained by integrating over the impact parameter and then the total cross section Q is obtained by summing up over Q_i as follows;

$$Q_i = 2\pi \int P_i b db, \quad (2.5)$$

$$Q = \sum Q_i. \quad (2.6)$$

In the present Landau-Zener calculation we use the linear trajectory model and the crossing

radius R_c for each product channel is estimated using eq. (1.2). The energy gain ΔE_i of the reaction is determined by

$$\Delta E_i = I_p(A^{q-1}) - I_t(\text{He}) - E_i, \quad (2.7)$$

where $I_p(A^{q-1})$ is the ionization potential of the charge-changed ion $A^{(q-1)+}$, E_i the excitation energy of the i -th level of the ion $A^{(q-1)+}$ and $I_t(\text{He})$ the ionization potential of He atom. The values of I_p and E_i are taken from the

table of Bashkin and Stoner.¹⁴⁾

2.2 General characteristics of the Landau-Zener cross section for a single crossing

Before going into the detailed calculation, we consider the general characteristics inherent in the present Landau-Zener model for the simple case of a single crossing.

As seen in eq. (2.2), the coupling matrix element H_{12} is dependent on q as well as on R_c . In order to see the features of the cross sections calculated by using Landau-Zener formula eq. (2.1) for a single crossing with H_{12} given by eq. (2.2), some examples are shown in Fig. 1. In Fig. 1(a) are shown the cross sections for various projectile charges q at a fixed collision energy of 600 eV/amu. In Fig. 1(b) are shown the cross sections for $q=8$ at different energies. The R_c -dependence of cross sections has more or less similar shape of curve, *e.g.*, there is an optimum region of R_c for the cross section have to an appreciable magnitude. The reason is that when R_c is too small H_{12} is so large that p is very small and then P is small, whereas when the R_c is too large H_{12} is so small that p is close to unity and then P is again small. In the region where $p \sim 0.5$, P has a maximum. These features are common for all cases and, therefore, such a shape of the

R_c -dependence is often called "reaction window". It is noted from the present analysis, however, that such a reaction window has a definite meaning for collision systems with the same q and the same collision velocity.

For low- q ions, the cross section has rather a narrow peak; this means that the cross section is large only when the crossing radius in an actual collision system happens to fall into such a narrow region of R_c . Because of the narrow R_c region, and also because of large separation of the adjacent n -states, the electron is transferred selectively into a particular single n -state whose crossing is located on the reaction window. On the other hand, for high- q ions, the shape becomes wide, and also the maximum of the cross section increases. This fact suggests that several n -states can be populated and the total cross section increases with q .

2.3 The Landau-Zener model for multi-curve crossings

Roughly speaking, the above-mentioned model for a single crossing explains qualitatively the results obtained from a series of our experiments. Actually, however, there are many crossings between the diabatic potential curves of the initial and final states. The next

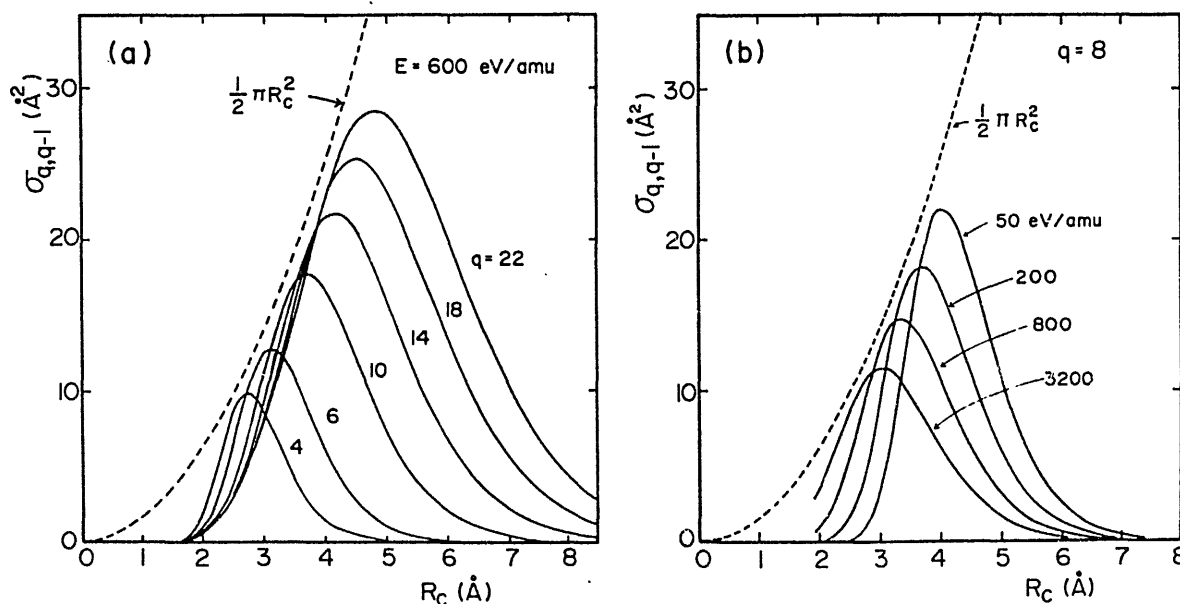


Fig. 1. The calculated single-crossing Landau-Zener cross sections for one-electron capture by multicharged ions A^{q+} from He as a function of the crossing distance R_c of potential curves. (a) The collision energy is fixed at 600 eV/amu and q is varied from 4 to 22. (b) Projectile charge q is fixed at 8 and the collision energy is varied from 50 to 3200 eV/amu.

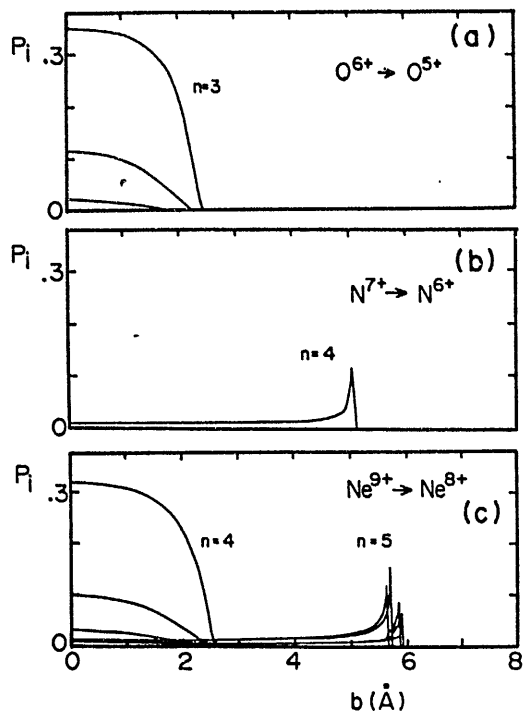


Fig. 2. Probabilities P_i of one-electron capture into various projectile levels (n, l) as a function of the impact parameter b at a collision energy of 600 eV/amu. (a) $O^{6+} + He$, (b) $N^{7+} + He$ and (c) $Ne^{9+} + He$.

step is to extend the single crossing model to the multi-curve crossings and to see how the model does work.

Three typical examples of actual collision systems are shown in Fig. 2(a), (b) and (c). In these figures, the transition probability P_i for the i -state of product ion is calculated by using eq. (2.4) for multi-curve crossings at a fixed collision energy of 600 eV/amu.

(a) $O^{6+} + He$ collision system (Fig. 2(a))

The dominant one-electron capture process has three final channels leading to the $1s^23s$, $1s^23p$ and $1s^23d$ states of product O^{5+} ion.⁶⁾ The crossing radii corresponding to these $n=3$ states are, respectively, 2.10, 2.33 and 2.41 Å, all of which are fairly smaller than the optimum radius (3.2 Å) shown in Fig. 1(a). The coupling matrix elements for $1s^23l$ states are so large that the diabatic transition probabilities p are very small. In that case, eq. (2.4) tells us that the two transitions at inner crossings are suppressed by the transition at the outer-most crossing, which has a dominant influence on total cross section. Other crossings corresponding to the $1s^24l$ and $1s^22l$ states are located

outside the reaction window and their contributions are negligibly small.

(b) $N^{7+} + He$ collision system (Fig. 2(b))

The dominant process is the electron transfer into the $1s4l$ ($l=s, p, d$ and f) states of product N^{6+} ion, and the corresponding crossings are located at fairly large distances around 5 Å in contrast to the case (a) above. As the coupling matrix element H_{12} between the initial and final states is very weak for such large R_c , the radial velocity v_b should be small at the crossing (see eq. (2.1)) to give a favorable value of p . Therefore, the transition at larger impact parameter is more favored. Since p is close to unity except for the glancing collision, it can be seen from eq. (2.4) that the inner crossings contribute to the reaction without being influenced strongly by the outer crossings. This fact leads us to the conclusions that each channel contributes to the total cross section almost independently of other channels and that the total cross section is nearly proportional to the number of the crossings.

(c) $Ne^{9+} + He$ collision system (Fig. 2(c))

This is a case of a wide reaction window (see Fig. 1(a)). Two groups of the crossings corresponding to the $n=4$ states and $n=5$ states of product Ne^{8+} ion fall into the reaction window. As seen in Fig. 2(c), the transition to the $n=4$ states is similar to the case (a) and the outer transition to the $n=5$ states is similar to the case (b). Both transitions contribute to the electron transfer reaction. Indeed, the corresponding double peak structure was observed in our energy-gain spectrum.⁷⁾ It is clear that the inner transitions ($n=4$) are not affected significantly by the outer transitions ($n=5$). This fact can be understood in a similar way to the case (b). Contributions from other channels leading to the $n=3$ and $n=6$ states are negligibly small, because their crossing radii are too small or too large.

It should be noted that these three cases provide us very good examples for understanding the properties of charge transfer process from the point of view of the potential crossing radius R_c . In the following sections, we calculate individual cross sections and compare them with the experimental results.

§3. Landau-Zener Cross Sections for Highly Stripped C, N, O, F and Ne Projectile Ions

As mentioned above, eq. (2.2), a revised form of the Olson-Salop's expression, is adopted as the coupling matrix element H_{12} and the excitation energies of product ions are referred to the book of Bashkin and Stoner.¹⁴⁾ Some excitation levels such as $O^{6+}(1s4s)$, $F^{6+}(1s^24f)$, $Ne^{7+}(1s^24f)$ and $Ne^{8+}(1s5s, 1s5g \text{ and } 1s4s)$ are not listed up in the book; these excitation energies are determined by extrapolation from the known sublevels.

Calculations of the cross sections have been carried out for almost all of the fully-stripped, H-like and He-like projectile ions of C, N, O, F and Ne. We did not calculate cross sections for two cases of F^{6+} and Ne^{7+} projectiles, because the dominant electron transfer is not one-electron process, but two-electron process leading to doubly excited states $2p3l$ of product F^{5+} and Ne^{6+} ions.⁷⁾ In the case of A^{7+} projectiles ($A=N, O$ and F), we observed transfer ionization process where two electrons are captured into autoionizing levels of product A^{5+} ions.^{4,7)} We neglect this process in the present calculation, because of its minor contribution to the electron transfer process.

In Table I are listed the calculated cross sections and the capturing levels n at the collision energy of 600 eV/amu together with the experimental data. Contributions from the levels which are not listed in the table are found to be negligibly small. The most important capturing levels deduced from the present model are quite consistent with our experiments. The agreement of the cross sections is almost satisfactory except for C^{4+} , C^{6+} , N^{6+} and O^{6+} , all of which have the crossing distances smaller than 2.5 Å. In such small distances our simple assumptions on the potential curves are invalid and the coupling matrix element H_{12} becomes inaccurate. The calculated partial cross sections for the two n -states in $Ne^{9+} + He$ collision are also in reasonable agreement with the experiment.

In Fig. 3 are compared the calculated total

Table I. One-electron capture cross sections for $A^{q+} + He$ collisions calculated using the multichannel Landau-Zener model (MLZ) are compared with the experimental data (Exp) of refs. 1 and 7. The capturing levels n are also listed. In parentheses are partial cross sections. The collision energy is 600 eV/amu. It should be noted that all the collision energies where experimental data are taken are not exactly the same, but vary from 430 to 780 eV/amu.*

A	q	n	Cross sections (Å ²)	
			MLZ	Exp
C	4	2	0	0.3
	5	3	14.9	15.2
	6	3	5.5	9.0
N	5	3	12.8	13.4
	6	3	6.1	14.2
	7	4	8.1	9.5
O	6	3	5.5	9.0
	7	4	14.5	10.9
	8	4	25.5	27.3
F	7	4	10.3	14.4
			(10.2)	(14.4)
	8	4	(0.1)	(0)
			26.7	26.7
Ne	8	4	26.0	28.0
			17.2	16.9
	9	5	(10.6)	(12.7)
			(6.6)	(4.2)

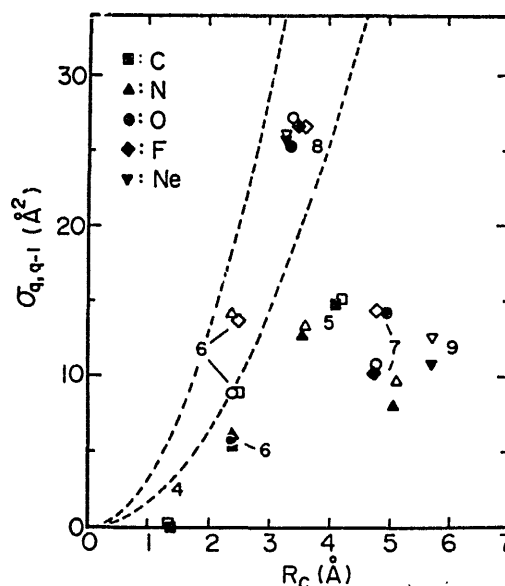


Fig. 3. The total one-electron capture cross sections versus the crossing radius R_c in $A^{q+} + He$ collisions calculated using multichannel Landau-Zener model (black symbols) are compared with the experimental data in ref. 7 (open symbols). Projectile charge q is written beside the symbols. The collision energy is around 600 eV/amu.

* Contributions of transfer ionization are subtracted from the measured total cross sections for $q=7$.

one-electron capture cross sections with the data measured for various projectile ions as a function of the crossing radius R_c . For the cases where several peaks were observed, the measured cross sections are shared among the respective states according to the observed peak intensities in the energy-gain spectra; Only data for stronger peaks are shown in the figure. When several sublevels were not resolved in the observed spectra, R_c is estimated from the peak position or from the weighted average of ΔE which contribute to the peak. An observed maximum in the cross section at R_c around 3.5 \AA is reproduced fairly well with the present model.

§4. Landau-Zener Cross Sections for Highly Stripped Kr^{q+} Projectile Ions ($q = 10, 15, 20$ and 25)

In the case of Kr^{q+} ions the accurate levels of $\text{Kr}^{(q-1)+}$ are unknown. We assume then that $\text{Kr}^{(q-1)+}$ ions have the H-like energy levels. This seems to be a reasonably good assumption for large q where an electron is captured predominantly into high Rydberg states. We further assume that each n -state has n sublevels corresponding to possible l .

In Fig. 4 are shown the calculated partial (P_i) and total (P) transition probabilities for the possible channels as a function of the

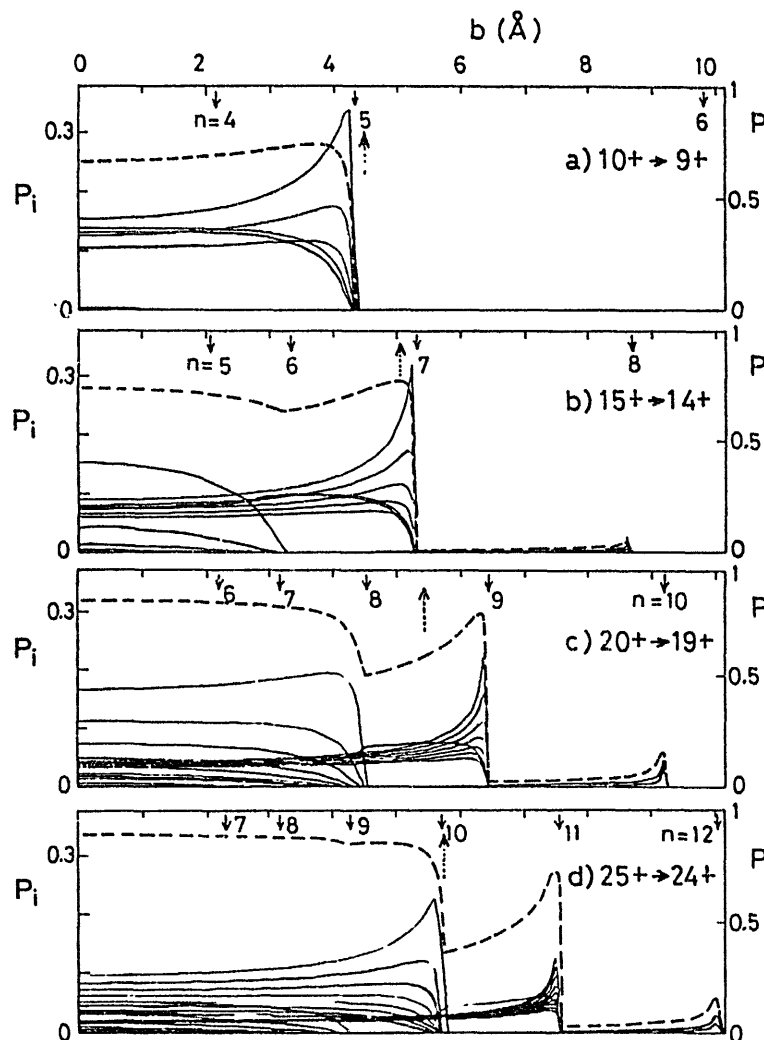


Fig. 4. The calculated probabilities P_i of one-electron capture into various states i of $\text{Kr}^{(q-1)+}$ for $\text{Kr}^{q+} + \text{He}$ collision system as a function of the impact parameter b . The collision energy is $q \times 1 \text{ keV}$. Total probabilities P are shown by the broken lines and its scale is shown on the right-hand ordinate. Crossing points between the product $\text{A}^{(q-1)+} + \text{He}^+$ system and the initial system are shown by the vertical arrows. The dotted arrows indicate the absorbing-sphere radii R_0 proposed by Olson and Salop (ref. 10). Projectile charges q are (a) 10, (b) 15, (c) 20 and (d) 25.

impact parameter at the collision energy of $q \times 1$ keV. As seen in Fig. 4, the most interesting features in these cases are that the number of the states contributing to the charge transfer processes increases with increasing q and that the collisions at large impact parameters have appreciably high reaction probabilities. These are due to the increased width of the reaction window with increasing q (Fig. 1(a)) and also due to the small energy separation between the adjacent levels of the product $\text{Kr}^{(q-1)+}$ ions. When only a limited number of the states with large crossing radius are available as in the cases of N^{7+} and $\text{O}^{7+} + \text{He}$ (Fig. 2(b)), only the near-grazing incidence to the crossing sphere can lead to the charge transfer reaction with considerable probabilities. This fact makes the total cross section relatively small in spite of large R_c . Contrary to those cases, it is shown when $q \geq 15$ that all collisions at the impact parameters smaller than a certain radius have appreciable probabilities of the reactions, i.e., not only the crossings located at large distances inside this sphere but also the crossings at smaller distances participate in the reactions. Especially for ions of $q \geq 20$, the collisions with the impact parameters smaller than a certain distance make the charge transfer probability nearly constant. In fact, the probabilities are generally larger than 80%, which may be compared with the absorbing-sphere model proposed by Olson and Salop.¹⁰⁾ They defined the radius R_0 from the condition that the diabatic transition probability p ($b=0$) becomes 0.86 at R_0 and assumed that the probabilities inside this sphere are unity. The radius of the absorbing sphere was calculated by using eq. (2.2) and indicated in the figures by the dotted arrows.

Partial cross sections are shown in Fig. 5, meanwhile total cross sections are shown in Fig. 6 with other experimental data and an empirical scaling law proposed by Müller and Salzborn.¹⁵⁾ No experimental data on partial cross sections are available. Since the separation of the energy-gain peaks corresponding to different n -states for these systems becomes so small in our energy-gain spectra, even the n -distributions could not be determined experimentally.⁹⁾ Therefore, the effective crossing distance R_c was deduced from the observed

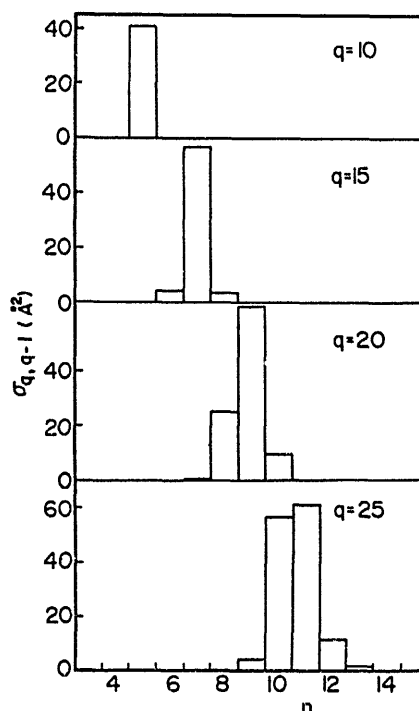


Fig. 5. Calculated distributions of one-electron capture cross sections over the principal quantum number n for Kr^{q+} ($q=10, 15, 20$ and 25) + He collisions. The collision energy is $q \times 1$ keV.

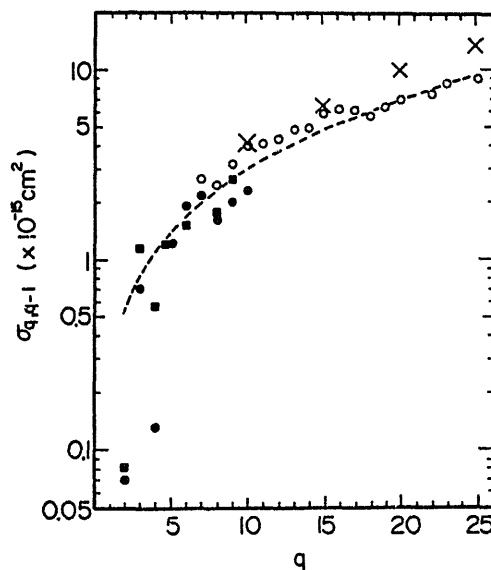


Fig. 6. Total cross sections for one-electron capture $\sigma_{q,q-1}$ as a function of the charge state q of projectile Kr^{q+} ions. \bullet : Cocke *et al.* (ref. 16) at $q \times 0.78$ keV, \blacksquare : Kusakabe *et al.* (ref. 17) at 0.286 keV/amu, \circ : Iwai *et al.* (ref. 9) at $q \times 1$ keV, \times : the present calculated results at $q \times 1$ keV/amu. The dashed curve represents the empirical scaling law of Müller and Salzborn (ref. 15).

peak position of the energy-gain spectra using eq. (1.2). On the other hand, the theoretical effective R_c was evaluated from the weighted

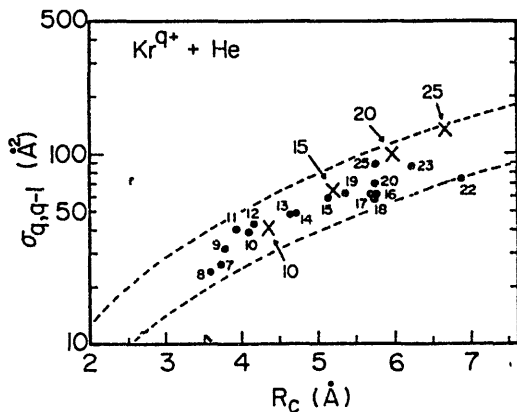


Fig. 7. Total one-electron capture cross section versus the effective crossing radius R_c in $Kr^{q+} + He$ collisions. \times : present results at $q \times 1$ keV. \bullet : experimental results by Iwai *et al.* (ref. 9) at $q \times 1$ keV. Two dashed curves represent $\frac{1}{2}\pi R_c^2$ and πR_c^2 , respectively.

average of the calculated energy gain ΔE . The results are compared in Fig. 7. It is clearly seen that both the calculated cross sections and effective crossing distances increase with q in agreement with the observed results and that both cross sections are between $\frac{1}{2}\pi R_c^2$ and πR_c^2 . Though more and more channels belong to higher n -states, our calculations are based on the assumption that there are no couplings between the adjacent channels. This assumption may somewhat overestimate the cross sections especially for the charge states q larger than 20.

The present calculation is based upon several assumptions and simplifications. We assumed, as the coupling matrix element H_{12} , an Olson-Salop's expression multiplied by a factor of 0.6 (eq. (2.2)). We neglected the interference between the neighboring channels. For high- q ions where no levels are known, the number of the channels was assumed to be proportional to the principal quantum number n . The Landau-Zener probability p (eq. (2.1)) becomes inaccurate in near-glancing collisions. No correction, however, was made for this case. We also neglected the orbiting effect in the present calculation. In spite of these assumptions and simplifications, the agreement between the present calculations and experiments is systematically good. Therefore, the present model helps us to get an insight of physics of one-electron capture processes by highly stripped ions from He atoms.

Acknowledgements

This work was carried out as a part of the Guest Research Program at the Institute of Plasma Physics, Nagoya University. The authors are grateful to Professor H. Kakihana, the Director of the Institute, and Professor Emeritus K. Takayama, the former Director of the Institute, for their encouragement throughout the present work. Thanks are also due to Professor T. Watanabe of the Institute of Chemical and Physical Research (RIKEN) for his interest and helpful discussion.

References

- 1) T. Iwai, Y. Kaneko, M. Kimura, N. Kobayashi, S. Ohtani, K. Okuno, S. Takagi, H. Tawara and S. Tsurubuchi: *Phys. Rev. A* **26** (1982) 105.
- 2) Y. Kaneko, T. Iwai, S. Ohtani, K. Okuno, N. Kobayashi, S. Tsurubuchi, M. Kimura, H. Tawara and S. Takagi: *Physics of Electronic and Atomic Collisions*, ed. S. Datz (North-Holland, Amsterdam, 1982) p. 697.
- 3) S. Ohtani, Y. Kaneko, M. Kimura, N. Kobayashi, T. Iwai, A. Matsumoto, K. Okuno, S. Takagi, H. Tawara and S. Tsurubuchi: *J. Phys. B* **15** (1982) L533.
- 4) T. Tsurubuchi, T. Iwai, Y. Kaneko, M. Kimura, N. Kobayashi, A. Matsumoto, S. Ohtani, K. Okuno, S. Takagi and H. Tawara: *J. Phys. B* **15** (1982) L733.
- 5) M. Kimura, T. Iwai, Y. Kaneko, N. Kobayashi, S. Ohtani, K. Okuno, S. Takagi, H. Tawara and S. Tsurubuchi: *J. Phys. B* **15** (1982) L851.
- 6) K. Okuno, H. Tawara, T. Iwai, Y. Kaneko, M. Kimura, N. Kobayashi, A. Matsumoto, S. Ohtani, S. Takagi and S. Tsurubuchi: *Phys. Rev. A* **28** (1983) 127.
- 7) H. Tawara, T. Iwai, Y. Kaneko, M. Kimura, N. Kobayashi, A. Matsumoto, S. Ohtani, K. Okuno, S. Takagi and S. Tsurubuchi: *Phys. Rev. A* **29** (1984) 1529.
- 8) H. Winter, E. Bloemen and F. J. de Heer: *J. Phys. B* **10** (1977) L453; D. Smith, N. G. Adams, E. Alge, H. Villinger and W. Lindinger: *J. Phys. B* **13** (1980) 2787; H. Winter: *Physica Scripta* **T3** (1983) 159; B. A. Huber: *Physica Scripta* **T3** (1983) 96.
- 9) T. Iwai, Y. Kaneko, M. Kimura, N. Kobayashi, A. Matsumoto, S. Ohtani, K. Okuno, S. Takagi, H. Tawara and S. Tsurubuchi: *J. Phys. B* **17** (1984) L95.
- 10) R. E. Olsen and A. Salop: *Phys. Rev. A* **14** (1976) 579.
- 11) S. E. Butler and A. Dalgarno: *Astrophys. J.* **241** (1980) 838.
- 12) R. E. Olson, E. T. Smith and E. Bauer: *Appl. Optics* **10** (1971) 1848.

- 13) A. Salop and R. E. Olson: *Phys. Rev. A* **13** (1976) 1312.
 - 14) S. Bashkin and J. O. Stoner, Jr.: *Atomic Energy Levels and Grotrian Diagrams I* (North-Holland, Amsterdam, 1975).
 - 15) A. Müller and E. Salzborn: *Phys. Lett.* **62A** (1977) 391.
 - 16) C. L. Cocke, R. DuBois, T. J. Gray and E. Justiniano: *IEEE Trans. Nucl. Sci.* **NS-28** (1981) 1032.
 - 17) T. Kusakabe, H. Hanaki, N. Nagai, T. Horinouchi and M. Sakisaka: *Physica Scripta* **T3** (1983) 191.
-

ONE-ELECTRON CAPTURE BY HIGHLY STRIPPED IONS
FROM HELIUM ATOMS
— FINAL-STATE ANALYSIS —

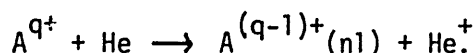
S. Ohtani
Institute of Plasma Physics
Nagoya University
Nagoya 464, Japan

One-electron capture processes in collisions between highly stripped ions and He atoms at low energies are discussed. For lower charged ion collisions, the cross sections oscillate strongly with increase of charge state, while for higher charged ion the cross sections tend to increase monotonically. Through a series of experimental investigation of the final states of collision products, it reveals that the cross sections are sensitive to the details of the potential curves of the collision systems.

INTRODUCTION

During the last decade, a great deal of information on electron capture processes in slow collisions between highly stripped ions and atoms has been accumulated. At XI ICPEAC in Kyoto and XII ICPEAC in Gatlinburg, we had symposia of collisional processes involving highly stripped ions and there both theoretical and experimental situation of electron capture collisions was reviewed [1,2]. There are a number of excellent review articles and proceedings of the symposia which have been devoted to the collision processes involving highly stripped ions: see, for example, Gilbody [3], Dalgarno [4], Janev and Presnyakov [5], de Heer [6, 7], the IAEA Technical Committee Meeting on Atomic and Molecular Data for Fusion [8], the Symposium on Production and Physics of Highly Charged Ions in Stockholm [9], and the NATO Summer School of Atomic Physics of Highly Ionized Atoms at Cargese [10].

As for the electron capture processes by highly stripped ions from multielectron targets, Salzborn and Müller [11] reviewed at the XI ICPEAC in Kyoto in 1979. There they discussed the general feature of cross sections dependent on the velocity and the charge state of projectile in slow collisions ($v < 1$ a.u.). In this paper we shall follow the scheme of their review but cannot cover all the new data of interest in connection with the fast increasing interest of this field. Therefore, we will focus on a part of this field and discuss the progress in the recent experimental studies of final-state-selected one-electron capture by highly stripped, slow ions from He atoms as the most simple multielectron targets as follows,



These collisions may take place very effectively in reactions of moderate exothermicity through the favored crossings in the diabatic potential curves. Final-state-selective studies are essential for unambiguous interpretation of the electron capture processes.

ION SOURCES

As one of the reasons of a rapid growth in this field, we would like to mention successful progress in the development of "new generation" (named by Crandall [12]) ion sources for slow ions.

Recoil ions, formed when fast heavy projectiles extracted from an accelerator impact gas atoms (e.g. Xe^{29+} at 4.5 MeV/amu on Ne gas target), are very slow and highly stripped. These slow ions (2 - 20 eV) extracted from the target cell can be used for collision experiments. Such experiments are being performed by Cocke et al. [13], Mann et al. [14], Kusakabe et al. [15], Aarhus group [16] and by some other groups. The property of providing localized, suddenly-charged in a short time, slow ions is uniquely suited to ion trap experiments of very slow collisions such as done by Sellin et al. [17] and Prior et al. [18]. The most powerful sources are considered to be an electron cyclotron resonance ion source (ECRIS)[19] and an electron beam ion source (EBIS)[20] for collision experiments in the low energy keV region. There are a number of new experiments using these ion sources. The present situation of these "new generation" ion sources and other important ones are summarized by Crandall [12], and the recent progress of the ion sources is reviewed by H. Winter [21].

TOTAL CROSS SECTIONS FOR ONE-ELECTRON CAPTURE

During the last years, systematic investigation of charge transfer collisions has been performed by Salzborn et al. [11] and subsequently done by Huber et al. [22] and Bliman et al. [23]. According to their measurements, the general feature of the total cross sections for one-electron capture $\sigma_{q,q-1}$ in the various collision systems with the same target atoms at low energies are as follows:

- 1) The cross sections are almost independent of impact energy, excepting low q projectile systems.
- 2) The cross sections generally increase with the primary ion charge state q . As an example, Fig. 1 shows total cross sections $\sigma_{q,q-1}$ in collisions of Bi^{q+} ions with He atoms as a function of the collision energy, measured by Schrey and Huber [24] using a miniature EBIS of Redhead type. In this figure, the cross sections for Bi^{4+} are very small and show a marked energy dependence in comparison with other $\sigma_{q,q-1}$ in the energy range studied.

Among a large number of one-electron capture cross sections investigated, such a behavior always occurs with high atomic number projectile with low charge states and He target systems. This behavior is considered to be due to the fact that, in these collision systems, the energy defect of the reaction is very small or negative (endothermic) in almost cases.

For higher q collision systems, the cross sections $\sigma_{q,q-1}$ show the weak energy dependence. This behavior is understood by the involvement of a lot of electron-capturing excited states of the product ion. The partial cross section for each specific transition of an electron terminating in a final state may have an individual energy dependence. The total cross section, however, should be made up by a sum over the involved partial cross sections with maxima at different collision energies and hence shows a faded energy dependence. Further, for highly but partially stripped ion collisions, the number of these states increases more and more with increasing q . The number of open channels in the reaction becomes so large that the electron capture process can be considered as decay of the initial input-channel, and then, due to its interaction with the quasicontinuum of final states, this process becomes quasistationary in character. Under these conditions, a scaling law of the cross section with q becomes possible since the decay concept remains valid in a wide q region.

In the above circumstances, many attempts have been made to find a general expression for the charge state q dependence of the one-electron capture cross section by scaling in terms of power laws. According to the scaling laws derived from systematic investigation of measured cross sections, the cross sections obey roughly a scaling of linear dependence of q : $q^{1.17}$ by Müller and Salzborn [25], $q^{1.1}$ by Huber and Kahlert [26] and $q^{1.0}$ by Bliman et al [33]. The theoretical consideration of the scaling laws was discussed by Janev and Hvelplund [28]. They showed the reduced representation of the cross sections in a wide region of the collision energy based on the theoretical consideration. In Fig. 2, are shown the experimental reduced cross sections as a function of the reduced energy for the cross sections for one-

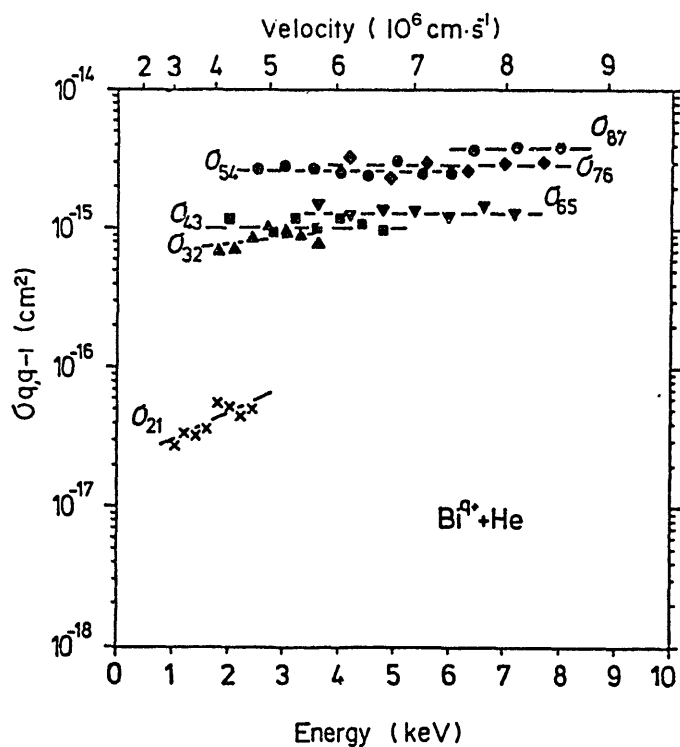


Fig. 1. Cross sections for one-electron capture $\sigma_{q,q-1}$ by Bi^{q+} ions incident on He. From Ref. [22].

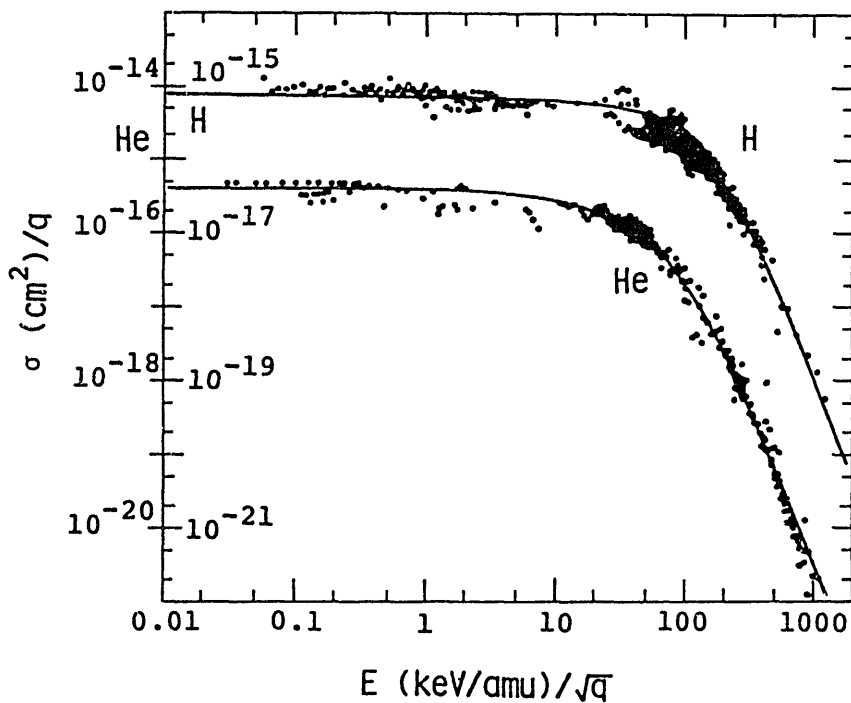


Fig. 2. Reduced cross sections for electron capture σ/q vs. reduced energy E/\sqrt{q} . Solid lines are fits to the experimental data ($q \geq 5$). References to the original data can be found in Ref. [27]. From Ref. [28].

electron capture by highly stripped ions ($q \geq 5$) from H and He targets together with their fitted curve. In low energy region, linear dependence of q is also seen. They also mentioned that the decay process of the initial channel plays an important role to discuss the scaling law for the collision systems involving many electrons at low energies and investigation of electron transfer in a quasimolecular system at the various crossings is necessary for further understandings. Meanwhile, in order to understand a detailed mechanism in the electron capture processes between highly stripped ions and multielectron atoms at low energies, the collision system between a highly stripped, simple ion having no more than a few electrons and He atom may be suitable because its electronic structure is simple enough to treat theoretically. As a typical example, hereafter, we would like to show the experimental work recently done by NICE group [29 - 37] in order to investigate the electron capture processes by highly stripped ions from He atoms. NICE group was organized by Kaneko and Iwai at Nagoya 1977 [34]. NICE means Naked Ion Collision Experiment. We have measured cross sections for one-electron transfer from a He atom into fully-stripped, hydrogen-like, helium-like and lithium-like ions of B^{9+} , C^{9+} , N^{9+} , O^{9+} , F^{9+} and Ne^{9+} at collision energies below 1.5 keV/amu. In Fig. 3, the total cross sections for one-electron capture at 0.8 keV/amu are shown, including highly stripped S^{9+} collisions. The lines are drawn to connect data for ions having the same iso-electronic sequences. The cross sections $\sigma_{q,q-1}$ oscillate strongly with q , around a dotted line which shows an empirical q -dependence $q^{1.17}$ [25]. Similar oscillations of $\sigma_{q,q-1}$ in the q -dependence have been observed by many investigators for the more complicated collision systems. This oscillatory behavior is interpreted in terms of the classical one-electron model [38], which becomes familiar at present.

According to the classical model, in the one-electron capture processes at low energies, an electron is captured into a selective level with a principal quantum number n . Such a level drastically changes from n to $n + 1$ at a particular quantum value of q when the q is increased. This level-change results in an increase of the crossing distance of diabatic potential curves: it causes a significant increase in the q -dependence of the cross sections. When the quantum number n is the same, the larger q gives the smaller interaction distance, causing gradual decrease in the cross section. After all, the q -dependent cross sections show a saw-tooth type oscillation. Though the classical model may be crude, the model has been found to be adequate for the case of He target [29, 30].

FINAL STATE ANALYSIS

In order to see whether an electron is captured selectively into a favored level and whether the oscillation is caused by the change of such a level, we have measured translational energy spectra of charge-changed incident ions. The final excited state of the ion after electron capture can be identified by the translational energy gain of the ion scattered in the forward direction. For the favored channel, capture occurs at a crossing in the potential curves during collisions, and the translational energy generally is increased, i.e., the potential energy difference between initial and final states is converted to translational energy. We have made a series of measurements of the energy gains of almost all the incident ions shown in Fig. 3 at low energies (1 and 2 keV/ q), to analyse the final states after electron capture. The measured energy gains ΔE are compared to the reaction energies calculated from the book of Bashkin and Stoner [36], and the final states of the charge-changed primary ions are determined.

Figure 4 shows the translational energy-gain spectra for low energy (1 keV/ q), fully stripped ions of C^{6+} and O^{8+} incident on He. In this figure, calculated energy levels are also indicated, corresponding to some principal quantum numbers n of the product C^{5+} and O^{7+} ions after electron capture, and it is clearly shown that only single peaks are observed which correspond to the $n=3$ for the product C^{5+} and the $n=4$ for O^{7+} . Selective electron capture into these levels is in good agreement with the prediction of the classical consideration in [29, 30]. The change of the final state, $n=3$ for $C^{6+} + He$ collision to $n=4$ for $O^{8+} + He$, should give rise to a

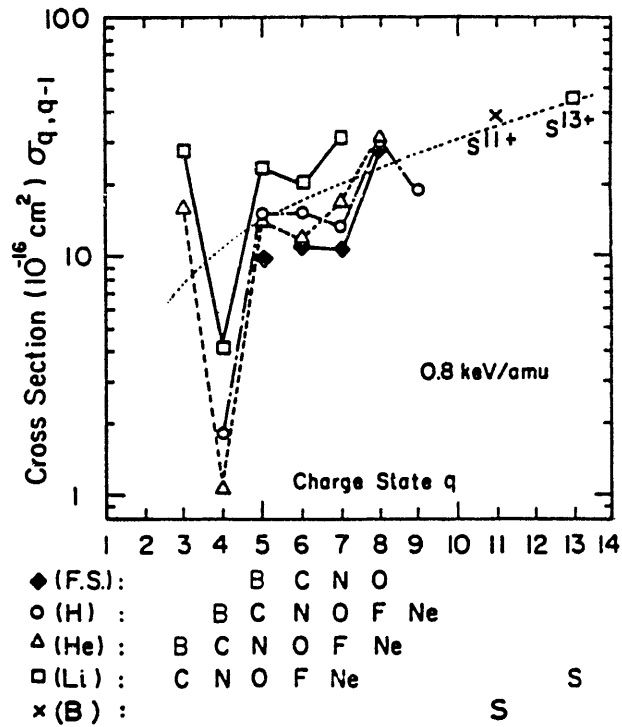


Fig. 3. Measured cross sections $\sigma_{q,q-1}$ at 0.8 keV/amu as a function of the ionic charge q of projectile ions. Dotted line is obtained from an empirical formula of Müller and Salzborn [25].

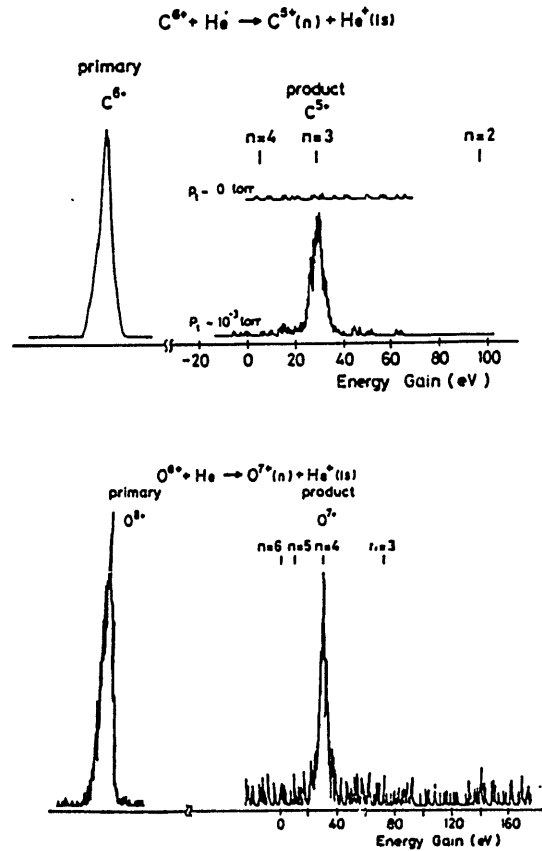


Fig. 4. Typical energy gain spectra of forward scattered C^{5+} and O^{7+} ions in $C^{6+} + He$ and $O^{8+} + He$ collisions at 1 keV/q.

similar. Therefore, such similarity should give the similarity in the energy spectra for the one-electron capture processes by various projectiles having the same charge state $q=6$ from He. For other collision systems, similarities in the energy spectra for different ions with the same q are seen in almost cases.

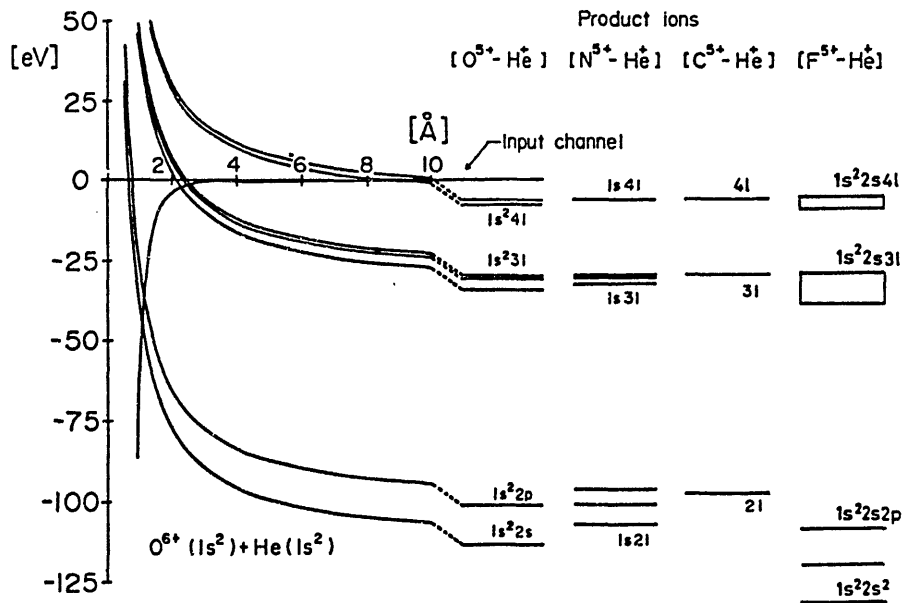
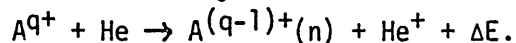


Fig. 6. Diabatic potential curves for one-electron capture process, $O^{6+}(1s^2) + He(1s^2) \rightarrow O^{5+}(1s^2n\ell) + He^+(1s)$, and energy diagrams for channels of one-electron capture into $O^{5+}(1s^2n\ell)$, $N^{5+}(1s n\ell)$, $C^{5+}(n\ell)$ and $F^{5+}(1s^2 2s n\ell)$ levels.

Therefore, we will classify and summarize the measured spectra according as the charge state q rather than the iso-electronic sequence of the incident projectiles. In Table 1, are summarized the principal quantum number n into which the electron is captured, the energy gain ΔE (eV) measured in the spectra and the calculated crossing radius R_C (Å) in the diabatic potential curves. In a few cases studied, there are weak peaks observed in the energy-gain spectra around the dominant peak. In this table, are shown the values of n , ΔE and R_C corresponding to such the dominant peaks. Good similarities of n , ΔE and R_C among the same q are also shown, in this table, for the various $A^{q+} + He$ systems. Furthermore, with increasing q , the n increases stepwisely, while the R_C shows non-monotonic increase. This behavior is shown in Fig.7. The dashed line is drawn in order to visualize the strong oscillation with q . As described earlier, the oscillation of the one-electron capture cross sections is thought to be caused by the capturing-level change and resultant drastic change of the crossing radius R_C . This prediction is seemed to be confirmed here qualitatively by observing R_C -oscillation with q .

However, there are some discrepancies between the prediction and the measurements. For instance, the change of the level from $n=3$ for C^{6+} to $n=4$ for N^{7+} , and from $n=4$ for F^{8+} to $n=5$ for Ne^{9+} should cause a significant increase in the q -dependent cross sections. But the cross sections, as seen in Fig.3, change little and/or decrease toward higher charge state. Therefore, it is expected that there should be an another rule in determination of the q -dependence of the cross sections for one-electron capture, in addition to the selection and its variation of the final capturing state.

Table 1 Principal quantum number n , energy gain ΔE (eV) and crossing radius R_c (Å), obtained from the dominant peaks in the energy gain spectra for the collision systems:



A \ q	3			4			5			6			7			8			9			
	n	ΔE (eV)	R_c (Å)																			
C	2	11	26	2	31	14	3	14	42	3	29	25										
N				2	24	18	3	16	36	3	30	24	4	17	51							
O							3	18	31	3	30	24	4	18	48	4	30	34				
F										3	29	25	4	18	48	4	28	36				
Ne													4	20	43	4	31	33	5	20	57	

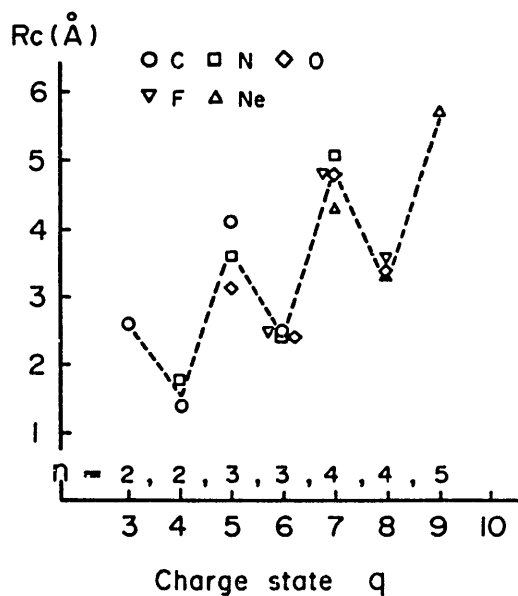


Fig. 7. Crossing radius R_c (Å) of one-electron capture processes in $A^{q+} + \text{He}$ collisions as a function of the ionic charge q of projectile ions, ($A = \text{C}, \text{N}, \text{F}$ and Ne). Principal quantum number n into which an electron is captured is also shown.

In order to search for the additional rule, we arranged the measured cross sections at 0.5 keV/amu as a function of the derived crossing radius R_C . According to this arrangement (see in [36]), the R_C -dependence of the one-electron capture cross sections does not increase monotonically but seems to have a peak structure. This fact implies that the electron capture process prefers the final states of the product ions which correspond to crossings at some suitable internuclear distances.

The existence of a maximum in the cross sections at a particular crossing radius has been reported by some investigators for various collision systems at different energy ranges [40, 41, 42, 43] and is often called the "reaction window". This window shape seems to be similar for the various cases reported. Accordingly, it tends to be believed to be universal for all the collision systems. This behavior is qualitatively understood by considering the exponential decrease of quasi-molecular-coupling with the crossing radius. It is, however, necessary to analyze more carefully the observed data before coming to such a conclusion, because there should always exist multicrossings in the diabatic potential curves for the collision systems. Even though the observed energy-gain spectrum consists of a single peak, this does not always guarantee the single crossing in the diabatic potential curve. In fact, the energy-gain spectra in the collision system, for example, between Li-like ions and He become broad indicating the contribution of a number of peaks corresponding to the levels with different orbital quantum number ℓ . We have no accurate idea on which and how many crossings do contribute to the observed apparent single peak in the energy-gain spectrum because of a limited energy resolution used in the experiments. For such a collision system where the sublevels having the same n but different ℓ result in many crossing closely located in the potential curve, an optical measurement can be a powerful complementary work, as described later.

Further experimental studies have been in progress for the collision systems of S^{11+} , S^{13+} and Kr^{q+} ($q=10-25$) with He in order to observe what happens in higher q projectile collisions. The measured energy spectra are shown in Fig.8 for some cases in the $Kr^{q+} + He$ systems at low energies (1 keV/ q). Though the energy levels for highly charged Kr^{q+} ions are not known, it should be noted that the energy spectrum in all cases studied here consists of the dominant "apparent" single peak with a relatively narrow width, and, in general, the values of $\Delta E/q-1$, the observed energy gain divided by the product charge state, becomes smaller with q , that is, the derived crossing radius R_C where an electron is transferred in the potential curves becomes consequently larger with q . We arranged once again the measured total one-electron capture cross sections as a function of R_C , as seen in Fig.9. In contrast to the result of the former arrangement for the collision systems involving relatively lower charge ($q < 10$) projectiles, the measured cross sections do not have a maximum at a particular R_C but seem to follow the classical cross section R_C rule.

We cannot clearly understand this phenomenon but may roughly consider as follows: At a given q and energy in slow collisions, there should be a favored region of R_C in the diabatic potential curves where the cross sections have large values, and when the proper crossings fortunately exist in this favored region, electron capture effectively occurs in the $A^{q+} + He$ system. The maximum R_C of this region becomes larger and the width of the favored region becomes wider with increasing q .

In the cases of lower q ($q < 10$) projectiles having no more than a few electrons, an opportunity that the proper final states fit into the favored $R_C(q)$ may strongly depend on the electronic structure of the product ($q-1$) ion and is accidentally afforded for particular projectiles, since the final states of such product ions should be located discretely for the smaller principal quantum number ($n \leq 5$) into which the electron is captured. In Fig.9, the projectiles whose cross sections are much smaller than $1/2\pi R_C^2$ may have not suitable final states for electron capture with their q and collision energy. According to multicrossing consideration of Landau-Zener type, for small R_C the cross section for electron transfer is much smaller than πR_C^2 , because, even if there are several crossings available, only a single outer-most crossing becomes effective. This should be reason why

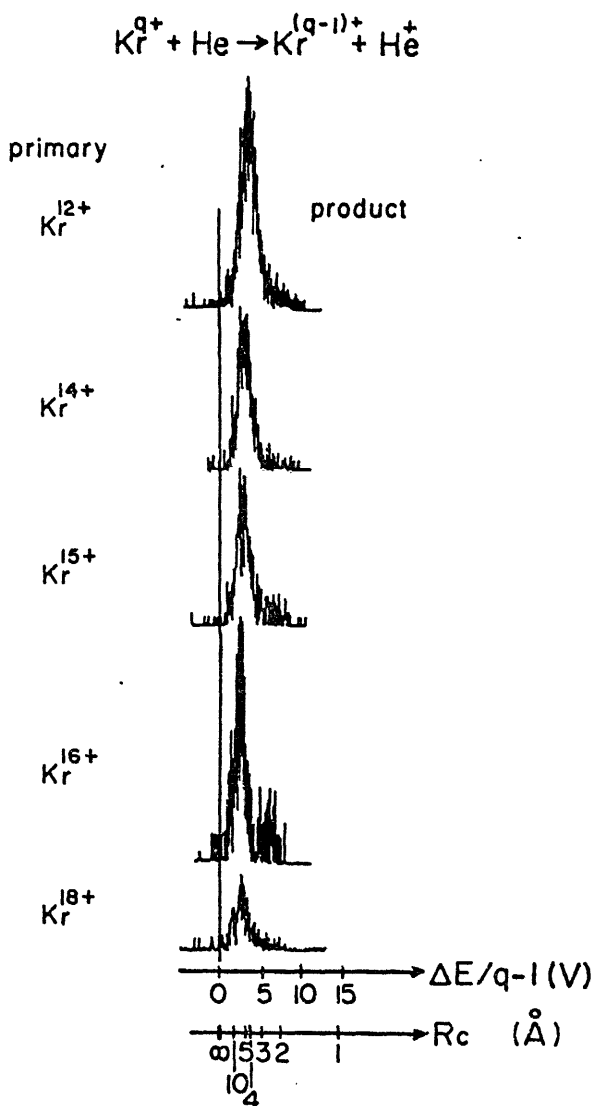


Fig. 8 Energy gain spectra of the product $Kr^{(q-1)+}$ in $Kr^{q+} + He$ collisions at 1 keV/q.

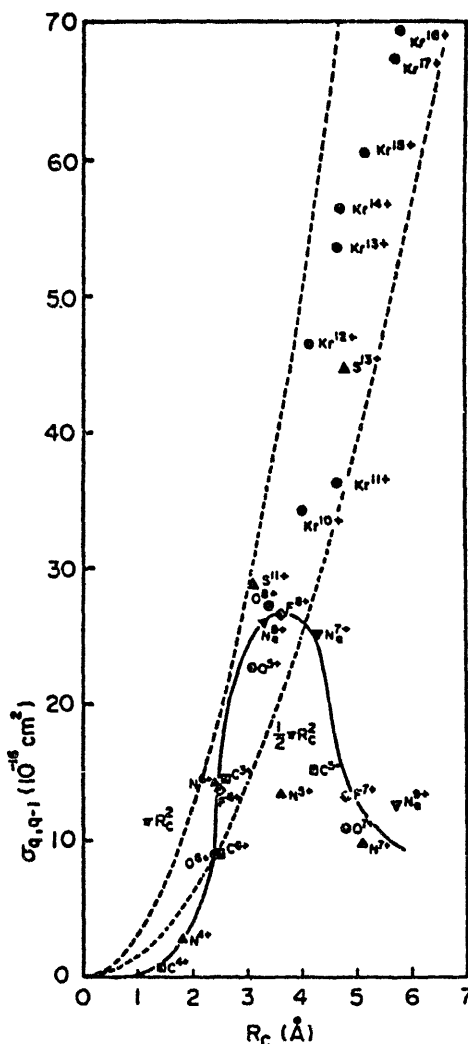


Fig. 9. Total cross sections for one-electron capture as a function of crossing radius R_c in slow $A^{q+} + He$ collisions. Dotted lines correspond to the classical cross sections.

The existence of maximum in the q -dependent cross sections was observed for the lower q projectiles at low energies.

On the other hand, higher charged ($q \geq 10$), but partially stripped projectiles may have abundant opportunities to capture an electron from He during collisions. For these projectiles, the electron should be transferred in the larger R_c region and into a larger principal quantum number around which a number of levels including sublevels are densely located. And the number of crossings increases with R_c and q . Under this situation, there are a fair chance in higher q collision for several final states to fit into the favored R_c with a broad width. In addition, the multi-crossing Landau-Zener consideration shows that when several crossings exist at larger R_c , all of them may contribute to the total electron transfer processes. Then even if the diabatic transition probability is small for a single crossing, the total cross sections should be larger with the number of the crossings. Therefore, for the observed collision systems between S^{q+} , Kr^{q+} and He where there should be a number of crossings available, the total cross section may increase with R_c and tend to come up to the maximum cross section πR_c^2 .

For the higher q collision systems where the electron is transferred into the densely

located levels of large n - simulated to quasicontinuum, it is expected that the total cross sections obey the scaling law as described earlier. The total cross sections for one-electron capture by Kr^{q+} from He are shown in Fig.10 as a function of the primary charge state q in slow collisions, together with an empirical scaling law of Müller and Salzborn. As seen in this figure, strong oscillation in the cross section is observed for lower q , but it tends to diminish toward higher q and the q -dependence of the measured cross sections becomes in good agreement with the empirical scaling of the cross sections.

In discussion of the electron capture process into quasi-continuum states, we want to refer to the width of favored region at large R_C for higher q collisions. For each energy spectrum of $\text{Kr}^{q+} + \text{He}$ system, the observed energy spread seems to be narrow. From a simple deconvolution, the half-width of favored R_C region is less than 1 Å at $R_C = 4.7$ Å for the collision system: $\text{Kr}^{14+} + \text{He} \rightarrow \text{Kr}^{13+}$ (product). This width seems to be much narrower than that expected from Landau-Zener calculation. This shows that the crossings in the narrow region at a given R_C in the diabatic curves of the collision system should be very effective and make an important contribution to the total cross sections. Such a conclusion is very similar to that of "absorbing-sphere model" of the multicrossing systems [46].

Above consideration is one of the possible discussions to pursue knowledge of electron capture process in the complicated collision systems such as highly stripped ion-multielectron atom collisions, through a series of our recent investigation.

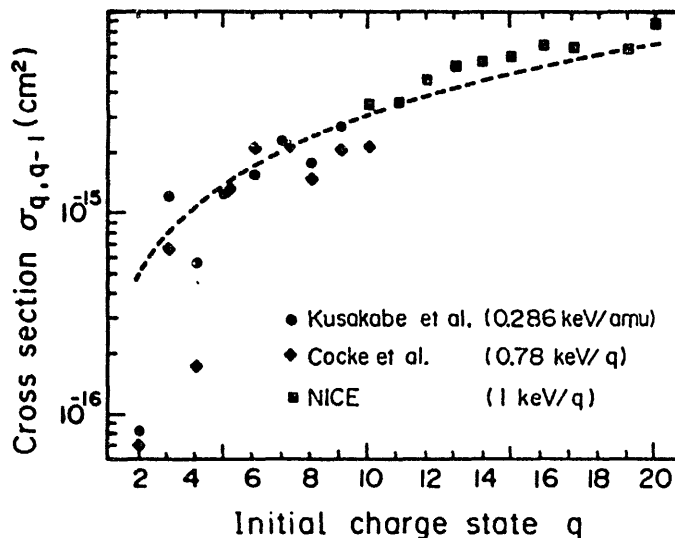


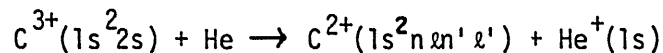
Fig.10 Total cross sections for one-electron capture as a function of the ionic charge q of projectile ions. Dotted line is obtained from an empirical formula of Müller and Salzborn [25], ●: Kusakabe et al. [15], ◆: Cocke et al. [44], ■: present results.

Very recently, many laboratories have engaged in intense investigation of final-state-selected electron capture processes by highly stripped ions from atoms in slow collisions, by aid of the translational energy spectroscopy method. Earlier studies of this kind was carried out by Panov et al. [46] for $\text{Ar}^{6+} + \text{He}$ in slow collisions below 120 keV. They measured the partial cross section for electron transfer into 4s, 4p, and 3d states of Ar^{5+} . Recently Mann et al. [47] observed

selective electron capture by Ne^{9+} and Ne^{10+} from rare-gas targets at energies below 500 eV using recoil ions. They continue doing a systematic work of electron transfer collisions. McCullough et al. [48] and Huber et al. [49] have observed the state-selective electron capture processes for low q collision systems in good energy resolution.

One of the advantages of this method is the small necessity of the primary ion intensity. Intensity of 10^3 counts/sec is sufficient to determine the energy spectra. Another is that the electron transfer into the ground state of the product ion can be observed. However, in order to observe the closely located final states such as ℓ states, it is hard to separate them in the energy spectrum at the present energy resolution as yet. As described before, spectroscopic studies of the radiative decay of the excited product ions may be used to obtain information on ℓ -state-selective capture processes.

Of course, if ℓ -states in the same n are discretely located in energy, it is possible to observe these states separately. Kimura et al. [33] observed ℓ -distributions of captured electrons in the reaction at 1 keV/ q ,



It is found that an electron is captured selectively into particular states of $\text{C}^{2+}(1s^2 2\ell 2\ell')$. The measured partial cross sections were compared with the Landau-Zener cross sections. Recently, Lennon et al. [50] measured these partial cross sections as a function of collision energy (3 - 18 keV). They observed that electron capture processes into the $\text{C}^{2+}(1s^2 2p^2)$ states involving a change in the electron-core configuration of the primary ion, contribute significantly to the total cross sections at higher energies. For the $\text{N}^{4+} + \text{He}$ collision, the reaction of electron transfer involving a change of core configuration is predominant compared with simple one-electron transfer in slow collisions [33].

The measurement of the ℓ -distributions in electron capture processes should be important to understand electron translational mechanisms such as the momentum transfer process to captured electron. There are several theories considering the ℓ -distributions in the cross sections. However, the measurements of the ℓ -dependent cross sections have been scarcely performed for highly stripped ion collisions at low energies, because we could not have an intense slow ion beam with higher charge state, by use of which it is possible to detect photons emitted after the collision. Recently, Afrosimov et al. [51] could measure the emission cross sections for the characteristic X-ray radiation accompanying the electron capture by C^{6+} and O^{8+} from H_2 at low energies, using EBIS source, "KRION-2" at Dubna. Bliman et al. [52] also measured the partial cross sections for electron capture into ℓ -sublevels in $n=3$ by C^{4+} and O^{6+} from H_2 , using their ECRIS source "MINIMAFIOS" at Grenoble, from optical spectroscopic measurements.

Very recently, detailed spectroscopic measurements have been performed by Gordeev et al. [53]. These experiments have been made as a collaboration between FOM (de Heer, Dijkkamp et al.) and Technical University Vienna (Winter et al.) and carried out at Groningen, using the MINIMAFIOS-type ion source. The cross sections for electron capture into different $n\ell$ state for A^{6+} ($\text{A} = \text{C}, \text{N}, \text{O}, \text{Ne}$) + He, H_2 collisions at low energies have been measured. They measured the absolute intensities of the various emitted lines corresponding to the transitions between different $n\ell$ levels of the product A^{5+} ions, and deduced emission cross sections σ_{em} . From the σ_{em} values they obtained the cross sections for electron transfer into $n\ell$ states, $\sigma_{n\ell}$, by taking into account all possible cascading effects. In Fig. 11 are shown the deduced $\sigma_{n\ell}$, together with $\sigma_n = \sum_{\ell} \sigma_{n\ell}$ and $\sigma_t = \sum_{n\ell} \sigma_{n\ell}$, for N^{6+} and $\text{O}^{6+} + \text{He}$ systems as a function of collision velocity. As seen in Fig. 11, the deduced cross sections σ_t are in good agreement with the previously measured results by Crandall [54] and Iwai et al. [30]. For $\text{A}^{6+} + \text{He}$ collisions, it is found that the electron is dominantly captured into the $n=3$ state and that there are good similarities between $\text{N}^{6+} - \text{He}$ and $\text{O}^{6+} + \text{He}$, both in the absolute value and in the velocity dependence of the cross sections.

These similarities among the same q are also in good agreement with the results before [35] (e.g. see in Fig.5 and 6). It is remarkable that σ_t and σ_n do not show significant dependence on the collision velocity, while $\sigma_{n\ell}$ show a strong redistribution of the ℓ -sublevel population over the studied velocity range. At present, theoretical calculations which can be compared directly with the observed data do not exist, the only available calculations dealing exclusively with fully stripped ion-atomic hydrogen collisions. However, the observed strong redistribution is rather unexpected. The theories predict more or less fixed ℓ -distributions over a wide velocity range. At a point of experimental view, since it is not easy to measure separately radiation lines from different ℓ states of the H-like product ions of the fully stripped ions-He collisions systems, we expect the theoretical calculation of the ℓ -dependent cross sections for electron capture by a simple, highly stripped ion from a He atom.

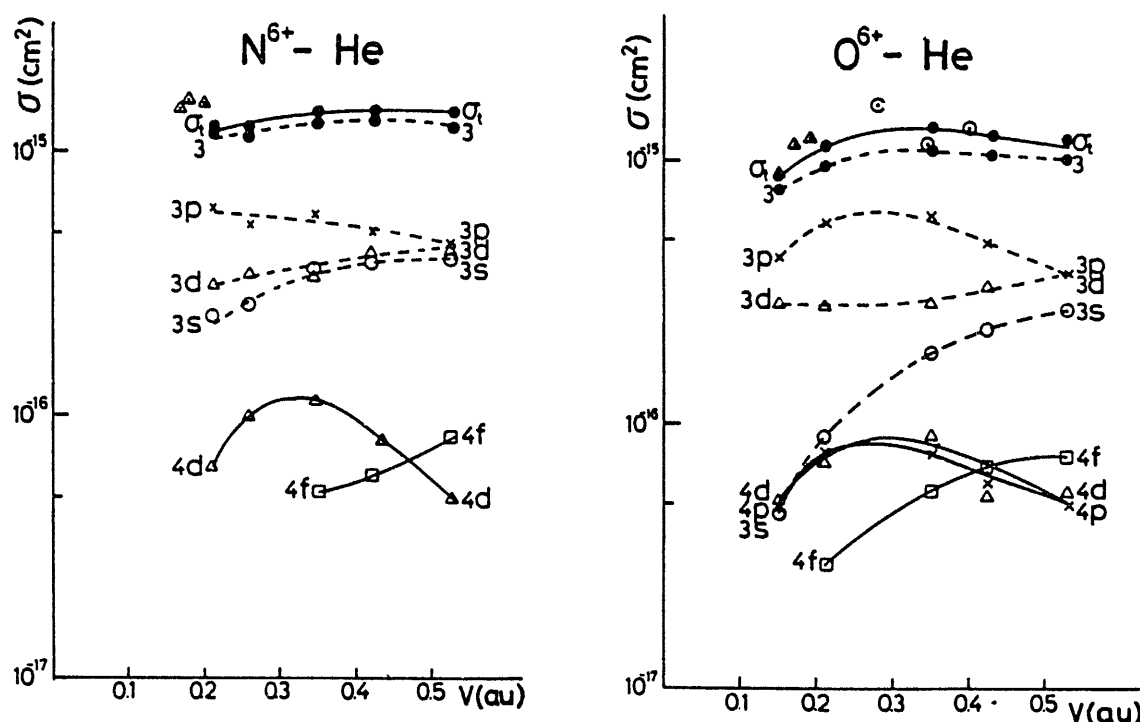


Fig.11. Partial $\sigma_{n\ell}$, σ_n and total σ_t cross sections for one-electron capture as a function of velocity in N^{6+} and $O^{6+} + He$ collisions. From ref. [52]. Δ : σ_t Iwai et al. [30]., \circ : σ_t Crandall et al. [54].

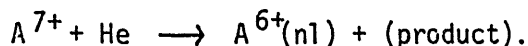
FURTHER REMARKS

One-electron capture processes in collisions between highly stripped ions and He atoms at low energies are discussed. The cross sections are very sensitive to the details of the potential curves of the quasimolecular collision system. Electron capture may take place effectively through the favored region of crossing radius R_c . For the lower q ion and He system, the crossing points are discretely located in the potential curves. Therefore, the value of the cross sections are determined by the coincidence of the specific crossing with the favored R_c . It may cause the drastic change of the q -dependent cross sections. On the other hand, for higher q collisions the system may have a large opportunity of overlapping each other because of the quasicontinuum state of the final channels. Therefore, the cross sections for electron capture by higher q ions become quasi-stationary in character and tend to agree with the cross sections derived from a scaling law.

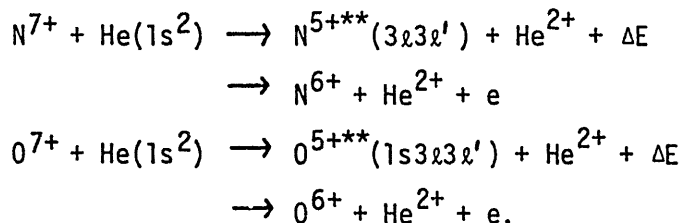
Finally, we would like to refer briefly to the transfer ionization processes, which are intensively investigated by several groups, and are reviewed by Niehaus [55],

Kishinevskii and Parilis [56] and by Müller [64]. Transfer ionization processes are essentially important for the multielectron target systems and may make a large contribution to other electron transfer processes. Final states in these processes have been analyzed mainly by measuring the energy spectrum of emitted electron during or after collision [57 - 61]. Winter et al. [57] have determined the total cross sections for electron production, σ_e , for rare gas ions and rare gas targets systems. Their results showed that σ_e values become larger for high q ion collisions, when the relevant transfer ionization processes become exothermic. Recently, Justiniano et al. [62] and Groh et al. [63] have measured the transfer ionization processes applying coincidence in charge state selection of both the projectile and target-ion. In their measurements of charge state distribution of target ions from two-electron capture, target ions with high charge state are formed in the transfer ionization process, with increasing q of projectile ions. Autoionizing states of the projectile formed after two-electron transfer or capture of inner-shell electrons from the target with subsequent Auger decay can become quite important when q is so high that these processes are exothermic. This experiment is powerful for understanding the transfer ionization mechanisms because the process can be distinguished from the direct ionization but the experiment can not give us information on the role of the final states in this collision system.

In Fig.12, the translational energy spectra are shown for the collision system:



It is also seen in this figure that there is good similarity among the spectral patterns for the same charge state of projectiles ($q=7$), irrespectively of ionic species. The dominant peaks at around 20 eV of energy gain observed in all the energy gain spectra are corresponding to the one-electron transfer into the $n=4$ of the product final state. This similarity results from the similarity among diabatic potential curves for the collision systems of $A^{7+} + \text{He}$, as described before. Besides the dominant peaks, there are weak peaks at around 70 eV in all the energy gain spectra observed for the A^{7+} collisions. In N^{7+} and $O^{7+} + \text{He}$ systems, these peaks are assigned as being due to the following transfer ionization via two-electron capture into the autoionizing states of N^{5+} and O^{5+} [32],



From the similarities of the diabatic potential curves and of the measured energy spectra with the same q for different ions, which are observed for the various charge state ($q=5,6,7,8$), the weak peaks at around $\Delta E=70$ eV for F^{7+} and Ne^{7+} collisions are thought to be due to the transfer ionization processes via two-electron capture into $F^{5+}(1s^2 3\ell 3\ell')$ and $Ne^{5+}(1s^2 2s 3\ell 3\ell')$, respectively, though it is not possible to assure this because no information on the energy levels of such doubly excited states is available presently.

Thus the translational energy spectroscopy may give us useful information regarding the final states of the transfer ionization processes, though we can not distinguish perfectly between transfer ionization and direct ionization. Further experiment such as a coincidence experiment between an energy-analyzed projectile-ion and a charge-separated target-ion would supply more detailed information.

ACKNOWLEDGMENTS

I am very grateful to many investigators who have sent me their latest, often unpublished results. As an expression of my appreciation of their generous help, I

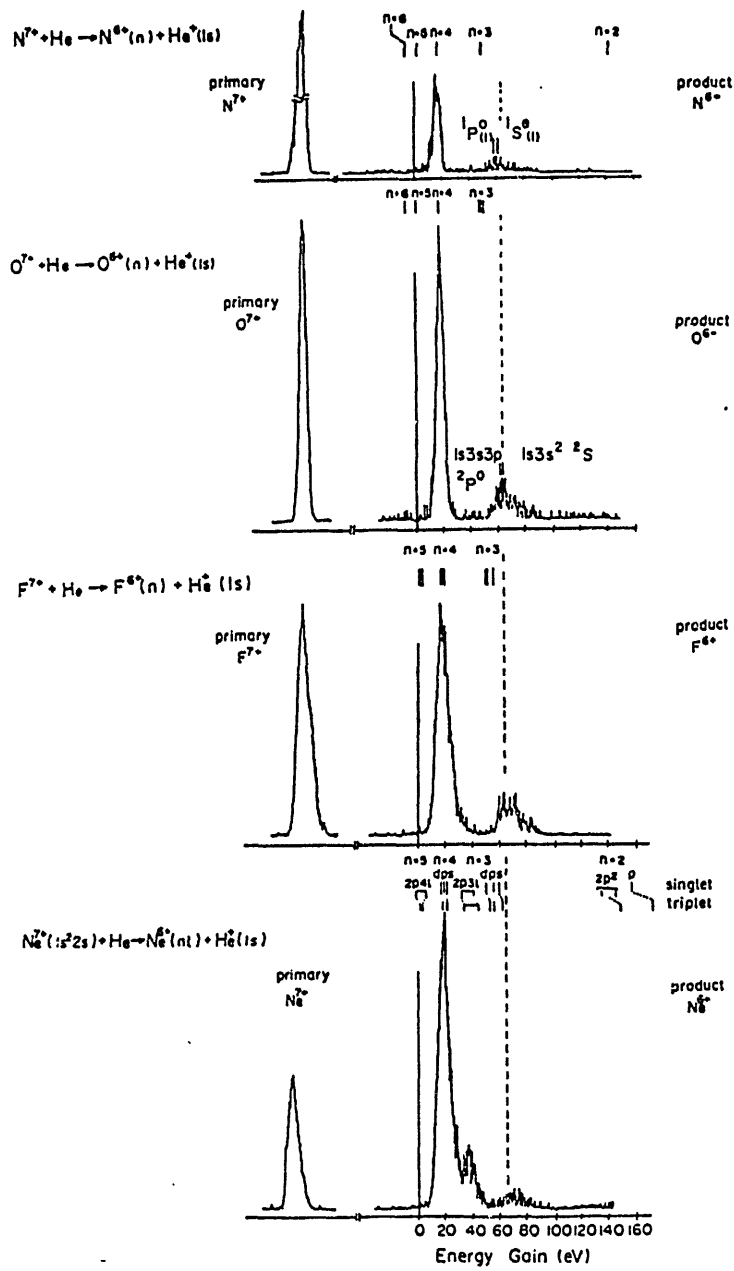


Fig.12. Energy gain spectra of forward scattered product ions A^{6+} in $A^{7+} + He$ collisions at 1 keV/q ($A = N, O, F$ and Ne). Weak and broad peaks at around 70 eV of energy gain are thought to be due to transfer ionization processes.

list here their names: V.V. Afrosimov, S. Bliman, C.L. Cocke, D. Dijkkamp, H.B. Gilbody, B.A. Huber, P. Hvelplund, T. Kusakabe, F.W. Meyer, M.H. Prior, I.A. Sellin and H. Winter. A review article of F.J. de Heer is very useful for studying this subject. I would like to thank all the members of NICE group for their collaboration and discussion through the experimental study of electron capture processes at Nagoya. Special thanks are due to A. Matsumoto and S. Takagi for helpful discussion and for preparing this manuscript.

REFERENCES

1. Symposium on electron capture by multiply charged ions, Proceedings ICPEAC XI, in Kyoto 1979, Invited Papers and Progress Reports, eds. N. Oda and K. Takayanagi, p.387 (North Holland, Amsterdam, 1980).
2. Symposium on collisions of multiply charged ions with atoms (dedicated to Jim McDonald) and other articles in Proceedings ICPEAC XII in Gatlinburg 1981, Invited Papers, ed. S. Datz (North Holland, Amsterdam, 1982).
3. H.B. Gilbody in Advances in Atomic and Molecular Physics, Volume XV, eds. D.R. Bates and B. Bederson, p.293 (Academic Press, New York, 1979).
4. A. Dalgarno in Advances in Atomic and Molecular Physics, Volume XV, eds. D.R. Bates and B. Bederson, p.37 (Academic Press, New York, 1979).
5. R.K. Janev and L.P. Presnyakov, Physics Reports 70, 1 (1981).
6. F.J. de Heer in Atomic and Molecular Processes in Controlled Thermonuclear 1979).
7. F.J. de Heer in Atomic and Molecular Physics of Controlled Thermonuclear Fusion, eds. C.J. Joachain and D.E. Post, (Plenum Press, New York and London, 1983).
8. Atomic and Molecular Data for Fusion in Physica Scripta, 23 no.2 (1981), edited by H.W. Drawin and K. Katsonis.
9. Production and Physics of Highly Charged Ions, Stockholm 1982, Physica Scripta T3, ed. L. Liljeby (1983).
10. Atomic Physics of Highly Ionized Atoms, Cargese 1982, ed. R. Marrus (Plenum Press, New York, 1983).
11. E. Salzborn, and A. Müller, Proceedings ICPEAC XI, in Kyoto 1979, Invited Papers and Progress Reports, eds. N. Oda and K. Takayanagi p.407 (North Holland, Amsterdam 1980).
12. D.H. Crandall, see [ref.9, p.249].
13. C.L. Cocke, R. DuBois, T.J. Gray, E. Jastiniano and C. Can, Phys. Rev. Lett. 46, 1671 (1981).
14. R. Mann, F. Folkmann and H.F. Beyer, J. Phys. B 14, 1161 (1981).
15. T. Kusakabe, H. Hanaki, N. Nagai, T. Horiuchi and M. Sakisaka, see [ref. 9, p.191].
16. Aarhus group, private communication from P. Hvelplund.
17. D.A. Church, R.A. Kenefick, W.S. Burns, I.A. Sellin, M. Breinig, S.B. Elston, S. Huldt, R. Holmes, J.-P. Rozet, D. Taylor and G.A. Glass, see [ref.9, p.71].
18. M.H. Prior, R. Marrus and C.R. Vane, Submitted to Physical Review A.
19. R. Geller and B. Jacquot, see e.g. [ref.9, p.19].
20. E.D. Donets, see e.g. [ref.9, p.11].
21. H. Winter in ref. 10.
22. B.A. Huber and H.J. Kahlert, J. Phys B 13, L159 (1980) and B.A. Huber, J. Phys. B, 809 (1980).
23. S. Bliman, S. Dousson, B. Jasquot and D. Van Houtte, J. Physique 44, 467 (1983).
24. H. Schrey and B.A. Huber, J. Phys. B 14, 3197 (1981).
25. A. Müller and E. Salzborn, Phys. Letters 62A, 391 (1977).
26. B.A. Huber and H.J. Kahlert, J. Phys. B 13, L159 (1980).
27. H. Knudsen, H.K. Haugen and P. Hvelplund, Phys. Rev A23, 597 (1981).
28. R.K. Janev and P. Hvelplund, Comments on Atomic and Molecular Physics, XI, 75 (1981).
29. Y. Kaneko, T. Iwai, S. Ohtani, K. Okuno, N. Kobayashi, S. Tsurubuchi, M. Kimura, H. Tawara and S. Takagi, Abstracts of ICPEAC XII in Gatlinburg 1981, ed. S. Datz, p.696 (North Holland, Amsterdam, 1981).
30. T. Iwai, Y. Kaneko, M. Kimura, N. Kobayashi, S. Ohtani, K. Okuno, S. Takagi,

- H. Tawara, and S. Tsurubuchi, Phys. Rev. A. 26, 105 (1982).
31. S. Ohtani, Y. Kaneko, M. Kimura, K. Kobayashi, T. Iwai, A. Matsumoto, K. Okuno S. Takagi, H. Tawara and S. Tsurubuchi, J. Phys. B 15, L533 (1982).
 32. S. Tsurubuchi, T. Iwai, Y. Kaneko, M. Kimura, N. Kobayashi, A. Matsumoto, K. Okuno, S. Takagi and H. Tawara, J. Phys. B 15, L733 (1982).
 33. M. Kimura, T. Iwai, Y. Kaneko, N. Kobayashi, A. Matsumoto, S. Ohtani, K. Okuno, S. Takagi, H. Tawara and S. Tsurubuchi, J. Phys. B 15, L851 (1982).
 34. S. Ohtani see [ref.9, p.110].
 35. K. Okuno, T. Iwai, Y. Kaneko, M. Kimura, N. Kobayashi, A. Matsumoto, S. Ohtani, S. Takagi, H. Tawara and S. Tsurubuchi, Phys. Rev. A28, (1983).
 36. H. Tawara, T. Iwai, Y. Kaneko, M. Kimura, N. Kobayashi, A. Matsumoto, S. Ohtani, K. Okuno, S. Takagi and S. Tsurubuchi submitted to Phys. Rev. A.
 37. A. Matsumoto, T. Iwai, Y. Kaneko, M. Kimura, N. Kobayashi, S. Ohtani, K. Okuno, S. Takagi and S. Tsurubuchi, submitted to J. Phys. Soc. Jpn.
 38. H. Ryufuku, K. Sasaki and T. Watanabe, Phys. Rev. A21, 745 (1980).
 39. S. Bashkin and J.P. Jr. Stoner, Atomic Energy Levels and Grotrian Diagrams I,II (North Holland, Amsterdam, 1975).
 40. H. Winter, E. Bloemen and F.J. de Heer, J. Phys. B 10, L599 (1977).
 41. D. Smith, N.G. Adams, E. Alge, H. Villinger and W. Lindinger, J. Phys. B13 2787 (1980).
 42. B.A. Huber see [ref.9, p.96].
 43. H. Winter see [ref.9, p.159].
 44. C.L. Cocke, R. DuBois, T.J. Gray and E. Justiniano, IEEE Trans. Nucl. Sci. NS-28 1032 (1981).
 45. A. Salop and R.E. Olson, Phys. Rev. A13, 1312 (1976).
 46. M.N. Panov, see [ref.11, p.437].
 47. R. Mann, C.L. Cocke, A.S. Schlachter, M. Prior and R. Marrus, Phys. Rev. Lett. 49, 1329 (1982).
 48. R.W. McCullough, M. Lennon, F.G. Wilkie and H.B. Gilbody, J. Phys. B 16, L173 (1983).
 49. B.A. Huber and H.J. Kahlert, submitted to J. Phys. B.
 50. M. Lennon, R.W. McCullough and H.B. Gilbody, to be published in J. Phys. B.
 51. V.V. Afrosimov, A.A. Basalaev, Yu. S. Gordeev, E.D. Donets, A.N. Zinov'ev, S. Yu. Ovchinnikov and M.N. Panov, Pisma Zh. Eksp. Fiz. 34, 332 (1981).
 52. S. Bliman, J.J. Bonnet, G. Chauvet, S. Dousson, D. Hitz, B. Jacquot and E.J. Knystautas, J. Phys. B 16, L243 (1983).
 53. Yu. S. Gordeev, D. Dijkkamp, A.G. Drentje and F.J. de Heer, Phys. Rev. Lett. 50, 1842 (1983).
 54. D.H. Crandall, Phys. Rev. A 16, 958 (1977).
 55. A. Niehaus, Comments on Atomic and Molecular Physics IX, 153 (1980).
 56. L.M. Kishinevskii and E.S. Parilis, Soviet Phys. JETP 28, 1020, (1969).
 57. H. Winter, Th. M. El-Sherbini, E. Bloemen, F.J. de Heer and A. Salop, Physics Letters 68A, 211, 1978.
 58. P.H. Woerlee, Th.M. El-Sherbini, F.J. de Heer and F.W. Saris, J. Phys. B 12, L235 (1979).
 59. R. Morgenstern, A. Niehaus and G. Zimmerman, J. Phys. B 13, 4811 (1980).
 60. R. Mann, H.F. Beyer, and F. Folkmann, Phys. Rev. Lett, 46, 646 (1981)
 61. H. Knudsen, P. Hvelplund, L.H. Andersen, S. Bjørnerlund, M. Frost, H.K. Haugen and E. Samsø, see [ref.9, p.101].
 62. E. Justiniano, C.L. Cocke, T.J. Gray, R.D. DuBois and C. Can, Phys. Rev. A24, 2953 (1981).
 63. W. Groh, A. Müller, C. Achenbach, A. Schlachter and E. Salzborn, Physics Letters 85A, 77 (1981).
 64. A. Müller, Progress report in ICPEAC XIII in Berlin 1983.

Translational-Energy Spectroscopy of One-Electron Capture Processes in $\text{He}^{2+}\text{-H}_2$ and -N_2 Collisions

Nobuo KOBAYASHI,[†] Tsuruji IWAI,^{††} Yozaburo KANEKO,^{*}
Masahiro KIMURA,^{***} Atsushi MATSUMOTO, Shunsuke OHTANI,
Kazuhiko OKUNO,^{*} Shoji TAKAGI, Hiroyuki TAWARA
and Seiji TSURUBUCHI^{****}

Institute of Plasma Physics, Nagoya University, Nagoya 464

(Received July 14, 1984)

Translational energy spectra of He^+ ions produced by one-electron capture processes in collisions of 0.8 and 2 keV He^{2+} with H_2 and 0.8 keV He^{2+} with N_2 have been measured with an electrostatic energy analyzer. The spectra show only a single broad peak with the energy gain of about 11 eV for all the cases. The peak in each spectrum becomes broader with the increase of the collision energy. It is found that the product He^+ is in the ground state and the capture process is associated with the dissociation and/or ionization of the product molecular ion.

Electron capture processes of He^{2+} ions in collisions with atoms and molecules are of great importance in the fields of thermonuclear fusion research and astrophysics. The cross sections for such processes have been widely measured by many workers, and a number of data have been compiled.¹⁾ For better understanding of the electron capture processes, translational energy spectroscopy of product ions provides useful information. Panov²⁾ studied the electronic states of the He^+ ions formed in collisions of He^{2+} with noble gas atoms, He, Ne, Kr and Xe, using a translational energy spectrometer. As far as we know, however, such a study has not been made with molecular targets.

We have systematically studied electron capture processes by highly charged ions, including fully stripped ions of B, C, N and O, in collisions with He.³⁾ Especially, the final state analysis of the product ions by a trans-

lational energy spectroscopy has provided valuable information for understanding electron capture processes by highly charged ions. In the present work, as one of the serial studies of such electron capture processes, we have measured the translational energy spectra of He^+ ions in collisions of He^{2+} with H_2 and N_2 at the collision energies of 0.8 and 2 keV.

He^{2+} ions are produced in an ion source of EBIS type (NICE-I)³⁾ by introducing ^4He gas. The ion beam of $^4\text{He}^{2+}$ extracted from the source is contaminated with H_2^+ ions, and therefore, cross section measurement has not been made. However, translational energy analysis of the product He^+ ions can be made with an electrostatic analyzer, because the energy of the product He^+ ions is roughly $2 V_{\text{acc}}$ (eV) while that of H_2^+ is $1 V_{\text{acc}}$ (eV), where V_{acc} is the acceleration potential of the ions in the ion source.

In Fig. 1(a) and (b) are shown the translational energy spectra of the product He^+ ions in the $\text{He}^{2+}\text{-H}_2$ system at the collision energies of 0.8 and 2 keV, respectively. The full width at half-maximum (F.W.H.M.) of the energy spread of the primary beam is about 1.5 eV. The spectra of the product He^+ ions show only a single peak and have a maximum at the energy gain of about 11 eV. The tails of the spectra at low energy gain side seem to be ex-

* Permanent address: Department of Physics, Tokyo Metropolitan University, Setagaya-ku, Tokyo 158.

** Permanent address: Department of Liberal Arts, Kansai Medical University, Hirakata, Osaka 573.

*** Permanent address: Department of Physics, Osaka University, Toyonaka, Osaka 560.

**** Permanent address: Department of Applied Physics, Tokyo University of Agriculture and Technology, Koganei, Tokyo 184.

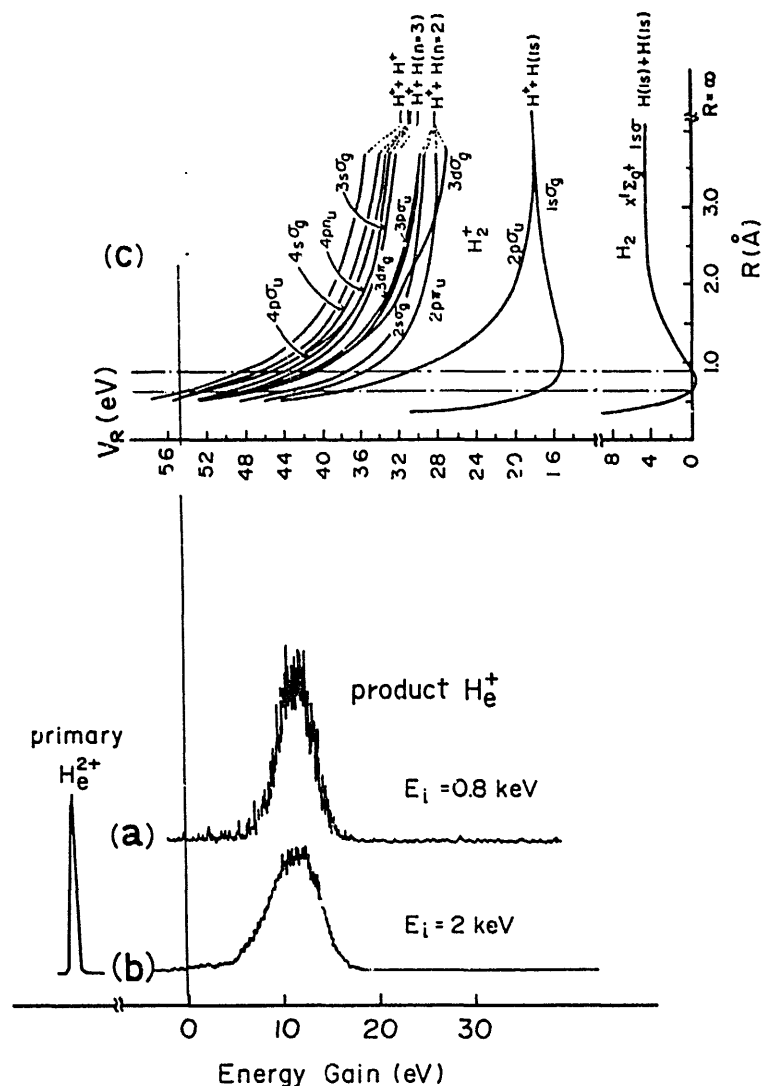


Fig. 1. Translational energy spectra of He^+ in the $\text{He}^{2+}-\text{H}_2$ system at the collision energies of 0.8 keV (a) and 2 keV (b), and the potential energy curves of H_2 and H_2^+ (c). The potential energy of 54.4 eV, corresponding to the ionization potential of He^+ , is joined to the origin of the lower energy gain spectra.

tended down to the negative energy gain (energy loss). In (b) of this figure, weak but appreciable signals are seen at the energy gain of several eV. However, this structure is attributable to the electron capture from residual gas or metal surfaces in the vacuum chamber, because such signals are observed even without the introduction of the target gas.

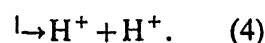
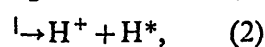
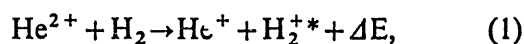
If the product He^+ and H_2^+ are in the ground electronic and vibrational states, the exothermicity of the reaction will be 39.0 eV. However, no peak has been found at such a large energy gain. On the other hand, if the electron is captured into the excited state of He^+ , for example $n=2$, the process must be endothermic and the excess energy is -1.81 eV for the

production of the ground electronic and vibrational state of H_2^+ . In the spectra, no appreciable peak has been observed at the energy loss side.

Nutt *et al.*⁴⁾ measured the total cross sections for the one-electron capture processes in the energy range from 0.6 to 15 keV and reported that the cross section is 2.7×10^{-16} cm^2 at 15 keV and gradually decreases down to 0.8×10^{-16} cm^2 at 0.8 keV. On the other hand, Shah *et al.*⁵⁾ and Khayralla and Bayfield⁶⁾ measured the cross sections for the formation of $\text{He}^+(2s)$ in $\text{He}^{2+}-\text{H}_2$ collisions in the energy range from 10 to 80 keV. Their results show that the cross section has a maximum of about 9×10^{-17} cm^2 around 60 keV

and sharply decreases with the decrease of the collision energy. From these results, the cross section of the formation of $\text{He}^+(n=2)$ is expected to be negligibly small compared to the total cross section for one-electron capture. The present result is consistent with their results, and therefore, the product He^+ is considered to be in the ground state. This means that most of the excess energy is converted to the internal energy of H_2^+ .

The internal energy converted to H_2^+ is estimated by subtracting the translational energy gain of the product He^+ (about 11 eV) from the excess energy of the reaction (39 eV). This energy is so much that the product H_2^{+*} cannot be stable and is dissociated to $\text{H}^+ + \text{H}^*$. Besides, the energy 39 eV is much larger than the sum of the ionization energy of H atom (13.6 eV) and the dissociation energy of H_2^+ (2.6 eV). Therefore, one-electron capture process in the $\text{He}^{2+} + \text{H}_2$ system can be associated with ionization in addition to dissociation of H_2^+ ; namely,



As a reference, the potential energy curves of H_2^+ are shown in Fig. 1(c). In this figure, the origin of the potential energy is taken to be at the ground state of H_2 . If all of the excess energy were converted to the internal energy of H_2^+ , that is to say $\Delta E=0$, the energy just equal to the ionization potential of He^+ (54.4 eV) should be transferred to the target H_2 . The potential energy of 54.4 eV is, then, joined to the origin of the energy gain spectra. Therefore, the potential energy corresponding to the peak of the translational energy spectra means the energy transferred to the target.

In Fig. 1(c), the Frank-Condon region of H_2 molecule is shown with two dashed lines. If the Frank-Condon vertical transition is important in the present case, the product molecular ions should be dissociated and $\text{H}^+ + \text{H}(n \geq 2)$ are expected to be produced through the repulsive state of H_2^{+*} (eq. 3). On the other hand, if the Frank-Condon principle is not held, the one-electron capture process in the

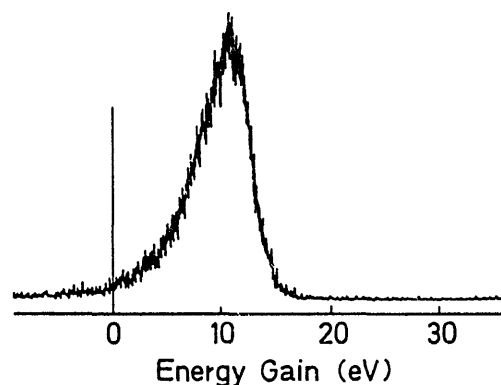


Fig. 2. Translational energy spectrum of He^+ in the $\text{He}^{2+}-\text{N}_2$ at the collision energy of 0.8 keV.

$\text{He}^{2+}-\text{H}_2$ system can be associated with the ionization (eq. 4).

When the potential curve of the left hand side of the reaction (3) is represented simply by a flat line, and that of the right hand side by a curve of the Coulomb repulsion force, the potential curves cross each other at 1.3 Å. It is well known that only a reaction channel which has a potential crossing within 3–5 Å can give large cross section of the order of 10^{-15} cm^2 and the channels whose crossing points are outside of this region cannot have appreciable cross section.⁷⁾ This is considered to be the reason that Nutt *et al.* reported a small cross section, $0.8 \times 10^{-16} \text{ cm}^2$ at the collision energy of 0.8 keV, for this reaction.

In Fig. 2 is shown the translational energy spectrum of the product He^+ by 0.8 keV He^{2+} incident on N_2 . The shape and the peak position are almost the same as those for H_2 target. From the energy consideration, the product He^+ is considered to be in the ground state. Since the ionization potential of He^+ is 54.4 eV and the translational energy released to the products is about 11 eV, the energy of about 43 eV is considered to be transferred to the internal energy of the target molecule. The appearance energy of N_2^{2+} is about 43 eV. Therefore, the one-electron capture process in the $\text{He}^{2+}-\text{N}_2$ system may also be associated with ionization as well as dissociation of N_2^+ .

Search for the ionized electrons or analysis of the charged products from target molecules is needed for further studies.

References

- 1) K. Okuno: IPPJ-AM-9. (Institute of Plasma

- Physics, Nagoya Univ., 1978).
- 2) M. N. Panov: *Electronic and Atomic Collisions*, ed. N. Oda and K. Takayanagi (North-Holland, 1980) p. 437.
 - 3) T. Iwai, Y. Kaneko, M. Kimura, N. Kobayashi, S. Ohtani, K. Okuno, S. Takagi, H. Tawara and S. Tsurubuchi: *Phys. Rev. A* **26** (1982) 105; S. Ohtani, Y. Kaneko, M. Kimura, N. Kobayashi, T. Iwai, A. Matsumoto, K. Okuno, S. Takagi, H. Tawara and S. Tsurubuchi: *J. Phys.* **B15** (1982) L533; K. Okuno, H. Tawara, T. Iwai, Y. Kaneko, M. Kimura, N. Kobayashi, A. Matsumoto, S. Ohtani, S. Takagi and S. Tsurubuchi: *Phys. Rev. A* **28** (1983) 127.
 - 4) W. L. Nutt, R. W. McCullough, K. Brady, M. B. Shah and H. B. Gilbody: *J. Phys.* **B11** (1978) 1457.
 - 5) M. B. Shah and H. B. Gilbody: *J. Phys.* **B7** (1974) 256.
 - 6) G. A. Khayrallah and J. E. Bayfield: *Phys. Rev. A* **11** (1975) 930.
 - 7) H. Winter, E. Bloemen and F. J. de Heer: *J. Phys.* **B10** (1977) L453; D. Smith, N. G. Adams, E. Alge, H. Villinger and W. Lindinger: *J. Phys.* **B13** (1980) 2787; B. A. Huber: *Physica Scripta* **T3** (1983) 96; H. Winter: *Physica Scripta* **T3** (1983) 159; H. Tawara, T. Iwai, Y. Kaneko, M. Kimura, N. Kobayashi, A. Matsumoto, S. Ohtani, K. Okuno, S. Takagi and S. Tsurubuchi: *Phys. Rev. A* **29** (1984) 1529.
-

ELECTRON CAPTURE IN I^{q+} ($q = 10-41$) + He COLLISIONS AT LOW ENERGIES

H. TAWARA, T. IWAI *, Y. KANEKO **, M. KIMURA †, N. KOBAYASHI **, A. MATSUMOTO, S. OHTANI, K. OKUNO **, S. TAKAGI and S. TSURUBUCHI ††

Institute of Plasma Physics, Nagoya University, Nagoya 464, Japan

One electron capture processes in I^{q+} ($q = 10-41$) + He collisions at low energies have been investigated. It is found that total cross sections for one-electron capture processes increase roughly linearly with increasing charge q of the incident ions and also increase with the square of the crossing radius R_c of the diabatic potential energy curves where the electron transfer takes place. These smooth increases are in contrast to those observed for ions with low charge $q < 10$.

1. Introduction

Recently the electron capture processes of highly ionized ions at low energies have been recognized to be important in many fields. A number of experimental [1] and theoretical [2] studies have been published. However, most of the experimental works have been limited to charge $q < 10$. Only few experimental results have been treated for ions with $q \geq 10$. Justiniano et al. [3] have recently reported their results of measurements of total cross sections for electron capture processes for Kr^{q+} and Xe^{q+} ions with the charge q up to 14. We have also presented our recent results of total cross sections for one-electron capture for Kr^{q+} ions with q up to 25 [4]. A significant difference has been found in electron capture processes between ions of $q < 10$ and those of $q \geq 10$. In the former, total cross sections for one-electron capture oscillate significantly as a function of the charge q and have a maximum at a particular crossing radius ($R_c \sim 3.5 \text{ \AA}$) [5]. On the other hand, total cross sections for the latter increase smoothly with increasing the charge and also with increasing R_c [4].

The present work is concerned with measurements of total cross sections for one-electron capture processes of I^{q+} ($q = 10-41$) ions in collisions with He atoms at low energies.

* Permanent address: Department of Liberal Arts, Kansai Medical University, Hirakata, Osaka 573, Japan.

** Permanent address: Department of Physics, Tokyo Metropolitan University, Setagaya-ku, Tokyo 158, Japan.

† Permanent address: Department of Physics, Osaka University, Toyonaka, Osaka 560, Japan.

†† Permanent address: Department of Applied Physics, Tokyo University of Agriculture and Technology, Koganei, Tokyo 184, Japan.

2. Experiments

The experimental apparatus is practically the same as that described previously [6]. HI gas is introduced into an electron beam ion source, NICE-1, up to 1×10^{-9} Torr. Using an electron beam of 9.1 mA/3.6 keV, I^{q+} ions with q up to 42 are observed with a very weak trace of I^{43+} . In the present work, two types of measurements have been done. Firstly, total cross sections for one-electron capture processes are measured by observing the intensity of charge-changed ions ($I^{(q-1)+}$) as a function of the target gas pressure. Secondly, by measuring the energy gain in collisions, the crossing radii of the diabatic energy levels where electron transfer takes place are determined. It is found that the observed results are nearly independent of the collision energy investigated over $0.75 \times q$ to $2.25 \times q$ keV.

3. Results

3.1. Dependence of total cross section on incident ion charge

The total cross sections of one-electron capture processes in I^{q+} + He collisions measured at the energy of $1.25 \times q$ keV are shown in fig. 1 as a function of the incident ion charge q , together with results for Kr^{q+} by Iwai et al. [4], Cocke et al. [7], Kusakabe et al. [8] and Justiniano et al. [3]. It is clearly seen that all these data for different ions with the same charge tend to lie on a single curve. The oscillation of the cross sections is noticed for ions of $q < 10$ as discussed before and can be explained in terms of a similar mechanism found in relatively light ions such as C, N and Ne ions, where a particular single or very few levels are found to play a key role in electron capture processes. On the other

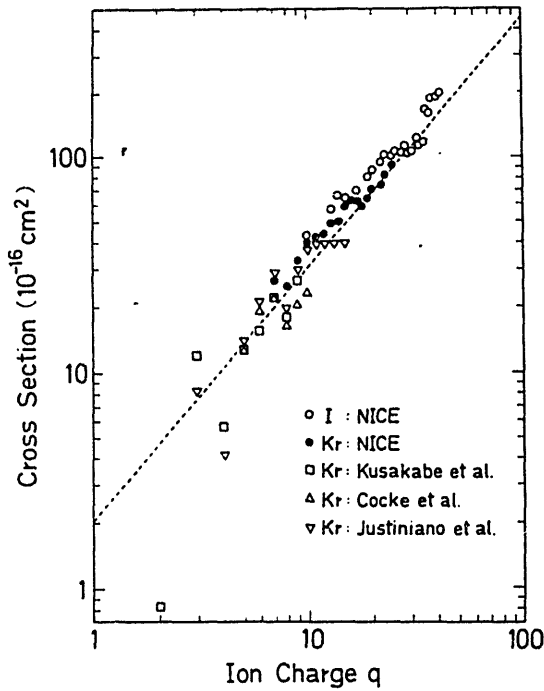


Fig. 1. Cross sections of one-electron capture processes in $I^{q+} + \text{He}$ and $\text{Kr}^{q+} + \text{He}$ collisions at around $1 \times q$ keV as a function of the ion charge q .

hand, the cross sections for ions with $q \geq 10$ increase relatively smoothly with increasing the incident ion charge q . Also in fig. 1 is shown a curve based upon a semi-empirical scaling law by Müller and Salzborn which was derived using data of ions with $q < 10$ [9].

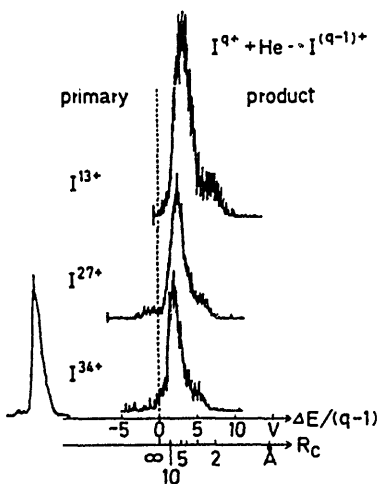


Fig. 2. Energy gain spectra in $I^{q+} + \text{He}$ collisions. Stronger peaks correspond to one-electron capture processes and weaker peaks possibly to transfer ionization.

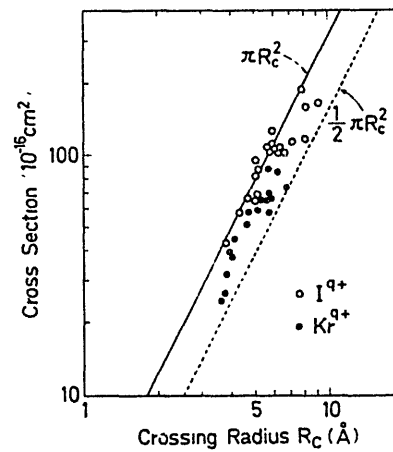


Fig. 3. Cross sections of one-electron capture processes in $I^{q+} + \text{He}$ and $\text{Kr}^{q+} + \text{He}$ collisions as a function of the crossing radius R_c .

3.2. Dependence of total cross section on crossing radius

The energy gain spectra have been observed for I^{q+} ions with q up to 38 and it is found that the observed peaks shift toward smaller values of $\Delta E/q$ (ΔE : the energy gain) with increasing q . Using the observed energy gain ΔE , the crossing radius R_c in diabatic energy levels of quasi-molecules can be determined by $R_c(\text{Å}) = 14.4(q-1)/\Delta E(\text{eV})$. It should be noted that all the observed energy gain peak looks like a single peak but, because of the limited energy resolution of the present experimental apparatus, corresponds to that averaged over a number of the possible levels contributing to the electron capture processes (see fig. 2).

In fig. 3 are shown the measured total cross sections for one-electron capture in $I^{q+} + \text{He}$ collisions as a function of the observed crossing radius R_c , together with our previous results for $\text{Kr}^{q+} + \text{He}$ collisions. From this figure it is clear that most of the observed cross sections increase roughly with the square of R_c and lie between the classical cross section ($\frac{1}{2}\pi R_c^2$) and the geometrical cross section (πR_c^2), indicating that the classical picture is valid for one-electron capture of ions with very high charge. This smooth increase of the cross section with increasing q is in significant contrast with those previously observed in ions with $q < 10$ [5].

4. Remarks

In the present work we have extended the previous measurements of one-electron capture processes for ions with q up to 41 and found that total cross sections are nearly constant over the energy range investigated and increase smoothly with increasing incident ion charge q and also with increasing the crossing radius R_c . This smooth variation is quite in contrast to that for ions

I. COLLISION PROCESSES

with $q < 10$ and can be understood qualitatively, assuming that a number of the excited states are available in one-electron transfer processes in heavy, highly ionized ions.

Unfortunately, little is known on the energy levels of ions in such a highly ionized state and it is not possible to get accurate information of the electron-capturing levels which are located mostly in the Rydberg states. However, the energy levels in which the electron is captured in such highly ionized ions can be assumed to be hydrogenic and, then, some estimation on the electron-capturing levels can be made. Typically, the electron is captured into $n = 5$ for I^{10+} ions and into $n = 15$ for I^{38+} ions which are in fairly good agreement with the classical model [10].

Based upon the hydrogenic energy levels, we have also tried to calculate total cross sections using the multi-channel Landau-Zener model [11] which is found to be able to reproduce quite well the present experimental results. We should also note that theoretical as well as experimental works are still limited for ions of $q > 10$. The fully detailed description will be given in a forthcoming publication.

This work was made as a part of the Guest Research Program at the Institute of Plasma Physics, Nagoya University.

References

- [1] S. Ohtani, *Electronic and Atomic Collisions*, eds., J. Eichler, I.V. Hertel and N. Stolterfoht (North-Holland, Amsterdam, 1984) p. 353.
- [2] R.K. Janev, B.H. Bransden and J.W. Gallagher, *J. Chem. Phys. Ref. Data* 12 (1983) 829.
- [3] E. Justiniano, C.L. Cocke, T.J. Gray, R. DuBois, C. Can and W. Waggoner, *Phys. Rev. A* 29 (1984) 1088.
- [4] T. Iwai, Y. Kaneko, M. Kimura, N. Kobayashi, A. Matsumoto, S. Ohtani, K. Okuno, S. Takagi, H. Tawara and S. Tsurubuchi, *J. Phys. B* 17 (1984) L95.
- [5] H. Tawara, T. Iwai, Y. Kaneko, M. Kimura, N. Kobayashi, A. Matsumoto, S. Ohtani, S. Takagi and S. Tsurubuchi, *Phys. Rev. A* 29 (1984) 1529.
- [6] K. Okuno, H. Tawara, T. Iwai, Y. Kaneko, M. Kimura, N. Kobayashi, A. Matsumoto, S. Ohtani, S. Takagi and S. Tsurubuchi, *Phys. Rev. A* 28 (1983) 127.
- [7] C.L. Cocke, R. DuBois, T.J. Gray and E. Justiniano, *IEEE Trans. Nucl. Sci. NS-28* (1981) 1032.
- [8] T. Kusakabe, H. Hanaki, N. Nagai, T. Horiguchi, I. Kinomi and M. Sakisaka, *Physica Scripta* T3 (1983) 191.
- [9] A. Müller and E. Salzborn, *Phys. Lett.* 62A (1977) 391.
- [10] H. Ryufuku, K. Sasaki and T. Watanabe, *Phys. Rev. A* 21 (1980) 745.
- [11] M. Kimura, T. Iwai, Y. Kaneko, N. Kobayashi, A. Matsumoto, S. Ohtani, K. Okuno, S. Takagi, H. Tawara and S. Tsurubuchi, *J. Phys. Soc. Japan* 53 (1984) 2224.

Electron capture processes of I^{q+} ions with very high charge states ($41 \geq q \geq 10$) in collisions with He atoms

H Tawara, T Iwai†, Y Kaneko‡, M Kimura§, N Kobayashi‡,
A Matsumoto, S Ohtani, K Okuno‡, S Takagi and S Tsurubuchi||
Institute of Plasma Physics, Nagoya University, Nagoya 464, Japan

Received 29 June 1984, in final form 14 August 1984

Abstract. One-electron capture processes of iodine (I^{q+}) ions with very high charge q up to 41 in collisions with He atoms at low energies have been investigated using energy gain spectroscopy. It is found that total cross sections increase with increasing charge of ions q , and also increase roughly with the square of the crossing radius R_c of the diabatic potential curves in the quasi-molecules where the electron transfer takes place. This smooth variation, in contrast to that in ions with low charge where only few crossings play a role, can be understood from the fact that a number of the crossings closely located in a relatively narrow region of R_c contribute to one-electron transfer processes in ions with high charge.

1. Introduction

Presently much attention is being paid to the investigation of electron capture processes of highly ionised ions at low energies, particularly because these processes are found to play a key role in high temperature plasmas. A number of experimental (Winter 1982, Mann *et al* 1982, Phaneuf 1983, Bliman *et al* 1983, Yan *et al* 1983, Lennon *et al* 1983, Nielsen *et al* 1984) and theoretical (Greenland 1982, Lin 1982, Janev *et al* 1983, Gallagher *et al* 1983, Janev 1983) works have been reported. Because of the limited availability of ion sources capable of producing high charge state ions, most of the experiments made so far are concerned mainly with ions with charge $q \leq 10$ and very few experimental results have been reported for ions with $q \geq 10$ (Bliman *et al* 1981, Justiniano *et al* 1981, Groh *et al* 1983, Phaneuf 1983). Recently Justiniano *et al* (1984) have measured total cross sections for one-electron capture processes of Kr^{q+} and Xe^{q+} ions with q up to 14, which are produced in high energy heavy-ion impact, in collisions with He, Ne and Ar target atoms. It should also be noted that in most of these experimental works only total cross sections have been measured and again only a few results on the final-state distribution measurements have been reported so far (Ohtani 1984).

In order to understand the mechanism of electron transfer processes involving highly ionised ions, we are concentrating our effort on investigating the following

† Permanent address: Department of Liberal Arts, Kansai Medical University, Hirakata, Osaka 573, Japan.

‡ Permanent address: Department of Physics, Tokyo Metropolitan University, Setagaya-ku, Tokyo 158, Japan.

§ Permanent address: Department of Physics, Osaka University, Toyonaka, Osaka 560, Japan.

|| Permanent address: Department of Applied Physics, Tokyo University of Agriculture and Technology, Koganei, Tokyo 184, Japan.

one-electron capture process by highly ionised ions A^{q+} from He atoms at low energies



through measurements of total cross sections by observation of the charge-changed ions $A^{(q-1)+}$ and of the final-state distribution and crossing radius R_c by observing the energy gain ΔE . R_c is determined through the following equation:

$$R_c(\text{\AA}) = 14.4(q-1)/\Delta E \text{ (eV)} \quad (2)$$

where only the Coulomb repulsion is assumed to be important in the diabatic potential. A series of our recent works have been published for relatively light but highly ionised ions including the fully stripped ions such as C^{6+} , N^{7+} and O^{8+} ions (Ohtani *et al* 1982, Tsurubuchi *et al* 1982, Kimura *et al* 1982, Okuno *et al* 1983, Matsumoto *et al* combinations (Huber 1983) and believed to be universal until recently. However, it was made clear that this is not true because this should be dependent on the charge of the ions as well as on the collision velocity (Tawara *et al* 1984, Kimura *et al* 1984).

Through these works it has been found that there are some distinct differences between electron capture processes of high- q ions and those of low- q ions in collisions with He atoms. For low- q ions, total cross sections show strong oscillation when plotted as a function of the charge of the ions, q (Iwai *et al* 1982). These results clearly indicate that the one-electron capture into few levels is a dominant mechanism which is supported with a single peak observed in the energy gain spectrum in most of the ions investigated. Also the cross sections, plotted as a function of the crossing radius determined from the energy gain ΔE , have a maximum at $R_c \approx 3.5 \text{ \AA}$ (Tawara *et al* 1984). This latter behaviour had previously been observed in various ion-atom combinations (Huber 1983) and believed to be universal until recently. However, it was made clear that this is not true because this should be dependent on the charge of the ions as well as on the collision velocity (Tawara *et al* 1984, Kimura *et al* 1984).

On the other hand, it was found that, for high- q ions, a number of crossings closely located in a relatively narrow region of R_c contribute to the electron transfer processes and, then, the total cross sections increase smoothly with increasing q and roughly with the square of R_c (Iwai *et al* 1984).

In the present work, following the previous work on Kr^{q+} ions (Iwai *et al* 1984), we report results of measurements on total one-electron capture cross sections and on crossing radii in collisions of I^{q+} ions with very high charge states (up to $q = 41$) with He atoms. To our knowledge, this is the highest charge state ever to be investigated at low energies.

2. Experimental apparatus

The experimental set-up used in the present work is shown schematically in figure 1 and is practically the same as that described in detail in a previous publication (Okuno *et al* 1983). Hydrogen iodide (HI) gas up to about 1×10^{-9} Torr measured with an ionisation gauge is introduced into an electron beam ion source, NICE-1, whose base pressure is typically 2×10^{-10} Torr. A typical charge spectrum of I^{q+} ions produced in the impact of 9.1 mA, 3.6 keV electron beams at a pressure of 8×10^{-10} Torr is shown in figure 2. In addition to impurity ions such as C^{q+} , N^{q+} and O^{q+} , very highly ionised I^{q+} ions up to $q = 42$ are clearly seen. A weak trace of I^{43+} ions is also observed on the tail of a big peak of $m/q = 3$ ions in an expanded scale. In fact since the ionisation potential of I^{42+} (i.e., $I^{42+} \rightarrow I^{43+} + e$) is 3.2 keV (Carlson *et al* 1971), I^{43+} ions is the

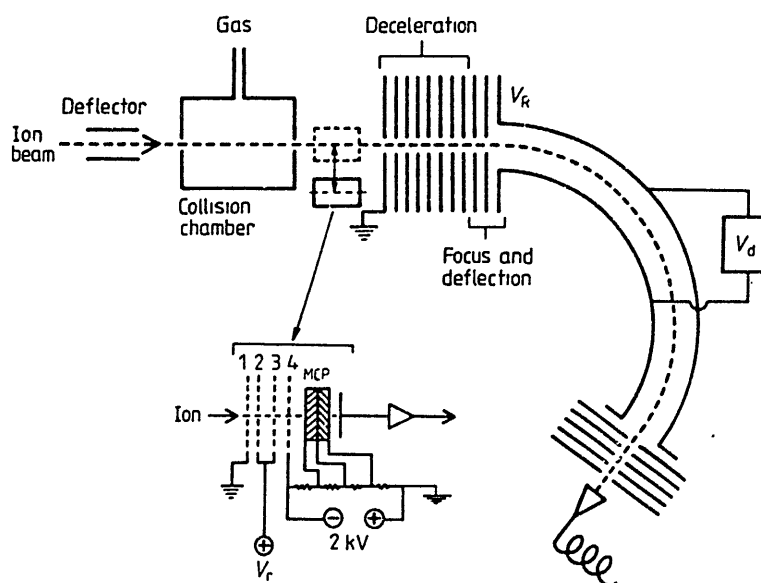


Figure 1. Schematic drawing of the present experimental apparatus.

highest charge state of iodine ions which can be produced by 3.6 keV electron beams. It is noticed in this ion charge spectrum that the charge distribution changes significantly at $q = 25$ because of the drastic change in the ionisation potential of ions at $q = 25$. I^{25+} ($Z = 53$) ions have the electron configuration of all O- and N-shell electrons ionised and only K-, L- and M-shell electrons left un-ionised. From this result, it is found that one of the keys relevant to producing such high charge ions is vacuum itself in the ion source which should be as low as 1×10^{-9} Torr. The ion beam intensities used are typically a few to ten thousands of counts per second, except for those in highest charge states which are about one thousand counts per second.

In the present work a new system for measuring total electron capture cross sections is introduced which is retractable when the energy gain spectrum needs to be measured. This retractable system, shown in an insert of figure 1, consists of four meshed

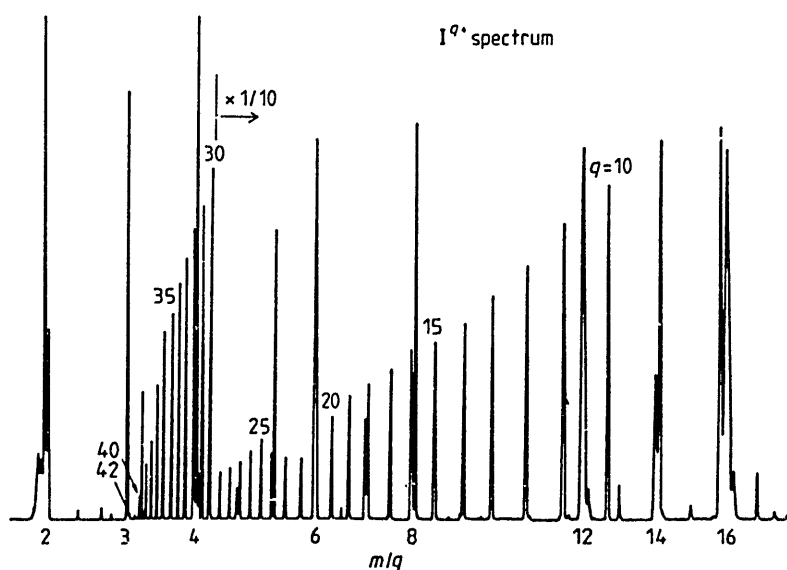


Figure 2. A typical charge distribution of I^{q+} ions produced in an EBIS (electron energy 3.6 keV, intensity 9.1 mA, source pressure 8×10^{-10} Torr).

electrodes, each having 90% transparency, and an ion detection system. The first mesh is grounded and on the second and third meshes, connected together, is applied the retarding positive voltage V_r . The ions retarded between the first and second meshes are accelerated through the fourth mesh at -2 kV and detected with a multichannel plate (MCP). The fourth mesh also serves as a reflector of secondary electrons produced at the surface of MCP. It should be noted that, in principle, no electron originating in these meshes can reach the MCP in the present configuration. By applying the retarding voltage on the retarding meshes, the variation of the number of ions arriving at the MCP is observed as shown in figure 3(a). The first flat part (on the left) of the intensity variation corresponds to the intensity of primary A^{q+} ions and the second flat part to that of the product (charge changed) $A^{(q-1)+}$ and $A^{(q-2)+}$ ions. Also seen in figure 3(a) is the third weak flat part corresponding to the double charge changed $A^{(q-2)+}$ ions which is confirmed to be produced through two-step processes. It is found that the third flat part due to double charge changed ions is negligibly small, compared with that due to single charge changed ions, at the pressure range investigated in the present

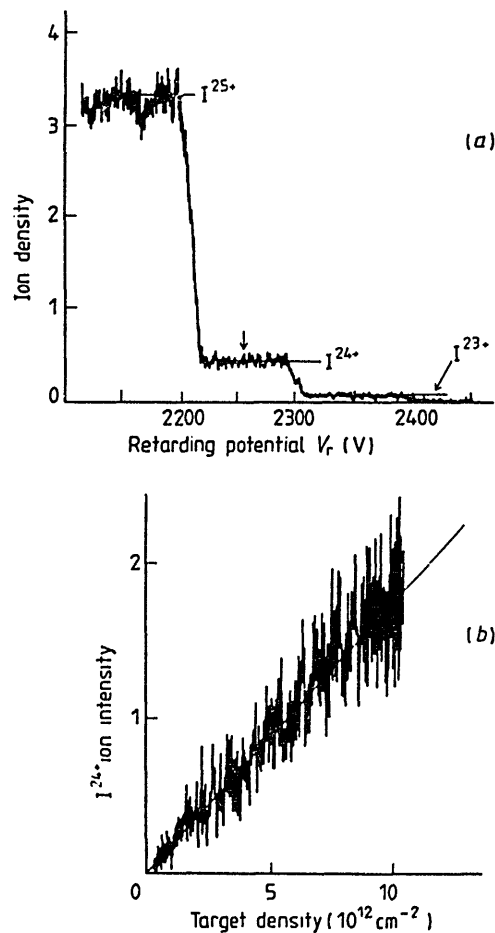


Figure 3. (a) Ion intensity variation as a function of the retarding voltage V_r in $I^{25+} + \text{He}$ collisions. The accelerating voltage is 2.25 kV. The flat part on the left corresponds to intensity of primary I^{25+} ions while the flat part in the middle to that of the charge changed I^{24+} and I^{23+} ions and the flat part on the right to that of the double charge changed I^{23+} ions which are produced through a two-step process. The arrow indicates the retarding voltage V_r where the growth curve (b) is obtained. (b) Growth curve of I^{24+} ions as a function of He target density.

work. To determine the growth rate of the product ions, the retarding voltage is fixed at the middle of the second flat part (shown by arrow). Then the growth curve of the product ions is obtained as a function of the target gas pressure shown in figure 3(b). From this growth curve, total one-electron capture cross sections are determined in the usual ways. It is confirmed that the cross sections determined in the present set up are in good agreement with our previous results (Iwai *et al* 1982) for O^{7+} , $O^{6+} + He$ and $N^{6+} + He$ collisions. Most of the experimental errors in the cross section measurements come from instabilities of the primary ions, determination of the slope of the growth rate curve and the target thickness determination. Total errors for the absolute values of the cross sections are estimated to be $\pm 30\%$.

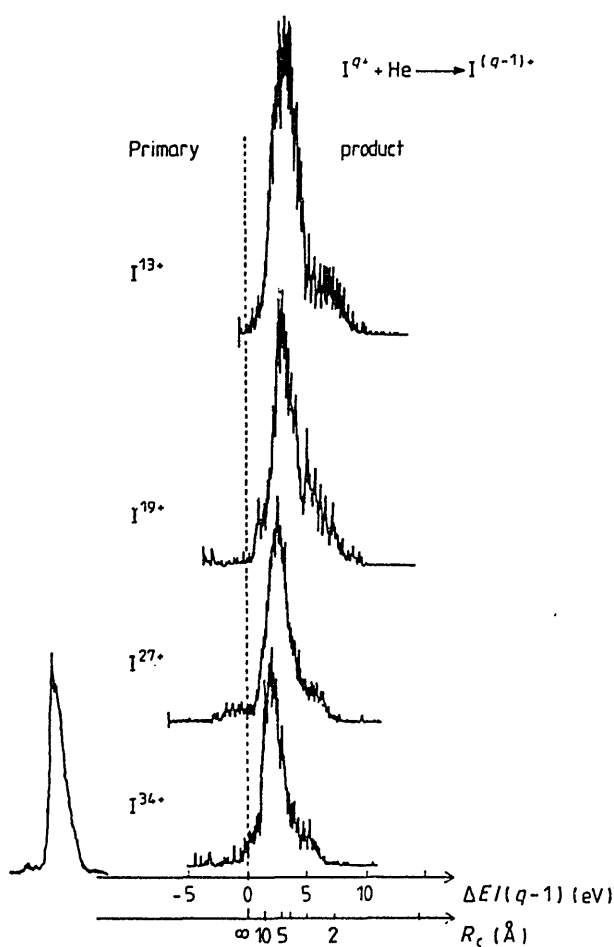


Figure 4. Energy gain spectra for $I^{q+} + He$ collisions ($q = 13, 19, 27$ and 34). Strong peaks correspond to the one-electron capture process whereas weak peaks on the right probably to the transfer ionisation process (see the text).

The energy gain spectra of I^{q+} ions ($q = 13, 19, 27$ and 34) at forward directions in collisions with He atoms at the energy of $1.25q$ keV are shown in figure 4. A detailed description of this energy gain spectrometer was given previously (Okuno *et al* 1983). The strong peaks in these energy gain spectra, which are only slightly broader than those of primary ions, are due to the one-electron capture processes of the incident I^{q+} ions and the second weak peaks (shoulders) at higher energy gain, though not well separated from the main peaks because of the limited energy resolution of the present

system, are believed to be due to indirect processes such as the transfer ionisation (see discussion later on). In this figure, the crossing radii determined are also shown. Uncertainties in the energy gain ΔE are estimated to be $\pm 15\%$ (Iwai *et al* 1984).

3. Experimental results

The measured total cross sections and the crossing radii for one-electron capture in $I^{q+} + \text{He}$ collisions are summarised in table 1(a) and also those in $\text{Kr}^{q+} + \text{He}$ are in table 1(b).

3.1. Total one-electron capture cross section

3.1.1. Energy dependence. The energy dependence of total cross sections for one-electron capture processes in $I^{q+} + \text{He}$ collisions is shown in figure 5 for ions with $q = 10, 15, 20, 25$ and 30 . As expected, the variation of cross sections with the collision energy is small and it can be assumed that the cross sections are constant over the energy range investigated in the present work, namely, $0.75q - 2.25q$ keV. In the following, all the cross sections and crossing radius R_c are referred to at $1.25q$ keV.

3.1.2. Charge dependence. The present results on total cross sections of one-electron capture processes for $I^{q+} + \text{He}$ collisions are shown in figure 6 as a function of the charge of the incident ion q . Also for Kr^{q+} ions our experimental results ($q \leq 25$) (Iwai *et al* 1984) and those by Cocke *et al* (1981) ($q \leq 10$), Kusakabe *et al* (1983) ($q \leq 9$) and Justiniano *et al* (1984) ($q \leq 14$) are shown together. All these results for different ions seem to lie on a single curve, although they are scattered. Below $q = 10$, the oscillation of the cross sections is clearly seen. In particular, the dips at $q = 2$ and 4 are significant. These dips can be understood in a way similar to those observed for light ions such as C, N, O and Ne, which had been discussed in detail previously (Iwai *et al* 1982, Tawara *et al* 1984, Kimura *et al* 1984). On the other hand, data for ions with $q \geq 10$ increase relatively smoothly with increasing charge of ions q . Some structure

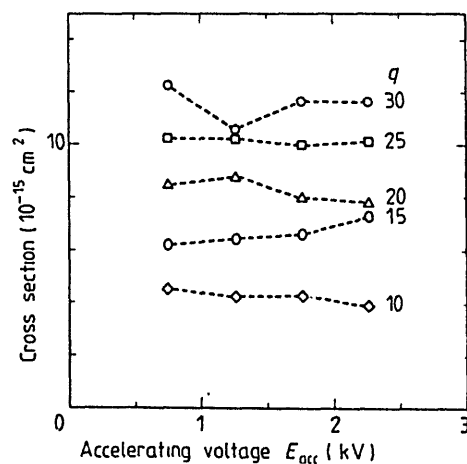


Figure 5. Energy dependence of cross sections for the one-electron capture process in $I^{q+} + \text{He}$ collisions ($q = 10, 15, 20, 25$ and 30). Total energy is represented by qE_{acc} .

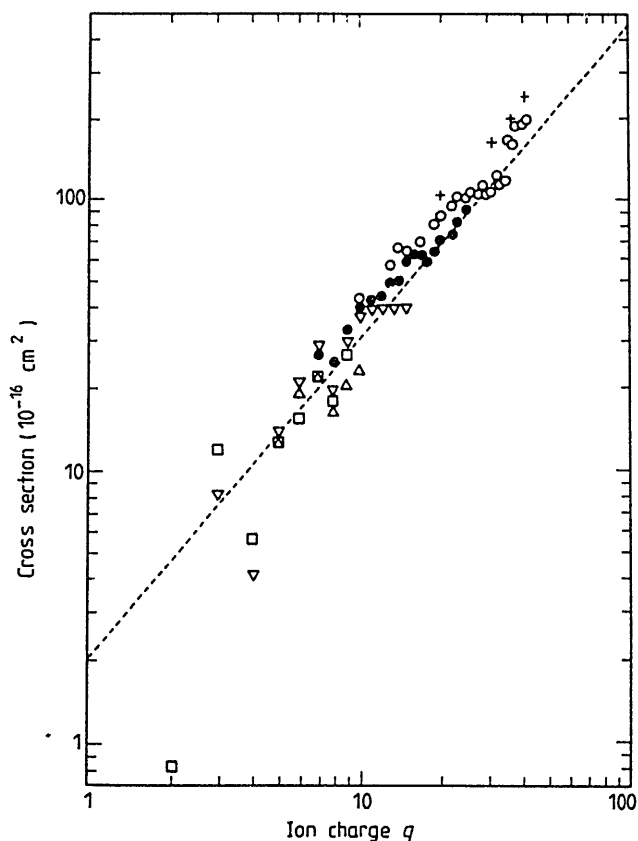


Figure 6. Cross sections for the one-electron capture process as a function of the charge q of ions: \circ , in $I^{q+} + \text{He}$ collisions at the energy $1.25q$ keV; \bullet , Kr^{q+} (Iwai *et al* 1984); \square , Kr^{q+} (Kusakabe *et al* 1983); Δ , Kr^{q+} (Cocke *et al* 1981); ∇ , Kr^{q+} (Justiniano *et al* 1984); $+$, the MCLZ model calculation; $---$, empirical formula of Muller and Salzborn (1977).

around $q = 25$ – 35 is seen in these data. Although we have no clear understanding of these structures at present, we suppose these are caused by different mechanisms from those observed in low q ions.

In figure 6 calculated cross sections (broken curve) based on an empirical formula proposed by Müller and Salzborn (1977) are also shown. Except for those with low q , this empirical formula ($\sigma_{q,q-1} = 2.07 \times 10^{-16} q^{1.17}$ (cm^2) for He) can reproduce these experimental results. This is somewhat surprising because this formula was derived from a number of experimental data for ions with $q \leq 10$.

Though a number of calculations of cross sections for electron capture processes in collisions between highly ionised ions and atomic hydrogen were made based on different approximations (Greenland 1982, Janev *et al* 1983), they are concerned mainly with those for ions with $q \leq 10$. Very few theoretical calculations of these cross sections for ions with $q \geq 10$ in collisions with He atoms have been reported (Suzuki *et al* 1984).

3.2. Energy gain measurements

3.2.1. *Crossing radius R_c .* The observed spectra of the energy gain, as shown in figure 4, seem not to differ very much for different I^{q+} ions over the charge states $41 \geq q \geq 10$. However, the shift of these peak positions toward smaller $\Delta E/q$ with increasing charge of the primary ions, q , is clearly observed. It should be noted that the energy resolution

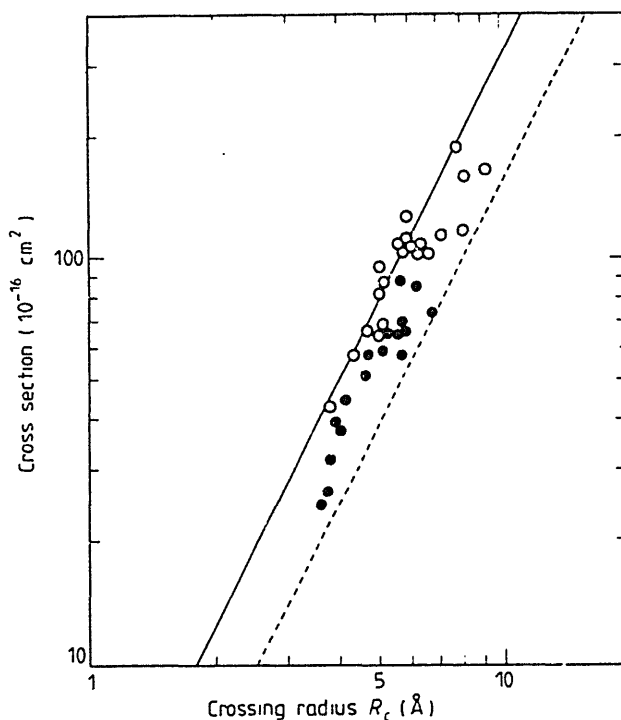


Figure 7. Cross sections for one-electron capture processes as a function of the crossing radius R_c in $I^{q+} + \text{He}$ collisions. \circ , I^{q+} ; \bullet , Kr^{q+} . The full curve represents the geometrical cross section (πR_c^2), whereas the broken curve represents the classical cross section ($\frac{1}{2}\pi R_c^2$).

of the present energy gain spectrometer is not good enough to separate possible peaks contributing to the observed peaks which correspond to the average energy gain spectra over a number of the capturing levels of ions. From the observed energy gain ΔE , the crossing radius R_c in quasi-molecules where the electron capture takes place is determined by equation (2). For high q ions the polarisation effect should become important. However, this effect is neglected in the present analysis. However, as seen in the present results the crossing radii for high- q ions are generally large. Thus the polarisation effect can be assumed to be minor. Therefore this polarisation is neglected in the present analysis.

The crossing radius R_c has been found to increase with the charge of primary ions q . The cross sections for I^{q+} ions are shown in figure 7 as a function of the crossing radius R_c thus determined, together with the previous data of Kr^{q+} ions. Though data are scattered, the cross sections increase roughly with the square of the crossing radius R_c , that is $\sigma_{q,q-1} \propto R_c^2$. It should be noted that almost all the observed cross sections lie between the geometrical cross section πR_c^2 and the classical cross sections $\frac{1}{2}\pi R_c^2$. This behaviour indicates that the classical picture of one-electron capture processes prevails for the ions with very high charge state investigated in the present work. As discussed previously, this smooth behaviour of the cross sections for ions with high charge as a function of R_c is quite in contrast with that for ions with charge less than 10. This difference can be understood from the fact that the cross sections for high- q ions increase with increasing R_c because there is not a single crossing but a number of densely populated crossings at large crossing distances which contribute to one-electron capture processes, though they are not separable in the present work, whereas those for low- q ions are dominated by few crossings (Kimura *et al* 1984).

3.2.2. *Electron-capturing level.* As mentioned before, no accurate information is available on the energy levels of I^{q+} ions with such very high charge. Therefore, it is not possible to accurately determine the levels where the electron of the He atom is captured in collisions. However, in such highly ionised heavy ions their energy level structure can be assumed to be hydrogenic and the energy of their excited states is given by $13.6q^2/n^{*2}$, n^* being the effective principal quantum number of the excited level. Thus, using the observed energy gain ΔE and the known ionisation potential of target atom V_i , n^* of the electron capturing level can be determined through the following relation:

$$\Delta E = 13.6q^2/n^{*2} - V_i \quad (3)$$

where ΔE and V_i are given in units of eV. In the present case, $V_i = 24.59$ eV for He atoms.

Typical correlations between the energy levels and observed energy gain spectra are shown in figure 8(a) and (b) for $I^{13+} + \text{He} \rightarrow I^{12+}$ and $I^{35+} + \text{He} \rightarrow I^{34+}$ processes, respectively. These energy levels are calculated by assuming only the Coulomb interaction between the product ions, namely $I^{(q-1)+}$ and He^+ . Clearly, the electron is captured mainly into the $n^* = 6$ state for $q = 13$ ions, whereas that for $q = 35$ ions is captured into the $n^* = 14$ state. Note that the electron is captured into the fairly narrow region of n^* of the ions. This fact is also noted in the energy gain spectra shown in figure 4 where the widths of the product ions are only slightly broader than those of the primary ions, indicating that a limited number of the levels contribute to the one-electron capture process. Also the energy diagrams corresponding to double electron capture processes are shown (by dotted curves) in figure 8. Stronger Coulomb interaction between $I^{(q-2)+}$ and He^{2+} ions results in sharp variation of the potential energy curves which often cross those corresponding to single electron capture processes. As seen in figure 8, the shoulders at higher energy gain may correspond to two electron capture processes into the autoionising states (transfer ionisation) which, followed by one-electron emission, result in the same charge state as that in single electron capture (Tsurubuchi *et al* 1982). Unfortunately no information is available

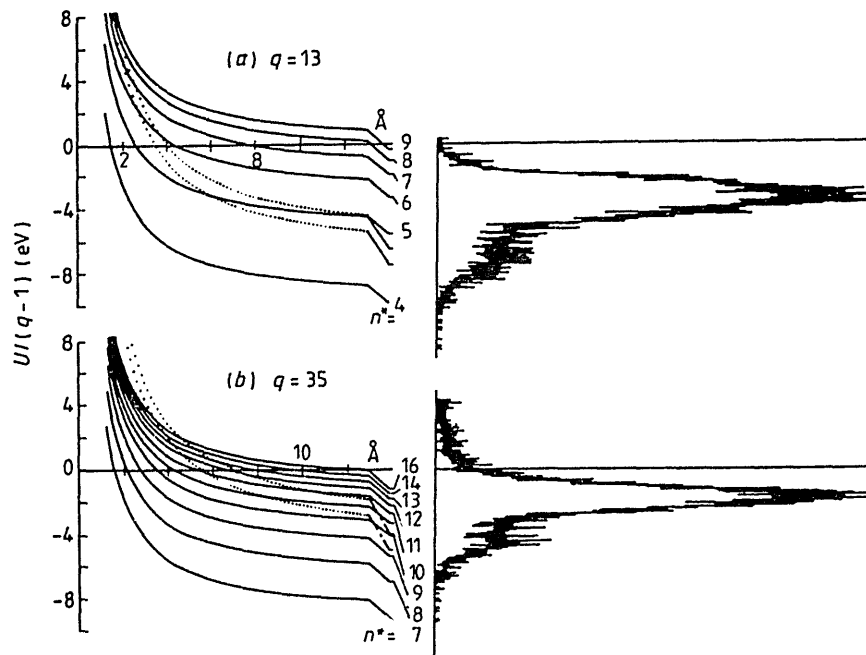


Figure 8. Energy diagrams compared with energy gain spectra in $I^{13+} + \text{He}$ and $I^{35+} + \text{He}$ collisions at an energy of $1.25q$ keV.

presently on the autoionising states of such highly ionised I ions. As discussed by several investigators (for example, Kamber and Hasted 1983), it is known that the energy gain spectra depend significantly on the scattering angle. However, the present energy gain spectra are obtained in a very forward direction of scattering. Therefore, processes other than the transfer ionisation can be responsible for the observed shoulder at higher energy gain.

In figure 9 the average quantum number n^* of the electron capturing levels is shown as a function of the charge of primary ions q . With increasing q , the principal quantum number n^* of the electron-capturing level becomes large, showing that the electron is captured into a higher quantum state ranging from $n^* = 5$ for $q = 10$ to $n^* = 15$ for $q = 40$.

It is also possible to estimate the principal quantum number n based on the classical model for electron transfer described previously (Ryufuku *et al* 1980, Iwai *et al* 1982). In the present work, the high Rydberg states are found to be responsible in the electron capture in highly ionised ions and, therefore, the effective charge of the core nucleus can be assumed to be equal to the real charge of ions; $Z_1^* = q$. The results estimated in this way are shown in figure 9 by a full curve. These results are in agreement within $\Delta n^* = \pm 1$ with those determined from the observed energy gain, indicating that the classical model is valid in estimating the electron-capturing levels in very highly ionised ion collisions. Asymptotically the following classical formula is obtained for large q :

$$n^* = \sqrt{2}(q/Z_2)^{0.75} \quad (4)$$

where Z_2 is the effective charge of target atom, meanwhile the experimental data fit for He by

$$n^* = 0.76q^{0.818}. \quad (5)$$

3.2.3. Multichannel Landau-Zener model calculation. As demonstrated previously, the multichannel Landau-Zener (MCLZ) model is quite useful in understanding the one-electron capture processes involving highly ionised heavy ions in collisions with He atoms at low energies (Kimura *et al* 1984). For $I^{q+} + \text{He}$ collisions, we have also tried

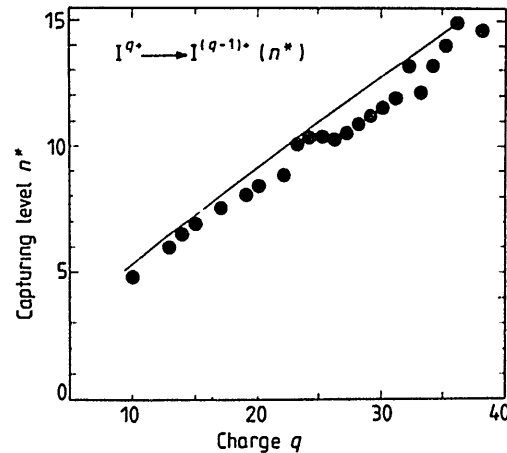


Figure 9. Average principal quantum number n of the electron capturing level as a function of the charge of ions q in $I^{q+} + \text{He} \rightarrow I^{(q-1)+}(n^*) + \text{He}^+$ processes. The full curve represents the classical estimation.

to reproduce the observed results using the MCLZ model. The calculated results of partial cross sections of one-electron capture in $I^{q+} + \text{He}$ collisions for $q = 20, 30, 35$ and 40 are summarised in table 2. In the present calculation, the following assumptions are made as they were in the previous work: (i) the energy levels are represented to be hydrogenic, (ii) each state of the principal quantum number n has n sublevels, (iii) no interference among the neighbouring crossings takes place and (iv) the transfer ionisation processes are neglected. Roughly 100 levels are taken into account in the calculation. These calculations are found to be in good agreement with the observed results as far as the electron capturing levels are concerned. For I^{35+} ions, the principal quantum number n^* of the electron capturing states which contribute most to one-electron capture processes is calculated to be $n^* = 14$, in agreement with the experimental result shown in figure 8(b). In all the cases, the calculated results on the electron capturing level reproduce the observed results quite well.

However, it should be noted that some discrepancies exist in total cross sections for one-electron capture processes (see tables 1 and 2). One of the important origins for these discrepancies might be the effective number of the sublevels which is assumed to be equal to the principal quantum number n^* . The overestimation of cross sections suggests that the number of the levels actually contributing to electron transfer is

Table 1. (a) Measured cross sections and crossing radii for one-electron capture process in $I^{q+} + \text{He}$ collisions. (b) those for $\text{Kr}^{q+} + \text{He}$ collisions (Iwai *et al* 1984).

(a)

q	Cross section (10^{-15} cm^2)†				R_c (Å)‡
	0.75 kV	1.25 kV	1.75 kV	2.25 kV	
10	4.56	4.25	4.25	3.88	3.81
13		5.70			4.31
14		6.65			4.75
15	6.20	6.45	6.60	7.33	5.01
17		6.92			5.18
19		8.16			5.05
20	8.48	8.74	7.98	7.78	5.20
22		9.53			5.06
23		10.3			6.68
24					6.72
25	10.2	10.3	9.98	10.1	6.31
26		10.8			5.69
27					5.69
28		10.5			5.84
29		11.2			6.00
30	12.3	10.6	11.7	11.7	6.08
31		10.7			6.40
32					8.04
33		12.7			5.95
34		11.4			7.20
35		11.7			8.16
36		16.6			9.27
37		16.0			8.22
38		18.9			7.89
40		18.7			
41		19.6			

Table 1. (continued)
(b)

q	Cross section (10^{-15} cm^2) [†]			R_c (Å) [‡]
	0.75 kV	1.0 kV	1.25 kV	
7		2.64		3.73
8		2.47		3.61
9		3.19		3.79
10		3.74		4.22
11		4.02		3.78
12		4.24		4.13
13		4.84		4.65
14		4.94		4.70
15		5.70		5.29
16		6.16		5.76
17		6.12		5.69
18		5.74		5.76
19	7.53	6.39	6.54	5.45
20		6.92	6.30	5.76
22		7.33		6.86
23		8.57		6.22
25		8.86		5.74

[†] Errors $\pm 30\%$ (see Iwai *et al* 1982).

[‡] Errors $\pm 15\%$ (see Iwai *et al* 1984).

smaller than assumed or the coupling potential has the l dependence or the interference among the neighbouring crossings is not negligible. A part of these discrepancies is also believed to be due to the fact that the observed results include not only one-electron capture processes but also contribution from indirect processes like transfer ionisation processes which is clearly indicated in figure 4 to be significant in such highly ionised ion+He collisions, whereas the calculation is purely due to the one-electron capture processes. In fact, contribution of the indirect process is estimated to amount to 15–20% in $I^{q+} + \text{He}$ collisions, being enhanced with increasing the charge of ions q (see figure 4). To clarify this contribution more experiments are needed such as the scattering angle dependence of the energy gain spectra and ejected electron spectroscopy and also accurate information on the energy levels of such highly ionised ions.

Table 2. Calculated partial cross sections for one-electron capture in $I^{q+} + \text{He}$ collisions at an energy of $1.25q$ keV using the MCLZ model. The numbers on the extreme right show experimental values.

q	Partial cross section (10^{-16} cm^2)															Total	Expt
	$n=6$	7	8	9	10	11	12	13	14	15	16	17	18	19			
20	0.06	23.0	68.1	9.0	0.08											100.1	87.5
30					0.4	20.6	81.2	59.2	1.3	0.9						174.9	106
35						0.05	5.87	53.4	88.5	46.8	10.7	1.2				206.5	117
40								1.7	27.3	83.7	83.1	37.6	9.0	1.4		243.9	187

4. Summary

In the present work we have demonstrated that our EBIS, NICE-1, with a relatively weak, continuous electron beam of 10 mA can produce I^{q+} ions with the charge as high as $q=41$ whose intensity is high enough to work on energy gain spectroscopy and found that one of the keys relevant to producing such high charge ions is vacuum in the ion source. Using these ions we have measured total cross sections for one-electron capture processes in $I^{q+} + \text{He}$ collisions at energies ranging from $0.75q$ to $2.25q$ keV and found they are nearly constant over the energy range investigated. In contrast to results for ions with low charge where significant oscillations are observed (Iwai *et al* 1982), these cross sections have been found to increase smoothly with the charge of the ions, agreeing with an empirical formula, and to increase with the square of crossing radius.

It should be noted that the observed energy gain spectra are only slightly broader than those of the incident ions, indicating that the electron is captured into the Rydberg states in a relatively narrow region of the principal quantum number n^* . This means that the electronic states with a limited number of the principal quantum number n are involved in one-electron capture process, though there should be a number of states closely spaced available. It should also be noted that, for He target atoms, the indirect processes like the transfer ionisation processes contribute significantly to one-electron capture processes in such highly ionised ion collisions.

It has also been found that there is a distinct similarity in both the size of cross sections and the electron capturing levels for the same q of ions irrespective of the nuclear charge of ions when the ion charge q is very high, as found in low q ions by Okuno *et al* (1983). Then, the ions can be treated as fully ionised in the electron capture processes. Therefore, based on the present results, some predictions such as the cross sections and electron capturing levels of electron capture processes can be made in collisions of He atoms with highly ionised metal ions like Fe, Mo, W, etc, which are most important in nuclear fusion researches.

Acknowledgments

This work was carried out as a part of the Guest Research Program at the Institute of Plasma Physics, Nagoya University. The authors are grateful to Professor H Kakihana, the Director of the Institute, and Professor Emeritus K Takayama, the former Director of the Institute, for their encouragement throughout the present work.

References

- Bliman S, Aubert I, Geller R, Jacquot B and van Houtte D 1981 *Phys. Rev. A* **23** 1703
- Bliman S, Bonnefoy M, Bonnet J J, Dousson S, Fleury A, Hitz D and Jacquot B 1983 *Phys. Scr.* **T 3** 63
- Carlson T A, Nester C W, Wasserman N and McDowell J D 1971 *At. Data* **2** 63
- Cocke C L, DuBois R, Gray T J and Justiniano E 1981 *IEEE Trans. Nucl. Sci.* **NS-28** 1032
- Gallagher J W, Bransden B H and Janev R K 1983 *J. Chem. Phys. Ref. Data* **12** 873
- Greenland P T 1982 *Phys. Rep.* **81** 131
- Groh W, Muller A, Schlachter A S and Salzborn E 1983 *J. Phys. B: At. Mol. Phys.* **16** 1997
- Huber B A 1983 *Phys. Scr.* **T 3** 96
- Iwai T, Kaneko Y, Kimura M, Kobayashi N, Matsumoto A, Ohtani S, Okuno K, Takagi S, Tawara H and Tsurubuchi S 1984 *J. Phys. B: At. Mol. Phys.* **17** L95

- Iwai T, Kaneko Y, Kimura M, Kobayashi N, Ohtani S, Okuno K, Takagi S, Tawara H and Tsurubuchi S 1982 *Phys. Rev. A* **26** 105
- Janev R K 1983 *Phys. Rev. A* **28** 1293
- Janev R K, Bransden B H and Gallagher J W 1983 *J. Chem. Phys. Ref. Data* **12** 829
- Justiniano E, Cocke C L, Gray T J, DuBois R D and Can C 1981 *Phys. Rev. A* **24** 2953
- Justiniano E, Cocke C L, Gray T J, DuBois R, Can C and Waggoner W 1984 *Phys. Rev. A* **29** 1088
- Kamber E Y and Hasted J B 1983 *J. Phys. B: At. Mol. Phys.* **16** 3025
- Kimura M, Iwai T, Kaneko Y, Kobayashi N, Matsumoto A, Ohtani S, Okuno K, Takagi S, Tawara H and Tsurubuchi S 1982 *J. Phys. B: At. Mol. Phys.* **15** L851
- 1984 *J. Phys. Soc. Japan* **53** 2224
- Kusákabe T, Hanaki H, Nagai N, Horiguchi T, Konomi I and Sakisaka M 1983 *Phys. Scr.* **T 3** 191
- Lennon M, McCullough R W and Gilbody H B 1983 *J. Phys. B: At. Mol. Phys.* **16** 2191
- Lin C D 1982 *Comment. At. Mol. Phys.* **11** 261
- Mann R, Cocke C L, Schlachter A S, Prior M and Marrus R 1982 *Phys. Rev. Lett.* **49** 1329
- Matsumoto A, Iwai T, Kaneko Y, Kimura M, Kobayashi N, Ohtani S, Okuno K, Takagi S, Tawara H and Tsurubuchi S 1983 *J. Phys. Soc. Japan* **52** 3291
- Muller A and Salzborn E 1977 *Phys. Lett.* **62A** 391
- Nielsen E H, Andersen L H, Barany A, Cederquist H, Hvelplund P, Knudsen H, MacAdam K B and Sorensen J 1984 *J. Phys. B: At. Mol. Phys.* **17** L139
- Ohtani S 1984 *Electronic and Atomic Collisions* ed J Eichler, I V Hertel and N Stolterfoht (Amsterdam: North-Holland) p 353
- Ohtani S, Kaneko Y, Kimura M, Kobayashi N, Iwai T, Matsumoto A, Okuno K, Takagi S, Tawara H and Tsurubuchi S 1982 *J. Phys. B: At. Mol. Phys.* **15** L533
- Okuno K, Tawara H, Iwai T, Kaneko Y, Kimura M, Kobayashi N, Matsumoto A, Ohtani S, Takagi S and Tsurubuchi S 1983 *Phys. Rev. A* **28** 127
- Phaneuf R A 1983 *Phys. Rev. A* **28** 1310
- Ryufuku H, Sasaki K and Watanabe T 1980 *Phys. Rev. A* **21** 745
- Suzuki H, Kajikawa Y, Toshima N, Ryufuku H and Watanabe T 1984 *Phys. Rev. A* **29** 525
- Tawara H, Iwai T, Kaneko Y, Kimura M, Kobayashi N, Matsumoto A, Ohtani S, Okuno K, Takagi S and Tsurubuchi S 1984 *Phys. Rev. A* **29** 1529
- Tsurubuchi S, Iwai T, Kaneko Y, Kimura M, Kobayashi N, Matsumoto A, Ohtani S, Okuno K, Takagi S and Tawara H 1982 *J. Phys. B: At. Mol. Phys.* **15** L733
- Winter H 1982 *Comment. At. Mol. Phys.* **12** 165
- Yan P G, van der Woude R, Dijkamp D and de Heer F J 1983 *Phys. Scr.* **T 3** 120

電子ビームイオン源用
水平設置超伝導コイルおよび
クライオスタットの製作

小林信夫、大谷俊介、金子洋三郎
岩井鶴二、奥野和彦、鶴淵誠二
木村正広、俵博之、日野利彦

名古屋大学プラズマ研究所・客員共同研究グループ

IPPJ-DT-84

1981年3月

(1980年2月17日受理)

名古屋大学プラズマ研究所

Design and Construction of a Horizontally Placed
Superconducting Magnet and its Cryostat for an
Electron Beam Ion Source.

N. Kobayashi, S. Ohtani, Y. Kaneko,
T. Iwai, K. Okuno, S. Tsurubuchi,
M. Kimura, H. Tawara and T. Hino

NICE Group for the Guest and Visiting
Research Program
Institute of Plasma Physics
Nagoya University

Abstract

An electron beam ion source nicknamed NICE-I (Naked Ion Collision Experiments) has been constructed at IPP for studies of atomic processes in fusion plasmas. A super conducting magnet is adopted to generate a strong, stable and homogenous magnetic field to compress a high density electron beam. The solenoid is 1 m long, the inner diameter is 100 mm and the maximum magnetic field is 2T. It is placed horizontally and coaxially with a liquid nitrogen (L-N₂) reservoir and a vacuum vessel. In order to fix their axes inmovable even when the reservoirs are cooled by L-N₂ and He, a structure having spokes strained uniformly like a wheel is used between the vacuum vessel and the L-N₂ reservoir and also between the L-N₂ reservoir and the solenoid bore. The electrodes, such as the electron gun, the drift tubes and so on, are mounted on the radiation shields fixed on the L-N₂ reservoir, and they are centered to the solenoid bore within the precision of 0.1 mm.

The evaporation rate of L-He is about 1.4 l/h, which is not so much larger than the estimated value. This provides a continuous operation for 16 hours with a charge of 50 l L-He including the precooling of the reservoir. The ultimate pressure 4×10^{-10} Torr is achieved in the vacuum vessel, and the residual gas pressure in the ionization region is expected to be much lower than 1×10^{-10} Torr. The consideration for mechanical strength and the heat conduction of the materials related to the design are described as well as the details of the structure.

Furter communication about this report is to be sent to the Research Information Center, Institute of Plasma Physics, Nagoya University, Nagoya 464 Japan.

目 次

1. はじめに	1
2. Cryo-NICE の概要	2
3. コイル用線材の選択	4
4. コイルボビン及び液体ヘリウム溜	5
5. クライオスタット	9
5.1 クライオスタットの構造	9
5.2 輻射シールド	10
A. 液体窒素溜	10
B. 輻射シールド板	13
5.3 液体ヘリウム溜くびの構造	14
5.4 真 空 槽	17
6. スポークを用いた超伝導コイルの固定	17
6.1 低温用材料	17
6.2 スポークによる超伝導コイルの懸下	21
A. 真空槽から液体窒素溜の懸下	22
B. 液体ヘリウム溜の固定	23
a. スポークによる懸下	23
b. 細いステンレス線を用いた補強	24
c. ガラス棒によるコイル-磁気シールド間の補強	24
7. 寒剤の消費量	26
7.1 寒剤の性質	26
7.2 予冷による寒剤の消費	26
7.3 熱流入による寒剤の消費	29
A. 液体窒素溜への熱流入	30
B. 液体ヘリウム溜への熱流入	30
8. おわりに	33

1. はじめに

我々は Naked Ion Collision Experiment (略して NICE) 計画用の多価イオン源として、超伝導コイルを使用した Electron Beam Ion Source (EBIS) 型イオン源(我々は Cryo-NICE と呼んでいる)の製作を行った。EBIS 型イオン源の原理は、磁場によって細くしぼられた電子ビームで原子や分子を電離し、生じたイオンを電子の空間電荷と軸方向にかけられた電位障壁によって閉じ込め、逐次電離によって多価イオンを生成するものである。したがって EBIS 型イオン源の製作にあたっては、高密度電子ビームの発散を防ぐために比較的均一度の高い強磁場の発生と同時に、イオン化領域を 10^{-10} Torr 以下の超高真空にして、残留ガスのイオンによって空間電荷が中和されないようにすることが必要である。

この要求にこたえるものとしては超伝導コイルの利用が考えられる。超伝導コイルは空心コイルに比較して小型で均一度が高い。同時にコイルを液体ヘリウムに浸して使用するので、コイルを収納するヘリウム溜の表面はクライオポンプとして利用出来る。このような利点から超伝導コイルを使用した EBIS 型イオン源がすでに実用化されている。ただし極低温で使用するものであるから、製作及び取扱い上のやっかいな問題もある。我々は Cryo-NICE の建設にあたって、超伝導コイルを使用した場合の得失について種々の検討を行い使用に踏み切った。その最大の理由は、イオン化領域が、軸方向に電位をかけるための移動管 (Drift Tube) と呼ばれる細い管に包まれており、この内部を超高真空に保つ有効な排気系を見い出すことが出来なかったためである。超伝導コイルを使用して、コイルボビン内に移動管を設置すればボビン表面はクライオポンプとして大きな排気速度をもっているから、移動管内を超高真空に保つことは容易である。さらに EBIS 型イオン源の特徴はパルス動作にある。パルスの導入された気体から生じたイオンをイオン化領域内に閉じ込め、価数が上がって電子ビームの空間電荷が中和された時点で、軸方向の電位障壁を取り払ってイオンを引き出した時に多価イオン生成効率は最も高い。したがってガス導入については、イオンの閉じ込め時間に比べてパルス巾を十分短くしかつ立上り、立下り時間の短い中性ガス入射が要求され、ガス噴射口附近には排気速度の大きなポンプが必要になる。この点でも超伝導コイルを利用することの利点は大きい。

Cryo-NICE で採用した超伝導コイルはコイル長 1 m, ボビン全長 1070 mm, ボビン内径 100 mm ϕ で、実験の都合上水平に設置されている。超伝導コイル及びクライオスタットの製作についてはすでに多くの解説がなされている。現在では超伝導用の線材も容易に入手出来るようになって小型のコイルであれば手造りも可能である。このコイルをガラス製の液体ヘリウムデュアー中に浸して使用すれば、数十 kG の磁場は容易に発生させることが出来る。しかし、超伝導コイルが物性実験と共に進歩したものであるために 解説の多くは物性実験家を対象としている。コイルはたてに設置する方が容易であり、物性実験用としてはそれで十分であるからたて型設置が基本になっている。Cryo-NICE 用の 1 m のコイルは大型の部類に入り、かつ

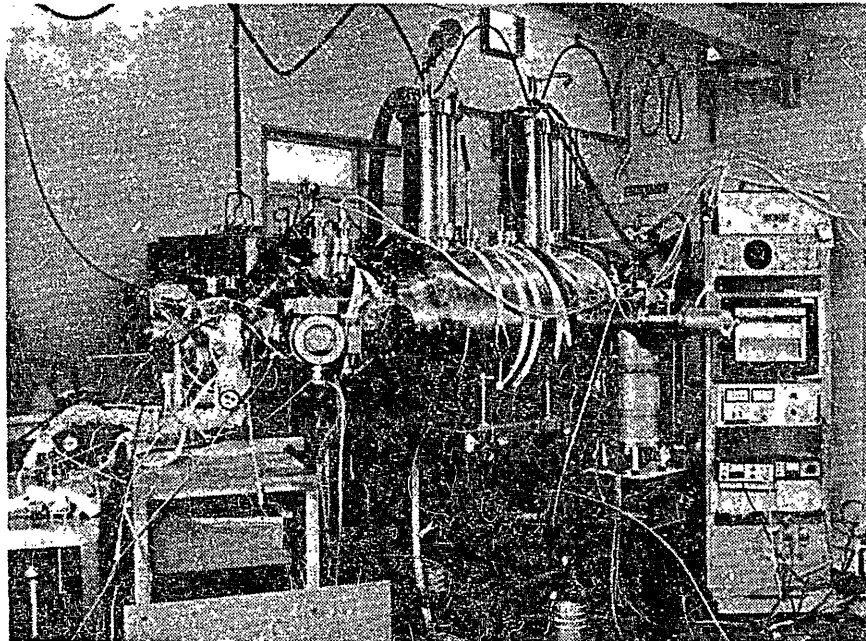
それをある程度の強度をもたせて水平設置するには多少の工夫が必要であった。

Cryo-NICE の多価イオン源としての特性その他については別の機会に報告することにして、この報文では低温装置としての Cryo-NICE の建設及びその建設に際して我々が学んだことについて報告する。

2. Cryo-NICEの概要

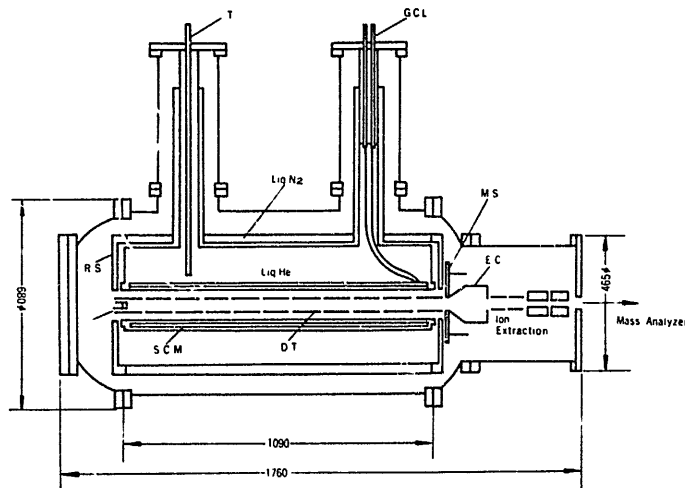
Cryo-NICE の概念図を1図に又その概要を表1に示す。電子銃から引き出された電子ビームは、このコイルによって発生する磁場でしぼられ、移動管にそったイオン化領域を通過した後、電子ビームコレクターに到達する。コレクターの直前には、軟鉄およびμメタルからなる磁気シールドがおかれており、ビームは発散してコレクターに捕集される。電位障壁が取り払われて電子ビームと一緒に流れ出たイオンは、コレクター後部にあるイオン引き出し電極のポテンシャルによって引き出され、レンズ系で収束した後質量電荷分析される。したがって、イオンソースを構成する電子銃、移動管、磁気シールド、コレクター、イオンレンズ系及び質量分析器は磁場(コイル)の中心軸と同軸に設置されていなければならない。特に電子ビームとコイルにより発生する磁場中心の軸合せには高い精度が要求される。

通常超伝導コイル用クライオスタットでは、コイルを収納している液体ヘリウム溜は構造材による熱伝導を可能な限り小さくするために、液移送口、電流導入口を兼ねた数本の肉薄パイプによって懸下されている。このような場合構造材として使用されている金属が冷却によって収縮するために、コイルの位置は室温時のそれに比べて数mmも移動してしまう。Cryo-NICE



N I C E 全 景

の場合、イオンソース構成部品をコイルボビンに固定出来れば、軸合せは容易であり、イオンをレンズ系を用いて質量分析器に導くことも可能である。しかし、高温の発熱体を極低温で動作させるコイルボビンに直接固定することは危険でもあり容易ではない。それ故我々は電子銃をはじめとするイオンソース構成部品は全て1図にR.S.で示された液体窒素温度の輻射シールド板に固定し、かつコイル軸と輻射シールドの軸は冷却時においても室温で設定した位置と0.1 mm以内の精度で一致させることを目標に設計を行った。そこで、上記のような一方向の収縮による移動をさけるため、コイルボビン、液体窒素溜、真空槽を同軸円筒形に設置し、ボビンと液体窒素溜、液体窒素溜と真空槽間を各々等方的に張ったスポークによって懸下する方式を採用した。又コイル近傍に強磁性体が設置されるので、クライオスタットの機械的強度についても検討を行い磁気シールドとの間に働く引力にも耐え得る構造とした。



1 図 Cryo-NICE 概念図

K : カソード A : アノード S.C.M. : 超伝導マグネット D.T. : 移動管
M.S. : 磁気シールド E.C. : 電子ビームコレクター G.C.L. : ガスクールリード
T : 液移送パイプ R.S. : 輻射シールド板

表 1 Cryo-NICE の概要

電 子 銃	Semi-immersed flow 方式
カ ソ ー ド	BaO 3 mmφ
電 子 加 速 電 源	10 kV 2 A
移 動 管 長	1000 mm
超 伝 導 コ イ ル 線 材	NbTi
磁 場 強 度	20 kG/90 A , 永久電流方式
コ イ ル ボ ビ ン 内 径	100 mmφ
ボ ビ ノ 全 長	1070 mm
液 体 窒 素 溜 体 積	23ℓ
液 体 ヘ リ ウ ム 溜 体 積	33ℓ

3. コイル用線材の選択

超伝導コイルの最大の利点は、いうまでもなく電気抵抗がゼロであるために電力消費がなく、かつ通常の空芯コイルに比較してはるかに小型化出来ることにある。永久電流方式で使用した場合、電源変動の影響を受けないから非常に安定度の高い磁場が得られる。現在では良い線材が開発されており、60kGまでは合金系のNbTi、それ以上200kG程度までは金属間化合物のNb₃Snを使用して比較的容易に高磁場を発生させることが出来る。

Cryo-NICEの20kGの発生は超伝導コイルにとっては弱磁場であってコイル製作上の問題はほとんどない。ただ超伝導コイルはクエンチして、超伝導状態がやぶれてノーマル状態におちることがある。我々のような未経験者にとって、大きなエネルギーを貯えているコイルがクエンチした状態というのは想像もし難い大変恐ろしいことのように思われる。そしてCryo-NICE運転中にクエンチし電子ビームは発散し、コイルのみならずイオンソース全体が破壊されてしまうのではないかといったことが心配される。事実過去にはNbTi線には低磁界不安定性とよばれる現象があって使用がそう容易でなかったり、training効果といわれて所定の磁場まで励磁してゆく際に数回のクエンチを経験するというようなことがあったようである。その後数百本の細い線材を束ねたmulti core wireにして線材の信頼度が向上するとともに、これに銅被覆をほどこして①線材の冷却効果を上げる、②局部的にノーマル状態におちても電流を銅にバイパスさせて超伝導線の温度上昇を防ぐ、③急激な磁束の変化が生じたとき銅中に渦電流が流れて緩和する等の改良がされ、現在では安定な線材が容易に入手出来るようになった。

クエンチの原因としては大まかにいって次のようなことが考えられる。①コイル自身の発生する強磁場中で機械的・磁氣的相互作用によってコイルが移動する。②コイル電源にパルスが入る。巻線後最初の励磁の際には、巻線のわずかなむらがあったりして①の原因でクエンチする可能性があるがその後は安定するものようである。Cryo-NICEのような低磁場用コイルではそのようなことはおこらないであろうとの予想であったが、幸にも我々はクエンチを経験しなかった。強磁場用コイルの場合でも線材をエポキシ樹脂でかためたり、銅被覆を厚くする等によってクエンチを防ぐことが可能である。

超伝導線には線材固有のパラメーターとして、超伝導状態になる温度T_cとその線材で発生し得る最高磁場H_cが決まっている。線材に垂直に磁場をかけた状態で、その線材に流し得る最大電流容量I_cを臨界電流という。I_cは磁場の強さの関数となっていて、各種線材によっても異なる。低磁場でI_cは大きく、磁場が強くなると共に減少しH_cでゼロになる。

Cryo-NICEのような20kG程度の低磁場用の場合には、励磁電流を大きくしてコイルの巻数を少なくした方が製作費は安上がりで、かつコイルのインダクタンスも小さくなって取り扱い易い。Cryo-NICEではI_cが大きく、同時にクエンチしにくい線材ということで銅被覆率の比較的高い線材を選択した。実際に使用した線材はI.G.C.社のCRYOSTRAND-Tiで、その定格およびコイル仕様を表2に示す。表に示された50kGにおけるI_cの値は短線の場合の値であっ

て、コイルにした時にはこの値より低くなる。それにしても 20kG の励磁に対しては十分余裕をもっており、励磁電流を大きくすればさらに高磁場の発生が可能である。

表 2 Cryo-NICE 用超伝導コイルの概要

線材	I.G.C. 社 CRYOSTRAND-Ti	ホルマル加工
線径	0.677 mm ϕ	
織条数	276	
Cu/Nb-Ti 比	2.0	
臨界電流	160 A (50 kG において)	ただし短線において
コイル巻数	17,732 ターン	12 層
磁場均一度	2.5 x 10 ⁻⁴	at 100 D.S.V.
線材全長	7,102 m	
自己インダクタンス	4.6	ヘンリー
電流導入	ガスクールリード	
電源定格	100 A	4 V
電流掃引率	100 A/10 min.	(0-60 A) 100 A/25 min. (60-90 A)

4. コイルボビン及び液体ヘリウム溜

物性実験などで使用される小型の超伝導マグネットの場合には、ボビンに巻線し、液体ヘリウムデュアー中にそのまま浸して使用される場合もある。ボビン材としては冷却時の収縮率が線材のそれとあまり異ならなければ何を使用してもよい。アルミ合金、真鍮、銅、ステンレス等が使用されるが、その中でもマグネットの軽量化のためにアルミ合金が多く使用される。

Cryo-NICE ではボビンの内側は超高真空で、その中心をビームが通るのでボビンは液体ヘリウム溜の一部をなしている。ボビンに巻線後両端フランジ部と溜との溶接を行う。それで、ボビン、溜ともに溶接が容易なステンレスを使用することにした。ステンレスとしては SUS 304 が入手しやすいが、切削加工後わずかではあるが磁化率の増大がみられる。

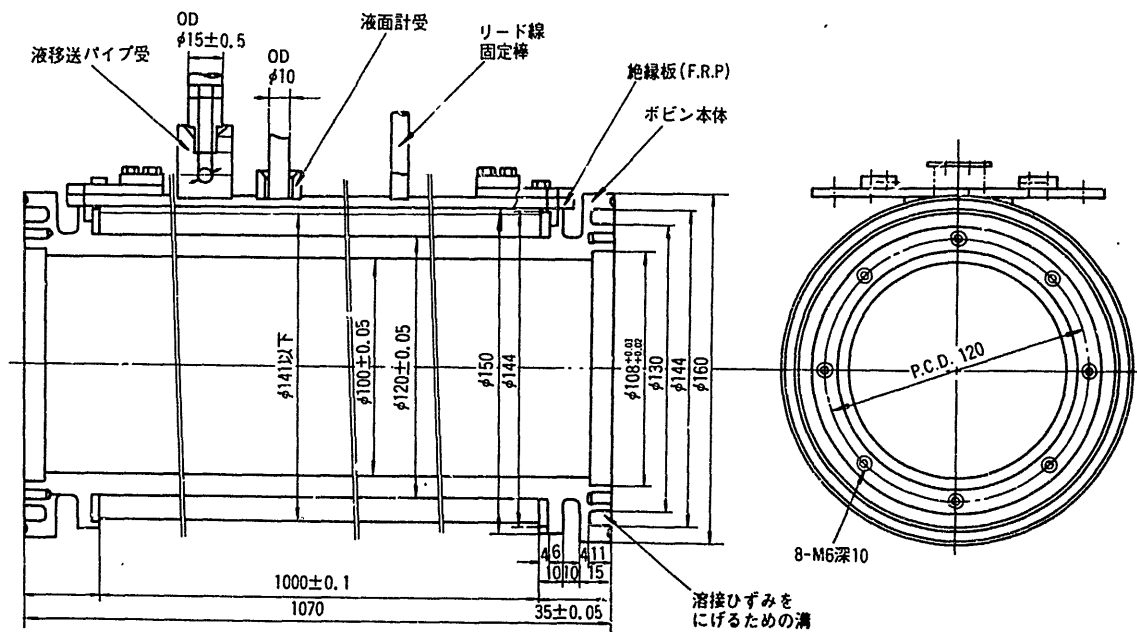
我々は、多少高価ではあるがそのような現象が少なく又溶接性も優れている SUS310-S を使用した。

ボビンは線巻の際コイル端の処理及び線材の継ぎ処理を行うためにコイル両端に 20~30 mm

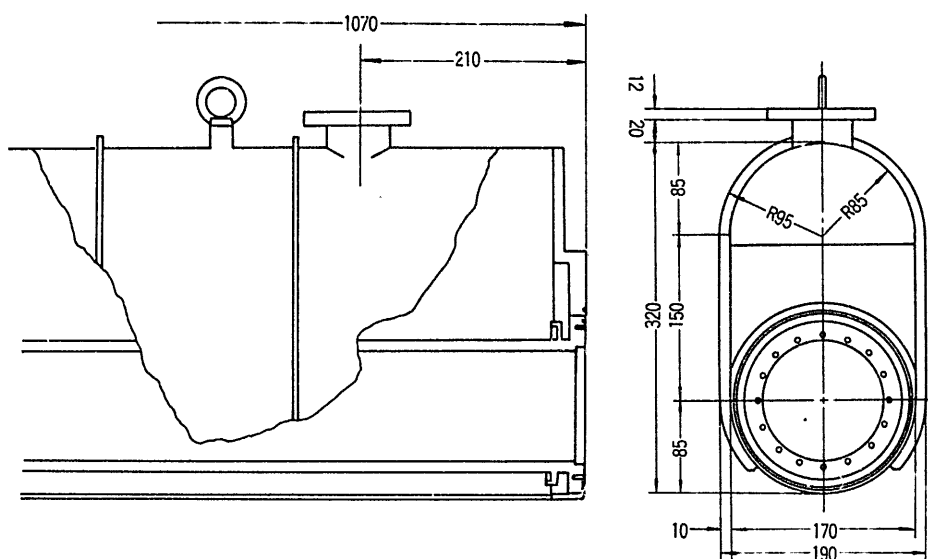
のスペースを取る。Cryo-NICE の場合ポビン全長はコイル長 1000mm にこのスペースとフランジ厚を加えて 1070mm となった。このように長いポビンにステンレス鋼を使用した場合、かなりの重量となるので少しでも肉厚を薄くしたいところである。しかしある程度の肉厚がないとポビンは自重及び線材の重みでたわむ。又、巻線の際には、前章で述べたような励磁中におこる線の移動をおさえるために、数kgの張力をかけて巻くので線材の張力によってポビン径は収縮する。Cryo-NICE の場合、特に前者のポビンのたわみは磁力線のたわみとなって直進するビームの不安定性の原因ともなりかねない。このたわみがどの程度まで許容されるかについては明確な判断は出来ないが、ビームと磁場中心を 0.1 mm の精度で一致させるという目標値からして 0.02mm におさえることにした。その結果ポビンの肉厚は 10mm となり、ポビン本体の重量は 56kg となった。しかし肉厚については次に述べる工作精度の点からもあまり薄くすることは出来なかった。

SUS 310-S は SUS 304 に比較して高価であるとともに加工性が多少劣る。しかし工作精度が悪い場合、特にポビン内・外径の中心が一致していない場合には、コイルはヘリウム溜に納められていて外部から見る事が出来ないので、コイル中心を決定することはむずかしい。かといって完成後に径方向の磁場分布を測定して磁場中心を決定することも困難である。それ故ポビン内径の中心がコイル中心となり、したがって磁場中心となるよう、ポビン工作にあたっては内外径の中心が $\pm 0.05\text{mm}$ の精度で一致することを要求した。1 m を越える SUS 310-S のポビン工作をこのよう内・外径ともに高い精度で行うことはそう容易なことではなく、工作工場探しに多少の苦勞が必要であった。ポビン材の SUS 310-S は山陽特殊鋼製鍛造品を使用し、工作は東京の富士機械株式会社が行った。

ポビンに線巻し必要な附属物を組み立てた後ヘリウム溜との溶接を行う。ポビン及び超伝導コイル組立図を 2 図に、液体ヘリウム溜の外観図を 3 図に示す。後に述べるようにコイル及び



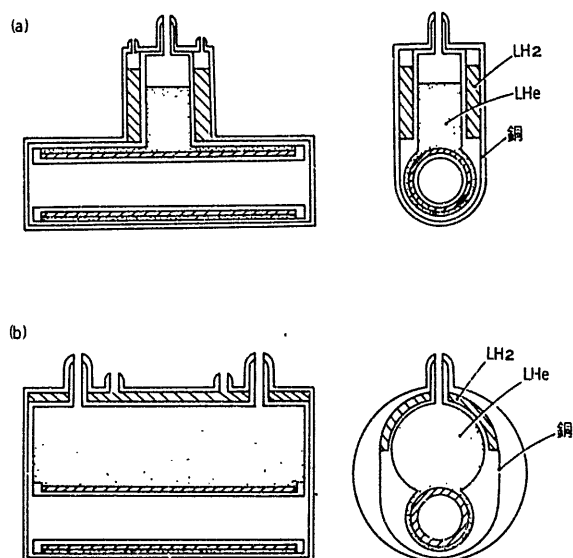
2 図 超伝導コイル組立図



3 図 液体ヘリウム溜外觀図

ヘリウム溜をスポークで懸下するためのスポーク受けがボビン両端にはめ合いで固定される。溶接の際の熱によってこのはめ合い箇所が熱ひずみを受け真円でなくなる可能性がある。そこで溶接部分からわずかに内側に切れ込み溝を入れて一部フランジの肉厚を薄くして、ボビン本体への熱伝導を小さくするとともにひずみはこの箇所でのげるようにした。

コイルは 4.2 K に冷却して使用するのでコイルが液面から出た状態で使用することは危険である。したがって 3 図に示されるような Cryo-NICE の溜では、コイル頂以下のスペースは無駄である。液体ヘリウムは高価であるので、極力デッドスペースを減らすことが望ましい。そのような無駄なスペースの少ない溜及びそれに合わせた一般的なクライオスタットの例を 4 図



4 図 一般的な水平設置型クライオスタットの例

に示す。我々は当初 (b) 図のような形状の溜を計画していたが、コイル長が長いために溶接が困難であると同時に機械的強度を保障することがむずかしいために 3 図に示した形状のものとなった。

ヘリウム溜にためた液体ヘリウムは外部からの熱流入によって絶えず沸騰しているから、長時間運転するためには時々ヘリウムを充填しなければならない。通電中に充填することは危険であるのでコイルの電流を切ってから充填する。超伝導コイルの場合、この手間はかなりかかりめんどろであるから一度充填したら長時間連続運転出来ることが望ましい。連続運転可能時間はヘリウム溜の体積と液体ヘリウムの蒸発量によって決まる。熱流入を小さく出来れば溜は小さくすむが、そうでない場合には大きくせざるを得ない。我々は液体ヘリウムの蒸発量を 1ℓ/h 程度と見積ったので、1日に1度の充填としてコイル頂以上の有効体積は 23ℓとした。ポビン、コイルを含むヘリウム溜全重量は 95 kg となり、超伝導コイルとしてはかなり大型のものとなった。

ポビンと溜が一体となっていて、かつコイル長の長い場合には室温から冷却してゆくときに全体が一様に冷却されるように注意しなければならない。冷却が一様でないと冷却箇所の局所的な収縮によってひずみが生ずる。ポビン又は溜の外壁の一方のみが 4.2 K まで冷却されると全長×1/300の収縮がおこる。この収縮力がポビンと溜の溶接部にかかり、溶接は破壊されてしまう。事実、Cryo-NICEの液体ヘリウム溜が完成した後に液体窒素温度でのリークテストを行った際、かなり長時間かけて冷却したにもかかわらず溶接部にクラックが入るという事故があった。その原因は、溜の外側から液体窒素をふりかけたためにポビンは冷却されず、溜のみが収縮したためであることが判明した。溶接部を強化すると共に均一に冷却されるよう注意することによって、その後このような事故は発生していない。後に述べるように、液体ヘリウムを充填する際、液溜を液体窒素温度から 4.2 K まで予冷するのに要する液体ヘリウムの量は冷却がうまく出来るかどうかによって大巾に異なる。したがって、コイル及び溜が一様に冷却されかつ冷却効率のよい液導入パイプの設置が大切である。Cryo-NICE では、液は 2 図に示されているコイル上部の液体ヘリウム移送用パイプ受けから 2 本のパイプに分けられて、コイル端からコイル長の約 1/3 の位置のコイル下部から注入される。そして蒸発したガスはコイル及び溜と熱交換した後に外部に排出される。

ポビン、液体ヘリウム溜の設計及びコイル組み立ては真空冶金 K.K で行い、溶接は日本真空工業で行った。

5. クライオスタット

5.1 クライオスタットの構造

クライオスタット（低温恒温槽）の製作で最も重要なことは、当然のことながら高温部から低温槽への熱流入を最小限におさえることである。特に超伝導コイルのように沸騰している液体ヘリウムの場合、ヘリウムの蒸発潜熱が小さいために、わずかな熱流入によって多量の液体ヘリウムが蒸発する。一番簡単な 4.2 K クライオスタットは液体ヘリウム貯蔵用デュアーである。簡単な液体ヘリウム・デュアーではヘリウム溜を液体窒素温度の輻射シールドで覆い、これを真空容器におさめてある。

水平設置型コイルの場合においても、簡単なクライオスタットとしては、4 図に示したように、液体ヘリウム溜を輻射シールドで覆いそれに合った真空容器に入れればよい。真空槽、輻射シールド、ヘリウム溜の各間隔は 2～3mm あればよいから、上手に製作すれば真空容器もあまり大きくなくてすむ。4 図にも見られるように、通常、液体ヘリウム溜は外部からの熱流入を小さくするために液移送口の細いくび状のパイプのみによって支持されている。したがって機械的には弱い。又くび上部とコイル中心までは 500～1000 mm の長さがあるために室温時に比べて冷却時にコイル中心は 1.5～3 mm 移動する。さらにこの移動はクライオスタットの構造によっては平行移動とは限らないからやっかいな問題である。

Cryo-NICE では 2 章で述べたように、磁場中心を冷却時においても 0.1 mm 以内の精度で固定させることを目標としたので、このような液移送口パイプによるつり下げ方式はとれない。そこで、懸下方式の原理としては、真空槽、液体窒素溜を円筒型にしてコイルボビンと同軸に設置し、等方的に張ったスポークによってまず真空槽フランジから窒素溜を、次に窒素溜からコイルボビンを懸下することとした。このような等方的に張ったスポークによるつり下げを行った場合、冷却による収縮は各スポークに均等な張力として働くから中心を移動させる力とはならないはずである。各溜の重量は全てこのスポークによって支え、各溜のくびの途中にはペローを入れて収縮による上へ引き上げようとする張力がかからないようにした。

スポークを用いて懸下した場合には、恒温槽への熱流入はくびからの分にこのスポークからの分が加わるから出来るだけスポークによる熱伝導は小さくおさえたい。スポークの本数及び径は懸下に必要な荷重によって決まるからある程度の長さが必要である。特に窒素溜からボビンをつるためのスポークは長くなる。さらにコイルボビンから上部につき出したような非対称な形状のヘリウム溜を等方的に張ったスポークで懸下するから、無駄な空間が多くなりこれを収納する真空槽は大きなものとなる。真空槽は可能な限り小さい方が良く、かつ工作上的の制約もあって Cryo-NICE 用真空槽の内径は 596 mm ϕ となった。輻射シールド用液体窒素溜については上に述べた完全円筒形に出来ず多少変形した形状となった。

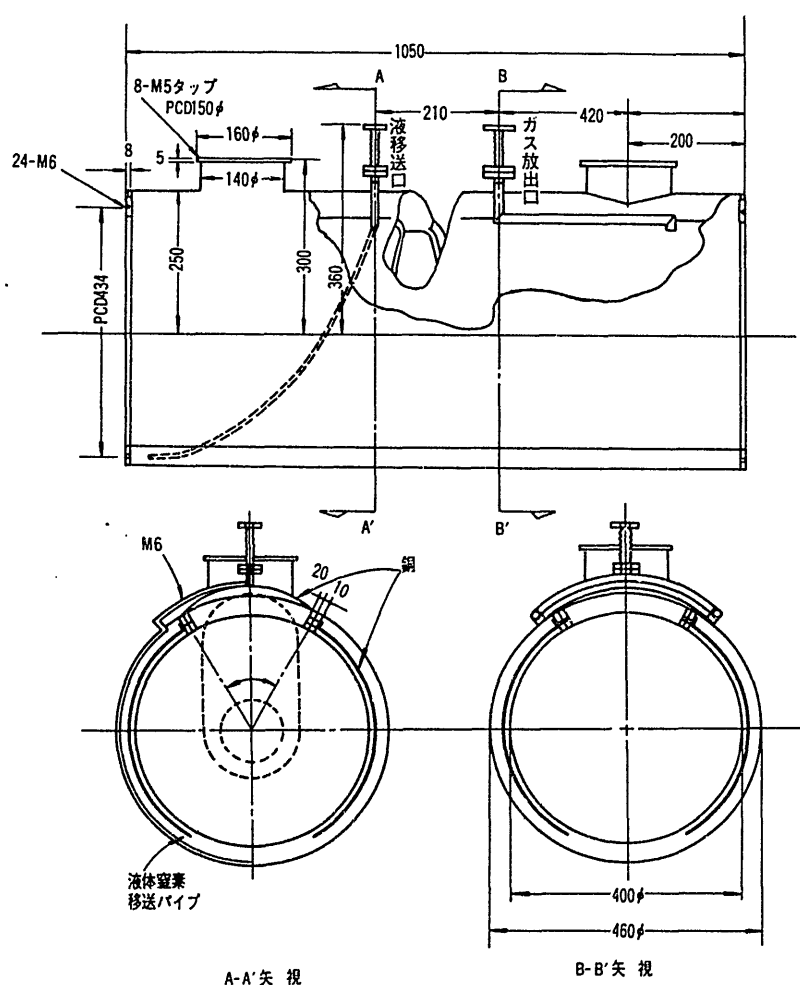
液体ヘリウム移送口については通常くび上端で溶接する。しかし今回のようなスポークによる懸下は初めての試みであり、溶接終了後にトラブルが生じた時のことが心配された。それ故

くび部については数種類のフランジを組み合わせて解体・組み立てが可能な構造にした。次に輻射シールド、くびの構造について述べる。

5.2 輻射シールド

A. 液体窒素溜

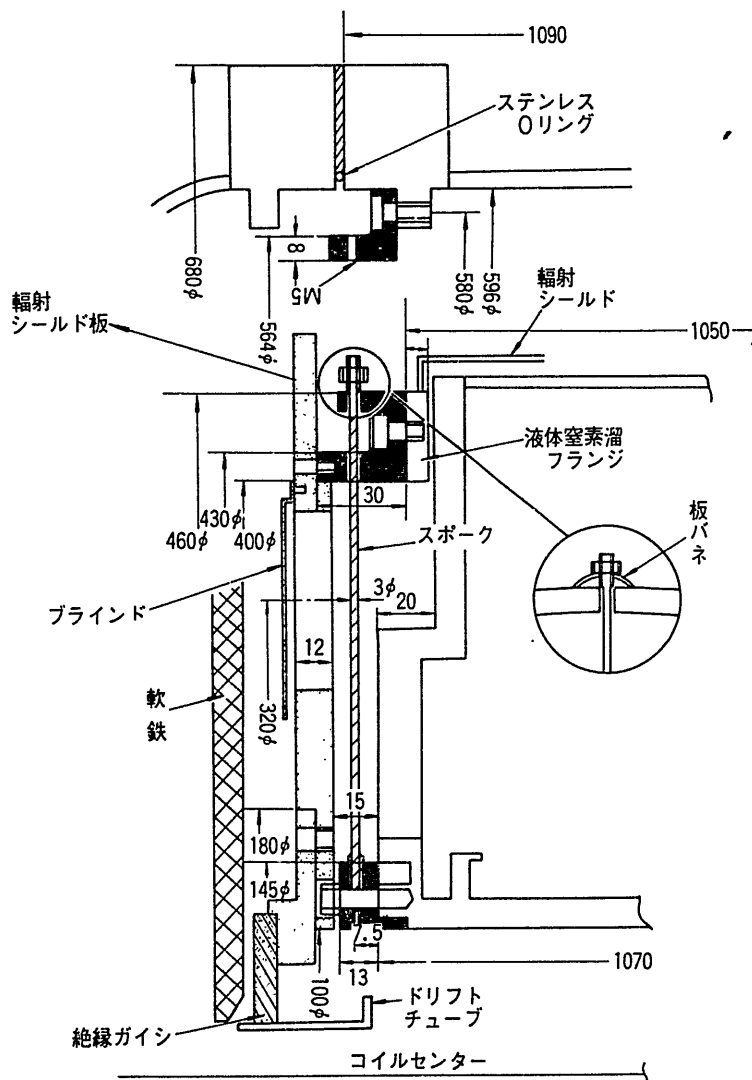
ヘリウム溜の高さは3図に示されているようにコイル中心から235 mmである。コイル中心を真空槽の中心に設置すると、ヘリウム溜頂部と真空槽内壁との間隔は61 mmである。この間に円筒形の液体窒素溜を設置し、真空槽からスポークを張ってこの溜を懸下する余裕はない。液体窒素溜は円筒の上部1/6を切り取り、その上に鞍形をした銅板をかぶせてヘリウム溜を覆うようにして、円筒の外径は460 mmφにおさえた。5図にその詳細を示す。



5図 輻射シールド用液体窒素溜

液体窒素移送口及びガス放出口は真空槽との接合の都合上ほぼ中央に位置している。ただし、液体窒素を注入して溜を室温から液体窒素温度まで予冷する際に、蒸発ガスによる冷却効果を上げるために移送口から溜の端までパイプをはわせてある。一方ガス放出口は溜の他方の端に位置しており、蒸発したガスは溜内を一巡して十分熱交換した後外部へ排出される。

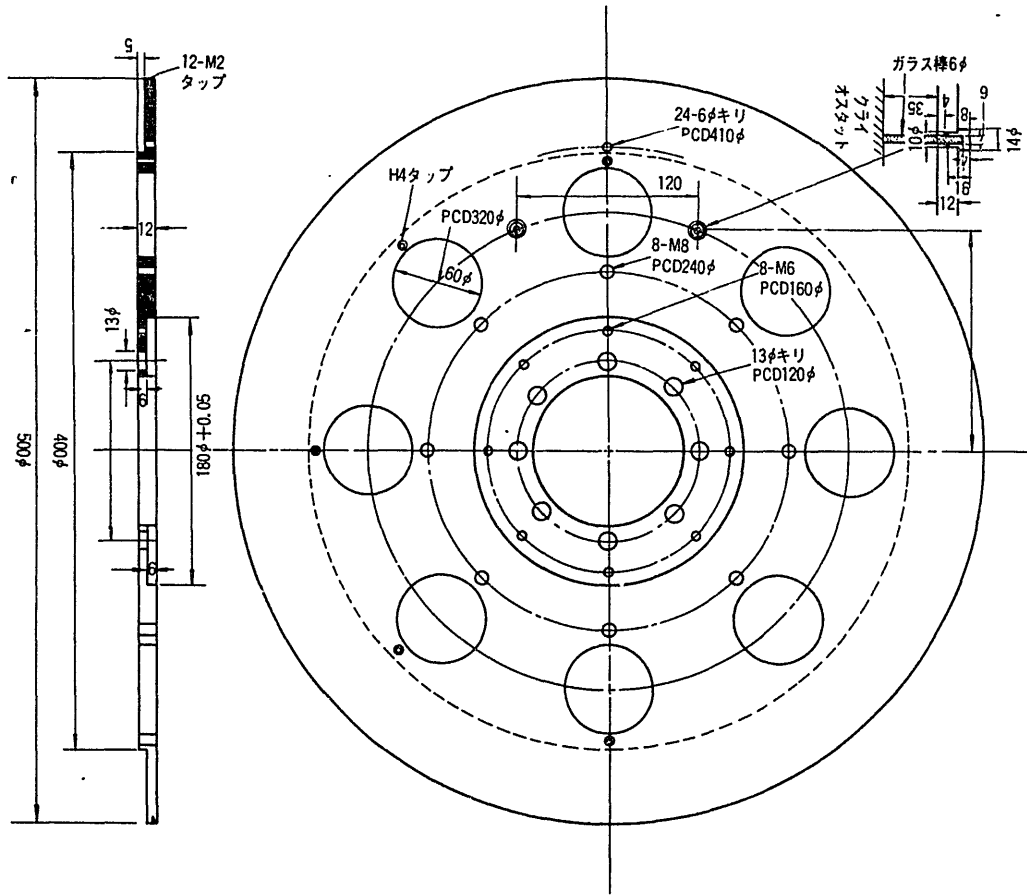
液体窒素溜が完全円筒でなくなったために、冷却時に変形する可能性がある。そこで6図に



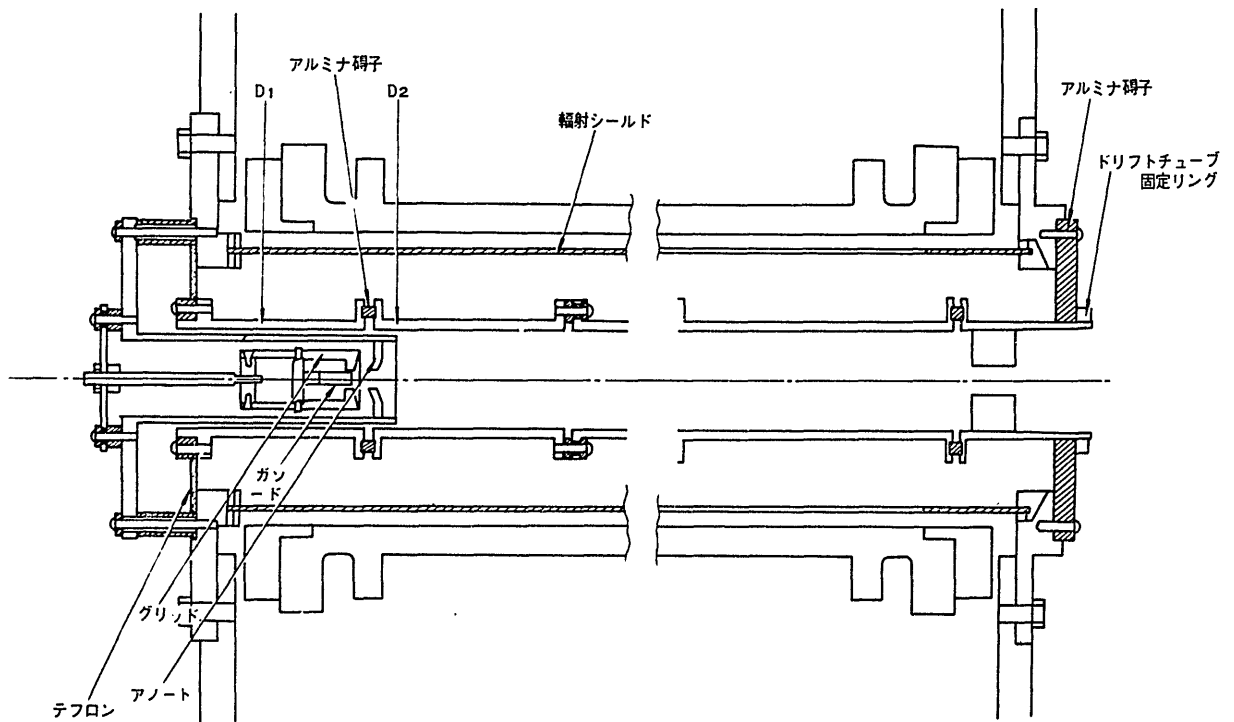
6図 スポーク支持用フランジとスポーク支持方法

示すように、溜の両端フランジは切断せずにリング状にして残し、そこにスポーク固定用フランジをネジ止めする。かつこのフランジに厚さ12mmの銅円板を取りつけた。このようにして、溜が冷却によって変形した場合にもスポーク固定用フランジは変形せずに真円を保つと同時に、銅製円板は液体ヘリウム溜の両サイドを覆うかたちとなって放射シールドを兼ねている。

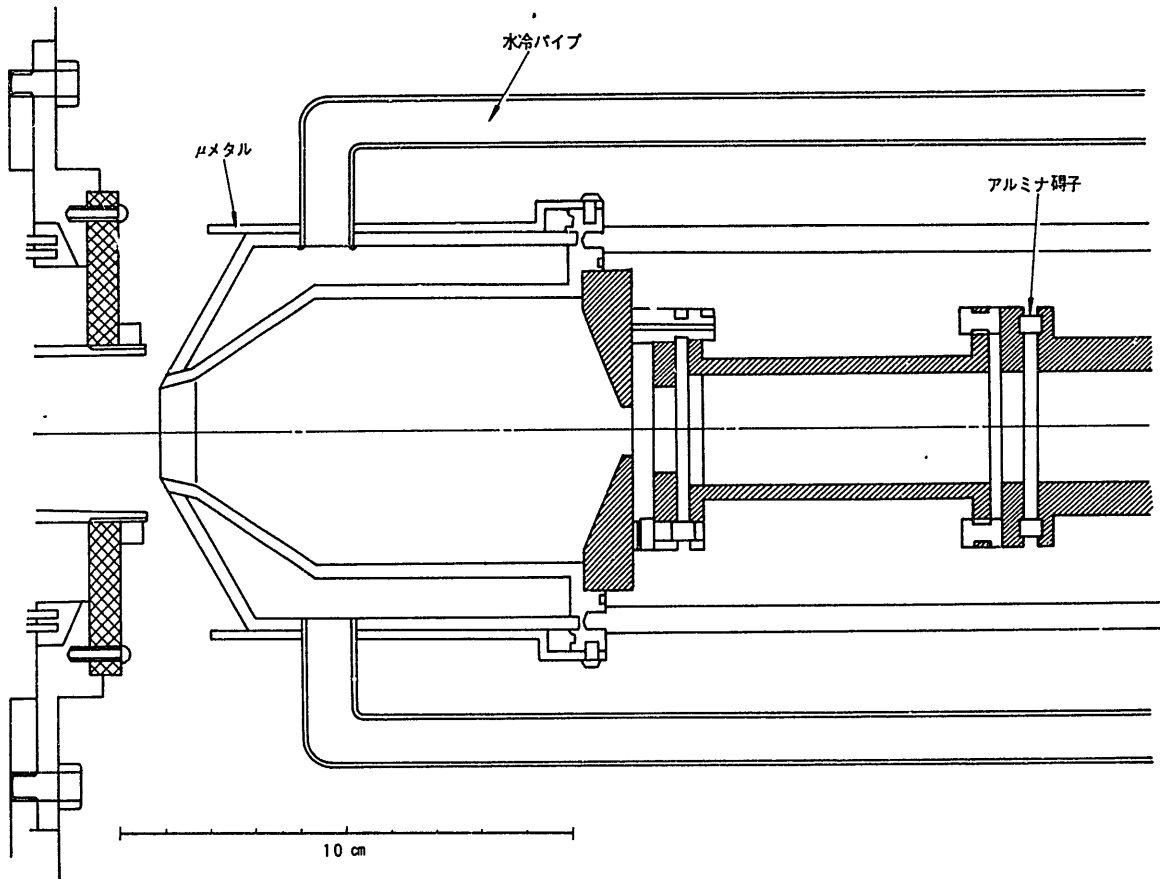
液体窒素溜は円筒形にして上部を切り取ったためにヘリウム溜の下部に位置することとなった。通常窒素溜は熱伝導率の大きな銅製とするが、Cryo-NICEの場合超高真空を要求するので溶接箇所からのリークを心配して溶接性のよいステンレス製とした。ステンレスの熱伝導率は小さいから、液体窒素が減少して液面が下がったときに上部の温度は上昇する。そこで溜内部に銅板を入れて常に銅板は液に浸っているようにして上部温度の上昇を防いだ。



7 図 シールド板詳細



8 図 コイルピン内の詳細



9 図 電子ビームコレクター及びイオンレンズ系

B. 輻射シールド板

液体窒素溜両サイドにある輻射シールド板の一方には電子銃，反対側には磁気シールド，電子ビームコレクター及びイオンレンズ系が設置される。又ポビン内の移動管，輻射シールドもこのシールド板によって支持される。輻射シールドの詳細を7図に，ポビン内の構成を8図に，電子ビームコレクター及びイオンレンズ系を9図に示す。

輻射シールド内はヘリウム溜外壁がクライオポンプとして働き大きな排気速度をもっているから真空度はよいと考えられる。しかし，輻射シールドと真空槽の間の空間の真空度が悪いと，移動管はこの真空槽側空間とつながっているために移動管端から残留ガスが流れ込みイオン化領域の真空度は向上されない。一方この空間を他の真空ポンプを用いて排気しようとすればかなり大型の超高真空装置が必要となる。そこで，両輻射シールド板に 60 mmφ の穴を8ヶ所ずつ計16ヶ所あけ，ヘリウム溜外壁のクライオポンプ作用を利用して真空槽側空間の排気を利用することとした。ただ穴をあけただけでは真空槽内壁からの輻射が入り込むので6図に示されているようにブラインドをおいて輻射シールドをしている。そのためあまり大きな排気速度は得られないが，500 l/sec 程度の排気速度になると期待される。450 l/sec のターボ分子ポンプ1台によって 5×10^{-8} Torr まで予備排気した後，液体ヘリウム及び液体窒素溜を液体窒素で冷却

した時点で真空度は 6×10^{-9} Torr になる。さらにヘリウム溜に液体ヘリウムを充填した時の到達真空度は 4×10^{-10} Torr に達する。この状態でターボ分子ポンプのバルブを閉じて真空度はほとんど変わらない。

ポビン内はさらに真空度を良くする必要があるから、真空槽側と通ずる箇所が無いよう 8 図に示すようにテフロンシートとアルミナ碍子を用いて遮蔽してある。ポビン・フランジと輻射シールド板との間隔は 2mm と狭く、コンダクタンスは小さくしてあるので、シールド板排気口を通して真空槽側残留ガス分子が入り込んでもポビン内へは到達しない。移動管の一方の端には電子銃を収納しかつ他端には内径 10 mmφ のリデューサーを挿入して移動管と真空槽側とのコンダクタンス C_1 を小さくおさえている。移動管内の排気は移動管接属部の間隙のコンダクタンス C_2 を通じて行く。したがって移動管内の真空度 P は真空槽側の真空度を P' としてポビン内の真空度は十分よいとすれば

$$P = C_1 / C_2 P'$$

で決まる。 C_1 は電子ビームコレクター側のリデューサーで決まるが、肉薄のアーチャーと仮定すると約 8 l/sec である。一方移動管の接合部は 10ヶ所あり、間隙は 3 mm で移動管内径は 34mm であるが、接合部のフランジ半分は絶縁碍子でふさがれている。この場合にも肉薄のパイプが並んでいると仮定すると C_2 は約 150 l/sec と見積られる。 $C_1 / C_2 < 1/10$ であるからイオン化領域の真空度 $P < 4 \times 10^{-11}$ Torr で、当初の目標 $P < 10^{-10}$ Torr に到達していると推定される。

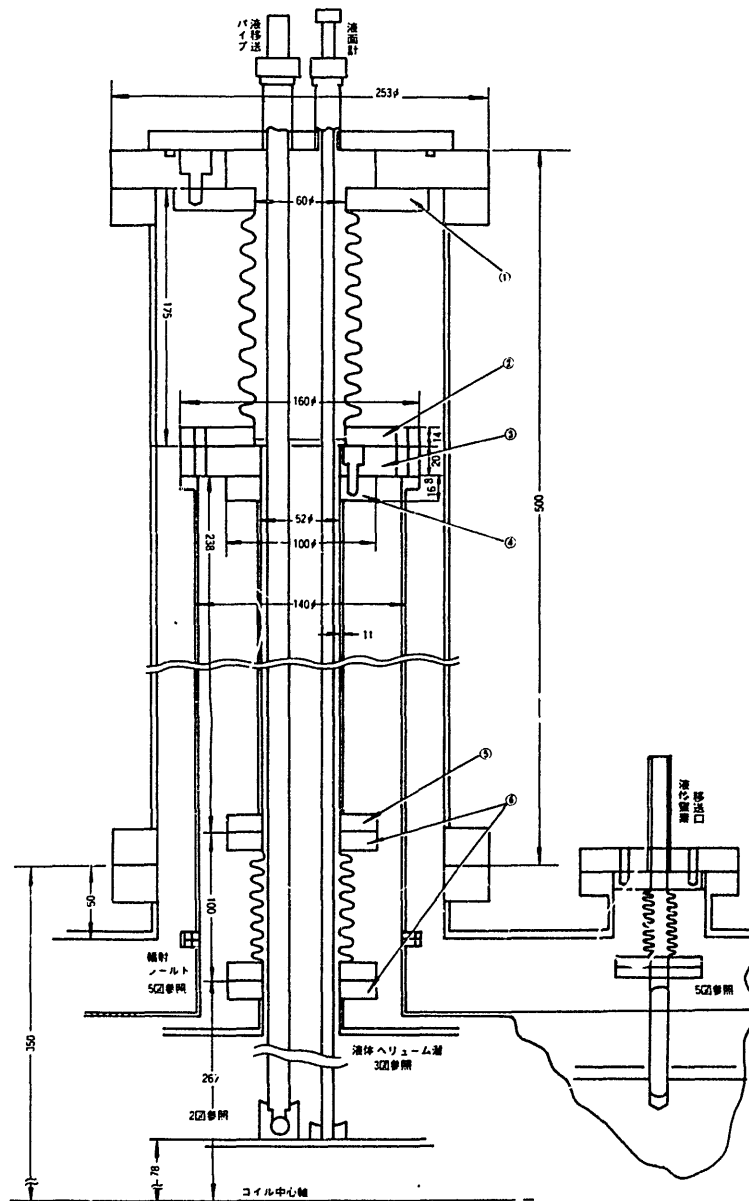
この場合、移動管からポビン壁が直接見える方が望ましい。特にガスをパルス導入する場合ポビン内壁の大きな排気速度を直接活用することが出来る。そのためには移動管も液体窒素温度に冷却されていることが必要である。さもないと高温の移動管からの輻射シールドが必要となって排気速度は極度に減少してしまう。Cryo-NICE では輻射シールド板に移動管を支持することによって、移動管も冷却してポビン間の輻射シールドは省略出来るようにしてある。安全のために電子銃附近のみ輻射シールドで覆ってある。ただし、電子銃、移動管には高圧がかかるので絶縁物を介して固定する。したがってこの絶縁物の熱伝導能力以上の熱流入、例えば電子ビームのごく一部でも移動管にあたるようなことがあると、移動管の温度が上昇するから、そのような事故が無いよう注意が必要である。

5.3 液体ヘリウム溜くびの構造

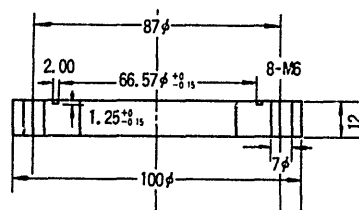
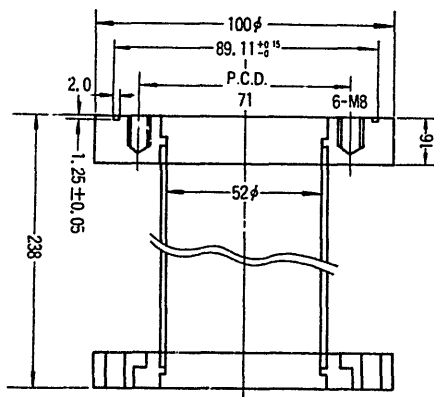
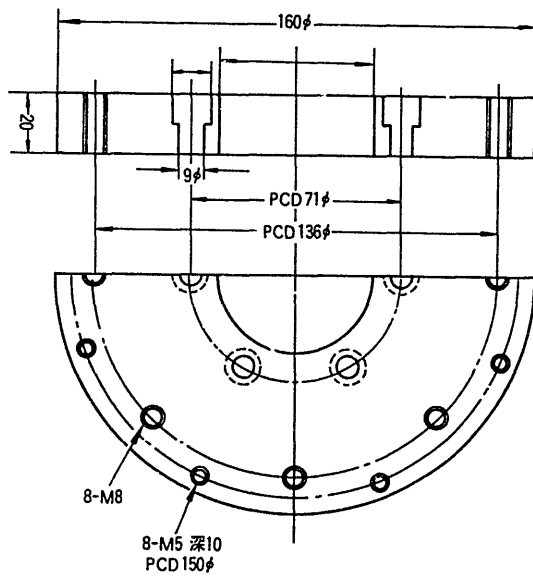
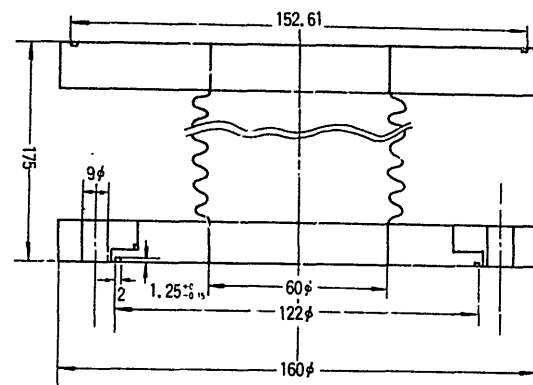
くびは 1 図ですでに示したように 2ヶ所あり、それぞれ液移送口、電流導入口となっている。共に同じ構造であるので液移送口について 10 図に示す。11 図には使用したフランジの詳細とガスケットには富士テルモ製ステンレス Oリングを使用したのでその規格を示す。くびの途中にはベローを入れて、冷却時の収縮力が液体ヘリウム溜にかからないようになっている。又溜頂部から 370mm のところで鞍型の輻射シールド板から煙突状に突き出た、くび部輻射シールドと

くびを接合させ冷却している。幾つもの部品を組み上げてゆく構造となっているので、一部に回転フランジを使用し上部にもベローを入れてある。

くびの上端は室温であるから、液体ヘリウム液面から上部フランジが覗けると輻射による熱流入が大きくなる。そこで、非常に簡便な方法ではあるがアルミ板2枚からなる輻射シールドを入れてある。



10 図 液体ヘリウム溜くび及び液体窒素移送口の構造



11 図 液体ヘリウム溜くび内のフランジ

5.4 真空槽

真空槽の概要はすでに1図に示してある。イオンソースの全長は1760 mmで、超伝導コイルを収納している部分のフランジ外径は680 mmφ、イオン引き出し部フランジ外径は465 mmφである。これら大口径フランジ部のガスケットには富士テルモ製ステンレスOリング E-24000 (680φ), F-465 を使用したが、イオン出射部フランジは着脱が容易であるということからEVAC社クランプ・チェーン型アルミOリングを使用した。それ以外のフランジはコンフラットフランジを使用し、排気系には排気速度 450 l/sec のターボ分子ポンプを使用した。バルブを使用しているのでポンプの実効排気速度は約 300 l/sec である。ポンプのみによる予備排気の時の到達真空度は 5×10^{-8} Torr である。

超高真空用真空槽としては300℃程度の焼出しをしたいところであるが、内部に超伝導コイルが収容されているので、焼出し温度は100℃以下におさえなければならない。

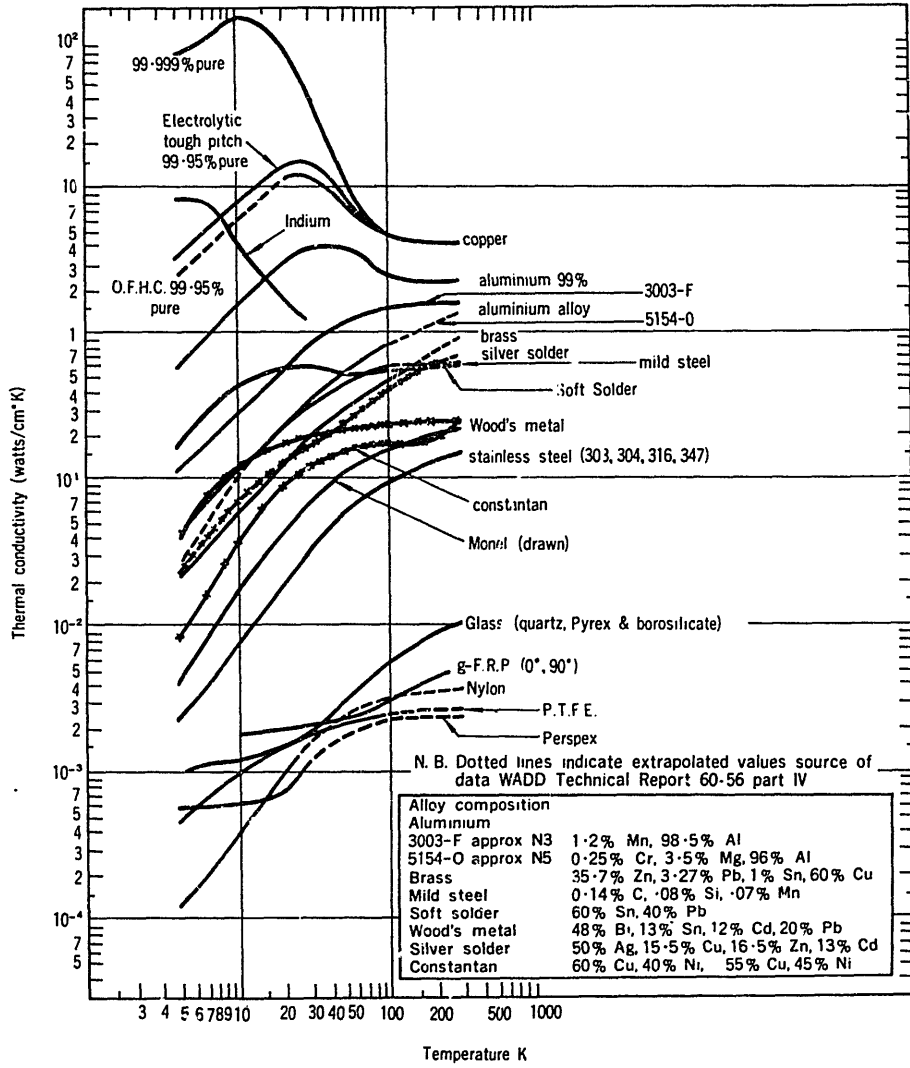
6. スポークを用いた超伝導コイルの固定

6.1 低温用材料

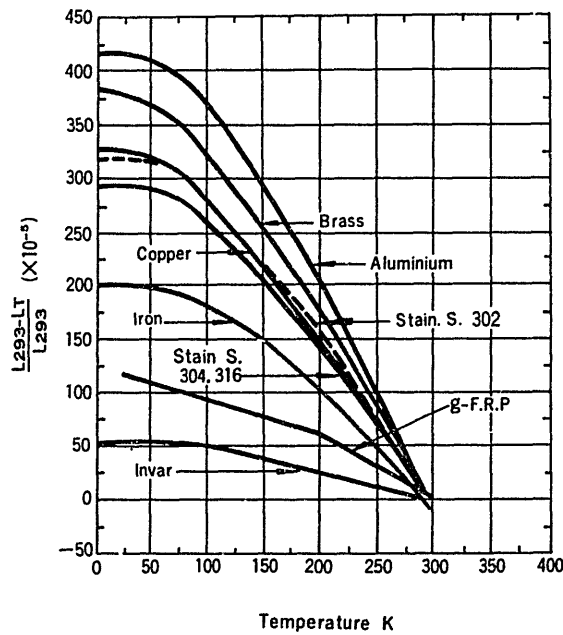
これまでも多少触れてきたように、クライオスタットの製作においては熱流入を抑えなければならない場合もあり、又逆に熱伝導を良くしなければならない場合もある。したがって熱絶縁材、熱良導体をうまく組み合わせることが必要である。各種材料は低温においてそれぞれに特徴的なふるまいを示すが、クライオスタット構造材の低温特性についてはこれまで具体的には何も述べずにきたので、ここで多少ふれておく。ただし広範な材料の各種特性については他の文献を参考にしてもらうことにして、ここではごく少数の材料についてその熱伝導率、熱収縮比及び低温強度について紹介する。

代表的な材料の熱伝導率を12図に、20℃を基準にした熱収縮比を13図に示す。低温における機械的強度の温度変化を表3に示す。

12図に見られるように熱伝導率は材料によって非常に多様であり、特に低温において変化が激しい。金属元素の場合熱伝導率は、図中の銅の場合に見られるように、純度及び格子欠陥の存在等によって大きく異なる。したがって熱伝導をよくする場合には純度のよい材料を選ぶと同時に工作後にはアニールをして使用する。一方合金の場合には、不純物散乱のために電子の熱伝導への寄与は小さくごく低温においてはフォノンによる伝達が主になるために、一般に熱伝導率は小さくかつ温度が下がると共に急激に減少する。非金属の場合の熱伝達はフォノンによるが、フォノン-フォノン散乱及び不純物散乱が熱抵抗になる。したがって非晶質や不純物の入った非金属の熱伝導率は非常に小さい。一方、水晶、サファイヤのような純物質の場合には伝導率は比較的大きく純金属の場合のように低温でピークを持つ。これらの単結晶では50～



12 図 各種固体の熱伝導率 BOC社 "Cryogenic Data Chart" より



13 図 20 °C を基準にした固体の収縮比

表 3 材料の低温強度

品名	米国規格	JIS相当※	成分処理	引張強さ (kg/mm ²)				降伏 (kg/mm ²)				JIS指定 (常温)			
				25 K		50 K		25 K		50 K					
				25 K	50 K	100 K	200 K	300 K	25 K	50 K	100 K		200 K	300 K	
高力アルミニウム合金	2014-T6	A3-X1	焼入後焼モドシ Si(0.05~1.2), Fe(1.0), Cu(3.9~5.0), Mn(0.4~1.2), Mg(0.2~0.8), Cr(0.1), Zn(0.25)	96	89	55	51	49	47.8	55	53	51	47	43	43
耐食アルミニウム合金	5056-HB4	A2-X2	加工硬化安定化処理 Si(0.03), Fe(0.4), Cu(0.1), Mn(0.5~0.2), Mg(4.5~5.6), Cr(0.05~0.2), Zn(0.1)	-	-	48	38	38	44.3	-	-	31	29	28	28
“	6061-T6	A2-X4	焼入後焼モドシ Si(0.4~0.8), Fe(0.7), Cu(0.15~0.4), Mn(0.15), Mg(0.8~0.2), Cr(0.15~0.35), Zn(0.25), Ti(0.15)	49	43	38	34	31	29.5	36	33	31	29	28	18.2
“	5052-HB4	A2-X1	加工硬化安定化処理 Si+Fe(0.45), Cu(0.1), Mn(0.1), Mg(2.2~2.8), Cr(0.15~0.35), Zn(0.1)	51	41	31	24	24	26.7	25	22	20	18	18	21.8
銅				49	42	40	29	22		7	7	7	7	8	
ベリリウム銅				-	-	15	13	13		-	-	12	11	10	
18-8ステンレス	304	SUS-27	焼 純	175	168	154	94	73		49	45	40	33	24	
18-12モリブデンステンレス	316	SUS-32	“	147	136	119	84	60		58	56	49	35	22	
チタン合金			Al(6), V(4) 焼純	183	170	146	117	98		178	160	138	108	91	
チタン				-	-	90	68	56		-	-	76	58	45	
ナイロブロン				-	-	19	14	6.3		-	-	-	-	-	
塩化ビニル				-	-	14	12	5.2		-	-	-	-	-	
ケル				-	-	11	10	4.2		-	-	-	-	-	
チタン				-	-	8	3.5	1.4		-	-	-	-	-	
マニラ				-	-	28	19	15		-	-	-	-	-	

※は形状によって文字が変わる

10 K で高純度の銅と同じ程度の熱伝導率をもつ。 Al_2O_3 の粉末を焼結したセラミックスやグラファイトのような多結晶質のものは液体窒素温度附近ではほぼ合金と等しい熱伝導率を持つが、ごく低い温度では良い熱絶縁材となるので、一種の熱スイッチとして利用される。

熱絶縁材としてはガラス、テフロンなどの非金属材料がすぐれているが、機械的強度が低いために構造材としてはあまり使用されない。構造材としてはステンレス鋼が強度と共に加工性にも優れているために多く使用される。非金属材料のうちでも、加工性は劣るが機械的強度に優れているものに F.R.P. がある。ガラス繊維を用いた G-F.R.P. の引張り強度はステンレスに比較して多少劣るが、降伏点を比較した場合にはあまり差はない。炭素繊維を用いた C-F.R.P. についてはステンレスよりも機械的強度に優れたものが開発されている。表 3 に示されているような焼鈍処理を行わない通常の場合のステンレス鋼の引張強度は約 50 kg/mm^2 である。それに対し、東レ炭素繊維を素材とした小林木型社製 C-F.R.P. の引張強度は 90 kg/mm^2 でステンレスの強度を優にしのいでいる。上記小林木型社製トレカ・コンポジットの機械特性を表 4 に示す。

表 4 C-F.R.P. の機械特性

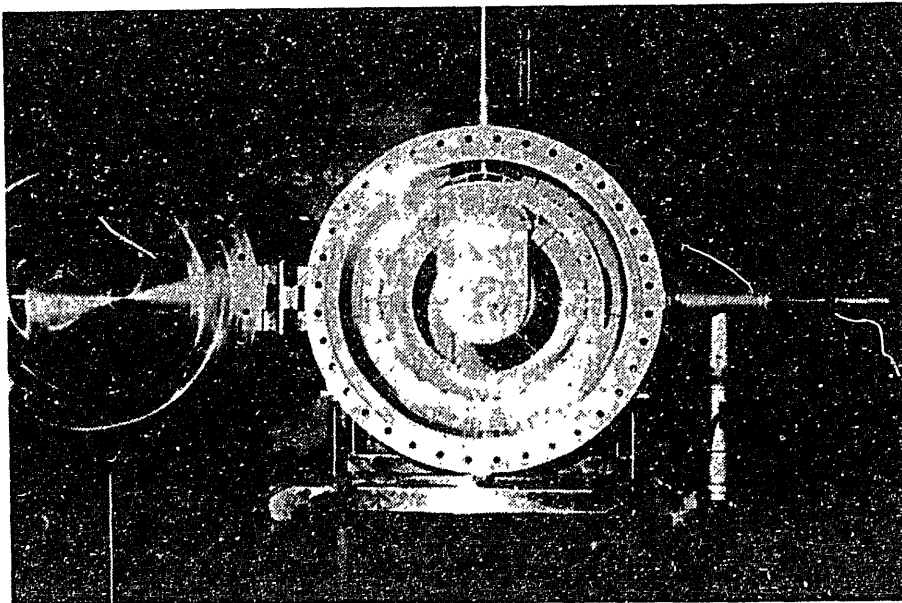
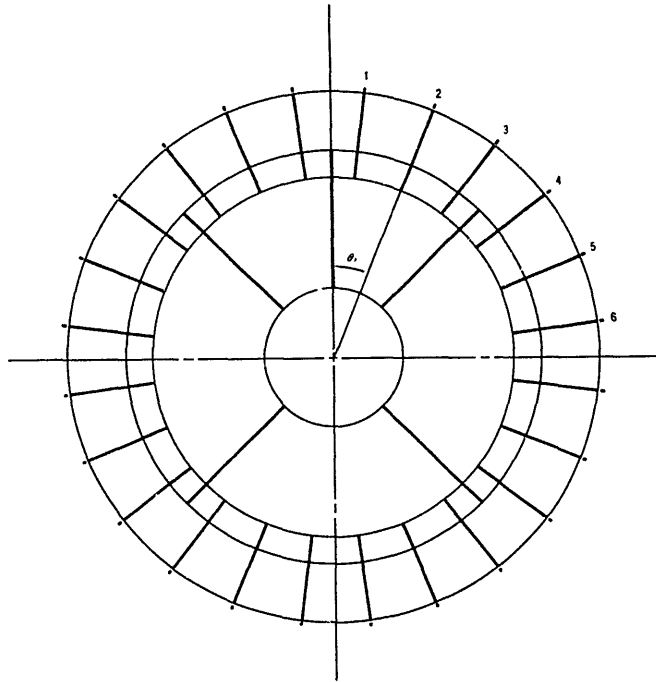
	23°C	-160°C
	kg / mm ²	kg / mm ²
引 張 強 度	63	54
圧 縮 強 度	49	53
曲 げ 強 度	85	84
曲 げ 弾 性 率	4900	5100

(小林木型製作所製 トレカコンポジット)

F.R.P. は繊維をエポキシ等の樹脂で固めてあるから、そのガス放出速度は樹脂のガス放出による。一般にエポキシ樹脂のガス放出速度は $10^{-6} \text{ Torr l/sec-cm}^2$ 程度と大きい。表面積が小さければあまり問題にならない場合もあるし、表面処理によっても放出速度を減少させることが可能である。又低温においては減少することも考えられる。我々は Cryo-NICE の設計開始当初スポーク材として F.R.P. の使用を計画したが以上の点について十分検討する余裕が無いために使用を断念し、ステンレスを使用することにした。F.R.P. の使用が可能であるならば、同一形状のもので比較した場合熱伝導はステンレスの $1/10$ におさえられる。スポークは短くしてクライオスタットの小型化と同時に十分に強度を持った懸下も可能である。ただし金属との収縮比が異なるので Cryo-NICE のように構造材として金属と併用する場合には注意が必要である。

6.2 スポークによる超伝導コイルの懸下

スポーク支持のための各フランジ及びスポーク支持方法についてはすでに3図に示した。全体のスポークの構成を14図に示す。液体窒素、ヘリウム溜の重量は各々約100kgであるから、真空槽からのスポークは200kgの荷重を懸下することになる。スポークは真空槽両端に2組あるから1組のスポークにかかる荷重は100kgである。



14図 懸下用スポークの構成

A. 真空槽から液体窒素溜の懸下

窒素溜をささえているスポークの本数は1組で24本である。このように本数を多くした理由は荷重を分散させて各スポークの荷重を小さくおさえるためである。溜をささえる役目をはたしているのは上半分のスポークだけであるが、今このスポークを均等に張って100kgの荷重をささえた場合の各スポークにかかる張力を求めてみる。各スポークと垂線がなす角を θ とし、スポークに上部から1から6までの番号をふるとスポークにかかる張力Fは

$$2F \sum_{i=1}^6 \cos \theta_i = 100 \text{ kg}$$

から $F = 13.1 \text{ kg}$ となる。したがって下部スポークも入れて全スポークを張った場合には、上部スポークには下部スポークに比べて13 kg 余計に張力が加わる。スポークが十分太ければ荷重による張力を無視し得る張力で均等にはることが出来る。スポーク径はなるべく太くしたいところであるが、スポークを通じて液体窒素溜への熱伝達が大きくなり液体窒素の蒸発が激しくなる。熱流入による液体窒素の蒸発量については次章にゆずるが、窒素溜への熱流入を10ワット程度におさえるためにスポーク径は $2.3 \text{ mm}\phi$ となった。

ステンレスの降伏点は表3に示されているように室温で 24 kg/mm^2 であるから $2.3 \text{ mm}\phi$ のスポークの降伏力は100kgである。窒素温度では 40 kg/mm^2 まで強度が増大するが、懸下作業は室温で行うから100kgが最大張力となる。 $2.3 \text{ mm}\phi$ のスポークの両端にネジ切りしてボルトで固定したのではネジ部の強度が低下する。したがって3図に示したようにスポーク両端の固定部は $5 \text{ mm}\phi$ のネジとなるよう、 $5 \text{ mm}\phi$ SUS-304 スタットから旋盤加工によって切り出した。スポークの細い部分の長さは液体窒素溜懸下用で77mm、ヘリウム溜懸下用で155mmである。旋盤加工時に入ったひずみ等でスポークが劣化している可能性もある。又、太い部分から急に細くなる形状をしている場合には、このタブ部分で強度の劣化がおりやすい。したがって計画通りの強度が保たれているかどうかを引張りテストを行って調べた。降伏点、引張り強度は各々 24 kg/mm^2 と 55 kg/mm^2 で劣化は認められなかった。

液体窒素溜を冷却してゆくと、溜およびスポーク固定用フランジは収縮する。スポークの両端をボルトで固定したままにすると、この収縮は全てスポークに張力としてかかる。13図に示された78Kにおけるステンレスの熱収縮比の値 2.8×10^{-3} を用いると、窒素溜フランジの半径は210mmであるから半径は0.59mm縮む。この収縮をスポークでささえようとする、300Kにおけるヤング率 $E = 21.1 \times 10^3 \text{ kg/mm}^2$ を用いても $F/S = (\Delta L/L) \times E = (0.59/77) \times 21 \times 10^3 = 160 \text{ kg/mm}^2$ となって、ステンレスの引張り強度を優に越えてスポークは切断されてしまう。

これを避けるために各スポークの一端に板バネをかませて上記の張力を緩和させた。非磁性のスプリング材として燐青銅、Cu-Be等について検討を行ったが、降伏力が小さく使用出来ない。ステンレス鋼にも硬化可能で降伏点の高い鋼材(SUS-630 H900°C, 耐力 120 kg/mm^2)が存在するようであるがその詳細について知ることが出来ずまた入手することも出来なかった。バネはコイル中心から約200mm程度離して設置しかつ小型のものですむので、鋼材にはK.S

鋼を使用した。肉厚 1 mm, 10 mm×25 mm の板を曲げて, 3 図に示したような三日月形をしたバネ定数 100 kg/mm , 最大荷重 200 kg の板バネを製作した。

実際の組み立ての際には真空槽 フランジと窒素溜 フランジ間の間隔よりわずかに短い治具を用意して, スポークの締め付けを調節しながら全周にわたってフランジ間隔が等しくなるように懸下を行った。したがって各スポークの張力は完全に均等にはならないが, 上記のようなバネを使用したことによって収縮による張力に対しては各バネは均等に沈み込むものと期待している。これを実測によって確認することはしていないが, Cryo-NICE の運転上支障をきたすようなことは現在まで起きていない。

B. 液体ヘリウム溜の固定

a. スポークによる懸下

ヘリウム溜の懸下に際しては, 窒素溜の場合に比較して熱流入をずっと小さく押えなければならぬ。その上, コイル近傍に磁気シールドを設置するので, コイルと磁気シールド間に働く引力にも耐え得る十分な強度で固定しなければならない。したがってヘリウム溜の固定には窒素溜とは異った困難がある。

金属の収縮比は 1 3 図に見られる通り, ごく低温ではほぼ一定となり 78 K と 4.2 K ではあまり変わらない。したがって窒素溜から非等方的な支持の仕方をしたとしても相対的な位置は冷却時においても変わらない。原理的には荷重に耐え得る最小限の径のスポークで吊り下げるだけでも, コイル中心の移動は無視出来る。ただしこのままでは振動してしまい, Cryo-NICE の溜が上に突き出た形状をしているために倒れてしまう。そこで, このような振動や倒れをある程度防ぐために, 14 図に示されているようにスポークは上部に 3 本, 下部に 2 本のスポークを用いほぼ等方的に張ることにした。

スポーク径は最上部のみが 3 mmφ で他は 2.3 mmφ である。スポークを通じての熱流入を抑えるためにスポークの本数は少なくしてある。上部 3 本のスポークにかかる, 荷重をささえるための張力は 30 kg と大きくなった。全スポークを 2.3 mmφ とした場合には, 耐力 100 kg に対してこの荷重のための張力 30 kg の割合が高く, 下部スポークを張った場合にあまり余裕がない。事実, 始めに最上部スポークにも 2.3 mmφ のものを使って組み立てたところ, しばらくしてコイル中心が下がってしまうことがあった。これは下部スポークを張りすぎて上部スポークの耐力を越えてしまったためにおこったことである。このようにスポークの耐力ぎりぎり懸下を行っているので, 安全を考えて最上部のみは 3 mmφ 耐力 175 kg のものを使用した。

その点上の材料の節で述べたように F.R.P. の使用が可能になれば, スポーク長を短くしてクライオスタットの小型化が可能ばかりでなく, スポークの本数を多くして十分な強度の懸下も可能になる。

液体窒素及びヘリウム溜をもし同時に冷却昇温が出来れば, 上にも述べた通りコイル中心

の窒素溜に対する相対位置の移動はない。したがって窒素溜懸下の時に使用したようなバネの使用は不必要である。しかし同時冷却も容易ではないし、特に同時昇温は熱絶縁が良いから不可能に近く、昇温時には窒素溜から温度は上昇する。このように両溜間に温度差が生ずると前に考察したのと同様に懸下用スポークの切断の可能性がある。そこで6図にすでに示されているように、窒素溜のときと同一の板バネを使用して収縮率のちがいによっておこるスポークへの負担を避けている。

b. 細いステンレス線を用いた補強

以上で一応はヘリウム溜の懸下は出来たが、このままではステンレスは曲げ、ねじれに弱いので軸方向の振動とか非対称型溜の横ゆれに対して不十分である。そこで窒素溜とヘリウム溜の空間に0.8 mmφのステンレス線を何本か張って補強を行った。横揺れに対しては、まずヘリウム溜頂部のくびを約1.5 mの線の中央で縛り、その線の両端をくびに近い方の窒素溜フランジに固定する。その際に線をボルトに巻きつけておくと、線はボルトの回転とともに引っ張られるからボルトの締めつけを調節すれば線の張り方を調節出来る。軸方向の振動防止には、まずコイルボビン両端で各4ヶ所づつ約1.2 mの線の1端を固定する。その線の他端を固定した箇所とは反対側の窒素溜フランジに固定する。この補強によって通常のクライオスタットとしては十分な強度をもって固定することが出来た。我々は作業のし易さを考えて0.8 mmφの線を使用した。十分な長さがとればこの補強用線材による熱伝達は無視出来るからもっと太いものも使用可能である。真空槽と窒素溜の間はスポークの本数も多く十分な強度を持っているので、我々は補強を行なわなかった。これと同様な方法で補強を行えばより強度のあるクライオスタットの製作が可能である。

c. ガラス棒によるコイル-磁気シールド間の補強

EBIS型イオン源では、磁場によってしぼられていた電子ビームはコイルを出た直後にコレクターに捕集される。コレクターでの捕集効率を良くするには、コレクター直前に磁気シールドを置いて磁場を発散させ、コレクター付近では磁場が存在しない状態が望ましい。Cryo-NICEでは磁気シールドは輻射シールド板に固定されている。

コイルと磁気シールドの間に働く引力はマクスウェルの応力によって求められる。強さHの様な磁場のある真空中におかれた磁性体に作用する引力は

$$T = 4.06 \times 10^{-8} S (H^2 - H'^2) \text{ (kg)}$$

で与えられる。ここでH, H'は共にガウス単位で、H'は磁性体が飽和してHと平行にもれている磁場の強さをあらわす。Cryo-NICEの最大磁場20 kGが発散せずにシールド板に吸収され、かつ飽和もしないとすると、 $S = 78.5 \text{ cm}^2$ であるとして $T = 1270 \text{ kg}$ に達する。このような大きな引力を、窒素溜とコイルボビン間に張った0.8 mmφのステンレス線4本でささえることは出来ない。いまちなみに、この引力を4本の線の径を太くしてささえようとすると線の径は、77 Kにおける降伏点の値 45 kg/mm^2 を用いて、 $\Phi = 2 \{1270 / (4 \times 45 \times \pi)\}^{1/2} = 3 \text{ mm}\phi$ となる。

一方このとき線は伸びるが、線の長さ 1000mmとし 300 K におけるヤング率 $21.1 \times 10^3 \text{ kg/mm}^2$ を用いて伸びを求めてみると $\Delta l = (l \cdot F) / (S \cdot E) = 1000 \times 45 / (21 \times 10^3) = 2.2 \text{ mm}$ となる。このように線も太くなって伝熱が無視出来なくなるし、コイルも移動する。

このように大きな力を材料の張力でささえることは問題が多い。Cryo-NICE では、輻射シールド板とヘリウム溜の間に直径 6mmφ のパイレックスガラス棒 2本を、コイル中心を通る鉛直線に対して対称な位置において、つかい棒にしこの引力をささえている。一般に材料の圧縮強度は大きいので、つかい棒方式は大きな応力に耐えることが出来るが、材料の長さはあまり大きく出来ないから熱伝導率の小さなものを選ばなければならない。その点ガラスは熱伝導率は非常に小さく、引張り、曲げ、ねじれの強度は小さいが、圧縮強度だけは 65 kg/mm^2 と大きい。6mmφ のガラスの両端が金属面にフラットにあたっており、かつコイルの移動方向と平行に設置されているとすると、2本のガラス棒の圧縮に対する耐力は $3.6 \times 10^3 \text{ kg}$ となる。

実際のガラス棒の固定方法については7図に示してある。銅製のボルトに 6mmφ の溝を切りこの溝にガラス棒を差し込んで、輻射シールド板の外からこのボルトをねじ込んで2本のガラス棒がほぼ均等な力でヘリウム溜外壁と接するようにする。後で取り出してみたところ、金属面との接触が完全にフラットでないために一部に細いヒビが入っていることがあったが、破壊されることもなく実用上は差支え無い。又棒の一端がボルトと密着しているために、ねじ込む際にねじれ応力がはたらいで割れることがあった。固定の際にこのようなねじれ力がかからないようにし、接触面をさらにフラットにする等の工夫をすれば、ほぼ所定通りの強度を発揮すると思われる。

ガラスは熱絶縁性はよいが機械的強度が小さいために、クライオスタットの構造材としてはあまり使用されない。しかし上述のように常に圧縮力のみが加わるように工夫すれば、その効用は大きいように思われる。ただし上記のような2つの構造物の間に入っている場合には冷却手順に注意をしなければならない。Cryo-NICE の場合には、内部構造物のヘリウム溜から先に冷却することが必要である。窒素溜から先に冷却すると窒素溜の収縮がこのガラスに加わり破壊の可能性がある。

以上のようにスポークを使用することによってコイル中心を固定させ、比較的強度もある水平設置型クライオスタットの製作が終了した。現在 Cryo-NICE の運転上支障になるような構造上の問題は起っていない。しかし当初の目標であった、冷却によるコイル中心の移動を 0.1 mm 以内におさえるという課題を本当に達成出来たかどうかについては、今のところ不明である。そのようなチェックをする余裕もないまま実用運転に突入してしまった。ただ運転開始後約半年経過した時点で点検したところでは、最初に設定した位置からのコイル中心の移動は認められなかった。

7. 寒剤の消費量

超伝導コイルを運転する際の寒剤の消費は2つに大別される。第1は、液体窒素及びヘリウム各溜に液を充填する時に、まず高温の溜を各液体温度まで予冷が必要である。その際に大型の装置であるとかかなり多量の寒剤を消費する。第2は、寒剤の充填終了後外部からの熱流入による蒸発である。前者の予冷に要する寒剤の消費は運転には直接役立たない損失であるから、熱流入を減らす努力は当然として、予冷効果の向上についても注意を払わなければならない。

7.1 寒剤の性質

一般に良く利用される寒剤としては、液体ヘリウム、水素、窒素、酸素などがある。これ等の寒剤のクライオスタット製作上必要と思われる性質を表5に示す。材料の冷却にとって重要な値は蒸発熱である。しかし蒸発したガスが材料と熱交換するような場合には、冷却能力としては蒸発熱とガスのエンタルピーによって決まる。各温度のガスのエンタルピーを表の下部に示してある。容積比は1ℓの液が気化して300 K, 1気圧のガスになったときの容積をあらわす。

表 5 各種寒剤の性質

液 体	He ⁴	H ₂	N ₂	O ₂
分 子 量	4.003	2.016	28.016	32.0
沸 点 (K)	4.2	20.39	77.35	90.0
沸点における液の比重 (kg/ℓ)	0.125	0.071	0.808	1.14
蒸 発 熱 (kcal/kg)	4.54	106	46.3	51.2
液体1ℓあたりの蒸発熱 (kcal/ℓ)	0.62	7.5	37.4	58.3
熱流入による蒸発量 (ℓ/W·h)	1.4	0.115	0.0230	0.0148
容 積 比 (300 K)	480	860	880	880
1気圧のガスのエンタルピー 4 K	7			
(kcal/kg) 20	28	170		
77	98	310	45	
300	376	1010	104	

1 kW = 0.239 kcal/sec

7.2 予冷による寒剤の消費

温度 T_2 の固体を温度 T_1 まで冷却するのに必要な熱量はエンタルピーの差

$$Q = \int_0^{T_2} C(T) dT - \int_0^{T_1} C(T) dT$$

である。mol 当りの比熱 C はデバイの式によってよく知られているように、デバイ温度 Θ に比べて十分高温では一定値 $3R$ に近づく。一方十分低温では

$$C \doteq 234 R (T/\Theta)^3 \quad T \ll \Theta$$

となる。 Θ は代表的な金属では数百 K であるから数十 K の温度領域では比熱は T^3 に比例する。したがってエンタルピーは T^4 に比例して温度が下がると共に急激に減少する。表 6 に種々の固体のエンタルピーの値を示す。

表 6 固体のエンタルピー

物質	エンタルピー [joule/g]								
	4 K	10 K	20 K	50 K	100 K	160 K	200 K	260 K	300 K
アルミニウム	$4.68 \cdot 10^{-4}$	$4.9 \cdot 10^{-3}$	$4.8 \cdot 10^{-2}$	1.85	17.76	54.4	84.8	135.0	170.4
銅	$1.3 \cdot 10^{-4}$	$2.4 \cdot 10^{-3}$	$3.4 \cdot 10^{-2}$	1.40	10.6	28.5	42.4	64.4	79.6
ニッケル	$9.8 \cdot 10^{-4}$	$7.1 \cdot 10^{-3}$	$4.1 \cdot 10^{-2}$	$9.3 \cdot 10^{-1}$	8.68	26.28	40.82	65.0	82.4
グラファイト	$1.68 \cdot 10^{-4}$	$3.3 \cdot 10^{-3}$	$3.8 \cdot 10^{-2}$	$7.0 \cdot 10^{-1}$	5.10	1.08	32.2	62.5	88.7
モネル	$9.0 \cdot 10^{-4}$		$4.6 \cdot 10^{-2}$	1.11	9.3		41.3		81.5
ウッドメタル	$5.16 \cdot 10^{-4}$		$3.31 \cdot 10^{-1}$						
黒鉛	$1.68 \cdot 10^{-4}$		$3.8 \cdot 10^{-2}$	$7.0 \cdot 10^{-1}$	5.10		32.2		88.7
パイレックス ガラス	$2.01 \cdot 10^{-4}$		$1.54 \cdot 10^{-1}$						
アラルダイト	$2.10 \cdot 10^{-3}$		$6.23 \cdot 10^{-1}$						
テフロン	$3.10 \cdot 10^{-3}$		$5.2 \cdot 10^{-1}$	4.88	19.51		75.9		

cal/g にするには 0.2390 を乗ずる。

真空技術講座 6 「真空技術常用諸表」(日本工業新聞社刊)

通常、超伝導コイルの予冷の手順は次のように行う。まず液体ヘリウム溜に液体窒素を満たして、コイル及び溜を 77 K まで冷却する。その後、液体窒素を追い出してから、ロータリーポンプで溜内を窒素の三重点 93.9 Torr 近くまで減圧し残った液を気化させて排気する。このようにすると、単に液体窒素の追い出しが完全に出来るばかりでなく、溜の温度を三重点温度 63.15 K まで下げることが出来る。その後液体ヘリウムの移送を行って 4.2 K まで冷却する。このような液体ヘリウムによる冷却を行う以前の処理によって材料のエンタルピーは大巾に減少し予冷に必要な液体ヘリウムの量をずっと少なくすることが出来る。ちなみに 77 K の銅のエンタルピーは約 1.8 cal/g であるが 63 K まで冷却すると約 0.9 cal/g と半減する。特に大型マグネットになればなるほど予冷に要する液体ヘリウムの量が増大するからこの予備冷却の効果は大きい。事実大型マグネットでは小型ヘリウム冷凍機を用いて 20 K 程度まで冷却した後、液体ヘリウムを充填する方法がとられている。銅の 20 K におけるエンタルピーは 8×10^{-3} cal/g に減少するから、わずかな量の液体ヘリウムで 4.2 K まで冷却出来、ただちに液は溜り始める。

一方寒剤の冷却能力は液の蒸発熱と蒸発したガスのエンタルピーによって決まる。ちなみにヘリウムの場合、1ℓの液の蒸発熱は表5に示したように0.62 kcal と非常に小さいが、それから蒸発したガスが完全に熱交換して300 Kまでなったとすると $(376 - 7) \times 0.125 = 46$ kcal もの熱量を吸収する。したがって蒸気のエンタルピーを上手に利用出来るかどうかによっても予冷に要する寒剤の消費量は大きく異ってくる。表7に材料の初期温度300 Kと77 Kの1kgの金属を蒸発熱だけで冷却した場合とガスのエンタルピーを利用して冷却した場合に要する寒剤の量を示す。

表7 材料の冷却に必要な寒剤の量

寒 剤		(ℓ/kg)		
		He ⁴		N ₂
材料の初期温度 K		300	77	300
蒸発熱のみ による冷却	アルミ	18	3.2	1.01
	ステンレス	9.2	1.4	0.53
	銅	8.6	2.2	0.46
ガスのエンタル ピーを利用した 場合	アルミ	1.6	0.22	0.64
	ステンレス	0.79	0.11	0.33
	銅	0.79	0.15	0.29

Jacobs, J.B. Advances in Cryogenic Engineering 18, 529 (1963)

BOC "Cryogenic Data Chart"

Cryo-NICE の場合コイルと液体ヘリウム溜の重量は約100 kgであるから、蒸気による冷却がほとんど出来なかったとすると77 Kから4.2 Kまでの予冷に140ℓの液体ヘリウムが必要になる。一方蒸気の熱交換が十分よくおこなわれるとすると11ℓですむ。この差はあまりにも大きいですが、設計の良し悪しによって予冷による消費量は大きく異なる。Cryo-NICEは横長コイルであるので2図のコイル組立図に示された、液移送パイプ受けから液は2本のパイプに分けられてコイル下部で2ヶ所からふき出す。実際に予冷に要する液体ヘリウムの量は15ℓ弱である。一般的にはコイル・溜全重量の1/3～1/2程度の量を予冷で消費するとのことであるから、Cryo-NICEの結果は非常によい結果であると思われる。

液体窒素の場合には、蒸発熱が37 kcal/ℓと大きいので蒸気による冷却が不十分な場合でも十分な場合との消費量の差はあまり大きくない。したがってヘリウムの場合とちがって、よほどのことがない限り予想値とそう異なることはない。

7.3 熱流入による寒剤の消費

寒剤への熱流入の原因としては次のようなことが考えられる。

- (1) 真空空間の残留ガスによる熱伝導
- (2) 真空空間を通しての輻射による熱流入
- (3) クライオスタット構造材を通しての熱伝導
- (4) ヘリウム溜くび及びくび内の液移送パイプ、液面計、電流リード等による熱伝導
- (5) くび上部室温部分からの輻射

このうち(1)は通常のクライオスタットでは無視出来る。(4)、(5)についてはこの部分を蒸発した低温のガスが流れているために熱の流入量を求めることはそう容易ではない。この問題については後にゆずり、まずスポークのような直接高温部分と接している構造材を通しての熱伝導と輻射による伝熱について述べる。

いま均一な断面積(A)をもつ長さℓの固体の両端の温度が T_1, T_2 であるとする、熱の流れる速さは

$$Q = \frac{A}{\ell} \left[\int_0^{T_2} \kappa dT - \int_0^{T_1} \kappa dT \right]$$

であらわされる。ここで κ は12図に示した熱伝導率で、その積分値は種々の固体について求められている。2,3の例について表8に示す。

表8 熱伝導率の積分値 $\int_0^T \kappa(T) dT$ watt/cm

温度 K	銅 (電解)	アルミ 99%	ステンレス	ガラス $\times 10^{-3}$	テフロン
6	8.0	0.176	0.0063	2.11	1.13
10	33	6.07	0.0293	6.81	4.4
20	140	27.6	0.163	20.0	16.4
76	686	220	3.17	175	130
100	802	284	5.28	292	187
200	1220	508	16.6	1030	442
300	1620	728	30.6	1990	702

輻射による熱流入についてはステファン・ボルツマンの式

$$Q = 5.67 \times 10^{-12} \bar{\epsilon} A (T_2^4 - T_1^4)$$

によって求められる。 $\bar{\epsilon}$ は2つの面の平均放射率でそれぞれの面の放射率を ϵ_1, ϵ_2 とし面積を A_1, A_2 とすると同軸円筒の場合

$$\bar{\epsilon} = \frac{\epsilon_1 \epsilon_2}{\epsilon_2 + A_1/A_2 (1 - \epsilon_2) \epsilon_1}$$

である。いくつかの材料の放射率の値を表9に示す。

表 9 材 料 の 放 射 率

	Surface temp K			
	4	28	77	300
Copper	0.0050		0.008	0.018
Silver	0.0044		0.008	0.02
Aluminum	0.011		0.018	0.03
Stainless steel 18-8			0.048	0.08
Silver plate on Copper		0.013	0.017	

Appl. Cryogenic Eng. p 154 (Vance and Duke)

BOC 社 “Cryogenic Data Sheet” より

A. 液体窒素溜への熱流入

スポークを通じた熱流入は、スポークの断面積が 0.0415 cm^2 、長さが 5.5 cm で本数が 48 本であるから $(0.0415/5.5)(30.6 - 3.17) \times 48 \div 10$ ワットとなる。輻射による熱流入は全てステンレス製と仮定すると 22 ワットである。この他に電子銃が輻射シールド板に固定されているので、フィラメントの発熱は全て液体窒素に吸収される発熱量は約 15 ワットである。したがって全部で 37 ワットの熱が窒素溜に流入する。この熱流入による液体窒素の蒸発量は表 5 の値を用いて 0.85 l/h と予想される。ところが実際には 2 l/h の窒素が蒸発してしまった。この原因についてははっきりした根拠は無かったが、輻射による熱流入が予想以上に大きいのではないかと考え、真空槽と窒素溜の空間に厚さ 80μ のアルミシートを両者にふれないように張って窒素溜を覆った。その結果、液体窒素充填直後は前と同様に蒸発は早いのが約 10 時間後には蒸発は減少してほぼ当初の予定に近い値におさまった。このことは、アルミシートからの輻射放出は窒素溜によって吸収されるために温度が下り、真空槽からの輻射吸収とつり合う温度

$$\bar{\epsilon}A(T^4 - 77^4) = \bar{\epsilon}'A'(300^4 - T^4)$$

におちつくためと考えられる。簡単のために $\bar{\epsilon}A = \bar{\epsilon}'A'$ とすると $2T^4 \div 300^4$ で $T \div 250 \text{ K}$ となる。このように輻射による伝熱が予想より大きく上まわった原因は、はっきりしない。窒素溜表面はバフ仕上げを施した。ステンレス表面には細かい穴が無数にあいておりバフ仕上げを行うとバフの膠質が研磨面に埋めこまれ、かなり入念な酸洗いによっても取りのぞけないといわれている。我々は表面を有機溶剤で洗浄しただけであるので、そのような表面処理によって悪い結果になったとも考えられるが、いずれにしても原因ははっきりしない。

B. 液体ヘリウム溜への熱流入

はじめにスポーク及びガラス棒からの熱流入を求めてみる。スポーク長は 15.5 cm で直径 3 mmφ のものが 2 本, 2.3 mmφ のものが 8 本使用されている。3 mmφ, 2.3 mmφ のスポーク各 1 本による伝熱は各々 1.4×10^{-2} , 8.5×10^{-3} ワットであるから全体で約 0.1 ワットである。熱流入による液体ヘリウムの蒸発量 1.4 l/W.h を用いるとスポークを通しての伝熱による蒸発量は 0.14 l/h となる。ガラス棒は 6 mmφ, 長さ 3.5 cm でボビン両端に各 2 本ずつ計 4 本使用している。1 本あたりの熱流入は 1.4×10^{-2} ワットで計 5.6×10^{-2} ワットであるから、これによる蒸発量は 80 cc/h となる。

輻射による熱流入を見積ろうとすると 4 K におけるステンレスの放射率が必要であるが表 9 には 4 K の値が欠けている。しかし結果にはあまり影響はないので 4 K についても 77 K の値を用いることにする。ヘリウム溜の表面積は $9.2 \times 10^3 \text{ cm}^2$, 輻射シールドの表面積は $1.5 \times 10^4 \text{ cm}^2$ である。輻射シールドはやはり全部ステンレス製であると仮定すると熱流入は 5.4×10^{-2} ワットであり、それによる蒸発量は 80 cc/h である。

くびを通しての熱流入量を見積ることは、先にも述べたようにそう容易ではない。くび内にはコイル励磁用電流リード、液面計等が納められている。これ等は直接室温部分と接しているから、蒸気による冷却効果を見積ると伝熱を見積ると大変大きな値となる。特にリード線からの熱流入は、銅の熱伝導率が大いから、たとえ 2 mmφ のリード線であっても 1 ワットを越えてしまう。又 15 mmφ 肉厚 0.5 mm^t の液移送パイプで 0.14 ワットとなる。しかし蒸発した低温ガスが流れているので、くび部の材料を通しての熱伝導はずっと小さくなる。

通常の金属製クライオスタットでは、経験的に液体ヘリウム蒸発量は 0.5 l/h ~ 1 l/h である。したがって我々はこの値にスポーク、ガラスによる伝熱と輻射伝熱による蒸発量約 300 cc/h を加算して、Cryo-NICE の蒸発量はいまうまくいって 1 l/h 弱、悪くて 1.3 l/h と見積っていた。実際に Cryo-NICE を運転してみたところ蒸発量は約 1.4 l/h となり、悪い方の見積りを多少越えてしまった。ヘリウム溜の有効体積は 23 l であるから 24 時間近い連続運転を見込んでいたが、実際には 16 時間程度に減少してしまった。ただ幸いにも Cryo-NICE を使用しての実験は連続運転が不可欠な条件ではないし、かつ 16 時間の運転時間は 1 日の実験時間としても十分であるので特に改良もせずに現在は使用している。

このように液体ヘリウムの消費量が、当初我々が楽観的に考えていた見積りをこえてしまった原因についていくつかのことが考えられる。第 1 に液体窒素の蒸発のところでも述べたように窒素溜の表面処理が不十分であったために輻射伝熱が見積りよりも大きい可能性がある。ただしこの点については判断が難しい。第 2 は最も可能性が高いと思われるが、くび部の構造があまりよくないために熱伝導が大いことが考えられる。事実、くび上部の室温部からの輻射シールド 1 つをとっても一般には細心の注意を払って製作するのに対して、我々は固定方式に注意が集中して十分な対策を講ずることが出来なかった。通常液移送パイプは液体ヘリウ

ム充填後引き抜いて熱流入を減らしている。又電流リードについても、途中でスイッチを入れて永久電流方式に切り換えた後に切り離す方法にすると液体ヘリウムの蒸発量はずっと少なくすることが出来る。我々の場合液移送パイプも多少工作精度が悪かったために引き抜くことが出来ず、固定したままで使用している。Cryo-NICE を用いた衝突実験に追われてこれ等の点について改良を行う余裕が無かったが、今後改良が行えれば液体ヘリウム蒸発量はまだ減少させることが可能ではないかと考えている。したがってこの点に関しても不十分ながらも我々の技術レベルからすればほぼ満足すべき結果ではないかと思われる。

8. お わ り に

この報文は、新しい技術の報告というよりも、ズブの素人がまがりなりにも使用可能な超伝導コイル及び超高真空クライオスタットを製作することが出来たという苦労話のようなものである。我々は超伝導コイルの実情については十分な知識を持っていないために、まずまずの結果だと考えているが、専門家の目からすればひどい誤解や思い過しがあるかもしれない。

Cryo-NICE の設計にあたっては共立出版の実験物理学講座の「低温」及び「磁気」中の“超伝導マグネット”が大変役に立ったが、この報文を書くにあたっても参考にさせていただいた。

Cryo-NICE のコイル及び液体ヘリウム溜を除く工作は全て京和真空機械製作所で行った。我々のめんどろな要求に心よく応じていただいた高松氏に感謝します。超伝導コイル及びクライオスタットの製作に関し全く無知であった我々の質問に対して心よく応じていただき、かつ各種資料も提供していただいた真空冶金K.Kの高野氏、野口氏に感謝します。又、種々の助言をいただいた都立大学理学部物理学科の久米、米満研究室の諸氏に感謝します。スポークの強度テストをしていただいた都立大学工学部機械学科の三沢氏に感謝します。コイルボビン用SUS-310 S 鍛造品の提供に御尽力いただいた山陽特殊鋼K.Kの森弘氏に謝意を表します。

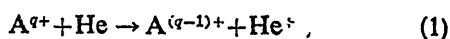
多価イオンの一電子捕獲断面積の 価数依存性に見られる振動

阪大理 木村正広

§1. はじめに

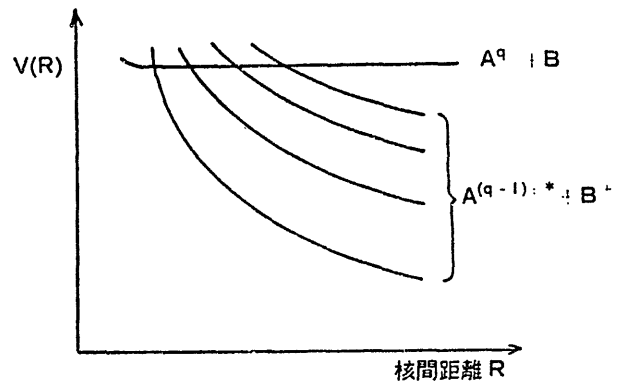
高電離イオンと中性原子・分子との衝突による電荷移行過程の研究には、最近特に強い関心が寄せられている。この方面の情報は核融合プラズマのエネルギー損失や中性粒子打込みによる加熱、ビームプローブ計測法と関連して高温プラズマの挙動を探る上で欠くことができない。¹⁾ 多価イオンが電子を捕獲した結果、反転分布が生じればX線レーザーへの発展も考えられる。²⁾ 星の大気や星間空間では水素やヘリウムとの衝突による電荷移行が多価イオンの平均電荷数を下げる働きもする。³⁾

以上のような応用面からの要請が強くなったことと、定常的に低エネルギーの多価イオンを引き出せるイオン源が開発されたことから多価イオン-中性原子の衝突研究は理論・実験とも1975年以降、活発に行われるようになった。^{4,5)} 名古屋大学プラズマ研究所では1977年、客員研究としてNICE (Naked Ion Collision Experimentの略) 計画が発足し、その間、多価イオン源として電子ビームイオン源 (EBIS: electron beam ion source) を建設し、いくつかの原子衝突実験を行ってきた。⁶⁾ その中に、低速度の多価イオンがヘリウム原子に衝突して一つの電子を捕獲する過程、



の断面積が q の変化に伴い激しく振動する現象がある。本稿ではこの現象を紹介し、その原因について考察する。

ここでいう低速度衝突とは、入射イオンの速度が捕獲される電子の原子内軌道速度より遅い衝突をいう。低速度の衝突では、入射イオンと標的原子とによって形成される準分子のモデルで衝突過程の議論ができる。多価イオン A^{q+} が中性原子 B に接近すると、核間距離 R に応じてそのエネルギー準位は連続的に変化してポテンシャル・エネルギー曲線を形成する。 $A^{(q-1)+}$ の基底状態およびいくつかの励起状態のイオン化エネルギーは B のイオン化エネルギーより高いのがふつうである。このため第1図に示すように、相対運動のエネルギーを除けば R の大きい位置では $A^{(q-1)+} + B^+$ の方が $A^{q+} + B$ よりエネルギーが低い。しかし、 A^{q+} と B



第1図 $A^{q+} + B \rightarrow A^{(q-1)+} + B^+$ 衝突系の透熱(diabatic)ポテンシャル曲線。

が近づくときはかなり接近するまでこの系のポテンシャル・エネルギーは大きくは変わらないのに対し、 $A^{(q-1)+}$ と B^+ が近づくときはクーロン斥力が働いてエネルギーはどんどん上がる。このために(1)式の左辺と右辺のそれぞれのポテンシャル曲線は核間距離が比較的大きい位置で交差する可能性が大きい。これらの交差点を経て電子の移行が起きると考えれば、一つの始状態から多数の終状態へのチャンネルが開けていることになる。価数 q が大きいほどこのチャンネル数は増えるので断面積はほとんど速度依存性をもたなくなり、一電子捕獲過程をモデル的に取扱うことが可能となる。標的が水素原子の場合の一電子捕獲に対して、種々のモデルが提案された。それらによると一電子捕獲過程の断面積 $\sigma_{q,q-1}$ は q^α に比例して単調に増加する。 α はモデルによって多少異なり、1~2の間の値をとる。⁴⁾

しかしこれらのスケーリング則は価数 q の大きい場合に妥当な近似であり、価数の小さい場合には疑問を残す。事実、1979~1980年に行われたCrandallらオークリッジ・グループのB, C, N, Oの多価イオンとHとの衝突実験では、 $\sigma_{q,q-1}$ は必ずしも q と共に単調には増加せず、イオン種によってさまざまな値を示した。⁷⁾ その後、Blimanらグルノーブル・グループも、C, N, O, Arの多価イオンと D_2 との衝突でスケーリング則からのずれを指摘している。⁸⁾ 簡単なスケーリング則が成立しないことをもっとも系統的にそして明確に示したのはNICEグループの実験である。

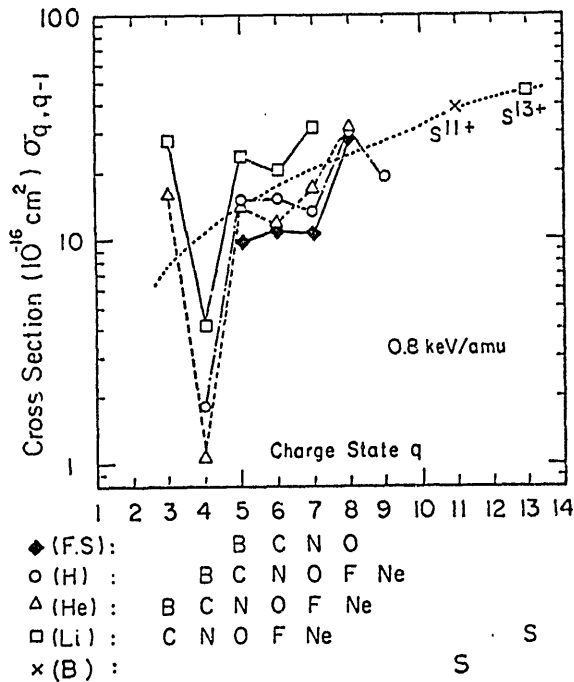
§2. NICEでの実験と古典的一電子モデル

多価イオン源として採用したEBIS型イオン源⁹⁾は、従来、核加速器用に開発されてきたものであるが、最近は原子衝突実験にも使われるようになった。NICE

では, B, C, N, O 等の裸イオン—電子が完全にはぎとられたイオン—をはじめとする多価イオンを定常的に引き出せて衝突実験に用いることができる。

次に He を標的原子とした一電子捕獲過程(1)の断面積の測定結果を示そう.¹⁰⁾ 多価イオン A^{q+} としては, 裸イオン ($B^{5+}, C^{6+}, N^{7+}, O^{8+}$), H 様イオン ($B^{4+}, C^{5+}, N^{6+}, O^{7+}, F^{8+}, Ne^{9+}$), He 様イオン ($B^{3+}, C^{4+}, N^{5+}, O^{6+}, F^{7+}, Ne^{8+}$), Li 様イオン ($C^{3+}, N^{4+}, O^{5+}, F^{6+}, Ne^{7+}, S^{13+}$) の i -等電子系列のイオンを網羅している。衝突エネルギー範囲は $1.5q-3.0q$ keV と狭いが, この範囲では大部分の断面積はエネルギーに依存しない。衝突エネルギーが 0.8 keV/amu の場合の一電子捕獲断面積を価数の関数として第2図に示す。折れ線は各等電子系列を結んである。これを見ると, $q=3, 5$ に当る断面積が $q=4$ のそれより一桁近く大きいなど, 明らかに実験誤差 ($\pm 30\%$) を上まわる断面積の振動構造がすべての等電子系列のイオンについて読み取れる。特に小さい q で振動が著しく, q が大きくなると共に振動は減衰して, Müller-Salzborn が実験的に出したスケーリング則¹¹⁾ (図の点線) に近づく。

一般に, 低速度での電荷移行の理論的取扱いは, <歪んだ固有関数で展開する方法 (PSS 法)> がもっとも正統的な方法とされている。しかし, 今の場合, B^{3+} ,



第2図 一電子捕獲断面積の価数依存性 (T. Iwai, et al.: Phys. Rev. A 26 (1982) 105 より転載)。

$C^{4+}+He$ 系についての Shipsey らの計算しかない。¹²⁾ 一方, 龍福・佐々木・渡部による <ユニタリー化された歪曲波近似 (UDWA) 法> は, 広いエネルギー領域において適用できることが特徴で, 標的原子が H の場合についての実験結果をかなりよく説明している。^{13, 14)} しかも低速度では, UDWA 法は <ポテンシャル曲線の交差にもとづく古典的一電子モデル> の計算と等価であることも彼らによって指摘された。¹⁴⁾ 彼らは標的原子が H 原子の場合を扱っているが, ここではこれを He におきかえた古典的一電子モデルによって, 観測した振動構造の説明を試みる。

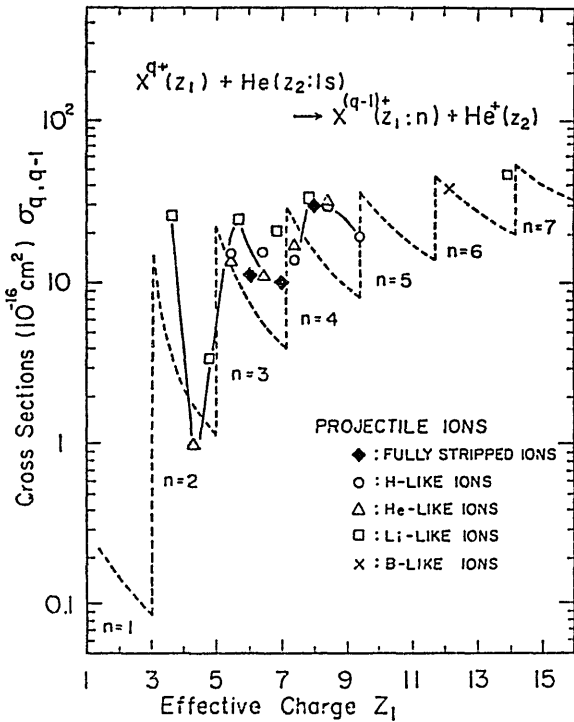
いろいろな衝突系を統一的に取り扱うために, $A^{(q-1)+}$ と He はそれぞれ有効核電荷 Z_1 と Z_2 の水素型のエネルギー準位をもつものと仮定する。したがってエネルギー準位はそれぞれ主量子数 n_1, n_2 を用いて $-Z_1^2/2n_1^2, -Z_2^2/2n_2^2$ と表わされる。こうすれば有効核電荷 Z_1, Z_2 はそれぞれ $A^{(q-1)+}, He$ のイオン化エネルギーから定まる。さて, A^{q+} と He とが近づいてきて, 核間距離 R で電荷の移行が起きると考えよう。移行する電子は, 始状態では He の基底状態にあり, A^{q+} からのクーロンポテンシャル $-Z_1/R$ の摂動を受ける。一方, 終状態では電子は $A^{(q-1)+}$ の励起状態 ($-Z_1^2/2n_1^2$) に移り, そのとき He⁺ から $-Z_2/R$ の摂動を受ける。このような摂動を受けた両状態のエネルギー準位が一致するという, いわゆる共鳴条件,

$$-Z_1/R - Z_2^2/2 = -Z_2/R - Z_1^2/2n_1^2, \quad (2)$$

が成立する R で電子が He から A^{q+} に移行すると考える。このときの R は第1図に示したポテンシャル曲線の交点の位置を与えることになる。しかし移行する電子には A^{q+} と He との間にポテンシャル障壁があり, R の減少と共にその高さも減少する。電子の移行が可能のためには始状態のエネルギー (上式の左辺) がこの障壁を越えるに十分なだけ両粒子が接近しなければならない。上の二つの条件を最初に満足する核間距離を R_n として, 電子移行の確率を $1/2$ とすれば,

$$\sigma_{q,q-1} = \frac{1}{2} \pi R_n^2 \quad (3)$$

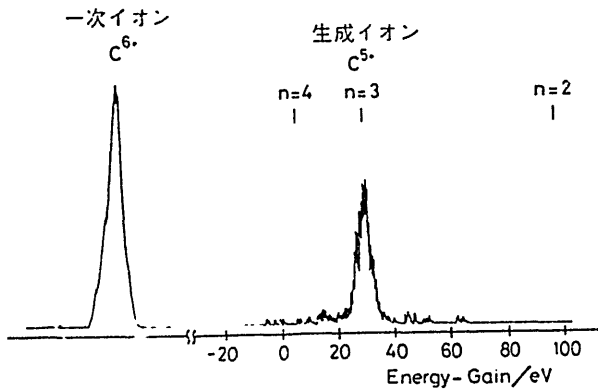
で電子捕獲断面積が与えられる。この式で計算した断面積を有効電荷 Z_1 の関数として示したのが第3図の破線である。 n ($\equiv n_1$) の値が1だけ増すごとに断面積は非連続的にジャンプする。また同図には実験データも整理しなおしてプロットしてある。両者の一致は必



第3図 有効核電荷の関数としての一電子捕獲断面積 (T. Iwai, et al.: Phys. Rev. A 26 (1982) 105 より転載)。

ずしもよくないが、古典的一電子モデルが非常に大胆な近似をしていることからみてやむをえない。しかし、このモデルは観測された、断面積の特徴的な振動構造の本質をついているように思われる。

低Zイオンではnの小さな準位へ電子が捕獲される。そこでは準位の間隔が大きいのでnの値が1だけ増えても断面積は大きく変化する。一方、高Zイオンでは大きなnに捕獲されるが、そこでは準位が密に分布しているためにnの変化による断面積の変化も小さい。



第4図 $C^0 + He \rightarrow C^{6+}(n) + He^+$ のエネルギー利得スペクトル。

これが高Zイオンで断面積の振動が減衰する原因である。

特定の準位nに選択的に電子が捕獲されるという考えは、古典モデルの重要な予測であるがはたしてそうであろうか。これを確かめる実験をNICEグループが目下行っている。電子を捕獲したイオンのエネルギー損失(または利得)スペクトルを観測し、これを解析することによりイオンのn分布が求まる。C^{4,5,6+}, O^{5,6,7,8+} イオンで調べた結果では、C⁴⁺ はn=2, O^{7,8+} はn=4, 残りはすべてn=3というように、特定のnに選択的に電子の移行が起きることが分った。

これらのn値は一電子モデルでの予測と一致する。その一例を第4図に示す。すなわち低エネルギーのA^{q+}+He衝突の一電子移行では、古典的一電子モデルがかなり良い指針となることが確かめられたといえよう。

さらに高いZのイオンについては、古典モデルの予測とちがって二つ以上の準位に電子が捕獲される可能性も無視できなくなるだろう。これは今後の興味深い課題である。

文 献

- 1) M.P.C. McDowell, ed.: *Atomic and Molecular Processes in Controlled Thermonuclear Fusion* (Plenum Press, 1979).
- 2) A. V. Vinogradov and I. I. Sobel'man: *Sov. Phys.-JETP* 36 (1973) 1115.
- 3) G. Steigman: *Astrophys. J.* 199 (1975) 642.
- 4) 理論的研究のレビューとしては; 松沢通生: JAERI-M8676 (日本原子力研究所, 茨城, 1980); R. E. Olson: *Electronic and Atomic Collisions*, ed. N. Oda and K. Takayanagi (North-Holland, Amsterdam, 1980) p. 391.
- 5) 実験的研究のレビューとしては; E. Salzborn and A. Müller: *Electronic and Atomic Collisions* ed. N. Oda and K. Takayanagi (North-Holland, Amsterdam, 1980) p. 407.
実験データ集としては; K. Okuno: IPPJ-AM-9, -10, -11 (名古屋大学プラズマ研究所, 1978); Y. Kaneko, T. Arikawa, Y. Itikawa, T. Iwai, T. Kato, M. Matsuzawa, Y. Nakai, K. Okuno, H. Ryufuku, H. Tawara and T. Watanabe: IPPJ-AM-15(同, 1980); Y. Kaneko, Y. Itikawa, T. Iwai, T. Kato, Y. Nakai, K. Okuno and H. Tawara: IPPJ-AM-20 (同, 1981).
- 6) H. Imamura, Y. Kaneko, T. Iwai, S. Ohtani, K. Okuno, N. Kobayashi, S. Tsurubuchi, M. Kimura and H. Tawara. *Nucl. Instrum. & Methods* 188 (1981) 233; 小林信夫, 大谷俊介,

- 金子洋三郎, 岩井鶴二, 奥野和彦, 鶴淵誠二, 木村正広, 俵博之, 日野利彦: IPPJ-DT-84 (名古屋大学プラズマ研究所, 1981); Y. Kaneko, T. Iwai, S. Ohtani, K. Okuno, N. Kobayashi, S. Tsurubuchi, M. Kimura and H. Tawara: *J. Phys. B* **14** (1981) 881.
- 7) D.H. Crandall, R.A. Phaneuf and F.W. Meyer: *Phys. Rev. A* **19** (1979) 504, **22** (1980) 379; L.D. Gardner, J.E. Bayfield, P.M. Koch, I.A. Sellin, D. J. Pegg, R. S. Peterson and D. H. Crandall: *Phys. Rev. A* **21** (1980) 1397.
- 8) S. Bliman, J. Aubert, R. Geller, B. Jacquot and D. van Houtte: *Phys. Rev. A* **23** (1981) 1703.
- 9) E.D. Donets: *IEEE Trans. NS-23* (1976) 897.
- 10) T. Iwai, Y. Kaneko, M. Kimura, N. Kobayashi, S. Ohtani, K. Okuno, S. Takagi, H. Tawara and S. Tsurubuchi: *Phys. Rev. A* **26** (1982) 105.
- 11) A. Müller and E. Salzborn: *Phys. Lett* **62A** (1977) 391.
- 12) E. J. Shipsey, J. C. Browne and R. E. Olson: *Phys. Rev. A* **15** (1977) 2166.
- 13) H. Ryufuku and T. Watanabe: *Phys. Rev. A* **18** (1978) 2005, **19** (1979) 1538, **20** (1979) 1828.
- 14) H. Ryufuku, K. Sasaki and T. Watanabe: *Phys. Rev. A* **21** (1980) 745.

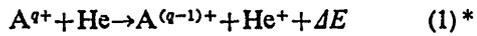
多価イオン ($q \leq 41$) による一電子捕獲

関西医大教養 岩井 鶴二

§1. はじめに

裸か、それに近い多価イオン(例えば O^{8+})や、価数の極めて高いイオン(例えば Kr^{23+})による電子捕獲反応は、原子物理学の問題として非常に興味があるだけでなく、核融合プラズマ中の不純物問題やX線レーザー開発の可能性などに関連して注目を集めている。²⁾ この研究のためには特別のイオン源が必要で、各国で競ってその開発が行われていたが、名大プラズマ研のNICE(Naked Ion Collision Experimentsの略)グル

ープでは既にそのための装置を完成し,³⁾ それを使って多価イオンによる He 原子からの一電子捕獲反応,



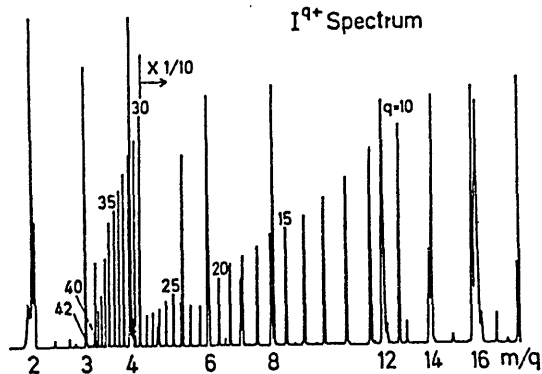
について, $q=3$ から 41 までにわたって系統的に調べ上げることに成功している.⁴⁻¹⁵⁾ その結果, 多価イオンによる一電子捕獲反応についての理解が深められたので紹介する.

§2. 実験でわかったこと

第1図にこのイオン源 (NICE-1) で得られた I^{q+} のマススペクトルを示す.¹⁵⁾ I^{42+} まで生成されていることがわかる.** 得られたイオンビームはエネルギー分布が半値幅で $0.8 \times q \text{ eV}$ と比較的狭く, 反応前後のイオンの運動エネルギーを測定することにより ΔE を求めることができる. ΔE が決まれば生成イオン $A^{(q-1)+}$ のエネルギー状態がわかることになる.

反応(1)について NICE グループの実験によってわかった特徴的なことを列記すると次の通りである.

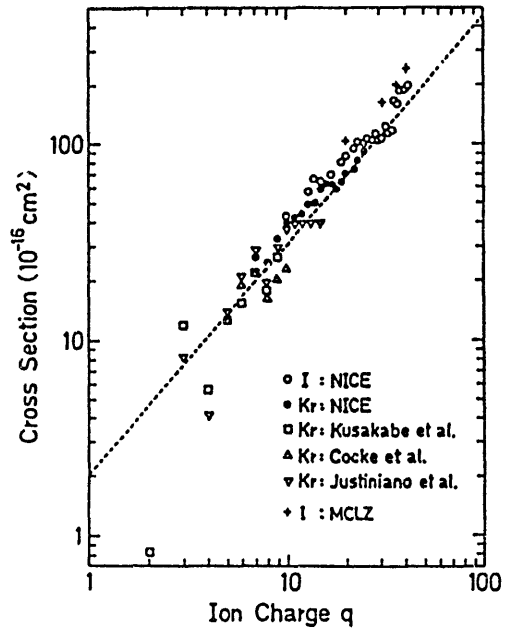
- 1) 価数 q が十分大きければ, 反応の様相は元素 A の種類によらず q のみで決まり, 同じ価数のイオンは同じ様に振舞う.
- 2) 電子は $A^{(q-1)+}$ のごく限られた n 準位 (n は主量子数) に選択的に捕獲される. 例えば $q=6$ では $n=3$ の準位に入り, $n=2$ にも $n=4$ にも入らない. $q=40$ では $n=15$ 程度の準位へ入ると推定される.



第1図 NICE-1 による I^{q+} ビームのマススペクトル, $m/q=2, 3, 4, 6, 8, 12, 14, 16$ などは不純物イオン (H. Tawara, et al.: J. Phys. B 18 (1985) 337 より転載).

* $A=B, C, N, O, F, Ne, S, Kr, I$ の各元素, ΔE は反応エネルギーで $\Delta E > 0$ のとき発熱反応.

** 沃素 ^{127}I は他に同位体がないために, H_2, He, C, N, O 等の不純物イオンと明瞭に分離できる.



第2図 He からの一電子捕獲断面積 (H. Tawara, et al.: J. Phys. B 18 (1985) 337 より転載).

- 3) 価数 q が 10 以下では反応(1)の断面積は q と共に振動しながら増加し, q が 10 以上では単調に増大して $q=41$ では $2 \times 10^{-14} \text{ cm}^2$ にも達する (第2図参照). これらの特徴のうち 1), 2) は第1表にまとめてある.

捕獲された電子が元素の種類に関係なく, 価数に固有な特定の準位に入ることがわかる. これはまた, 十分に価数が高ければ, 残った芯電子による遮蔽はほぼ完全で, A^{q+} はあたかも正電荷 qe をもった点電荷と考えてよいことを示唆している. 第1表にも見られる断面積の q に対する振動については, 既に木村がこの欄で紹介し,¹⁾ 簡単な古典的一電子モデルで定性的に説

第1表 一電子捕獲断面積と電子捕獲準位. 上段は断面積の実測値 (10^{-15} cm^2) で, 括弧内は準位の主量子数 n .

$A \backslash q$	3	4	5	6	7	8	9
C	1.9 (2)	0.1 (2)	1.5 (3)	0.9 (3)			
N		0.3 (2)	1.4 (3)	1.4 (3)	1.1 (4)		
O			2.3 (3)	1.1 (3)	1.3 (4)	2.7 (4)	
F				1.9 (3)	1.8 (4)	2.8 (4)	
Ne					3.0 (4)	2.9 (4)	1.9 (5)

明できることが示されているので、以下にはそのモデルの要点だけを述べる。

§ 3. 古典的一電子モデル

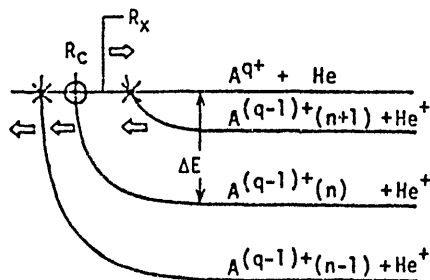
反応 (1) は第 3 図のような透熱ポテンシャル曲線の交差点を経て起ると考える。ここで反応系 $A^{q+} + He$ のポテンシャル曲線は直線で、生成系 $A^{(q-1)+} + He^+$ のそれはクーロン斥力だけで近似できるものとする。

He の $1s$ 電子が He^+ からの束縛を脱して A^{q+} の引力圏に進むためには、 A^{q+} と He^+ とが或る距離 R_x よりも接近することが必要である。古典モデルでは、 R_x の内側でかつ最も R_x に近い交差点 R_c を経て電子が移行すると考え、そのときの電子の移行確率を $1/2$ として、断面積を $\sigma = (1/2)\pi R_c^2$ とする。

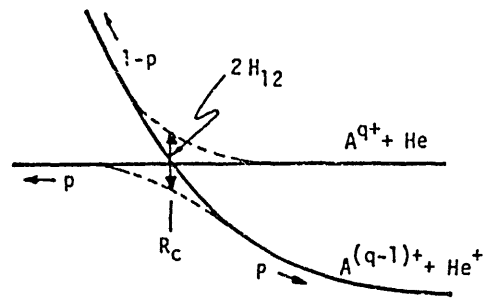
この古典的一電子モデルは、 $q < 10$ の場合に見られる断面積の無数に対する振動を定性的に説明することに成功し、また捕獲電子の入る準位の主量子数を正確に予言することができたが、大きな欠陥のあることも分った。このモデルによれば、断面積は $(1/2)\pi R_c^2$ で与えられるので、 R_c と共に単調に増大してゆく筈である。一方第 3 図のポテンシャル曲線を仮定すれば、実験で ΔE を求めることにより R_c は一義的に決まる。こうして得た R_c の関数として実測の断面積をプロットすると、 $q < 10$ では期待に反して、ある R_c のところで極大を示しそれ以上の R_c で減少してしまう。また q が 10 以上になると断面積の振動が急速に消えて q と共に単調に増大する様になるのも、このモデルでは理解しにくい。

§ 4. Landau-Zener (L-Z) 理論

第 4 図のような透熱ポテンシャル曲線の交差がある場合の交差点付近での遷移については、古くから有名な Landau-Zener の理論がある。反応系 $A^{q+} + He$ と生成系 $A^{(q-1)+} + He^+$ の間に相互作用があれば、相対



第 3 図 古典的一電子モデルの説明図。



第 4 図 L-Z 理論の説明図。

速度が無限小の極限では二つのポテンシャル曲線は交わることができず (Wigner の非交差則)、点線の様になる。これは断熱ポテンシャル曲線であって $(AHe)^{q+}$ 分子のエネルギー状態に対応する。しかし相対速度が有限の場合には二状態間に遷移の確率が生ずる。L-Z 理論によれば、系が透熱ポテンシャル曲線に沿って交差点を通過する確率は

$$p = \exp(-2\pi H_{12}^2 / v_b \Delta F) \quad (2)$$

で与えられる。ここで v_b , ΔF はそれぞれ交差点 R_c での相対速度 (動径方向) と透熱ポテンシャル曲線の勾配の差である。また H_{12} は反応系と生成系の相互作用ポテンシャルの行列要素で、断熱ポテンシャルの間隔の $1/2$ になっている。系が断熱ポテンシャルに沿って進行する確率は $(1-p)$ になるから、衝突完了時に系が反応系から生成系に移っている確率は

$$P = 2p(1-p) \quad (3)$$

で与えられる。この有名な L-Z 理論は今迄実際の系について実験と厳密に比較されることが殆どなかった。それはポテンシャル曲線や H_{12} について正確に知られている系が殆どなかったからである。多価イオンによる一電子捕獲反応は、上述の様に透熱ポテンシャル曲線が簡単な関数でかなり正確に近似でき、 H_{12} についても理論的に取扱い易い。つまり L-Z 理論検証のためにも多価イオンの電子捕獲反応は格好の材料となる。

さて、反応 (1) における H_{12} についての理論はいくつかあるが、¹⁶⁻¹⁸⁾ そのいずれでも H_{12} は $\exp(-R_c^3)$ に比例する形で表わされ R_c の増大と共に急速に減少する。従って R_c の大きいところでは p は 1 に近い。一方 R_c が十分小さければ p は 0 に近くなる。一電子捕獲の確率は (3) 式から p が 1 でも 0 でも $P=0$ であり、 $p=1/2$ のとき $P=1/2$ で最大となる。つまり R_c が適当な大きさのときだけ P が有限の値をもつ。

これ迄は生成系のポテンシャル曲線を一本しか考えなかったが、実際には第 3 図の様に n の異なる準位に

対応したポテンシャル曲線が多数ある。そのどれかの交差点が上述の様な適当な核間距離の範囲にあれば、その準位への電子捕獲が起るわけで、古典論と同様、価数の低い場合の断面積の振動も、断面積が R_0 の適当なところで極大を示すことも、共に説明できる。

§ 5. Multi-Channel-Landau-Zener (M-C-L-Z) モデル

L-Z 理論では、断面積の R_0 依存性は q が小さいほど鋭く、 q が増すにつれて極大が R_0 の大きい方にずれると同時に幅も広がる。ところで、 q が増すにつれて電子を捕獲する準位の n が大きくなることは既に見た通りである。 n が大きくなれば準位の間隔はつまってくるから、 n の異なる複数の準位が反応に寄与する可能性が生ずる。価数が10以上になると断面積の振動が消えるのはその故かと思われる。しかし実測された ΔE の幅は $q=30$ 程度になっても余り広くならず、反応に寄与する準位はせいぜい $n, n \pm 1$ の3通りほどと考えられる。一方 n の増大に伴い、 l の異なる副準位の数は n に比例して増加する。従って q が大きくなると非常に沢山の副準位が反応に寄与するだろう。これらの副準位はすべて反応系のポテンシャル曲線と交差するので、こうした多数の交差点を經由して反応が起ると考えねばならぬ。そこで木村らは各交差点での遷移確率 p に (2) 式を用い、反応の起る全確率 P は (3) 式の代りに考え得るすべてのチャンネルについての合計と考えて計算を試みた。¹⁴⁾ これを Multi-Channel-Landau-Zener (M-C-L-Z) モデルと言う。この計算で得た全断面積を第2図の+印で示す。粗い近似のわりには実験との一致はかなりよい。* またこの計算から推定される生成イオンの n 分布は $q=20$ の場合、 $n=8, 9, 10$ が 25:60:10 の割合であって、比較的狭い準位に集中していることも実験結果とよくあう。さらに、こうして得られた全断面積は交差点の平均値を \bar{R} とするとほぼ $\pi \bar{R}_0^2$ に近く、 q が10以上では再び古典論の予測が当る様になることが分る。

§ 6. おわりに

価数 q が 3~41 という広い範囲にわたって多価イオンによる一電子捕獲反応を系統的に調べた結果、その

* 裸イオンとHについては回転結合も考慮して M-C-L-Z 理論が Janev ら¹⁰⁾ によって行われている。

反応機構についてかなりの程度理解することができたと言えよう。反応 (1) は He を標的にしているが、これはたまたま実験がし易いからで、ここで分った反応機構は標的がH原子になっても変ることはないと思われる。多価イオンの振舞はその元素の種類によらず価数のみで決まることが分ったから、ここで得た Kr^{25+} の結果は Fe^{25+} (H様イオン) の振舞とほぼ同じであり、 I^{41+} の結果は Nb^{41+} (裸イオン!) の振舞とほぼ同じ管である。これら金属多価イオンとH原子との反応に関する知見は核融合研究で最も強く要求されているものだが、その実験は容易でない。ここに紹介した結果はその様な困難な実験が可能になる迄の中継ぎとしても十分役に立つ筈である。

文 献

- 1) 木村正広: 日本物理学会誌 37 (1982) 763.
- 2) S. Ohtani: *Electronic and Atomic Collisions*, ed. J. Eichler, I.V. Hertel and N. Stolterfoht (North-Holland, 1983) p. 353.
- 3) 小林信夫, 他: IPPJ-DT-84 (名古屋大学プラズマ研究所, 1981).
- 4) Y. Kaneko, T. Iwai, S. Ohtani, K. Okuno, N. Kobayashi, S. Tsurubuchi, M. Kimura, H. Tawara and S. Takagi: *Physics of Electronic and Atomic Collisions*, ed. S. Datz (North-Holland, 1982) p. 697.
- 5) T. Iwai, et al.: Phys. Rev. A 26 (1982) 105.
- 6) S. Ohtani, et al.: J. Phys. B 15 (1982) L533.
- 7) S. Tsurubuchi, et al.: J. Phys. B 15 (1982) L733.
- 8) M. Kimura, et al.: J. Phys. B 15 (1982) L851.
- 9) K. Okuno, et al.: Phys. Rev. A 28 (1983) 127.
- 10) S. Takagi, et al.: Nucl. Instrum. & Methods 215 (1983) 207.
- 11) A. Matsumoto, et al.: J. Phys. Soc. Jpn. 52 (1983) 3291.
- 12) H. Tawara, et al.: Phys. Rev. A 29 (1984) 1529.
- 13) T. Iwai, et al.: J. Phys. B 17 (1984) L95.
- 14) M. Kimura, et al.: J. Phys. Soc. Jpn. 53 (1984) 2224.
- 15) H. Tawara, et al.: J. Phys. B 18 (1985) 337.
- 16) R.E. Olson, E.T. Smith and E. Bauer: Appl. Opt. 10 (1971) 1848.
- 17) R.E. Olson and A. Salop: Phys. Rev. A 14 (1976) 579.
- 18) S.E. Butler and A. Dalgarno: Astrophys. J. 241 (1980) 838.
- 19) R.K. Janev, D.S. Belic and B.H. Bransden: Phys. Rev. A 28 (1983) 1293.

LIST OF IPPJ-AM REPORTS

- IPPJ-AM-1* "Cross Sections for Charge Transfer of Hydrogen Beams in Gases and Vapors in the Energy Range 10 eV–10 keV"
H. Tawara (1977) [Published in *Atomic Data and Nuclear Data Tables* 22, 491 (1978)]
- IPPJ-AM-2* "Ionization and Excitation of Ions by Electron Impact –Review of Empirical Formulae–"
T. Kato (1977)
- IPPJ-AM-3 "Grotrian Diagrams of Highly Ionized Iron FeVIII-FeXXVI"
K. Mori, M. Otsuka and T. Kato (1977) [Published in *Atomic Data and Nuclear Data Tables* 23, 196 (1979)]
- IPPJ-AM-4 "Atomic Processes in Hot Plasmas and X-Ray Emission"
T. Kato (1978)
- IPPJ-AM-5* "Charge Transfer between a Proton and a Heavy Metal Atom"
S.Hiraide, Y. Kigoshi and M. Matsuzawa (1978)
- IPPJ-AM-6* "Free-Free Transition in a Plasma –Review of Cross Sections and Spectra–"
T. Kato and H. Narumi (1978)
- IPPJ-AM-7* "Bibliography on Electron Collisions with Atomic Positive Ions: 1940 Through 1977"
K. Takayanagi and T. Iwai (1978)
- IPPJ-AM-8 "Semi-Empirical Cross Sections and Rate Coefficients for Excitation and Ionization by Electron Collision and Photoionization of Helium"
T. Fujimoto (1978)
- IPPJ-AM-9 "Charge Changing Cross Sections for Heavy-Particle Collisions in the Energy Range from 0.1 eV to 10 MeV I. Incidence of He, Li, Be, B and Their Ions"
Kazuhiko Okuno (1978)
- IPPJ-AM-10 "Charge Changing Cross Sections for Heavy-Particle Collisions in the Energy Range from 0.1 eV to 10 MeV II. Incidence of C, N, O and Their Ions"
Kazuhiko Okuno (1978)
- IPPJ-AM-11 "Charge Changing Cross Sections for Heavy-Particle Collisions in the Energy Range from 0.1 eV to 10 MeV III. Incidence of F, Ne, Na and Their Ions"
Kazuhiko Okuno (1978)
- IPPJ-AM-12* "Electron Impact Excitation of Positive Ions Calculated in the Coulomb-Born Approximation –A Data List and Comparative Survey–"
S. Nakazaki and T. Hashino (1979)
- IPPJ-AM-13 "Atomic Processes in Fusion Plasmas – Proceedings of the Nagoya Seminar on Atomic Processes in Fusion Plasmas Sept. 5-7, 1979"
Ed. by Y. Itikawa and T. Kato (1979)
- IPPJ-AM-14 "Energy Dependence of Sputtering Yields of Monatomic Solids"
N. Matsunami, Y. Yamamura, Y. Itikawa, N. Itoh, Y. Kazumata, S. Miyagawa, K. Morita and R. Shimizu (1980)

- IPPJ-AM-15 "Cross Sections for Charge Transfer Collisions Involving Hydrogen Atoms"
Y. Kaneko, T. Arikawa, Y. Itikawa, T. Iwai, T. Kato, M. Matsuzawa,
Y. Nakai, K. Okuno, H. Ryufuku, H. Tawara and T. Watanabe (1980)
- IPPJ-AM-16 "Two-Centre Coulomb Phaseshifts and Radial Functions"
H. Nakamura and H. Takagi (1980)
- IPPJ-AM-17 "Empirical Formulas for Ionization Cross Section of Atomic Ions for
Electron Collisions –Critical Review with Compilation of Experimental
Data–"
Y. Itikawa and T. Kato (1981)
- IPPJ-AM-18 "Data on the Backscattering Coefficients of Light Ions from Solids"
T. Tabata, R. Ito, Y. Itikawa, N. Itoh and K. Morita (1981)
- IPPJ-AM-19 "Recommended Values of Transport Cross Sections for Elastic Collision and
Total Collision Cross Section for Electrons in Atomic and Molecular Gases"
M. Hayashi (1981)
- IPPJ-AM-20 "Electron Capture and Loss Cross Sections for Collisions between Heavy
Ions and Hydrogen Molecules"
Y. Kaneko, Y. Itikawa, T. Iwai, T. Kato, Y. Nakai, K. Okuno and H. Tawara
(1981)
- IPPJ-AM-21 "Surface Data for Fusion Devices – Proceedings of the U.S–Japan Work-
shop on Surface Data Review Dec. 14-18, 1981"
Ed. by N. Itoh and E.W. Thomas (1982)
- IPPJ-AM-22 "Desorption and Related Phenomena Relevant to Fusion Devices"
Ed. by A. Koma (1982)
- IPPJ-AM-23 "Dielectronic Recombination of Hydrogenic Ions"
T. Fujimoto, T. Kato and Y. Nakamura (1982)
- IPPJ-AM-24 "Bibliography on Electron Collisions with Atomic Positive Ions: 1978
Through 1982 (Supplement to IPPJ-AM-7)"
Y. Itikawa (1982)
- IPPJ-AM-25 "Bibliography on Ionization and Charge Transfer Processes in Ion-Ion
Collision"
H. Tawara (1983)
- IPPJ-AM-26 "Angular Dependence of Sputtering Yields of Monatomic Solids"
Y. Yamamura, Y. Itikawa and N. Itoh (1983)
- IPPJ-AM-27 "Recommended Data on Excitation of Carbon and Oxygen Ions by Electron
Collisions"
Y. Itikawa, S. Hara, T. Kato, S. Nakazaki, M.S. Pindzola and D.H. Crandall
(1983)
- IPPJ-AM-28 "Electron Capture and Loss Cross Sections for Collisions Between Heavy
Ions and Hydrogen Molecules (Up-dated version of IPPJ-AM-20)"
H. Tawara, T. Kato and Y. Nakai (1983)

- IPPJ-AM-29 "Bibliography on Atomic Processes in Hot Dense Plasmas"
T. Kato, J. Hama, T. Kagawa, S. Karashima, N. Miyanaga, H. Tawara, N. Yamaguchi, K. Yamamoto and K. Yonei (1983)
- IPPJ-AM-30 "Cross Sections for Charge Transfers of Highly Ionized Ions in Hydrogen Atoms (Up-dated version of IPPJ-AM-15)"
H. Tawara, T. Kato and Y. Nakai (1983)
- IPPJ-AM-31 "Atomic Processes in Hot Dense Plasmas"
T. Kagawa, T. Kato, T. Watanabe and S. Karashima (1983)
- IPPJ-AM-32 "Energy Dependence of the Yields of Ion-Induced Sputtering of Monatomic Solids"
N. Matsunami, Y. Yamamura, Y. Itikawa, N. Itoh, Y. Kazumata, S. Miyagawa, K. Morita, R. Shimizu and H. Tawara (1983)
- IPPJ-AM-33 "Proceedings on Symposium on Atomic Collision Data for Diagnostics and Modelling of Fusion Plasmas, Aug. 29 – 30, 1983"
Ed. by H. Tawara (1983)
- IPPJ-AM-34 "Dependence of the Backscattering Coefficients of Light Ions upon Angle of Incidence"
T. Tabata, R. Ito, Y. Itikawa, N. Itoh, K. Morita and H. Tawara (1984)
- IPPJ-AM-35 "Proceedings of Workshop on Synergistic Effects in Surface Phenomena Related to Plasma-Wall Interactions, May 21 – 23, 1984"
Ed. by N. Itoh, K. Kamada and H. Tawara (1984)
- IPPJ-AM-36 "Equilibrium Charge State Distributions of Ions ($Z_1 \geq 4$) after Passage through Foils – Compilation of Data after 1972"
K. Shima, T. Mikumo and H. Tawara (1985)
- IPPJ-AM-37 "Ionization Cross Sections of Atoms and Ions by Electron Impact"
H. Tawara, T. Kato and M. Ohnishi (1985)
- IPPJ-AM-38 "Rate Coefficients for the Electron-Impact Excitations of C-like Ions"
Y. Itikawa (1985)
- IPPJ-AM-39 "Proceedings of the Japan-U.S. Workshop on Impurity and Particle Control, Theory and Modeling, Mar. 12 – 16, 1984"
Ed. by T. Kawamura (1985)
- IPPJ-AM-40 "Low-Energy Sputterings with the Monte Carlo Program ACAT"
Y. Yamamura and Y. Mizuno (1985)
- IPPJ-AM-41 "Data on the Backscattering Coefficients of Light Ions from Solids (a Revision)"
R. Ito, T. Tabata, N. Itoh, K. Morita, T. Kato and H. Tawara (1985)

- IPPJ-AM-42 “Stopping Power Theories for Charged Particles in Inertial Confinement Fusion Plasmas (Emphasis on Hot and Dense Matters)”
S. Karashima, T. Watanabe, T. Kato and H. Tawara (1985)
- IPPJ-AM-43 “The Collected Papers of Nice Project/IPP, Nagoya”
Ed. by H. Tawara (1985)

Available upon request to Research Information Center, Institute of Plasma Physics, Nagoya University, Nagoya 464, Japan, except for the reports noted with*.

